Role of the Receptor for Advanced Glycation End-products (RAGE) in the Immune Sensing of Nucleic Acids

Dissertation

zur

Erlangung des Doktorgrades (Dr. rer. nat.)

der

Mathematisch-Naturwissenschaftlichen Fakultät

der

Rheinischen Friedrich-Wilhelms-Universität Bonn

vorgelegt von

Damien Bertheloot

aus

Roubaix (Frankreich)

Bonn März, 2016

Angefertigt mit Genehmigung der Mathematisch-
Naturwissenschaftlichen Fakultät der Rheinischen Friedrich-
Wilhelms-Universität Bon

1. Gutachter: Prof. Dr. med. Eicke Latz

2. Gutachter: Prof. Dr. rer. nat. Sven Burgdorf

Tag der Promotion: 06.07.2016
Erscheinungsjahr: 2016

À mes parents, sans qui rien de ceci n'aurait été possible

Acknowledgments

First, I would like to thank the members of the Jury, Professor Eicke Latz, Professor Sven Burgdorf, Professor Matthias Geyer and Professor Wolfgang Lück for accepting to judge and grade this work.

I would specially like to thank Eicke, not only for giving me the chance to work in his laboratory, but also for his supervision. All along this journey, Eicke has been an amazing mentor, always full of ideas and advice that were indispensable to the work presented here and that have helped shape the scientist I have become.

I would also like to thank the collaborators I had the chance to work with. First of all, I would like to thank Cherilyn Sirois for starting this project, for her help at the beginning of my work on RAGE and to let me become a full member of the “RAGE team”. I am immensely grateful to Professor Natalio Garbi for his precious help throughout the project. Natalio was always available and ready to share ideas and advice on how to proceed with the project. He never hesitated to help me with in-vivo experiments even when this meant sitting in front of a flow cytometer until 3am. I am also greatly thankful to Christine Schmidt-Mbamumyo for her help and skilled work. Many thanks go to Allison L. Naumovski who was an amazing source of help and support throughout the good and the bad times. Thanks also go to Roland Kolbeck who made this collaboration possible. I would like to thank Tsan Sam Xiao and Tengchuan Jin for their help and crucial contribution to the understanding of how RAGE interacts with nucleic acids. I also thank Sudhir Agrawal and Idera Pharmaceuticals for relentlessly providing us with the TLR7-, TLR8- and TLR3-sepcific RNA agonists. Many thanks go to Zeinab Abdullah for being such a friendly source of help and advice. I would also like to thank the members of the FACS Core facility, Peter Wurst, Andreas Dolf and Elmar Endl for their help with FACS sorting of RAGE expressing cells. Many thanks also go to Thomas Zillinger, Ana Herzner and Eva Bartok for their help and reagents.

I would like to warmly thank all members of the AG Latz, past and present, for their continuous support, jokes and happy spirit. I am especially thankful to Gabor L. Horvath who has not only been a great housemate for several years but has also

been an important source of help throughout my PhD. I would like to thank Pia Langhoff for spending so much effort in organising the lab and keeping it running. Pia was also of great help on “bone-marrow days”. I am also grateful to Olivia Van Rey for her help and her happy spirit. Thanks also go to Max Roth and Anne Alfter who, together with Olivia took care of the RAGE knockout mice. My thanks also go to Guddrun Engels and Rainer Stahl for their technical support.
I would like to specially thank the members of the Original Dream Team: Andrea Stutz, Karin Pelka, Dominic and Christine De Nardo. Andrea and Karin have been a constant source of advice and support throughout my PhD. They have been indispensable friends that have made the hard times bearable. Dominic has been and still is a scientific model for me and together with Christine, was always an immense source of support and crucial advice.

I would like to thank my friends Allison Williams and Jérôme Heuper who field my life in Bonn with happy moments. They have been a great support for me during my PhD thanks to their spiritual and culinary skills. Many thanks must also go to Alison for accepting to read through this thesis and for her input.

I am eternally indebted to my family. My parents have been an immense source of support and encouragements throughout my life. They have helped me believe in myself and never doubted me. To them I must say *Mille Mercis*. I am also very thankful to my big sisters, Céline and Élodie, who have also been a constant source of support and love in my life.
I would like to also thank my adoptive German parents, Christa and Thomas, who have accepted me as part of their family and always made me feel at home.
Last but certainly not least, I would like to most deeply thank Jen for being such a constant source of scientific ideas, spiritual support and love. Jen continually stood by my side in the good and bad times that flourished along this long journey. I am lucky to have her and will eternally be grateful.

Declaration – Erklärung

An Eides statt versichere ich, dass die vorgelegte Arbeit – abgesehen von den ausdrücklich bezeichneten Hilfsmitteln – persönlich, selbständig und ohne Benutzung anderer als der angegebenen Hilfsmittel angefertigt wurde, die aus anderen Quellen direkt oder indirekt übernommenen Daten und Konzepte unter Angabe der Quelle kenntlich gemacht sind, die vorgelegte Arbeit oder ähnliche Arbeiten nicht bereits anderweitig als Dissertation eingereicht worden ist bzw. sind, kein früherer Promotionsversuch unternommen worden ist, für die inhaltlichmaterielle Erstellung der vorgelegten Arbeit keine fremde Hilfe, insbesondere keine entgeltliche Hilfe von Vermittlungs- bzw. Beratungsdiensten (Promotionsberater oder andere Personen) in Anspruch genommen wurde sowie keinerlei Dritte vom Doktoranden unmittelbar oder mittelbar geldwerte Leistungen für Tätigkeiten erhalten haben, die im Zusammenhang mit dem Inhalt der vorgelegten Arbeit stehen.

Datum Unterschrift

Teile dieser Dissertation sind in den folgenden Publikationen enthalten:

- Bertheloot D., Naumovski A.L., Langhoff P., Horvath G.L., Jin T., Xiao T.S., Garbi N., Agrawal S., Kolbeck R. and Latz E., *RAGE enhances TLR responses through binding and internalization of RNA*.
(Under peer review at the Journal of Immunology)

- Sirois, C.M., Jin, T., Miller, A.L., **Bertheloot, D.**, Nakamura H., Horvath G.L., Mian A., Jiang J., Schrum J., Bossaller L., Pelka K., Garbi N., Brewah Y., Tian J., Chang C., Chowdhury P.S., Sims G.P., Kolbeck R., Coyle A.J., Humbles A.A., Xiao T.S., Latz E., 2013. *RAGE is a nucleic acid receptor that promotes inflammatory responses to DNA*. Journal of Experimental Medicine.
doi: 10.1084/jem.20120201

Abstract

Nucleic acid recognition is an important mechanism that enables the innate immune system to detect both microbial infection and tissue damage. To minimize the recognition of self-derived nucleic acids, all nucleic acid sensing signaling receptors are sequestered away from the cell surface and are activated either in the cytoplasm or in endosomes. In endosomes, nucleic acid sensing relies on members of the toll-like receptor (TLR) family. In conditions of infection or damage, however, the immune system must allow recognition of extracellular nucleic acids. But, how these are sensed and internalized is not yet completely understood. Entry of nucleic acids has long been considered to rely on microbe or cell debris uptake into cells before release of their contents including the nucleic acids. It is now clear that free extracellular nucleic acids exist, which can be detected and internalized thanks to extracellular receptors.

The receptor for advanced glycation end-products (RAGE) is a multiligand cell surface receptor that has been studied the past twenty years for its role in development of a plethora of inflammation states such as those occurring during microbial infection, sterile injury, neurodegeneration, auto-immunity and cancer. RAGE was shown to trigger inflammatory signals, promote immune cell maturation, proliferation and motility thereby sustaining and exaggerating the inflammatory state. To do so, RAGE senses heterogeneous types of molecules that accumulate during such inflammatory conditions and which often can trigger expression of RAGE itself. These ligands include advanced glycation end-products (AGEs), amyloid fibrils such as amyloid-β, members of the S100 protein family and high-mobility group box 1 (HMGB1).

Data presented in this thesis introduces nucleic acids as new class of ligands for RAGE. First, data demonstrate the binding of DNA to RAGE extracellular domain and localizes this binding to the V and C1 immunoglobulin-like domains. Biochemical assays and crystallography analysis show that DNA binds with RAGE through interaction between the DNA phosphate backbone and a positively charged amino-acid surface present on RAGE V-C1 domain. Flow cytometry and confocal microscopy experiments show that stimulatory DNA, a specific activator of the endosomal DNA receptor TLR9, is recruited at the surface of cells expressing RAGE and thereby internalized more efficiently. Thus, RAGE expression increases subsequent TLR9 activation and downstream NFκB activity.

Since DNA binds to RAGE in a base-unspecific manner, a potential interaction of RNA with RAGE is further analyzed in the second part of this thesis. Results first prove that single stranded RNA (ssRNA) indeed binds to RAGE. Comparing DNA and RNA binding to RAGE, competing assays show that RNA binds to RAGE at a similar site than DNA. Confocal microscopy and flow cytometry experiments show that RAGE expression at the cell surface recruits RNA and promotes internalization that can be abrogated by truncation of RAGE V-C1 domain. As for TLR9, RAGE expression increases the activation of the RNA-specific receptors, TLR7, TLR8 and TLR13. Confirming these results, RAGE deficiency strikingly reduces the activation of bone marrow cells upon stimulation with a TLR13-specifc RNA agonist. Deeper analysis of mechanisms involving RAGE in TLR-dependent RNA-sensing show that the effect of RAGE relies on actin polymerization and dynamin-dependent cell internalization. Furthermore, truncation of RAGE intracellular signaling domain indicates that direct RAGE downstream signaling is negligible.

Finally, study of the effect of RAGE on double stranded RNA (dsRNA) sensing presents contradictory results. Indeed, although TLR3-specific dsRNA binds to RAGE efficiently, RAGE expression inhibits TLR3 activation. Surprisingly, upon cell stimulation with a dsRNA synthetic analog, poly (I:C), RAGE expression increases immune activation, indicating a possible role for RAGE in cytosolic RNA sensing.

Together, these results illustrate RAGE as a pivotal membrane receptor for nucleic acids. Hence, data presented in this thesis indicates that RAGE is an integral part of the endosomal nucleic acid sensing system and calls for further analysis of the role of RAGE in cytosolic nucleic acid sensing and potentially non-coding RNA-mediated cell-to-cell communication.

Table of Contents

List of Figures

1. Introduction

2. Materials and Methods

3. Results – Part 1: RAGE is a cell surface DNA sensor that promotes TLR9-dependent inflammatory responses

4. Results – Part 2: RAGE senses RNA at the cell surface and promotes TLR7-, TLR8- and TLR13-dependent inflammatory responses

5. Discussion

Abbreviations

ADAM10	Disintegrin and metalloproteinase domain-containing protein 10
AEP	Asparagine endopeptidase
AGEs	Advanced glycation end-products
Ago1/2	Argonaute 1/2
AIM2	Absent in melanoma 2
AP-1	Activator protein 1
AP-1/2	Adaptor protein-1/2
AP1	Activator Protein 1
APCs	Antigen-presenting cells
APP	Amyloid precursor protein
ARFs	Adenosine diphosphate ribosylation factors
Asn	Asparagine
Aß	Amyloid-beta
ATP	Adenosine triphosphate
BCA	Bichoninic acid (assay)
BCAM	Basal cell adhesion molecule
BCR	B-cell receptor
CAMs	Cell adhesion molecules
cAMP	Cyclic adenosine monophosphate
Cav-1	Caveolin-1
Cdc42	Cell division control protein 42
cDCs	Conventional dendritic cells
cGAS	Cyclic-GAMP synthetase
CLRs	C-type lectin receptors
co-IP	Co-immunoprecipitation
CREB	cAMP-responsive-element-binding protein
DAMP	Damage-associated molecular pattern
DC	Dendritic cell
DEC-205	Lymphocyte antigen 75, also CD205
DMEM	Dulbecco’s Modified Eagle Medium
DMSO	Dimethyl sulfoxide
DNA	Desoxyribonucleic acid
Dnase I	DNA endonuclease 1
dNTPs	deoxyribose-containing nucleotide triphosphates
DPBS	Dulbecco’s PBS
dsDNA	double-stranded DNA
dsRNA	Double-stranded RNA
ECD	Extra-cellular domain
EDTA	Ethylenediaminetetraacetic acid
EF-1a	Elongation factor 1-alpha
ELISA	Enzyme Linked Immunosorbent Assay
EMSA	Electrophoretic mobility shift assay
ER	endoplasmic reticulum

ERK1/2	Extracellular signal-regulated kinases 1/2
esRAGE	Endogenous secretory RAGE
Evs	extracellular vesicles
FACS	Fluorescence-activated cell sorting
FceRI	Fc-eupsilon-Receptor I
FcgR	Fc-gamma receptor
FCS	Foetal Calf serum
FH1	formin homology domain 1
fLuc	Firefly luciferase
FRET	Förster resonance energy transfer
Gag-pol	HIV group specific antigen and reverse transcriptase
gAMPs	Granular anti-microbial peptides
GEF	guanine nucleotide exchange factors
GEF	Guanine nucleotide-exchange factors
GFP	Green fluorescent protein
gLuc	Gaussia luciferase
gp96	Endoplasmin
GPCRs	G protein-coupled receptors
GSK3b	Glycogen synthase kinase 3 beta
GTPases	Guanosine triphosphate hydrolase
HDL	High-density lipoprotein
HMGB1	High-mobility group box 1
HMW	High molecular weight
Hprt	Hypoxanthine-guanine phosphoribosyltransferase
HTRF	Homogeneous Time Resolved Fluorescence
IC	Immune-complex
ICAM-1	Intercellular adhesion molecule 1
IFI16	g-interferon-inducible protein 16
IFN	Interferon
IgE	Immunoglobulin E
IgG	Immunoglobulin G
IκB	NFκB inhibitor
IKK	IκB kinase
IL-1 or 6	Interleukine-1 or 6
IL-1β	Interleukine-1 beta
IL-1R	Interleukine-1 receptor
IRAK	IL-1 receptor associated kinases
IRF3/7	Interferon regulatory factor 3/7
JAK2	Janus kinase 2
JNK	c-Jun N-terminal kinases
KO	Knock-out
LMW	Low molecular weight
lncRNA	long-non-coding RNA
LPS	Lipopolysaccharide
LRR	Leucine-rich repeats
LTR	Long terminal repeat

MAL	MyD88 adaptor like
MAPK	mitogen-activated protein kinase
MARCO	Macrophage receptor with collagenous structure
MD-2	Lymphocyte antigen 96
MDA5	Melanoma differentiation-associated protein 5
mDia1	Diaphanous-related formin 1
MEK	MAPK/ERK kinase
MHC	Major histocompability complex
miRNA	micro-RNA
MKK6	MAPK kinase 6
MMP9	Matrix metallopeptidase 9
mRNA	messenger RNA
mtRNA	Mitochondrial RNA
MyD88	Myeloid differentiation primary response gene 88
ncRNA	non-coding RNA
NETs	Neutrophil extracellular traps
NFκB	Nuclear factor-kappa-B
NLRs	NOD-like receptors
NO	Nitric oxide
NOD	Nucleotide-binding oligomerization domain
NOX1	NADPH oxidase 1
NS-RNA	Non-stimulatory RNA
ODN	Oligodeoxynucleotide
ORF	Open reading frame
ORN	Oligoribonucleotide
PAMP	Pathogen-associated molecular pattern
PCR	Polymerase chain reaction
PI3K	Phosphoinositide 3-kinase
PKB	Protein kinase B
PKC	Protein kinase C
PKR	Protein kinase R
poly (I:C)	Polyinosinic:polycytidylic acid
PRR	Pattern recognition receptor
qPCR	Quantitative PCR
Rab	Ras related protein
Rac-1	Ras-related C3 botulinum toxin substrate 1
RAGE	Receptor for advanced glycation end-products
RAGE ΔCyt	Cytosolic-domain truncated RAGE
RAGE ΔVC1	VC1-domain truncated RAGE
RAGE FL	RAGE full-length
Ras	Rat sarcoma protein
RhoA	Ras homolog gene family member A
RIG-I	Retinoic acid inducible protein I
RIP1	Receptor-interacting protein 1
RLRs	RIG-I-like receptors
RNA	Ribonucleic acid

ROCK	Rho-associated protein kinase
ROS	Reactive oxygen species
SID-1	Systemic RNA Interference Deficiency-1
siRNA	Small interfering RNA
SLE	Systemic lupus erythematosus
SNP	Single nucleotide polymorphism
SR-A	Scavenger receptor A
sRAGE	Soluble RAGE
Src	Proto-oncogene tyrosine-protein kinase
ssDNA	Single-stranded DNA
ssRNA	Single-stranded RNA
STAT1/3	Signal transducers and activators of transcription
STING	Stimulator of interferon genes protein
TagRFP	Tag-Red fluorescent protein
TANK	TRAF family member-associated NFκB activator
TBK1	TANK-binding kinase-1
TFAM	Mitochondrial Transcription Factor A
TGF-b	Transforming growth factor beta
TGF-bR	Transforming growth factor beta receptor
TIR	Toll-IL-1-resitence domain
TLR	Toll-like receptor
TLRsC	C-terminal domain of TLRs
TLRsN	N-terminal domain of TLRs
TNFa	Tumor necrosis factor alpha
TRAF3 or 6	TNF-associated factor 3 or 6
TRAM	TRIF-related adaptor molecule
TRIF	TIR domain-containing adaptor-inducing IFN-b
UNC93b1	Unc-93 homolog B1
VCAM-1	Vascular cell Intercellular adhesion protein 1
VSV-G	Vesicular stomatitis virus glycoprotein G
WT	Wild-type

1. Introduction

1.1 Immunity: *Veni, Vedi, Vici*?

The organism in its environment

We live surrounded by microorganisms, most of which are potentially infectious and therefore referred to as pathogens. Yet we only rarely become ill. This is due to a strong defense system that comprises several layers of complex and regulated mechanisms. When the body encounters a microorganism, the first line of defense is mainly physical and chemical. Our skin represents an important physical barrier that keeps pathogens from entering deeper into our organism. Chemical elements such as anti-microbial enzymes secreted in the mucosal surfaces block or kill pathogens before they enter the body.
But not all microorganisms are bad. Some help our body in daily tasks such as digestion and even participate in the defense of our body against microbial threats. The best example for this is the microorganisms present in the gut flora (1). They help to metabolize nutrients that the host's own digestive system is unable to process. They contribute to the antimicrobial defense by directly secreting acids that disrupt the bacterial cell wall or by promoting secretion of host anti-microbial proteins (AMPs) through the activation of Paneth cells. They also modulate the function of the second layer of the host's anti-microbial defense, namely the immune system.

The immune system

The immune system is divided into two distinct components: the innate immune system and the adaptive immune system. The innate immune system is readily available since birth and can directly combat a wide range of pathogens by secretion of antimicrobial and cytotoxic molecules as well as engulfment and further destruction of the pathogens in specialized cells during a process called

phagocytosis. In contrast, the adaptive immune system is responsible for a pathogen-specific and long lasting anti-microbial response. This response is developed upon first encounter with a particular pathogen and depends on 1) the production of antibodies specific to this pathogen and 2) the development of immunological memory, which can confer a lifelong protection against reinfection with the same pathogen. Both innate and adaptive immune responses act in concert and provide regulative feedback to each other. The innate immune system is often the first to act against a new pathogen and once activated, it licenses the adaptive immune system for specific recognition and destruction of the newly encountered pathogen. The adaptive immune system will then feedback onto the innate immune system to modulate a more adequate response.

The immune system actively recognizes and combats microbial pathogens. To this end, it must fulfill four main tasks.

- First, it must detect the presence of an infection. This is done by both white blood cells of the innate immune system that provide an immediate response and by lymphocytes of the adaptive immune system.
- The immune system must then contain or even eliminate the infection. It therefore brings into play immune effector functions such as the complement system, the production of antibodies by lymphocytes of the adaptive immune system and destructive tools provided by lymphocytes and innate white blood cells.
- To avoid damaging the body, the immune system must also self-regulate and failing to do so can lead to the development of allergies and autoimmune diseases.
- Finally, to protect the organism against frequent infection with the same pathogen, the immune system must develop an immunological memory to any newly encountered threat to provide an immediate and stronger immune response against reinfection with the same pathogen.

Vaccination is an important medical tool that uses this last feature of the immune system to prepare our organism to fight against pathogenic microorganisms, even before first encounter. The immune system is activated using a mixture of pathogen-derived molecules (antigens), which will be the target of new antibodies, together with immunogenic compounds that are known to strongly activate the innate immune system triggering the activation and regulation of the adaptive immune system.

The innate immune system: PAMP and DAMP recognition by PRRs

Innate Immune Cells

When a pathogen breaches the physical and chemical barriers formed by the skin and the mucosal epithelia of the airways and the gut, they are rapidly met by cells and molecules, which produce an immediate innate immune response. Most cells of the innate immune system derive from a common myeloid progenitor and are usually classified in four main groups: macrophages, granulocytes, mast cells and dendritic cells.

Macrophages reside in most tissues and originate from the maturation of the blood circulating monocytes. In normal conditions, macrophages act mainly as scavenger cells where they clear the body of dead cells and cell debris by phagocytosis. However, upon infection and since macrophages are present in most tissues, they are often the first innate immune cells to act against microorganisms. They engulf and kill invading microbes and clear infected cells. Perhaps even more importantly, macrophages are often the first to generate inflammation through secretion of signaling proteins called cytokines that will activate and recruit other immune cells further promoting the inflammation.

There are three types of granulocytes, namely neutrophils, eosinophils and basophils. These short-lived cells are mostly present in the circulation system until they infiltrate inflamed tissues. Neutrophils are the most important and numerous granulocytes (2). Specialised for intracellular killing of microbes, neutrophils can recognise and bind many pathogens. After phagocytosis, they are able to directly kill microbes by means of enzymes and anti-microbial peptides present in intracellular acidic granules. Neutrophils can secrete cytokines, release granular anti-microbial peptides (gAMPs) and enzymes that can degrade virulence factors and the bacterial cell wall, thereby directly killing microbes present in the extracellular milieu. To restrict and then kill microbes, neutrophils are also able to release a mixture of chromatin and gAMPs forming the so-called neutrophil extracellular traps (NETs) in a process often lytic for the neutrophils (3). Eosinophils and basophils are also capable of phagocytosis and contain intra-cellular acidic granules filled with enzymes and anti-microbial peptides. Eosinophils and basophils are less abundant than neutrophils and are believed to mainly play a role in the host's defence against

parasites too big to be internalised by neutrophils and macrophages. They are also thought to be involved in the development of allergies.

Mast cells differentiate in tissues and are found mainly around blood vessels or under the mucosal layers of the gut and the airways. Like granulocytes, mast cells contain granules that can be released upon cell activation. These cells are mainly studied for their role in allergic reactions. In fact, they express a high level of cell surface Fcε receptor (FcεRI) that possess high binding affinity for a type of antibody specific to allergenic molecules, namely immunoglobulin E (IgE). This confers IgE coated mast cells a high reactivity towards allergens, triggering rapid release of pro-inflammatory mediators and inducing recruitment of other immune cells such as eosinophils, basophils, T and B lymphocytes. This further amplifies the inflammatory response and the production of IgE specific to the allergen.

Since the main function of dendritic cells is to bridge the innate and adaptive components of the immune system, they are considered to be one of the most critical cell types of the immune system. Dendritic cells are believed to originate from both myeloid and lymphoid progenitor cells. Immature dendritic cells migrate from the bone marrow, through the blood stream before infiltrating tissues. Like macrophages and neutrophils, dendritic cells are capable of phagocytosis as they continually ingest large amounts of the extracellular fluid and its components in a process called macropinocytosis. Antigens derived from engulfed and degraded pathogens are presented by dendritic cells to T lymphocytes of the adaptive immune system and thereby initiate the specific anti-microbial response. Upon encounter with a pathogen, these antigen-presenting cells (APCs), can also be directly activated through the sensing of pathogen derived molecules. They subsequently secrete cytokines and other signals, which are vital for a complete activation of T lymphocytes and the modulation of both innate and adaptive immune responses.

Innate Immune Receptors sense infection and tissue damage

Activation of stromal and innate immune cells by pathogen relies on the recognition of pathogen-derived molecules otherwise called pathogen-associated molecular patterns (PAMPs). These molecules are common to many pathogens and are of diverse nature such as peptidoglycans, oligosaccharides and lipopolysaccharides (LPS) of the bacterial cell wall, or nucleic acids derived from the viral or bacterial

genome. Microbial-derived molecules are sensed by the so-called pattern recognition receptors (PRRs), proteins present either at the plasma membrane, in the cytoplasm or compartmentalized in intracellular membrane structures like the endosome. In 1989, Charles Janeway was the first to introduce the concept of pattern recognition by receptors that would link innate and adaptive immune systems (4). First research in the field of PRRs was done to find the receptor for LPS, an immune-stimulatory component of endotoxin derived from Gram-negative bacterial cell wall. Intense research was carried out until, 10 years after Janeway's postulate, Toll-like receptor (TLR)4 was finally proven to be the receptor for LPS (5-7). These seminal studies established the TLRs as real PRRs. Following this finding, other receptor families have been demonstrated to act as PRR. Numerous plasma membrane proteins of the C-type lectin receptors (CLRs) family were shown to sense a large array of heterogeneous ligands and mediate their endocytosis (8). For example, DEC-205 was recently shown to bind CpG-rich DNA molecules (9). Furthermore, numerous cytoplasmic nucleic acid-sensing receptors were discovered. These include the RNA sensors of the retinoic acid-inducible gene I (RIG-I)-like receptors (RLRs) RIG-I (10) and melanoma differentiation-associated protein 5 (MDA5) (11) or the nucleotide-binding oligomerization domain (NOD)-like receptors (NLRs) absent in melanoma 2 (AIM2) (12) and the γ-interferon-inducible protein IFI16 (13). Very recently, the DNA sensing enzyme cyclic-GAMP synthetase (cGAS) was discovered to act upstream of STING to induce an interferon (IFN) response (14, 15).
Several other receptors were shown to act as PRRs in certain conditions, like several members of the scavenger receptor family such as the scavenger receptor type-A (SR-A) or the receptor for advanced glycation end-products (RAGE), which will be described in greater details later on.

PRRs evolved to recognise pathogen-derived molecules and usually enable the immune system to differentiate between self and non-self. However, it has become apparent that, in the presence of tissue damage, certain PRRs are able to recognise misplaced or specifically secreted self-molecules that are referred to as damage-associated molecular patterns (DAMPs). Such molecules can be of various natures and found misplaced in the extracellular milieu like nucleic acids in association with nuclear proteins, uric acids, adenosine tri-phosphate (ATP) or actively secreted like the alarmin high mobility group box 1 (HMGB1). As for PAMPs, DAMPs are sensed by cells of the innate immune system and will trigger an inflammatory response and subsequent tissue repair.

1.2 Toll-like receptors

Toll-like receptor discovery

The Toll-like receptors (TLRs) were one of the first families of PRRs to be discovered and have now been the subject of intense research for 15 years (16). The first steps in the field of TLR research were made in *Drosophila melanogaster* with the discovery of Toll, a protein showed to promote dorsoventral polarity in the early phases of *D. melanogaster* embryo development (17). It was further demonstrated that Toll activation upon infection induced expression of the antifungal peptide Drosomycin, proving the involvement of Toll in the anti-microbial response (18, 19). In tobacco plants, a similar defence mechanism against mosaic virus was found to involve the N protein, a receptor containing an amino-terminal end similar to Toll (20). This conserved N-terminal domain was later found in the mammalian IL-1 receptor (IL-1R) cytoplasmic domain. This domain, conserved across the plant and animal kingdoms, was consequently called Toll–IL-1-resistence (TIR) domain. Moreover, other mammalian protein receptors had been found to have even more similarity to Toll than IL-1R. These proteins were predicted to have TIR domains and leucine-rich repeats similar to those found in Toll (21). These receptors, first named human Toll (hToll), were later re-named as Toll-like receptors (TLRs). At first, no function was attributed to mammalian TLRs but the structural similarity they shared with D. melanogaster Toll and mammalian IL-1R imposed suspicion for their involvement in innate immunity. Proof for this suspicion only came when TLR4 was identified as receptor for LPS (5-7). However, TLR4 was found to be a weak binding partner for LPS. Later studies showed that in reality, TLR4 senses formation of the complex of LPS with MD-2 (22, 23). Following the first discovery of TLR4 as LPS receptor, several other members of the TLR family were shown to sense other microbial components and it was eventually demonstrated that there are ten TLRs in human and twelve in mouse.

Heterodimers of TLR2 with TLR1 or TLR6 as well as TLR5 and TLR11 localise to the plasma membrane (**Fig. 1.1**). TLR3, TLR7, TLR8 and TLR9 localise to the intracellular endosomal compartment. Furthermore, TLR4 can be found both at the plasma membrane and in the endosome when activated by LPS.

Ligand recognition by TLRs and downstream signaling

All TLRs evolved to sense specific PAMPs (**Fig. 1.1**). At the plasma membrane, TLR2-TLR1 heterodimers recognize triacylated lipopeptides (24) while the TLR2-TLR6 heterodimers sense diacetylated lipopeptides (25). TLR2 was also shown to sense many other microbial components of diverse natures such as peptidoglycan from gram-positive bacteria, fungal zymosan or hemaglutinin protein from the measles virus (26). TLR5 was shown to sense flagellin, a component of bacterial flagella (27). TLR5 also plays an important role in the regulation of the gut adaptive immunity via activation of TLR5 expressing lamina propria dendritic cells (28). Mouse TLR11 was found to be specifically activated by infection with uropathogenic *Escherichia coli* bacteria although no specific bacterial molecule was identified as ligand for TLR11 (29). It was only later shown that when in complex with TLR12, TLR11 contributes to resistance against *Toxoplasma gondi* by sensing profilin-like proteins (30, 31).

Upon ligand binding by surface TLRs, downstream signal transduction is triggered by the recruitment of TIR-containing adaptor protein myeloid differentiation primary response gene 88 (MyD88). MyD88 associates with TLRs through interaction between TIR domains present in both proteins. In the case of TLR2 and TLR4, recruitment of MyD88 requires prior binding of MyD88 adaptor like (MAL) adaptor protein which also contains a TIR domain (32, 33). Following recruitment of MyD88, several members of the IL-1 receptor associated kinases (IRAK) family, namely IRAK1, IRAK2 and IRAK4, are engaged through interaction of their death-domains with MyD88 and form a large complex called the Myddosome (34). This enables activation of TNF-associated factor 6 (TRAF6), a ubiquitin-ligase able to activate transcription factors nuclear factor-κB (NFκB), activator protein 1 (AP1) and cAMP-responsive-element-binding protein (CREB) via IκB kinase (IKK)-α/β- or mitogen-activated protein kinases (MAPKs)-dependent pathways (35-40). Once activated, these transcription factors promote the expression of pro-inflammatory cytokines such as interleukine-6 (IL-6) and tumor necrosis factor alpha (TNFα).

Interestingly, TLR4 and TLR5 were also shown to trigger downstream signaling independently of MyD88 by recruiting the adaptor protein TIR domain-containing adaptor-inducing IFN-β (TRIF). In the case of TLR4, receptor endocytosis is a pre-requisite for the secretion of type-I IFN (41). TLR4 engages TRIF through interaction with an other TIR-domain containing adaptor protein TRIF-related adaptor molecule (TRAM) (41, 42). Upon ligand binding, TLR5 recruits TRIF in a TRAM-independent

manner (43). Recruitment of TRIF to TLR4 and TLR5 induces activation of TNF-associated factor 3 (TRAF3) followed by engagement of TANK-binding kinase-1 (TBK1) and IKK-ε, which in turn phosphorylate the interferon regulatory factor 3 (IRF3). Phosphorylation enables IRF3 dimerization and translocation to the nucleus where it induces expression of type-I IFN (44-46). Recruitment of TRIF also leads to activation of receptor-interacting protein 1 (RIP1) and further TRAF6-dependent NFκB activation (47).

More TLRs are present in intracellular vesicles called endosomes. Interestingly, all endosomal TLRs were shown to sense microbial nucleic acids. TLR9 was discovered for its ability to sense CpG-rich single stranded DNA (48-51). TLR7 and TLR8 recognize G- and U-rich single stranded RNA (ssRNA) (52-55) and TLR3 is activated by double stranded RNA (56). Finally, mouse TLR13 recognises bacterial 23s ribosomal RNA (rRNA) (57, 58).

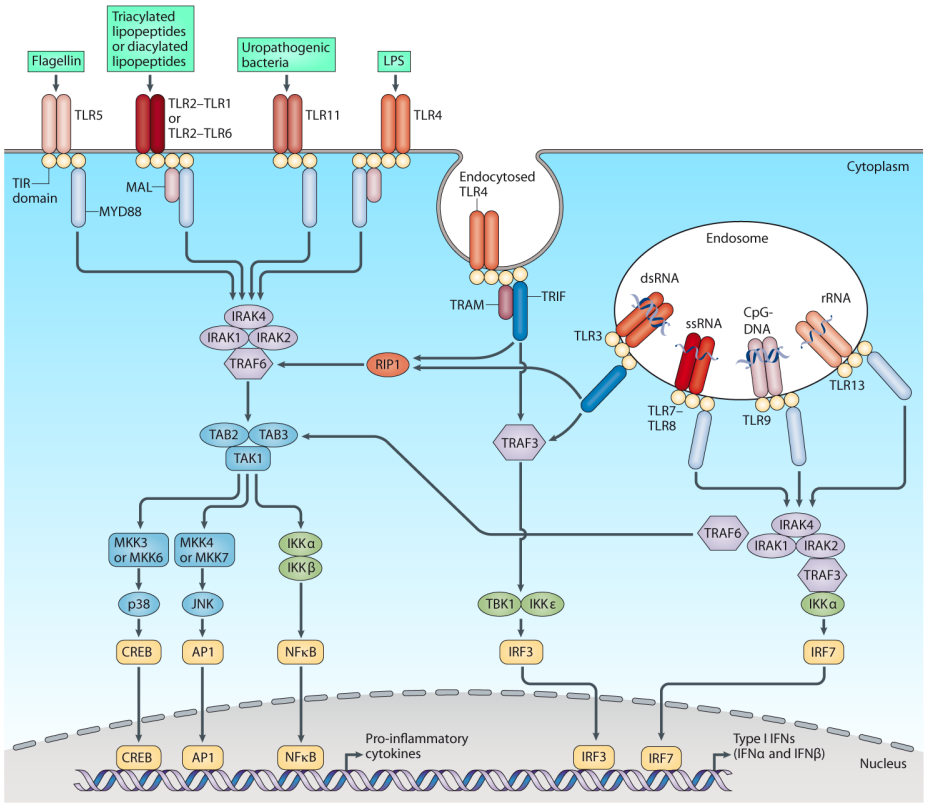

Figure 1.1 Toll-like receptors – Ligands and Signaling.
Upon ligand binding, TLR signaling requires recruitment of adaptor proteins MyD88, MAL, TRIF or TRAM. Downstream of MyD88, formation of the Mydosome complex containing IRAK1, 2 and 4 induce activation of TRAF3 or TRAF6 leading to IRFs-dependent type-I IFN production or NFκB-, AP1- and CREB-dependent pro-inflammatory pathways, respectively. On the other hand, recruitment of TRIF leads to activation of IRF3 and subsequent production of type-I IFN or, through RIP1, leads to TRAF6-dependent pro-inflammatory pathways.
Note: This figure was modified from (16) *and used here with license agreement with the Nature publishing group.*

Once activated, TLR7, TLR8, TLR9 and TLR13 recruit the adaptor proteins MyD88 and after formation of the Myddosome by recruitment of IRAK1, 2 and 4, activate TRAF3. This leads to IKKα-dependent phosphorylation and dimerization of IRF5 and IRF7 (59, 60) and promotes expression of type-I IFN. Upon formation, the Myddosome can also recruit TRAF6 (61), which, as described above, results in NFκB activation followed by up-regulation of pro-inflammatory cytokines expression. In contrast with other endosomal TLRs, TLR3 recruits TRIF (62) and induces activation of IRF3 as well as RIP1-dependent TRAF6 downstream signaling (47, 63).

Modulation of endosomal TLR activation

Recognition of nucleic acids by endosomal TLRs is tightly regulated by several mechanisms that enable maturation of both ligand and receptor as well as co-localisation and interaction in the endo-lysosomal compartment.

Trafficking of endosomal TLRs

Trafficking of endosomal TLRs is a first step for regulation of their function. All TLRs are produced at the membrane of the endoplasmic reticulum (ER) where protein folding was shown to depend on N-glycosylation and binding of the chaperone protein gp96 (64). TLRs from the ER traffic through the Golgi compartment and translocate to the endosome where signaling occurs (65, 66). This mechanism mainly depends on UNC93b1, a trans-membrane protein mostly present in the ER. A mutation in the Unc93b1 gene was shown to abrogate the response of TLR3, TLR7 and TLR9 and was consequently called triple-deficient mutant (3d-mutant) (67). This finding revealed the importance of UNC93b1 for nucleic acid sensing by endosomal TLRs. UNC93b1 was later proposed to regulate trafficking of the TLRs by escorting them to the endosome (68, 69). A recent publications stated that a tyrosine-based sorting motif (YxxΦ) present in UNC93b1 differentially regulates mouse and human endosomal TLRs (70, 71). The YxxΦ motif of human UNC93b1 was shown to interact with adaptor proteins (AP)-1 and AP2, which proved to be crucial for UNC93b1 trafficking to the endosome but seemed to be dispensable for TLR7, TLR8 and TLR9 stimulation, implying that UNC93b1 trafficking to the endosome is dispensable for TLR7-9 to function (71).

Enzymatic maturation of endosomal TLRs

Once trafficked to the endosome, compartment acidification occurring during endosomal maturation is critical for TLR7, TLR8 and TLR9 activation. Indeed, use of endolysosomal maturation inhibitors such as bafilomycin A and chloroquine (both able to disrupt the endolysosome acidification) inhibited sensing of CpG DNA by TLR9 (72, 73), nucleoside analogues by TLR7 and TLR8 (74, 75), and dsRNA by TLR3 (76). Interestingly, in-vitro study of the interactions of TLR9 with ssDNA and TLR3 with dsRNA showed higher affinity when placed in acidic conditions (pH 5.5) (77, 78). Since then, it was demonstrated that upon translocation towards the endolysosome, TLRs are cleaved to produce functional receptors in a process involving several proteases such as cathepsins and asparagine endopeptidase (AEP) (54, 79-81). Interestingly, these lysosomal proteases were already known to depend on acidification and to have an important role in antigen-processing and presentation to cells of the adaptive immune system (82).

TLR3 cleavage was shown to depend on cathepsins B and H (83) and it was soon after proved to be important for sensing of dsRNA (84). This study showed that the cleaved N-terminal fragment (TLR3N) remained associated with the membrane bound fragment (TLR3C) and that both TLR3N and TLR3C were necessary for dsRNA sensing.

Cleavage of TLR9 proved to rely on the collaboration of AEP and cathepsins in a multi-step processing fashion (81, 85, 86). Interestingly, as for TLR3, cleaved N-terminal fragment (TLR9N) was shown to stay associated with TLR9C and the presence of both fragments was necessary for DNA recognition (87). This implied the existence of a conserved common regulation mechanism for endosomal TLRs activation.

Mouse TLR7 cleavage was shown to mainly depend on cathepsins (81). Unsurprisingly, cleaved N-terminal domain of mouse TLR7 (TLR7N) was also found to stay associated with the membrane-bound C-terminal fragment (TLR7C) by formation of a disulfide bond (54). However, unlike mouse TLR7, human TLR7 and TLR8 are cleaved by proprotein convertase of the furin family (88, 89). This protease functions at neutral pH indicating the possible cleavage of TLR7 and TLR8 soon after synthesis. The TLR7N fragment produced by proteolytic processing of TLR7 was then found to remain bound to the TLR7C fragment and to be essential for correct trafficking of TLR7N-C complex to the endosome (90). Moreover, the products of TLR8 cleavage by the combined activity of cathepsins and proprotein convertase

were shown to associate after cleavage (89). However, no evidence for the role of the TLR8N fragment in receptor activation was then provided.

Internalization of nucleic acids

A third regulation process that limits endosomal TLRs activation is the need for nucleic acids to reach the endolysosome where further processing by nucleases enables recognition by the corresponding TLRs. There are several endocytic mechanisms that allow internalization of endogenous or pathogen-derived nucleic acids. Apoptotic cell debris and bacteria are phagocytized, viruses engage different endocytosis pathways while extracellular nucleic acids are internalized by receptor-mediated pathways either directly or opsonized by complexation with protein or phospholipids (**Fig. 1.2**, (91-93)).

Phagocytosis is an active and highly regulated mechanism mostly occurring in the specialised cells of the innate immune system, namely macrophages, granulocytes and dendritic cells. Phagocytosis relies on specific cell surface receptors and is mediated by Rho-family GTPases (94). For phagocytosis initiation, certain cell surface receptors must recognise their ligands to initiate actin polymerization and further membrane remodelling. These receptors include the mannose receptor, the Fc-gamma receptor (FcγR), complement receptors, scavenger receptors and dectin-1. These receptors can bind directly to the target particles as, for example, Dectin-1 receptor, which is known to bind β-glucans at the surface of *Candida albicans* in a mechanism enabling its phagocytosis (95, 96). Phagocytic receptors can also bind to the particles after their opsonization. For example, FcγR binds to IgG antibodies present at the surface of bacteria (97) and engages their phagocytosis.

Viruses enter cells by different mechanism of endocytosis such as macropinocytosis, clathrin-mediated endocytosis and caveolar/lipid-raft-dependent endocytosis. Before internalization, viruses often bind to the cell surface. Binding to the plasma membrane occurs either via interaction with attachment factors or via interaction with specific virus receptors. Attachment factors merely enable virus recruitment at the cell surface. Viruses binding to such proteins use the cell incessant endocytosis mechanisms as entry portal. However, specific virus receptors not only bind viruses to the cell but also induce changes in the virus, trigger cell signaling and internalization. This specificity of binding is an important determinant for cell tropism and species specificity. It also specifies the type of endocytosis used, which is often beneficial for the virus. For example, human immunodeficiency virus 1 (HIV-1) uses

binding of two distinct cell surface receptors inducing conformational change, which enables fusion (98) and internalization via macropinocytosis (99, 100).

After internalization, acidification of the endosomal compartment will not only be critical for maturation of the TLRs but also for the lysis of internalized pathogen thereby liberating the nucleic acids they contain. These will potentiate a TLR-dependent immune response.

Finally, entry of extracellular nucleic acids can be achieved by binding to cell surface receptors such as scavenger receptors, complement receptors and the Fc-receptors. For example, the class A scavenger receptors MARCO and SR-A were shown to bind CpG-DNA and increase their uptake by macrophages (101). SR-A receptor was later shown to bind dsRNA at the surface of human lung epithelial cells (102).

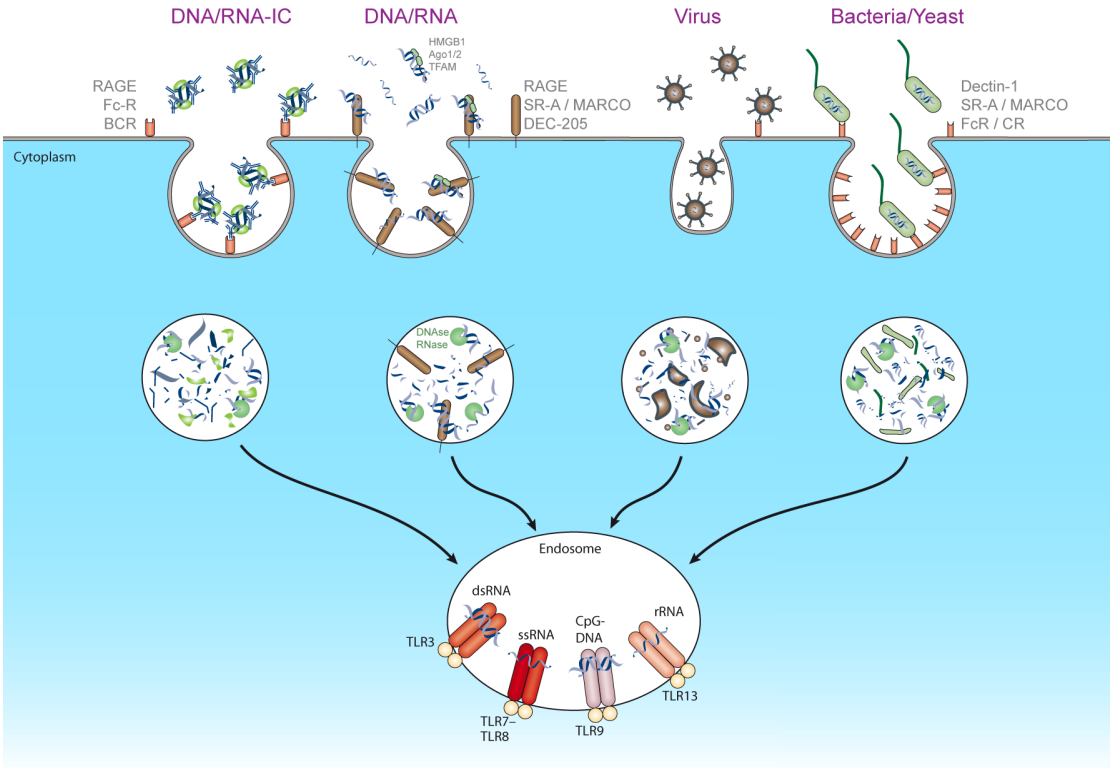

Figure 1.2 Internalization of nucleic acids.
Extracellular nucleic acids can enter cells in different forms. They can be either opsonised in complex with antibodies and nuclear proteins forming immune complexes (IC) which enable their capture by recpetors such as Fc-receptors (FC-R) or B-cell receptor (BCR). Nucleic acids may also be captured directly or complexed with other proteins and lipids and interact with surface proteins such as RAGE, SR-A, MARCO or DEC-205. Finally, nucleic acids can be internalised inside microorganisms such as viruses and bacteria and will require the microorganism proteolysis to be realised and trigger immune response through activation of endosomal TLRs.

A recent study demonstrated that the endocytic receptor DEC-205, expressed at the surface of dendritic cells and B cells, senses extracellular CpG-rich DNA and increases its uptake, thereby facilitating TLR9-dependent DC maturation and B cell activation (9). Moreover, FcγR is known to promote binding and internalization of nucleic acids present inside immune complexes such as found during the development of systemic lupus erythematosus (SLE) (103, 104). In opposition to the role of FcγR in SLE, the complement protein C1q was shown to bind DNA of dying cells promoting their degradation by DNase I (105). This indicated the importance of C1q in down-regulation of immune activation. Interestingly, C1q deficiency is associated with development of SLE (106, 107).

Structure of endosomal TLRs: further clues on activation mechanism

All TLRs are composed of an intracellular TIR-domain, a single trans-membrane domain and an extracellular leucine-rich repeat (LRR) domain. TLR3 has 23 LRRs while TLR7, 8 and 9 possess 26 LRRs. Furthermore, TLR7, TLR8 and TLR9 LRR domains are divided into two separated clusters by a flexible stretch of amino-acids forming a loop between LRR 14 and 15 called the Z-loop. The recent publication of human TLR3, TLR8 and TLR9 crystal structures in complex with their ligands has brought more insight into the mechanisms governing the endosomal TLR activation and provided further evidence for the requirement of their enzymatic processing.

The solved crystals of the extra-cellular domain (ECD) of TLR3 presented a horseshoe-like conformation of its LRR domain (108, 109). Except for one side of the horseshoe, the LRR was mostly masked by N-linked glycosylation. The dsRNA binding site was therefore proposed to lie in the only glycan-free surface. Solving the crystal structure of mouse TLR3 in complex with dsRNA provided the last piece of the puzzle (110). This crystal showed that two TLR3 ECDs dimerize around a molecule of dsRNA. Each TLR3 ECD bound dsRNA at two sites located on opposite ends of the horseshoe. Both TLR3 ECDs interacted with each other at their C-termini thereby improving stability of the complex.

A TLR9 ECD crystal in complex with agonistic and antagonistic DNA was solved very recently and revealed, as for TLR3, a horseshoe-like conformation of the LRR (49). More importantly, this crystal revealed that TLR9 ECD exists as a monomer, which can bind to either agonistic or inhibitory DNA with its N-terminal fragment (LRR 1-10). However, the DNA agonist used not only binds one TLR9 ECD on the N-terminal

fragment but also triggers dimerization by binding to the second TLR9 ECD on its C-terminal fragment. The crystal further showed that while both cleaved and un-cleaved TLR9 bound to DNA, only cleaved ECDs were able to dimerize. This explained the previously mentioned studies demonstrating that TLR9 cleavage was crucial for its activity. Moreover, histidine residues clustered at the DNA-binding interphase, which could explain why acidic conditions are optimal for DNA-binding. Finally, dsDNA and methylated DNA had much weaker binding affinity with TLR9 ECD and reduced dimerization. This is in agreement with previous findings showing that DNA methylation strongly reduces its agonistic activity (51).

Several crystal structures of the TLR8 ECD were recently published, each shedding more light on the TLR8 activation mechanism (53, 111, 112). Similarly to TLR3 and TLR9, crystal structures revealed that TLR8 ECD has a horseshoe-like conformation and can form dimers even in the absence of ligands. The first structure (112) presented the crystal of human TLR8 ECD in complex with small synthetic agonists CL075, CL097 and R848. Interestingly, the ECD dimerization interface approximately localised to the middle of the horseshoe (between LRRs 8 to 18) while C- and N-termini stayed relatively separated (53 Å). Two synthetic molecules bound at two sites of the dimer interface: LRR11 to LRR14 - LRR16* to 18* interface and LRR11* to LRR14* - LRR16 to LRR18 interface. Upon binding, conformational change occurred by rotation of the horseshoe, which induced a rapprochement of the C-termini from 53 Å to 30 Å. The authors concluded that upon ligand binding to full-length TLR8, this rotation movement would lead to closer proximity of the intracellular TIR domains from both dimer partners and, in turn, could mediate downstream signaling. Surprisingly, when trying to solve the crystal structure of TLR8 ECD with real ssRNA (53), the authors found that TLR8 failed to bind to full ssRNA and instead bound to two degradation products: uridine and short UG di-ribonuclotides. Uridine interacted with TLR8 ECD dimers at the same site as previously found for small synthetic molecules (112). UG bound at the concave surface of LRR10 to LRR13 with part of the Z-loop (residues 469 to 474) and therefore seemed to not contribute to the TLR8 ECD dimerization. However, when testing the binding of each component to TLR8 ECD, the authors found that uridine bound to TLR8 with a much weaker affinity than R848. But when in combination with full length RNA, uridine bound to TLR8 with an affinity similar to R848. Therefore, although the second site was dispensable to activate TLR8 upon stimulation with synthetic ligand, it proved to be essential for activation with ssRNA. Furthermore, these crystal structures confirmed that TLR8 cleavage products remain associated and further indicated their contribution to ligand recognition and receptor dimerization.

Up to now, there is no crystal structure of TLR7. However, knowing that both receptor sequences are highly similar and together with the fact that TLR7 and TLR8 likewise sense R848 and ssRNA, it is fair to forecast the TLR7 activation mechanisms to be similar to those of TLR8.

Nucleic acid digestion promotes endosomal TLR activation

The finding that TLR8 senses degradation products of RNA is even more remarkable in the context of two new studies, which showed that TLR9 activity depends on DNase II, the only DNase present in the phago-lysosomal compartment (113, 114). Chan and colleagues showed that DNase II knockout prevented TLR9 activation by CpG-A DNA but had no effect on CpG-B DNA stimulation. CpG-A DNA is larger than CpG-B DNA and forms complex multimeric structures that are DNase II sensitive and promote a strong IFN response in peripheral blood mononuclear cells (PBMCs). On the contrary, CpG-B DNA exists as a linear ssDNA, is resistant to DNase II digestion and only induces a weak IFN but stronger pro-inflammatory cytokine release from PBMCs (115, 116). Knowing the ligand for TLR9 to be ssDNA, it is thus understandable that CpG-A DNA would need to be digested to bind and activate TLR9. Stimulation with a synthetic 11-12mer mimetic of DNase II digestion product, activated conventional dendritic cells (cDCs) even in the absence of DNase II. Moreover, stimulation of cDCs with bacterial DNA, mainly composed of dsDNA, also required DNase II activity. Confirming these results, Pawaria and colleagues reported that TLR9-dependent activation of B cells with DNA-immune complexes required DNase II activity (114). Similarly to CpG-A DNA, DNA-containing immune complexes form large structures that would need prior processing to stimulate TLR9.
Until now, no study pinpointed the actual enzyme(s) responsible for RNA degradation preceding TLR8 activation. However, it is very likely that such an enzymatic process exists that would increase endosomal concentration of uridine and other short sequences potentiating TLR8 activation following previously described structural mechanisms (53).

In summary, activation of endosomal TLRs by specific nucleic acid sequences is a highly regulated process with several checkpoints: nucleic acid ligands need to be internalised and processed, TLRs have to be present in the right compartment and activated by proteolytic cleavage that requires compartment acidification which is also required for stronger ligand-receptor interaction.

1.3 Receptor for advanced glycation end-products (RAGE)

RAGE expression and structure

The *Ager* gene locus coding for the receptor for advanced glycation end-products (RAGE) is located on the reverse strand of chromosome 6 (32,180,968-32,184,324), in close proximity with the genes encoding for TNFα and MHC class III in human and mouse. *Ager* is 3,36 kb long and contains 11 exons, all expressed in the main variant of full-length RAGE. The transcript is 1,492 kb long and codes for a 404 amino acid long protein. RAGE is a type 1 transmembrane protein of the immunoglobulin superfamily. It is composed of three extracellular immunoglobulin-like domains (V, C1, and C2), one trans-membrane domain and a short cytoplasmic domain (**Fig. 1.3**). Gene sequence alignment and structure comparison studies suggested that RAGE appeared in mammals and evolved from a family of cell adhesion molecules (CAMs), with the basal cell adhesion molecule (BCAM) being its closest relative. In agreement with this hypothesis, RAGE still promotes cell spreading and cell-cell adhesion (117).

Up to approximately 20 splice variants of RAGE have been found in human and mouse from which, however, only a minor part are translated (118). Indeed, more than 50% of RAGE splice variant were predicted to follow the non-sense mediated mRNA decay pathway (118). Over all, the two major variants detectable in vivo and that display functions are the membrane bound, full-length RAGE and a soluble variant (RAGE_v1 or esRAGE) resulting from inclusion of part of intron 9 and deletion of exon 10 with a frame-shift before exon 11 creating a unique C-terminal sequence (**Fig. 1.3**).

In physiological conditions, RAGE expression is low in all tissue except for the lung where RAGE is constitutively expressed and localizes to type I epithelial cells (119).

Under certain inflammatory conditions such as cancer, diabetes, chronic inflammation or in neurodegenerative disorders, RAGE expression is increased and can be found in endothelial cells and smooth muscle cells of the vasculature, in neurons and microglial cells of the central nervous system (CNS) as well as in distinct immune cells such as T and B cells, monocytes, dendritic cells and granulocytes (120-130).

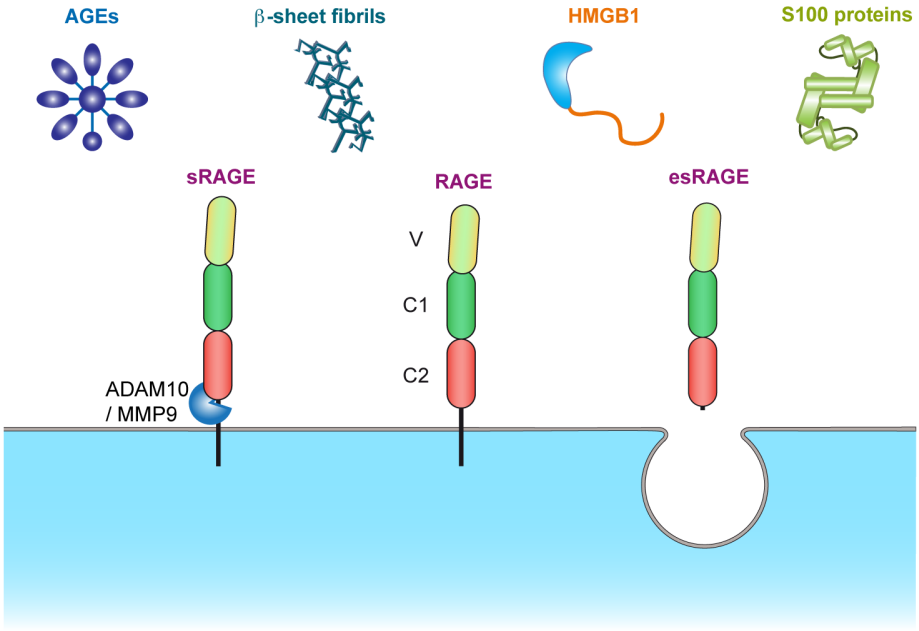

Protein sequence:

```
        10         20         30         40         50         60
MAAGTAVGAW VLVLSLWGAV VGAQNITARI GEPLVLKCKG APKKPPQRLE WKLNTGRTEA V
        70         80         90        100        110        120
WKVLSPQGGG PWDSVARVLP NGSLFLPAVG IQDEGIFRCQ AMNRNGKETK SNYRVRVYQI
       130        140        150        160        170        180
PGKPEIVDSA SELTAGVPNK VGTCVSEGSY PAGTLSWHLD GKPLVPNEKG VSVKEQTRRH C1
       190        200        210        220        230        240
PETGLFTLQS ELMVTPARGG DPRPTFSCSF SPGLPRHRAL RTAPIQPRVW EPVPLEEVQL C2
       250        260        270        280        290        300
VVEPEGGAVA PGGTVTLTCE VPAQPSPQIH WMKDGVPLPL PPSPVLILPE IGPQDQGTYS
       310        320        330        340        350        360
CVATHSSHGP QESRAVSISI IEPGEEGPTA GSVGGSGLGT LALALGILGG LGTAALLIGV
       370        380        390        400
ILWQRRQRRG EERKAPENQE EEEERAELNQ SEEPEAGESS TGGP
```

cDNA exon splicing:

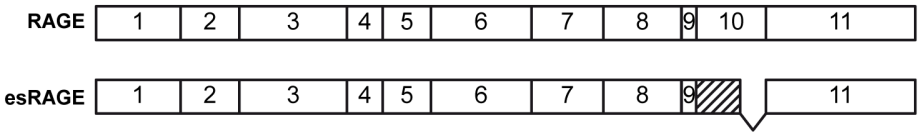

Figure 1.3 RAGE isoforms and ligands.
RAGE possesses three extracellular immunoglobulin-like domains (V, C1 and C2), one transmembrane domain and a short cytosolic tail. Three main RAGE isoforms exist: a membrane-bound full-length isoform (RAGE), a soluble version containing only the extracellular domains resulting from alternative splicing (esRAGE) and another soluble version similar to esRAGE and resulting from surface protein shedding (sRAGE).
Four main RAGE ligand families are represented as cartoons (please see text for more details). The protein sequence of RAGE is indicated with colour coding corresponding to each extracellular domain. Underlined sequence represents predicted binding site for mDia-1. Exon splicing of both RAGE and esRAGE are indicated. Hatched box represents intron 9 inclusion.

Importantly, the promoter region of *Ager* gene was shown to possess binding sites for transcription factors such as NFκB (-1543 and -587 bp) and SP1 (-245 and -40 bp) (125, 131).

Biochemical studies showed that the V- and C1-domains form an independent structural unit separated from the C2-domain by a flexible linker (132). Crystal structure of the V-C1 ectodomains confirmed the structural unit formed by the V and C1 domains with the presence of several interdomain hydrogen bonds and hydrophobic interactions (133, 134). Structure analysis found a highly positively charged surface along both V and C1 domains and predicted this surface to be responsible for binding of mostly negatively charged ligands. Further biochemical and structural studies revealed RAGE ectodomain to exist as a pre-formed tetramer via interaction of V and C1 domains across molecules and which extends to larger oligomers upon ligand binding (135, 136). Several studies found the V-C1 structural unit to be the ligand-binding domain of RAGE with the V-domain being the main contributor to the ligand-receptor interaction (132, 137-142). Only one ligand was found to bind to the C2-domain (S100A6) and was shown to induce cell apoptosis while a similar molecule (S100B) that binds to the V-C1 domain was shown to induce cell proliferation (139).

RAGE: one receptor fits many ligands

The literature suggests that a heterogeneous group of molecules exist as ligands for RAGE (**Fig. 1.3**), including advanced glycation end-products (AGEs) (143), β-sheet fibrils (like amyloid-β) (124), several members of the S100 protein family (140) and the alarmin high mobility group box 1 (HMGB1) (144). This diversity of ligands identified RAGE as a key modulator in the development of pathologies such as diabetes (145, 146), cardiovascular diseases (147, 148), Alzheimer's disease (149), systemic lupus erythematosus (SLE) (150, 151), sterile inflammation and cancer (152).

Advanced Glycation end-products (AGEs)

RAGE was first identified as receptor for advanced glycation end-products (AGEs), the role from which its name originated (143). AGEs are produced by the non-

enzymatic reaction between reducing sugars and proteins, lipids or nucleic acids. AGE formation is enhanced by inflammatory conditions, during renal failure, hyperglycemia or in certain oxidative stress conditions, all of which are often associated with diabetes or aging (153). AGEs can form either locally or more generally. The former is exemplified by joint amyloid, which is composed of AGE-β2-microglobulin and is found in patients with dialysis-induced amyloidosis. RAGE was found to mediate recognition of this type of amyloid by mononuclear phagocytes in the arthritic joint and was shown to promote further monocyte chemotaxis (154). In diabetes, the presence of RAGE and AGEs is found to be increased in the vasculature and other tissues (155). Interaction of AGEs with RAGE at the surface of endothelial cells was shown to induce expression of vascular cell adhesion molecule-1 (VCAM-1), an adhesion molecule that mediates early stages of atherosclerosis by recruiting peripheral blood cells (148, 156). This adds to the intrinsic adhesion function of RAGE and argues for RAGE as an important mediator of immune cell chemotaxis in early stages of inflammation.

Amyloid- β (Aβ)

RAGE expression is increased during development of neurodegenerative diseases and localizes to the site of senile plaques in neurons, microglia and endothelial cells (124, 157, 158). Interestingly, RAGE was found as one major cell surface binding protein for amyloid-β (Aβ) (124, 159). Aβ originates from the cleavage of the transmembrane β-amyloid precursor protein (APP) leading to the generation of 40 or 42 amino acids long Aβ, which can form soluble oligomers, beta sheets containing fibrils, and insoluble aggregates. When accumulating in the brain tissue, Aβ induces cell inflammation, neuronal cell death and extended neurodegeneration. RAGE was shown to mediate internalization of Aβ by neurons and to promote pro-inflammatory signaling in neurons and microglia, thereby contributing to synaptic dysfunction, general neuroinflammation and Aβ accumulation (160-162). Confirming these results, blockade of RAGE prevented Aβ aggregates-induced neurotoxicity (137). It is also worth noting that RAGE was shown to mediate the transport of Aβ across the blood-brain barrier and promoted Aβ accumulation in the brain (163, 164).
As mentioned previously, RAGE can bind to other types of amyloid fibrils such as those found in the joints of long-term hemodialysis patients (154).

S100 protein family

Members of the calcium ion binding S100 protein family have proved to be important cytosolic mediators of several cellular processes such as calcium homeostasis, energy metabolism, cell growth and differentiation (165). However, some S100 proteins have been shown to be secreted in a multitude of pathological conditions such as cancer (139, 166-169), myocardial injuries (170, 171) and airway diseases (172). Interestingly, most extracellular functions of S100 proteins seem to be occurring through RAGE although they induce different outcomes depending on the cells targeted. S100B was shown to promote neuron survival and neurite outgrowth, S100A6 promotes a RAGE-dependent production of reactive oxygen species (ROS) and apoptosis (139). Like S100B, S100A11, once secreted from cancerous keratinocytes, was found to signal through RAGE to promote cell survival and proliferation (167). Similarly, S100P was shown to promote cell survival and proliferation through RAGE in colon cancer (169, 173). S100A8/A9 heterocomplex was found to promote RAGE-mediated tumor cells growth (174) or endotoxin-induced cardiomyocytes dysfunction (171). S100A7 was shown to have chemotactic function towards granulocytes and this depended on RAGE (175). Finally, S100A12 sensed by RAGE induces production of mucin in the respiratory tract, thereby promoting chronic airway diseases such as severe asthma (172).

High mobility group box-1 (HMGB1)

High mobility group box-1 (HMGB1) is one of the most important but also most complex ligands of RAGE. HMGB1 binding to RAGE was demonstrated shortly after RAGE discovery (144) and RAGE proved to mediate the previously described role of HMGB1 in neurite outgrowth during the development of the nervous system (144, 176). HMGB1 was first described for its role in the nucleus where it binds to DNA and thereby regulates chromatin structure and gene expression (177-179). A few years later, HMGB1 was shown to be actively secreted by macrophages and monocytes stimulated with LPS (180-182) or by necrotic cells promoting inflammation through activation of monocytes (183). Similarly to some S100 proteins, extracellular HMGB1 was shown to act as chemoattractant for myeloid cells (184), smooth muscle cells (185) and mesangioblasts thereby promoting muscle tissue repair (186). In DCs,

HMGB1 release and sensing by RAGE was shown to be critical for homing to the lymph nodes and further cross-activation of T lymphocytes (128-130). In endothelial cells, HMGB1 was further shown to promote expression of RAGE and surface adhesion proteins (ICAM-1 and VCAM-1) as well as inducing RAGE-dependent cytokine production (187-189). A further role of RAGE in extracellular HMGB1 sensing was recently found in the context of sterile injury. HMGB1, originating from a brain injury, signaled through RAGE in the lung mediating pulmonary dysfunction after lung transplantation (190, 191). Interestingly, microglial-expressed RAGE had also shown to mediate part of HMGB1 deleterious function in the ischemic brain (192).

Fueling the complexity of HMGB1 biology, HMGB1 was found to form complexes with cytokines and immune-stimulatory molecules exacerbating their activity (193). Interestingly, in immune complexes, HMGB1 was found to bind to DNA increasing TLR9 activation through a RAGE-dependent DNA internalization mechanism (126, 194). Furthermore, oxidation states of released HMGB1 showed to be mutually exclusive and gave HMGB1 either pro-inflammatory and pro-survival function or chemotactic and pro-apoptotic properties (195, 196). For example, reduced HMGB1 secreted by cancer cells during anti-cancer treatment bound to RAGE and through induction of autophagy promoted local cell survival. However, stimulation with oxidized HMGB1 induced cell apoptosis (197).

RAGE signaling

As described earlier, RAGE engages many ligands and is expressed in a rather large array of cell types and tissues. It is therefore not surprising for RAGE signaling to be complex and devoid of a general scheme that could be applied to every circumstance (198). It seems clear that many factors influence RAGE downstream signaling including the cell type studied, the activating ligand and the presence of other co-receptors. As previously underlined with the description of RAGE ligands, a large variety of outcomes derive from RAGE signaling**,** namely cell maturation, proliferation, migration, autophagy, apoptosis and inflammation (**Fig. 1.4**).

One factor that seems to modulate many signals downstream of RAGE is mammalian Diaphanous-related formin 1 (mDia1). mDia1 is a cytosolic protein and member of the formin protein family, which modulates actin and microtubule

polymerization and thereby controls cell migration and division. mDia1 binds to the cytoplasmic domain of RAGE via interaction between the formin homology domain 1 (FH1) of mDia1 and RAGE amino-acids 364 to 368 (QRRQ, see **Fig. 1.3**) (199, 200). mDia1 is essential for activation of Rho-family GTPases downstream of RAGE. In several cell types, the Rho-family GTPases Ras-related C3 botulinum toxin substrate 1 (Rac-1) and cell division control protein 42 (Cdc42) become activated by RAGE (199, 201, 202). Indeed, once phosphorylated by the non-receptor tyrosine kinase Src (GTP-bound form), Rac-1 and Cdc42 activate the serine/threonine kinase PKB leading to activation of NFκB (202). Via activation of the serine/threonine c-Jun N-terminal kinases (JNK), Rac-1 also induces activation of AP-1 (202).

Moreover, through NADPH oxidase 1 (NOX1)-dependent ROS production, Src and Rac-1 activate the PI3K, PKB and GSK3β phosphorylation cascade leading to increased cell migration and vascular repair (201).

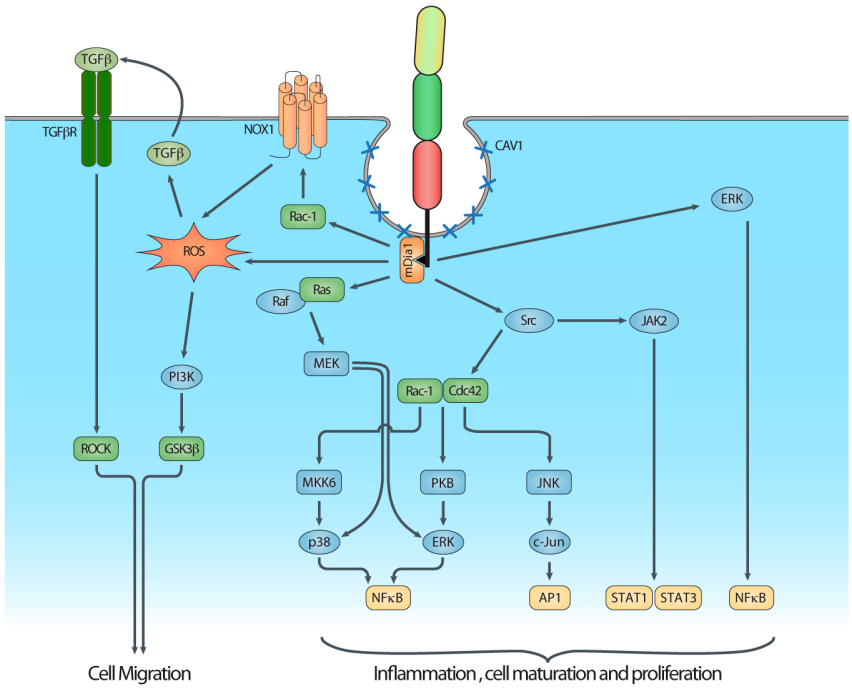

Figure 1.4 RAGE signaling.
Upon binding of certain ligands, RAGE downstream signaling involves caveolin (CAV-1)-dependent internalization and recruitment of the adaptor mDia-1. This leads to activation of Ras, Rac-1 and Cdc42 Rho-family GTPases, which will lead to MAP kinase- and c-Jun kinase-dependent phosphorylation cascade. Activation of p38, ERK and c-Jun will trigger activation of NFκB and AP-1 transcription factors. Together with activation of the JAK/STAT pathway, these will increase expression of pro-inflammatory and cell proliferation genes. RAGE activation also leads to ROS production and promotes cell migration through PI3 kinase- or TGFβ-dependent pathways.
This cartoon represents only the main pathways known for RAGE downstream signaling and is non-exhaustive.

ROS-induced cell migration following RAGE activation was also suggested to occur through up-regulation of TGF-β expression leading to increased activation of its putative receptor TGF-βR and further signaling through RohA and ROCK (203, 204). A similar mechanism involving the Ras GTPase has also been found downstream of RAGE. Upon activation, Ras engages MAPK/ERK kinase (MEK), further triggering ERK1/2- and p38 MAPK-dependent NFκB activation (205-207). However, there is also evidence for the direct binding of ERK1/2 with RAGE cytosolic domain indicating a possible Cdc42/Rac-1/Ras independent RAGE signaling (208). Furthermore, a study revealed the possible HMGB1-induced activation of p38 MAPK downstream of Rac1/Cdc42 pathways, which requires prior activation of MKK6 (209).
Moreover, upon ligand binding, RAGE was shown to mediate activation of Janus kinase 2 (JAK2) leading to phosphorylation of signal transducer and activator of transcription 1 (STAT1) and STAT3 and their translocation to the nucleus (210, 211).

Regulation of RAGE function

The first regulation mechanism that controls RAGE activity depends on post-translational modification. Indeed, RAGE possesses two N-glycosylation site, (Asn25 and Asn81) that seem to promote ligand binding to RAGE. In fact, S100A12 binding to RAGE was shown to be promoted by N-glycan (212). Moreover, study of a single nucleotide polymorphism (SNP) showed that the G82S mutation induced by the SNP led to an increased in N-glycosylation of Asn81, which increased binding of S100B to mutant RAGE (213). This further comforted the idea that N-glycosylation of the RAGE ectodomain is important for ligand binding.
Post-translational shedding of RAGE from the cell surface triggers negative regulation of RAGE. Metalloproteinases ADAM10 and MMP9 were shown to cleave RAGE extra-cellular domain in close proximity to the plasma membrane leading to the release of a soluble form of RAGE (sRAGE) containing all Ig-like domains (**Fig. 1.3,** (214, 215)). Shedding could be induced by PMA in a protein kinase-C (PKC) dependent manner (215). Further studies showed that RAGE shedding could be induced by increased Ca^{2+} levels (induced by ionomycin treatment) (216). Moreover, activation of several G protein-coupled receptors (GPCRs) was later found to promote RAGE shedding by ADAM10 and MMP9 (217).

Soluble RAGE not only regulates full-length RAGE activity by decreasing the proportion of membrane-bound and therefore signaling-competent RAGE. In fact, production of soluble RAGE, that is either by alternative splicing (esRAGE) or by shedding (sRAGE), procures a source of decoy receptor capable of ligand binding but unable to induce signaling. The level of soluble RAGE has been proposed as both a biomarker in many pathological conditions and as pharmacological tool that could be used to reduce RAGE effects in disease development (218, 219). This fits with the previous use of purified RAGE ectodomain as inhibitor for RAGE, which induced a dramatic reduction of tumor growth (123). A noteworthy study showed that esRAGE antagonizes tumorigenesis (220). Moreover, Koch and colleagues proposed an additional mechanism by which soluble RAGE could inhibit signaling (133). They predicted that the presence of soluble RAGE in the extracellular milieu could interfere with the oligomerization necessary for RAGE activation. As previously described, RAGE exists as an oligomer in the absence of ligand. It is however believed that upon ligand binding, the increasing size of RAGE oligomers would be responsible for signaling by a clustering of the intracellular domains. Formation of heterodimers of membrane-bound RAGE with soluble RAGE would thus decrease clustering of the intracellular domain and therefore inhibit signaling.

Furthermore, RAGE translocation to the plasma membrane was shown to be modulated in endothelial cells. Frommhold and colleagues showed by immuno-histochemistry that, upon trauma-induced inflammation, RAGE was rapidly (20 minutes) translocated to the cell surface (221, 222). Similar results could be found upon TNFα stimulation (222). This translocation of RAGE to the cell surface happened within only a few minutes, which led the authors to predict the presence of readily available intra-cellular storage of RAGE in endothelial cells.

There is also some evidence for a requirement of RAGE internalization prior to signaling. This would not be uncommon. In fact, receptor endocytosis as a mechanism enabling signaling has been known for some time to be important for many cell surface receptors (223). Interestingly, RAGE internalization upon ligand binding was shown to be important for transduction of ERK-dependent signaling (224). Confirming these findings, diaphanous-related formins are known to be essential for actin remodeling during formation of cell membrane filopodia and help endosomal mobility (225). Further evidence for RAGE internalization is the fact that RAGE interacts with an important component of caveolae, namely caveolin-1 (Cav-1) (226). In fact, in smooth muscle cells, ligand binding to RAGE induced a Cav-1 and

Src-dependent ERK1/2 and p38 MAPK activation leading to NFκB nuclear translocation and further induction of IL-6 expression (226). RAGE-dependent STAT3 activation was also dependent on Src activation and intact caveloa (226). This is in agreement with a study showing that, upon treatment of Schwann cells with anti-RAGE antibodies, RAGE recycles in a Cav-1/Src dependent manner (227). It is also worth noting that this work showed that internalized RAGE could encounter endogenous RAGE ligand, S100B, and following recycling to the plasma membrane, would promote S100B secretion.

Together, this data suggests that RAGE binds ligands at the cell surface and further triggers their uptake, via caveolae, into intracellular compartment where signaling occurs.

1.4 Project rationale and thesis aims

Nucleic acids of microbial origins have been extensively studied for their role in sensing of infection by the host immune system. They are now under special scrutiny. Indeed, when originating from the organism itself, nucleic acids function as danger signals. In normal conditions, they promote tissue repair but they can also be deleterious when the immune system fails to regulate itself and engages into auto-immunity. While several origins exist for extra-cellular nucleic acids, their sensing is limited to the endosomal TLRs. However, how such extra-cellular nucleic acids are internalized before further activation of their putative receptors is only poorly understood.

The first hint of a function of RAGE in nucleic acid sensing came from the work of collaborators who demonstrated the importance of RAGE as a transporter of DNA/HMGB1 complex towards TLR9 (126). While undertaking collaborative work for this publication, Dr. Cherilyn M. Sirois and Prof. Eicke Latz found for the first time that RAGE could bind directly to stimulatory DNA. This discovery was the first milestone for a project aiming to evaluate the role of RAGE in DNA internalization and trafficking towards the endosome and TLR9. This project produced a publication, which was the fruit of a collaborative effort (228). The results presented in the first part of this thesis briefly summarize the most important discoveries presented by this publication and mainly focus on the work done by the author of the present thesis. This work aimed at evaluating the effect of RAGE expression on the TLR9-

dependent immune activation following extracellular stimulation with CpG-rich DNA and to investigate a possible interaction between RAGE and TLR9 in these settings.

The results presented in the second section of this thesis ask whether RAGE also affects RNA sensing. Several aims emerged, each bringing answers to this question. First, biochemical experiments aimed at confirming the possible interaction of RNA with RAGE ectodomain. Ensuing work further investigated the biological influence of RAGE expression on the recruitment of RNA to the plasma membrane and its subsequent internalization. Furthermore, gain and loss of function studies examined the role of RAGE in the immune activation induced by extracellular stimulation with TLR3, TLR7, TLR8 or TLR13 specific RNA agonists. Finally, experiments were designed to further comprehend the cellular mechanisms involved in RAGE-RNA complex internalization and considered the possible induction of direct RAGE signaling downstream of RNA binding.

The work described in this thesis presents nucleic acids as new ligands for RAGE and helps with the general understanding of RAGE function in the development of pathologies involving extracellular nucleic acids such as SLE. This work further calls for evaluation of nucleic acid as pharmaceutical therapeutic to combat or prevent development of such deleterious pathologies. This thesis also opens the way for further investigation into the role of RAGE in other functions entrusted to nucleic acids in the extra-cellular milieu.

2. Materials and Methods

2.1 Materials

List of instruments

Instrument Name	**Company**
Aria flow cell sorter	BD
Centrifuge 5424, for 1.5 mL tubes	Eppendorf
Rotor: FA-45-24-11	
Centrifuge 5810 R, for 15/50 mL tubes and 96 well plates	Eppendorf
Rotor: A-4-81 & F-34-6-38	
Chilling Jar, freezing container	True North
Cooling centrifuge 5430 R, for 1.5 mL tubes	Eppendorf
Rotor: FA-45-24-11 Kit	
DMIL LED, tissue culture microscope	Leica
EV202, electrophoresis power supply	Consort
EV243, electrophoresis power supply	Consort
Fortessa flow cytometer	BD
L2, L20, L200, L1000 micropipettes (0.1µL to 1mL)	Rainin
MACSmix tube rotator	Miltenyi
Mr. Frosty, freezing container	Nalgene
NN-E245W, microwave oven	Panasonic
Novex mini cell, gel electrophoresis chamber	Life technologies
Odyssey Western-Blot scanner	LICOR
Pipet boy acu, pipetting device	Integra Biosciences
PS304 Minipac II, electrophoresis power supply	APELEX
Quant 6, qPCR cycler	Life Technologies
SpectraMax i3, multi-function plate reader	Molecular Devices
TALI, cell counter	Life Technologies
TCS SP5, Confocal microscope	Leica
VersaDoc 4000 MP fluorescent gel scanner	BioRad
Xcell II Blot Module, blotting chamber	Life technologies

List of plastic apparatus and consumables

Product Name	**Company**
0.45 µm filters, 0.22 µm filters	Merck Millipore
1.5 mL Tubes	Eppendorf
14 mL tubes for bacteria MiniPrep culture	VWR
15 mL and 50 mL Tubes	Greiner bio-one
2 mL Tubes	Sarstedt
5 mL, 10 mL and 25 mL serological pipettes	Greiner bio-one
96 well ELISA plates	Nunc
96 wells plates for cell culture	Greiner bio-one
Cell strainer (70 µm)	VWR
MaxiSorp 96-well ELISA plate	Nunc
Needles	Braun Meslungen
Pipette tips filtered and unfiltered	Rainin
Syringes	BD Bioscience
T175 Tissue culture flask	Greiner bio-one
T75 Tissue culture flask	Greiner bio-one
U-shape white 96 wells plate	Costar
V-shape 96 wells plate	Greiner bio-one

List of Kits and Reagents

Product Name	**Company**
4-12% NuPAGE Bis-Tris gels 1.5 mm, 10 well/15 well	Life Technologies
Agarose	Biozym
Ampicillin	Sigma Aldrich
Benzonase nuclease	Sigma
Bichoninic acid (BCA) assay	Thermo Scientific
Bovine serum albumin (BSA)	Roth
Coelenterazine	Promega
Complete protease inhibitor	Roche
Cytochalasin D	Sigma Aldrich
DRAQ5	eBioscience
Dulbecco's Modified Eagle Medium (DMEM), high glucose,	Life Technologies

with glutamine	
Dulbecco's Phosphate Buffered Saline (DPBS)	Life Technologies
Dynabeads Protein A	Life Technologies
Dynabeads Streptavidin	Life Technologies
Dynasor	Sigma Aldrich
ELISA substrate solutions	BD Bioscience
Erythrocyte lysis buffer	Miltenyi
Ethidium bromide	Sigma Aldrich
Ethylenediaminetetraacetic acid (EDTA*, 0.5 M, pH 8.0*)	Life Technologies
GeneJuice	Merck Millipore
Glycerol	Merck
Human IL-8 ELISA	BD Biosciences
Isopropanol	Roth
LB Agar (Lennox L agar, *10 g Peptone 140, 5 g Yeast Extract, 5 g NaCl, 12 g Agar per 1 L*)	Life Technologies
LB Medium (Luria/Miller, *10 g Tryptone, 10 g Yeast Extract, 10 g NaCl per 1 L*)	Roth
LDS sample buffer (*4x, 8% LDS, 40% glycerol, 2.04 mM EDTA, 0.88 mM SERVA Blue G, 0.7 mM Phenol Red, 564 mM Tris, pH 8.5*)	Life Technologies
Methanol	Roth
MOPS buffer (*20x, 50 mM MOPS, 50 mM Tris 0.1% SDS, 1 mM EDTA, pH 7.7*)	Life Technologies
Mouse IL-6 HTRF kit	Cisbio
Mouse TNFα HTRF kit	Cisbio
NaCl	Roth
Nonidet P-40	AppliChem
Passive lysis buffer (5x)	Promega
PCR master mix (2x)	Fermentas
Phenylmethylsulfonyl fluoride (PMSF)	Roth
Phosphate Buffer Saline (PBS, 10x)	Pan Biotech
Poly-L-lysine solution (0.01% m/v)	Sigma Aldrich
Polyvinylidene fluoride (PVDF) membrane, Immobilon-FL	Merck Millipore
PureLink Quick Gel Extraction Kit	Life Technologies
PureLink Quick Plasmid Maxiprep Kit	Life Technologies
PureLink Quick Plasmid Miniprep Kit	Life Technologies

Reducing agent (*10x, 500 mM dithiothreitol in stabilized form*)	Life Technologies
Restriction enzymes (FastDigest NotI, AscI, MreI)	Fermentas
RNeasy Plus Mini Kit	Qiagen
RPMI-1640 high glucose, with glutamine	Life Technologies
SecinH3	Tocris
Sodium dodecyl sulfate (SDS)	Sigma Aldrich
SteadyGlow	Promega
StemPro Accutase	Life Technologies
T4 DNA Ligase, HC	Fermentas
Tris Acetate EDTA (TAE) pH 8,5 (*50x, 2M Tris, 1M acetic acid, 50mM EDTA*)	Roth
Tris Buffer Saline (TBS, *10x, 400 mM Tris, 3 M NaCl, pH 7.4*)	Santa Cruz
Tris HCl pH 7.4 (*1M stock*)	Roth
Tris-Glycine (*10x, 0.25M Tris, 1.92M glycine, pH 8.5*)	Thermo Scientific
Triton X-100	Roth
Trypan-Blue, dead cell staining	Sigma Aldrich
Trypsin-EDTA (0.05%)	Life Technologies
Tween 20	Roth
β-mercaptoethanol	Sigma Aldrich

List of antibodies

Antibody Target	**Host**	**Company**	**Cat. Number**
GFP (Aequorea victoria)	Rabbit	Life Technologies	A11122
human RAGE	Mouse	Merck Millipore	MAB5328
human TLR9	Rat	eBioscience	14-9099-82
TagRFP	Rabbit	Evrogen	AB233
human β-actin	Rabbit	LICOR	926-42210

List of primers and DNA sequences

Name	**Cloning primer sequence**
R790	5′-TTTGGCGCGCCTGCCACCATGGCAGCCGGAACAGCAGTTGG-3′
R791	5′-AAAGCGGCCGCTCACCGCCTTTGCCACAAGATGAC-3′
R792	5′-AAAGCGGCCGCTCAAGGCCCTCCAGTACTACTCTC-3′

R1107	5′-TTTTGGCGCGCCTGCCACCATGG-3′
R1108	5′-TTTTGCGGCCGCAGGCCCTCCAGTACTACTCTCGCC-3′
R1161	5′-GGACCGATCCAGCCTCCGCG-3′
R1162	5′-ACCTACTACTGCCCCCCACAGAC-3′
R1163	5′-CTGTGGGGGGCAGTAGTAGGTCCCCGTGTCTGGGAGCCTGTG-3′
R1164	5′-TTTGCGGCCGCTCAAGGCCCTCC-3′

Name	**qPCR primer sequence**
Ager – forward	5′-AGAACATCACAGCCCGGATT-3′
Ager – reverse	5′-TTCCTGTGTTCAGTTTCCAT-3′
Tlr4 – forward	5′-AGCCATTGCTGCCAACATCA-3′
Tlr4 – reverse	5′-GCCAGAGCTACTCAGAAAC-3′
Tlr9 – forward	5′-TGAGCCACACCAACATCCTG-3′
Tlr9 – reverse	5′-GTCACCTTCACCGCTCCTGT-3′
Tlr13 – forward	5′-TGTCTGCTCTGGTGGACTTG-3′
Tlr13 – reverse	5′-GAGGAGTGAAGGCGTCTTTG-3′
Hprt – forward	5′-TGAAGTACTCATTATAGTCAAGGGCA-3′
Hprt – reverse	5′-CTGGTGAAAAGGACCTCTCG-3′

Name	**Stimulatory RNA and DNA sequences**
TLR7-RNA	5′-ACUG1CG1AG1CUU-X-UUCG1AG1CG1UCA-5′
TLR8-RNA	5′-YUGCUGCCUUUG-X-GUUUCCGUCGUY-5′
TLR3-RNA	5′-CAAGGCAAGCAUUCG$(C)_{35}$-3′
	5′-CGAAUGCUUGCCUUG$(I)_{35}$-3′
Sa19-RNA	5′-GGACGGAAAGACCCCGUGG-3′
NS-RNA	5′-AAAAAAAAAAA-Z-AAAAAAAAAAA-5′
2006-DNA	5′-TCGTCGTTTTGTCGTTTTGTCGTT-3′
2137-DNA	5′-TGCTGCTTTTGTGCTTTTGTGCTT-3′
1826-DNA	5′-TCCATGACGTTCCTGACGTT-3′

Note: TLR7-, TLR8-, TLR3- and NS-RNA oligoribonucleotides were synthesised and generously provided by Idera Pharmaceuticals.
G1 is 7-deazaguanosine, X is 1,2,3-propanetriol, Y is 1,3-propanediol and Z is a glycerol linker. Underlined sequences define complementary sequences.

Solutions

Name	Buffer protocol
1x RIPA lysis buffer	For 10 mL: 5 ml 2x RIPA lysis buffer stock, 4.6 mL ddH_2O, 0.4 mL 25x complete protease inhibitor, 5 µL 100 µM PMSF.
1x TBS (-T)	For 1L: dilute 50 mL 20x TBS buffer in 950 mL double distilled H_2O (ddH_2O). Final concentration: 20 mM Tris, 150 mM NaCl, pH 7.4. **Note**: for TBS-T, add 1mL Tween 20 (0.1% v/v)
2x RIPA lysis buffer stock	For 500 mL: 2.4 g Tris base, 8.8 g NaCl, 2 mL 0.5 M EDTA, 10 mL Triton X-100, 1 g SDS, 100 mL, 450 mL ddH_2O; pH to 7.4; adjust volume to 500 mL and filter through 0.2 µm filter.
Complete DMEM culture medium	Purchased DMEM medium was completed with 10% fetal calf serum (FCS), 100U/mL penicillin and 100µg/mL streptomycin
Complete RPMI culture medium	Purchased RPMI-1640 medium was completed with 10% fetal calf serum (FCS), 100U/mL penicillin and 100µg/mL streptomycin
ELISA diluent	For 50 mL: dilute 5 ml FBS in 45 mL PBS.
ELISA IL-8 capture buffer	For 1L: 7.13 g $NaHCO_3$, 1.59 g Na_2CO_3; add 750 mL ddH_2O; pH to 9.5 with 10N NaOH; adjust volume to 1L and store at 4ºC.
EMSA assay buffer	For 50 mL: mix 0.44g NaCl, 2.5 mL 1M Tris pH7.4 and 5 mL glycerol. Adjust to 50 mL with ddH_2O. Final concentration: 150 mM NaCl, 50 mM Tris pH7.4, 10% glycerol
Glycine-methanol transfer buffer	For 1L: 10 mL 10x Tris-Glycine buffer, 150 mL methanol, 840 mL ddH_2O; store at 4ºC. Final concentration: 25 mM Tris, 192 mM glycine, 15% methanol (v/v).
MOPS running buffer	For 1L: dilute 50 mL 20x MOPS buffer in 950 mL ddH2O. Final concentration: 2.5 mM MOPS, 2.5 mM Tris, 0.005% SDS, 0.05 mM EDTA, pH 7.7
TBS - 3% BSA	For 500 mL: 15 g BSA, 25 mL 20x TBS buffer, adjust to 500 mL with ddH_2O; mix until completely dissolved; filter through 0.2 µm filter and store at 4ºC.
Tween-TBS - 3% BSA	For 500 mL: 15 g BSA, 25 mL 20x TBS buffer, 500 µL Tween 20, adjust to 500 mL with ddH_2O; mix until completely dissolved; filter through 0.2 µm filter and store at 4ºC.

2.2 Methods

Cloning strategy

For all cloning experiments, primers were synthesised by Metabion. PCR mix was purchased in a pre-mixed form containing the Taq DNA polymerase. General PCR program was as follows (unless specifically stipulated):

- *Step 1*: 94ºC - 60s
- *Step 2*: 94ºC - 30s
- *Step 3*: 65ºC - 60s
- *Step 4*: 72ºC - 60s/kb

x35

- *Step 5*: 72ºC - 120s

Design of full-length RAGE coding pRP plasmid – *Escherichia coli* bacteria containing the *Ager* coding sequence (gene bank number: DQ896821) in a pLenti plasmid (Precision Lenti-ORF library, GE Dharmacon) were cultured for 16h in 7mL LB medium supplemented with ampicillin (0.1mg/mL). Plasmid DNA was then purified using the PureLink Miniprep kit following manufacturer's protocol. *Ager* coding sequence was extracted by PCR using primer pair R790/R792. This enabled not only extraction of the *Ager* coding sequence but also addition of a 5' AscI and a 3' NotI restriction sites. PCR product was directly purified using the PureLink Quick Gel Extraction kit and digested with FastDigest AscI and NotI restriction enzymes. pRP plasmid was also digested using the same restriction enzymes (please refer to annex 7.1 for pRP plasmid sequence). Restriction products were subsequently electrophoresed in a 1% agarose gel containing ethidium bromide for DNA staining and run in 1x TAE buffer at 100V for approximately 20 min. Bands corresponding to either *Ager* or opened pRP plasmid were isolated and DNA was purified using PureLink Quick Gel Extraction kit. *Ager* coding sequence was inserted into pRP plasmid by incubating both purified *Ager* insert and opened pRP plasmid together with T4 DNA Ligase for 30 min at 22ºC.

Design of cytosolic domain truncated RAGE coding pRP plasmid - *Ager* coding sequence was extracted from the Precision Lenti-ORF plasmid by PCR using primer pair R790/R791. This enabled extraction of *Ager* coding sequence until the start of

the cytoplasmic domain and addition of a 5' AscI and a 3' NotI restriction sites. PCR product was then processed as described for the full-length *Ager* sequence.

Design of RAGE-colour coding pRP plasmid – *Ager* coding sequence was extracted by PCR using the previously described full length RAGE pRP plasmid as DNA template and R1107/R1108 primers. This enabled extraction of *Ager* sequence between AscI-NotI restriction sites without the 3' end stop codon. PCR product as well as pRP plasmid were then digested with AscI and NotI restriction enzymes. Insert was ligated into opened pRP plasmid by incubation with T4 DNA Ligase for 30 min at 22ºC. TagRFP or mCitrin color coding sequences were obtained by digestion of already existing plasmids with NotI and MreI FastDigest restriction enzymes. pRP plasmid containing *Ager* coding sequence with deleted stop codon was also digested using NotI/MreI restriction enzymes. Digested insert and plasmid were loaded on a 1% agarose gel. Bands were isolated and gel-purified as described above. TagRFP and mCitrin sequences were then inserted in 3' of the *Ager* coding sequence by incubation of insert and plasmid with T4 DNA Ligase for 30 min at 22ºC.

Design of V-C1 domain truncated RAGE-color coding pRP plasmid – Sequence coding for *Ager* membrane localization signal was extracted by PCR using full-length *Ager* plasmid (described above) as DNA template with R1161/R1162 primer pair. This added a 3'-end sequence corresponding to the start of RAGE C2 domain. *Ager* coding sequence from the C2 domain (in 5') down to the 3' NotI restriction site was extracted by PCR using R1163/R1164 primer pair. This enabled addition of a 5' sequence corresponding to the 3' end of RAGE membrane localization signal. Products from both PCR were purified as described previously. Purified PCR products were then mixed and complementary sequences were annealed for 5 cycles in absence of primers. Double strand was then completed on both side of annealed sequences with added primers R1161 and R1164 for another 30 cycles. PCR product was subsequently digested with FastDigest AscI and NotI restriction enzymes, loaded onto a 1% agarose gel containing ethidium bromide and isolated band were gel purified as described before. Insert was finally ligated into AscI-NotI opened pRP plasmid containing either TagRFP or mCitrin fluorescent proteins coding sequences by incubation with T4 DNA Ligase for 30 min at 22ºC.

After ligation, all plasmids were transformed into DH5α competent *Escherichia coli* bacteria: 15µL competent bacteria were incubated on ice for 30 min with 3 µL ligation mix. DNA-bacteria mix was then incubated for exactly 1 min at 42ºC directly followed

by 2 min on ice. Bacteria were further resupended with 300 µL LB medium and incubated at 37ºC for 1h. 100 µL bacteria suspension was spread onto an LB agar plate containing ampicillin (0.1 mg/mL) and incubated at 37ºC for 16h. Single clones were picked using a L200 pipette tip and injected into 7 mL LB medium before 16h incubation at 37ºC. Plasmid DNA was purified using PureLink Miniprep kit. Glycerol stocks were prepared by adding 600 µL bacteria culture to 400 µl 50% glycerol (v/v in H_2O) and subsequent freezing at -80ºC. After test-digest (using FastDigest NotI/AscI or NotI/MreI enzyme pairs) and sequencing (ordered at GATC Biotech), plasmid DNA stocks were prepared by incubating a "scrape" of still frozen glycerol stock from previously generated clonal bacteria in 500 mL LB medium containing ampicillin (0.1mg/mL) for 16h at 37ºC. Finally, plasmid DNA was purified using PureLink Maxiprep kit. DNA Stocks were frozen at -20ºC for long-term storage.

Other plasmids – NFκB-gLuc and EF-1α-fLuc reporter plasmids were generously donated by Dr. Thomas Zillinger. The NFκB-gLuc plasmid contained the Gaussia luciferase-coding gene (gLuc, *Gaussia princeps*) under the control of an NFκB target promoter (containing five NFκB transcription factor binding sites). Gaussia luciferase was used because it is secreted upon expression therefore enabling simple read-out of NFκB activity. The EF-1α-fLuc plasmid contained the Firefly luciferase-coding gene (fLuc, *Photinus pyralis*) under the control of the constitutive EF-1α promoter. The effect of immune activation on EF-1α expression is negligible and was therefore used as a measurement of "background" cell activity and viability.
Viral packaging vector (Gag-pol) coding for HIV group specific antigen (Gag) and reverse transcriptase (pol) as well as viral envelope vector (VSV-G) coding for glycoprotein G of the Vesicular stomatitis virus (VSV) were obtained through a donation by Dr. Doug T. Golenbock, University of Massachusetts Medical School (UMASS). When transfected into cells together with a pRP transfer vector, these plasmids enable the formation of HIV-like viral particles able to infect mammalian cells and integrate the cDNA sequence contained between the two long terminal repeats (LTRs) present in the transfer vector.

General cell culture

TLR-expressing human embryonic kidney (HEK) 293 cells were purchased from InvivoGen. HEK293T, expressing the large T antigen of simian virus 40, were from

ATCC. HeLa cells were obtained courtesy of Professor Friedemann Weber's laboratory (Marburg, Germany). U373 glioma epithelial cells expressing TLR9-YFP fusion protein either alone or together with RAGE were produced by Dr. Cherilyn Sirois at the University of Massachusetts Medical School (UMASS).

Cells were routinely cultured in DMEM completed with 10% fetal calf serum (FCS), 100U/mL penicillin and 100µg/mL streptomycin. Depending on the usage, cells were cultured in T175 or T75 flasks and grown until reaching a confluence of 90%. They were then detached from the flask using either Trypsin (containing 2mM EDTA) or Stem Pro Accutase and passaged 1:5 (HEK293, HEK293T) or 1:10 (HeLa) to a new flask. To produce cell stocks, cells from an early passage (passage 2-3) were centrifuged and resuspended in FCS containing 10% DMSO. Immediately after resuspension, cells were transferred to cryo-tubes and placed in freezing container filled with isopropanol. Freezing containers were stored at -80°C for 24h. Cryo-tubes were finally transferred to -150°C for long-term storage.

Cells to be used for experiments were placed in a 50 mL tube and centrifuged at 340g for 5 minutes. Supernatant was discarded and cells were resuspended in 5 mL complete DMEM. After a 5-fold dilution of the cell suspension in trypan blue (to stain dead cells), cell density was assessed with a Neubauer hemocytometer. Cells present in the four outer corners of the chamber were counted and cell density was calculated using the following equation:

$$density = \left(\frac{count}{4}\right) \times 5 \times 100 = x \,.\, 10^6 cells/mL$$

Cell suspensions were diluted to the appropriate density and cells were seeded into tissue culture plates. Plates were left untouched on the sterile bench for 10 minutes to enable cells to sediment in a homogeneous manner to the bottom of the wells.

Generation of stable cell lines

Cells stably expressing RAGE were produced using a HIV-based retrovirus system. cDNA sequences coding for full-length or mutant human RAGE in fusion with either TagRFP or mCitrine fluorescent protein were transferred to a pRP plasmid between two LTR sites (as described previously, see Cloning strategy). On day 1, HEK293T cells were seeded at a density of $3x10^6$ cells per 10 cm tissue culture dish. On day 2, HEK293T cells were transfected with 10 µg Gag-pol plasmid and 1µg of VSV-G

plasmid together with 10 µg of pRP plasmid coding for RAGE-TagRFP or RAGE-mCitrine. Plasmids were diluted as desired in serum-free DMEM, combined with a cationic lipid based transfection reagent (GeneJuice) and further incubated 20 min at room temperature to allow formation of DNA-cationic lipid complexes. DNA-containing cationic lipid complexes were then added to HEK293T cells in the absence of FCS. After 6 hours incubation at 37°C, 5%CO_2, FCS was added to a final concentration of 10%. On day 3, cell supernatants were replaced by new complete DMEM containing 30% FCS and incubated for 48h at 37°C, 5% CO_2. On day 4, target cells were seeded in 6 well plates at a density of 1.10^5 cells (HeLa) or 2.10^5 cells (HEK293) per well in 3 ml of complete DMEM (10% FCS) and incubated at 37°C with 5% CO^2 overnight. 72h post-infection (day 5), virus-containing supernatants were harvested, filtered with a 0.45 µm PVDF syringe filter and applied to the target cells (3mL per well). After 24h, supernatants were removed from infected cells and replaced by fresh complete DMEM containing 10% FCS. Cells were expanded until reaching density of 80% in a T175 tissue culture flask. Cells positive for fluorescence were finally sorted using an Aria flow cell sorter with help from the FACS Core facility in Bonn, Germany.

Bone marrow isolation and stimulation

Eleven-week-old C57/BL6 WT and RAGE-deficient (KO) female mice were anesthetized using isofluoran vapours and subsequently sacrificed by cervical dislocation before harvesting femur and tibia bones. Bone marrow cells were isolated by flushing cut bones with 5mL complete RPMI medium per bone and using a 25-gauge needle. Cells were thoroughly resuspended and subjected to erythrocyte lysis. Finally, cell suspensions were filtered through a 70µm cell strainer and counted prior to plating and stimulation.

Cells were stimulated with TLR13 agonist (Sa19-RNA, 0.1µg/mL and 0.5µg/mL), TLR9 agonist (ODN 1826, 0.1 µM) or LPS (0.1µg/mL). TNFα and IL-6 cytokine secretion in the cell supernatant was sampled over 4h at different time points and quantified using mouse TNFα or IL-6 HTRF kit (please see below for detailed protocol). Animal experiments were performed in accordance with German animal protection law.

Enzyme-linked immunosorbent assay (ELISA)

HEK293-XL cells stably expressing TLR9 were seeded in 96-well plates at a cell density of 3.10^4 cells/well. After overnight incubation at 37ºC, 5% CO_2, cells were transiently transfected with non-tagged full-length RAGE or a control plasmid encoding for mCherry using GeneJuice transfection reagent. On the following day, cells were stimulated with a gradient of ODN 2006. Cells were also stimulated with the cytokine TNFα as control for RAGE-indepenent immune activation. Cells were then incubated at 37ºC for 16h. After incubation, 96-well plates were centrifuged at 340 g for 5 min and cell supernatant was harvested and frozen until use in ELISA. For quantification of human IL-8 secretion in the cell supernatant, MaxiSorp 96-well plates were coated with capture antibody diluted in coating buffer and incubated overnight at 4ºC. Plates were then washed 3x in wash buffer before blocking with PBS containing 10% FBS for 1h at room-temperature. After another three washes, standard and diluted supernatants (1:2) were incubated on the plate for 2h at room temperature. Following incubation, plates were washed 5x and subsequently incubated for 1h with working detector containing both biotinylated detection antibody and streptavidin-bound horseradish peroxidase (HRP). Finally, plates were washed a total of seven times before adding HRP-substrate solution. Plates were incubated approximately 20 min before adding sulfuric acid stop solution. Absorbance at 450nm was measured using SpectraMax i3 plate reader. Quantification of IL-8 cytokine concentration was finally calculated by fitting absorbance of each well to the standard curve.

Luciferase Assays

HEK293-XL cells stably expressing TLR7, TLR8, TLR9 or TLR13 were seeded in 96-well plates at a cell density of 3.10^4 cells/well. After overnight incubation at 37ºC, 5% CO_2, cells were transiently transfected with non-tagged full-length RAGE or a control plasmid encoding for mCherry, together with an NFκB (5xκB) driven luciferase reporter, using GeneJuice transfection reagent. On the following day, cells were stimulated with TLR specific DNA or RNA agonist at the indicated doses. As specificity control, cells were stimulated with TLR7/8 specific small synthetic agonist R848 or a non-stimulatory RNA (NS-RNA) at the specified doses. To control for RAGE-indepenent immune activation, cells were also stimulated with

cytokine TNFα or IL-1β at the indicated doses. Cells were then incubated at 37ºC for 6h, 16h (Results – Part 2) or 20h (Results – Part 1). After incubation, 96-well plates were centrifuged at 340g for 5 min. To measure NFκB-dependent release of gaussia luciferase, cell supernatants were subsequently harvested and transferred to a new 96-well plate. 25µL of each sample was then transferred to a U-shape white 96-well plate before adding 25µL of diluted Coelenterazine (1µg/mL in water).
When using cell endocytosis inhibitors, EF-1α-driven firefly luciferase reporter was used to control for cell viability. To measure firefly luciferase activity, cells were lysed in 50µL passive lysis buffer directly after supernatant harvest. Cells were incubated in lysis buffer for 10 min with orbital rocking. 25µL of cell lysate was then transferred to a U-shape white 96-well plate before adding 25µL of Steady-Glow luciferase reagent. For gaussia and firefly luciferase, luminescence emission was immediately measured with SpectraMax i3 plate reader.

Homogeneous Time Resolved Fluorescence (HTRF)

TNFα and IL-6 cytokines secretion from mouse bone marrow cells was quantified using homogeneous time resolved fluorescence (HTRF). This system is based on Förster resonance energy transfer (FRET). Two antibodies targeting different epitopes on the same target molecule are mixed together with a sample containing the antigen. When binding to the target antigen, both antibodies are placed in close proximity enabling energy transfer between a donor fluorescent molecule, europium cryptate, placed on one antibody and an acceptor fluorescent molecule, XL665, placed on the other antibody.
Bone marrow cells were stimulated as described above. Several 30µl samples of supernatant were taken over time (30 min, 1h, 2h, 3h and 4h post-stimulation). At the end of the stimulation time, all samples and standard were incubated overnight with donor/acceptor antibody mix. Finally, fluorescence emission at 620 nm (donor) and 665 (acceptor) were measured and the ratio 665nm/620nm was calculated prior to determination of cytokine concentration by fitting sample data to the standard curve.

Confocal Imaging

To study membrane binding of RNA to RAGE, µ-Slide 8 well microscopy dishes were first pre-coated by incubation with 200µL poly-L-lysine (0.01% m/v) for 30 min at

37ºC. Dishes were then washed twice with PBS. HEK293-XL TLR8-HA cells expressing either RAGE FL or RAGE ΔVC1 fused to a C-terminal Tag-RFP were then seeded in 200µL complete DMEM at a cell density of 1.10^5 cells/well. After overnight incubation at 37°C, 5% CO_2, cells were incubated at 37ºC for 15 min with 5 µM final concentration of biotinylated RNA or DNA labelled with streptavidin-AlexaFluor488 (20 min incubation of 50 µM biotin-RNA/DNA and 10 µM streptavidin-AlexaFluor488 in PBS) or with FAM labelled ORN Sa19. Supernatants were then replaced by complete DMEM medium containing DRAQ5 (1:2000) and cells where incubated for an extra 10 min at 37ºC before imaging.

To study RAGE-dependent internalization of RNA, HeLa cells expressing RAGE FL or RAGE ΔVC1 fused to a C-terminal TagRFP were seeded in µ-Slide 8 well microscopy dishes in 200µL complete DMEM and at a cell density of 2.10^4 cells/well. After overnight incubation at 37°C, 5% CO_2, cells were incubated for 5 min at 37ºC with 5µM biotinylated RNA labeled with streptavidin-AlexaFluor488 (as described above). Cells were then washed twice in PBS and either directly fixed (5 min time point) or incubated for a total time of 60 min at 37ºC, 5% CO_2. Cells were fixed in 3% PFA containing DRAQ5 (1:2000) and incubated at 37ºC for 30 minutes before PBS wash and imaging.

Live and fixed cells were imaged with a Leica SP5-AOBS-SMD confocal microscope.

Imaging settings:	Image size: 2048x2048 pixels, 16 bits, 246 µm/pixel
	Scan mode: XYZ
	Pinhole opening: 110 µm
	Sequential Scan with 4 channels
	400 Hz, 4 line averaging
Objective:	63x objective, water immersion
Laser power:	Argon laser, 20%
	Helium/Neon (HeNe), ON
	Diode-pumped solid-state (DPSS), ON
Transmitted light:	488 (20%), 561 (20%), 633 (10%)
PMT settings (measured spectrum):	AlexaFluor 488: 499-542 nm
	TagRFP: 567-629 nm
	DRAQ5: 642-789 nm

For RNA internalization, confocal images from three independent experiments were analysed using Cell Profiler software ((229), www.cellprofiler.org). RAGE channel was used to define primary objects first using a global threshold enhancement followed by a 3-class Otsu algorithm. Fluorescence intensity of the RNA channel was then used to quantify the median correlations of RNA to RAGE in a pixel-by-pixel basis calculation of Pearson's correlation coefficient within the objects. An area shape filtering for eccentricity was finally used to exclude linear membrane staining to put the focus on intracellular vesicles.

Western Blot analysis

Samples were prepared using NuPAGE LDS loading buffer together with NuPAGE reducing buffer and separated by NuPAGE 4-12% Bis-Tris poly-acrylamide gels in MOPS running buffer and at 100V for approximately 2h30. After gel electrophoresis, proteins were transferred to Immobilon-FL PVDF membranes using glycine-methanol transfer buffer at 32V for 1h30. Membranes were blocked in 3% BSA (w/v) diluted in TBS. Immunoblotting was performed in 0.1% Tween-TBS containing 3% BSA (w/v). Primary antibodies were diluted as follow: mouse monoclonal anti-human RAGE, 1:500; rat monoclonal anti-TLR9, 1:500; rabbit monoclonal anti-β-actin, 1:1000; rabbit polyclonal anti-TagRFP, 1:5000. Donkey anti-mouse or anti-rabbit antibodies conjugated to either IRDye680 or IRDye800 were used as secondary antibodies and diluted at $1:2.10^4$. Infrared signal was finally detected using Odyssey scanner (LI-COR).

Co-Immunoprecipitation (co-IP)

For co-immunoprecipitation of TLR9 and RAGE, U373 glioma epithelial cells stably expressing either TLR9-YFP fusion protein alone or together with RAGE were used. Cells were stimulated for 1h at 37ºC with medium alone or with 1 µM CpG ODN 2006 untagged or tagged with biotin. Cells were subsequently washed with cold PBS and then lysed in RIPA lysis buffer complemented with 0.1µM PMSF and 1x complete protease inhibitor. 50 µL of protein A Dynabead slurry was washed once with 200 µL cold PBS complemented with 0.02% Tween-20. Beads were then incubated 10 min with 1µg rabbit anti-GFP (in 200µL PBS-0.02% Tween-20). After protein concentration measurement using BCA assay kit, lysate concentrations were

adjusted across all samples by adding lysis buffer and 730 µg total protein was used per co-IP. Beads were washed once with 200µl PBS-0.02% Tween-20 before protein lysate was applied to the beads (1mL final volume). Lysates were incubated with anti-GFP antibody-coated beads for 2h30 at 4ºC using rotational mixing (MACSmix tube rotator). Beads were finally washed 3x in PBS-0.02% Tween-20 and subsequently boiled at 95ºC for 5min with 30 µL reducing western-blot loading buffer. Proteins captured on the beads were resolved by SDS-PAGE. Bound TLR9 and RAGE were detected by western blot as described previously.

Electrophoretic mobility shift assay (EMSA)

RNA molecules labeled with Oregon-green or 6-Carboxyfluorescein (Fluo-RNA) were incubated at a fixed concentration of 250 nM with increasing amounts of purified RAGE ectodomain (V-C1-C2, from 1 to 10 µM) or BSA (10 µM) as negative control. To assess the specificity of the interaction, electrophoretic mobility of Fluo-RNA (250 nM) with V-C1-C2 protein (2.5 µM) was competed with increasing concentrations of either unlabeled RNA molecules (corresponding to the sequence of the labeled RNA), CpG ODN 2006 or GpC ODN 2137 (RNA or 2006/2137-DNA; 0.63-40 µM, except for Sa19-RNA; 0.63-20 µM). All binding assays were prepared in assay buffer and at room temperature, allowing 10 min incubation time. Samples were loaded on NuPAGE 4-12% Bis-Tris poly-acrylamide gradient gels and electrophoresed at 90 V for 5h in TBE buffer with light protection. Oregon green or FAM fluorescence was detected using VersaDoc 4000 fluorescence imaging system with 90s exposition time.

Fluorescence-activated cell sorting (FACS)

To study the cell surface interaction of RAGE with RNA, HEK293-XL cells expressing either TLR7-HA or TLR8-HA together with RAGE FL or RAGE ΔVC1 fused to mCitrine were used. Cells detached from the tissue culture dish with StemPro Accutase were resuspended in complete DMEM and subsequently seeded in a V-shape 96-well plate (1.10^5 cell/well). Cells were then incubated at 37ºC for 15 min with 5 µM biotinylated RNA previously labeled with streptavidin-AlexaFluor647 (as described in confocal imaging section). Cells were then washed in FACS buffer

(PBS, 1% FCS) and kept on ice prior to fluorescence detection using Fortessa flow cytometer.

Quantitative Real-Time PCR (qPCR)

Bone marrow cells were harvested and stimulated as described above. At the end of the experiment, unstimulated cells were lysed in RLT buffer complemented with 1% (v/v) β-mercaptoethanol. Total RNA was subsequently isolated with RNeasy Mini Kit (Qiagen) following the manufacturer's protocol. Concentration of isolated RNA was quantified by measuring absorbance of RNA solutions at 260 nm using SpectraMax i3. 1 µg RNA from each sample was then used to synthesize cDNA using an oligo-dT(18) primer: mRNA and oligo-d(T) were mixed and incubated at 65ºC for 5min. Samples were then placed on ice for 2 min before adding 1x reaction buffer (stored as a 5x), 0.5 mM dNTPs, 5 mM DTT and 200U SuperScript III Reverse Transcriptase. Samples were subsequently incubated at 50ºC for 50 min followed by 5 min at 85ºC. cDNA mix was diluted 1:200 in water before use in qPCR. The amount of cDNA was determined using the Maxima SYBR Green/ROX qPCR Master Mix mixed with mRNA-target specific primers (listed above) and each cDNA sample. PCR was finally run on QuantStudio 6 qPCR cycler. Gene expression was normalized to expression of the housekeeping gene *Hprt* (normalized threshold cycle, ΔCt). For analysis, data was transformed to power ΔCt (pΔCt) where pΔCt = $2^{\Delta Ct}$ to take into account the exponential nature of the PCR reaction.

3. Results – Part 1: RAGE is a cell surface DNA sensor that promotes TLR9-dependent inflammatory responses *

3.1 DNA binds to RAGE extra-cellular V-C1 domain

To determine whether immune-stimulatory DNA binds to RAGE, purified His-tagged V-C1-C2 ectodomain was incubated with an increasing amount of A-, B- and C-type CpG DNA. As analysed by Alpha-Screen homogenous binding assay, all CpG types bound to RAGE at low nanomolar apparent affinities (**Fig. 3.1A**). CpG-A bound the most efficiently to V-C1-C2. CpG-B had a slightly lower affinity than CpG-A while CpG-C presented the smallest affinity of the three types of DNAs to RAGE ectodomain. To further characterize the structural basis for DNA binding to RAGE, V-C1-C2-His peptide was incubated with either full length CpG-B 2006 DNA (24 nt) or with different 3'-truncated DNA with sizes ranging from 20 nucleotides down to 7 nucleotides (**Fig. 3.1B**). Interestingly, DNA molecules smaller than 15 nucleotides could not interact with RAGE. The binding affinity of CpG-B to V-C1-C2 was size dependent, longer DNA presenting a stronger affinity to the peptide than smaller ODNs. Double- or single-stranded CpG-B DNA had similar binding affinity to V-C1-C2 (**Fig. 3.1C**). Surprisingly, bases were dispensable for the interaction. Indeed, phosphodiester- or phosphorothioate-linked deoxyribose backbone lacking bases also interacted with V-C1-C2-His peptide with a low nanomolar apparent affinity (**Fig. 3.1D**). Phosphorothioate-linked (PS) deoxyribose backbone had a greater affinity with RAGE than phosphodiester-linked (PO) backbone. Together, these results show that DNA binds to RAGE ectodomain in a size-dependent but sequence-independent manner. The fact that structurally heterogeneous types of CpG DNA bind to RAGE with different affinities suggests that RAGE binds preferentially to more complex structures of DNA where CpG-A, a more branched form of DNA, has the best affinity to RAGE. To identify the DNA binding site present in RAGE, different recombinant constructs of the RAGE ectodomain, either full-length (V-C1-C2), V-domain alone (V), V-C1-domains (V-C1) or C1-C2-domains (C1-C2) were incubated together with

* A modified version of some of the results discussed in this thesis section was published in the Journal of Experimental Medicine: Sirois et al. 2013, (228), annex 7.2.

an increasing amount of CpG-B ODNs (**Fig. 3.2A**). Full length V-C1-C2 peptide had the strongest affinity with DNA. V-domain alone or together with C1-domain (V-C1) also presented a strong affinity to DNA. On the contrary, the peptide containing C1-C2 domains (C1-C2) showed no binding affinity to DNA. Interestingly, full-length V-C1-C2 peptide had a stronger affinity to CpG DNA than V- or V-C1-domains. This result suggests that C1 and C2 domains have a stabilization role enabling a better binding of DNA to the V domain. This is in agreement with the known role for RAGE V-domain, which was previously shown to be essential for the interaction with other RAGE ligands (198).

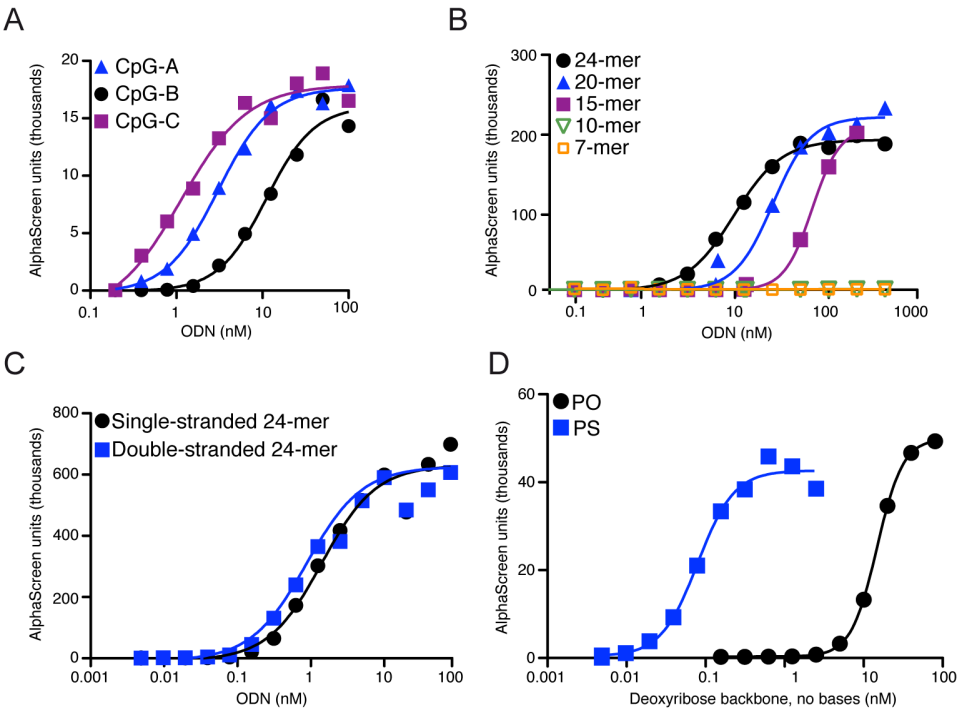

Figure 3.1 DNA binds to the extracellular domain of RAGE.
Indicated concentrations of ODN were incubated with 40 nM his-tagged RAGEV-C1-C2 and binding was assessed by AlphaScreen. Binding of phosphodiester backbone containing CpG type A, B and C DNA (A) or ODN 2006 full-length (24-mer) and 3' truncated ODN of different length based on same sequence (B) or single stranded 24-mer ODN 2006 and 24-mer ODN 2006 annealed to its complementary strand (C) were compared for binding to RAGE. (D) Deoxyribose backbone containing either phosphodiester (PO) or phosphorothioate (PS) type linkage in the absence of nucleobase was incubated with RAGE and tested for binding.
Experiments presented in this figure were performed by Dr. Cherilyn M. Sirois and were part of the manuscript published in the Journal of Experimental Medicine (228). *Please refer to manuscript Material and Method section for more technical details (please see joined manuscript).*

Our collaborators (T. Sam Xiao laboratory) further determined the crystal structures of the RAGE V-C1 domain in complex with either a 22 nucleotides-long dsDNA molecule derived from vaccinia virus genomic repeat sequences (PDB accession number 3S59, **Fig. 3.2B**) or with a 22 nucleotide-long CpG motif-containing dsDNA molecule (PDB accession number 3S58). In summary, both crystal structures had a resolution of 2.8-Å and 3.1-Å respectively.

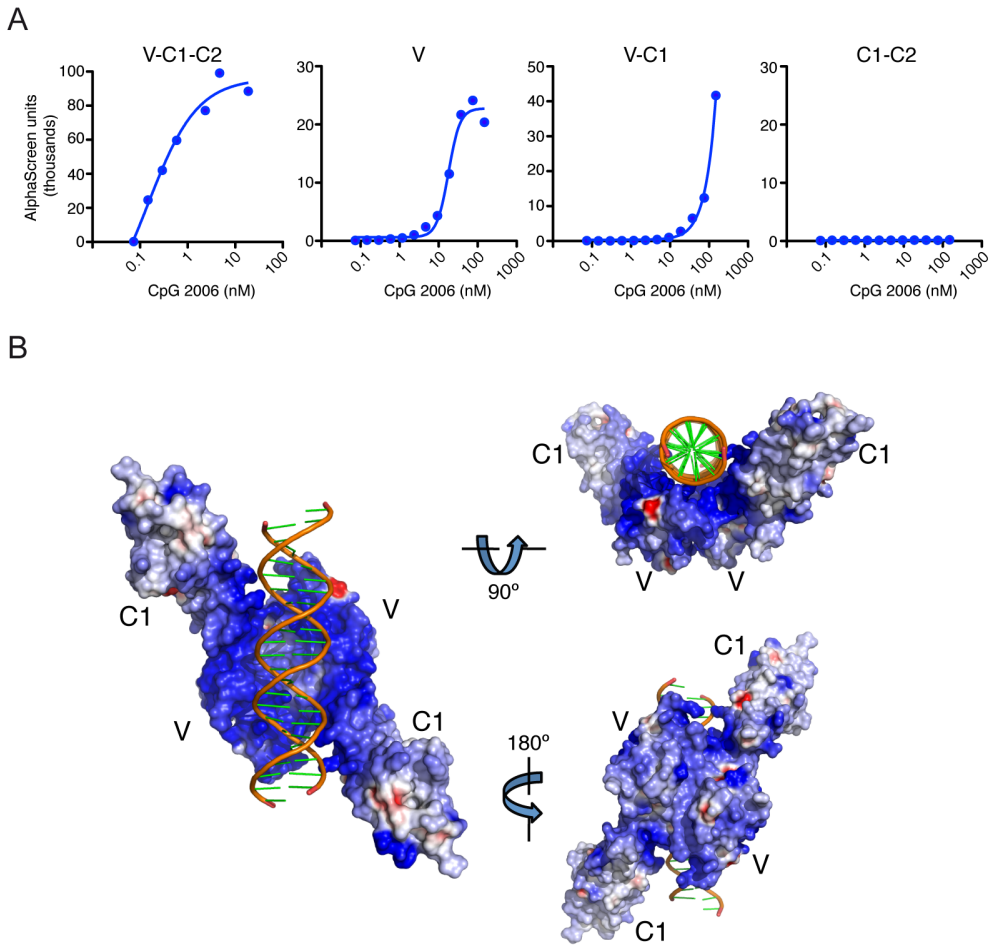

Figure 3.2 RAGE extracellular V-C1 domain is essential for binding of DNA.
(A) Localisation of DNA binding site in RAGE extracellular domain was analysed by AlphaScreen upon incubation of indicated concentrations of ODN 2006 with 40nM of either full-length RAGE extracellular domain (V-C1-C2) or isolated V domain (V), V-C1 domain (V-C1) and C1-C2 domain (C1-C2). (B) Representation of the solved structure of two RAGE V-C1 domains in complex with a 22 nucleotides-long dsDNA molecule derived from vaccinia virus genomic repeat sequences (PDB accession number 3S59). Electrostatic charge surface of RAGE is shown on a scale of -10 kT/e (red) to +10 kT/e (blue) in three different orientations. The bound dsDNA is shown as an orange ribbon.
Experiments presented in this figure were performed by Dr. Cherilyn M. Sirois (A) and Tengchuan Jin (B) and were part of the manuscript published in the Journal of Experimental Medicine (228). *Please refer to manuscript Material and Method section for more technical details (please see joined manuscript).*

The structures were solved using molecular replacement based on two previously published structures of V-C1 domains of RAGE (PDB accession numbers 3CJJ and 3O3U,(133)). The two structures were nearly identical except for the two DNA sequences. They presented the formation of a “trans” homodimer with two V-C1 monomers bound in a dyad conformation with their V-domains located at the dimer interface. One dsDNA molecule was bound in the pocket formed by the dimer. The dimer formed by interaction of the hydrophobic surfaces present on both V-domains showed an accumulation of highly positively charged amino acids at the protein:DNA interface (in blue), where the complementary negatively charged backbone of the dsDNA molecule was integrated.

3.2 DNA is recruited at the surface of cells expressing RAGE

To study the interaction of DNA with RAGE at the cell surface, an inducible expression system was first used. Cells transduced with the gene coding for human RAGE in fusion with mCitrine and under the control of a TRE-Tight tetracycline-inducible promoter were treated with doxycycline for 24h to induce RAGE expression (**Fig. 3.3A**). Cells either expressing RAGE (RAGE on) or kept without doxycycline (RAGE off) were stimulated with 1µM ODN 2336 (CpG-A) labeled with AlexaFluor647. Analysis of cell fluorescence by flow-cytometry showed a marked increase in mCitrine fluorescence indicating the efficiency of the 24h doxycycline treatment and RAGE expression. Interestingly, RAGE-on cells bound more DNA than RAGE-off cells. There was a positive correlation between the amount of DNA bound by the cells and their RAGE expression. Cells that were not treated with doxycycline showed a slight binding of DNA when compared with non DNA-stimulated cells. However, this RAGE-unspecific binding of DNA remained much lower than the binding induced by RAGE expression. To further characterize the binding of DNA to RAGE at the cell surface, two constructs were designed to code either for full-length RAGE (RAGE FL) or for V-C1 truncated RAGE (RAGE ΔVC1) in fusion with a C-terminal cytoplasmic TagRFP fluorescent protein (**Fig. 3.3B**). HEK 293 cells stably expressing either construct were used to study the binding of DNA to RAGE by confocal microscopy (**Fig. 3.3C**). Cells were stimulated with 5µM biotinylated DNA labeled with streptavidin AlexaFluor488. After 15 minutes stimulation at 37°C, cells were washed and incubated with medium containing DRAQ5 for another 10 minutes

to stain nuclei before live imaging. Cells expressing RAGE FL presented a strong accumulation of fluorescent RAGE at the cell-to-cell boundary. This is expected since the V and C1 domains of RAGE were previously shown to dimerize in a trans conformation (**Fig. 3.2B**).

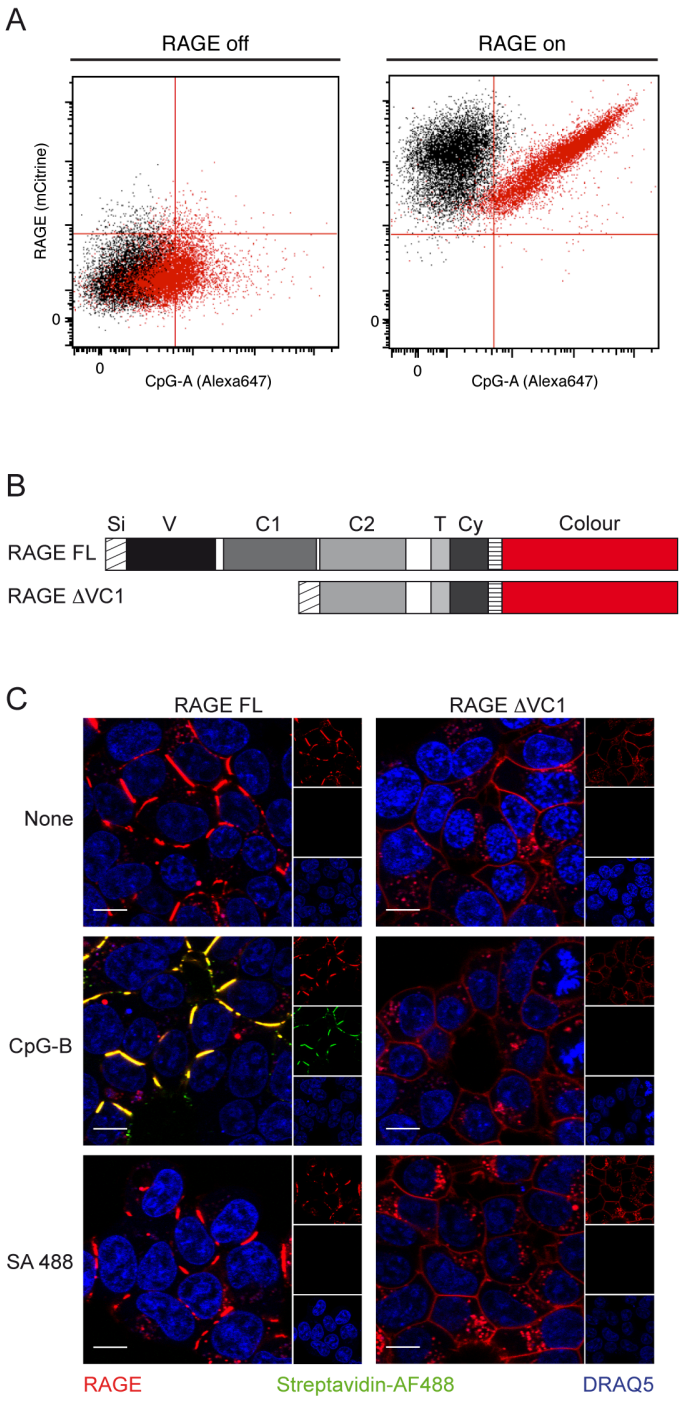

Figure 3.3 DNA is recruited at the surface of cells expressing RAGE.
Note: For detailed legend, please see opposite page.

On the contrary, cells expressing RAGE ΔVC1 did not show such accumulation of fluorescence and conserved a homogeneous repartition of the receptor along the membrane. After stimulation with labeled DNA, cells expressing RAGE FL recruited a pronounced amount of DNA at their cell surface, which almost entirely co-localized with RAGE. Cells expressing RAGE ΔVC1 showed no cell surface recruitment of DNA, strengthening our previous finding that localized the DNA binding site to the V-C1 domains of RAGE. To control for the specificity of the binding, cells were also stimulated with streptavidin AlexaFluor488 alone. No AlexaFluor488 fluorescence signal was detected at the surface of either RAGE FL or RAGE ΔVC1 expressing cells confirming the specificity of the DNA binding to RAGE.
Together, these results show that DNA binds to RAGE extracellular V and C1 domains not only in-vitro but also at the surface of living cells.

3.3 Protocol establishment for read-out of the impact of RAGE on the immune response to DNA stimulation

To analyze the effect of RAGE on the immune activation induced by CpG DNA stimulation, a tertracycline-inducible system identical to the one described previously (**Fig. 3.3A**) was used.

Figure 3.3 DNA is recruited at the surface of cells expressing RAGE.
(A) HEK293T cells transduced with tetracycline-inducible RAGE-mCitrine coding gene were left un-induced (RAGE off, black population) or treated to induce RAGE expression (RAGE on, black population) and then incubated on ice with 1 μM Alexa Fluor 647-labelled ODN 2336 (CpG-A, red populations), washed, and analysed by flow cytometry. Data is representative of three similar experiments. (B) Schematic representation of the RAGE-fluorescent protein fusion constructs used in confocal microscopy. (C) HEK293-XL cells stably expressing RAGE FL or RAGE ΔVC1 fused to TagRFP were stimulated with biotinylated ODN 2006 (CpG-B) labelled with streptavidin-AlexaFluor488 (5 μM) for 15 min at 37°C. DRAQ5 was used as nuclear staining. To control for binding specificity, cells were also incubated with streptavidin-AlexaFluor488 alone. Cells were finally imaged live by confocal microscopy. Main images represent merged channels corresponding to RAGE-TagRFP (red), labeled RNA (green) and DRAQ5 (blue). Scale bars represent 10 μm. Split channels are represented on the right with the same color-coding.
Experiment presented in (A) was performed by Dr. Cherilyn M. Sirois and was part of the manuscript published in the Journal of Experimental Medicine (228)*. For more technical details concerning experiment in (A), please refer to the manuscript Material and Method section of the manuscript (please see joined manuscript).*

Cells expressing either TLR9, tetracycline-inducible-RAGE or TLR9 together with tetracycline-inducible-RAGE were treated for 24 h with doxycycline to induce protein expression (+ Dox) or left without doxycycline for the same period of time (- Dox). Cells were then stimulated with an increasing dose of CpG-B ODN 2006 and TNFα as control for RAGE-independent immune activation (**Fig. 3.4A**). TLR9 or TNFα-receptor activation was assessed by quantification of interleukine-8 (IL-8) cytokine release (ELISA). RAGE expression, upon doxycycline treatment, was controlled by western-blot using unstimulated cells lysed in SDS loading buffer (**Fig. 3.4B**). Interestingly, cells expressing both TLR9 and RAGE upon doxycycline treatment showed an increased immune response to CpG-B DNA stimulation compared to - Dox cells. However, cells expressing only TLR9 but that were still treated with doxycycline showed the same increased activation. This result implicated that the rise in IL-8 release was RAGE-independent and triggered by doxycycline. Of note, cells only expressing RAGE and lacking TLR9 did not respond to CpG-B DNA stimulation either with or without doxycycline treatment. Moreover, upon TNFα stimulation, cells treated with doxycycline showed almost no increase in IL-8 secretion compared to cells left without doxycycline (**Fig. 3.4A**, right panel). This suggested that the effect of doxycycline was specifically targeting TLR9 activation sensitizing cells to CpG-B DNA stimulation without activating them directly. Moreover, background expression of RAGE was noticeable in the cells transduced with the tetracycline-inducible RAGE construct even without doxycycline treatment when compared to the TLR9 only expressing cells (**Fig. 3.4B**). This effect could be due to traces of doxycycline in the bovine serum used for cell culture or due to an imperfect control of the promoter by the TET-repressor. This background expression of RAGE together with the doxycycline effect on TLR9 activation made this experiment unreliable and difficult to analyse.

Consequently, a new protocol was established, using transient transfection of RAGE and a reporter plasmid for assessment of NFκB activation. This reporter plasmid contained the sequence coding for gaussia luciferase (gLuc) under control of an NFκB-target promoter. Cells of the control group were transfected with a plasmid coding for mCherry fluorescent protein enabling visual control for transfection efficiency. Cells expressing either TLR9 or TLR7 were transfected with previously described plasmids. After 24h, cells were stimulated with a gradient of CpG-B DNA (ODN 2006) or TNFα and incubated for 16h prior to gLuc activity measurement in the cell supernatants (**Fig. 3.4C**). Although CpG DNA stimulation induced a substantial

secretion of gaussia luciferase, indicating robust NFκB activation, only a very poor effect of RAGE was noticeable.

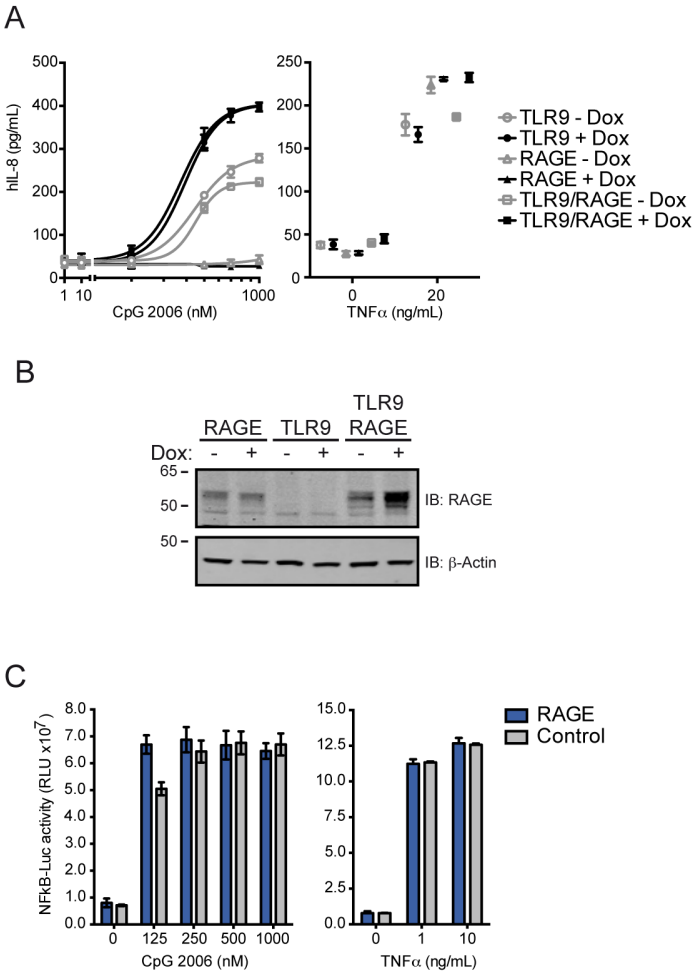

Figure 3.4 Protocol establishment for read-out of the impact of RAGE on the immune response to DNA stimulation.
(A) HEK293 cells expressing either TLR9, tetracycline-inducible-RAGE or TLR9 together with tetracycline-inducible-RAGE were left un-treated (- Dox) or treated for 24 h with doxycycline to induce protein expression (+ Dox). Cells were subsequently stimulated for 16h with a dose titration of ODN 2006 and TNFα as a control for RAGE-independent immune activation. After incubation, cell supernatant was harvested and concentration of IL-8 cytokine was measured by ELISA. Data are shown as mean ± SD for double experimental replicates and are representative of at least 3 independent experiments. (B) Unstimulated cells from (A) were lysed in LDS-loading buffer after harvest of supernatants. Samples were analyzed by Western-blotting for RAGE expression. Anti-β-actin antibodies were used for loading control. (C) HEK293-XL cells stably expressing human TLR9 were transiently transfected with an NFκB-driven luciferase reporter together with full length non-tagged human RAGE or mCherry as control. Cells were stimulated for 20h with a dose gradient of ODN 2006 and TNFα prior to readout of luciferase activity in cell supernatants. Data is shown as mean ± SD for triple experimental replicates.

When comparing to cells transfected with mCherry, RAGE significantly increased NFκB activation only at the lowest stimulation point (125nM). However, no dose-dependent increase of gaussia luciferase secretion was detected since even the lowest dose of CpG DNA induced a near-maximum luciferase expression. This indicated that the concentrations of CpG DNA used were too high and "over-loading" the cells, reducing the effect of RAGE. RAGE however showed no effect on TNFα stimulation at either doses used. Together, this pre-experiment indicated that RAGE could have a specific effect on DNA sensing at lower doses of CpG-B DNA, revealing the necessity of using a broader gradient of DNA concentrations.

3.4 RAGE increases TLR9-dependent NFκB activation in response to DNA stimulation

To further study the impact of RAGE on DNA sensing through TLR9, the previously established reporter assay was used, this time with a gradient of DNA extended to lower doses (**Fig. 3.5**). Additionally, to better understand the mechanism by which RAGE affects DNA induced NFκB activation, a second RAGE construct lacking the cytosolic domain was designed (RAGE ΔCyt, **Fig. 3.5A**). RAGE cytosolic domain was previously proposed to serve a signaling function upon binding of other RAGE ligands such as S100 proteins and AGEs. Consequently and as for other RAGE ligands, if binding of DNA to RAGE induced a direct signaling cascade through interaction of RAGE cytosolic domain with adaptor proteins like mDia-1, RAGE ΔCyt should abolish any such RAGE-dependent effect. Moreover, to examine the role of TLR9 in the DNA-induced immune response downstream of RAGE, TLR7 expressing cells were treated identically to TLR9 expressing cells. As expected, cells expressing TLR9 showed a dose-dependent increase in gaussia luciferase release upon CpG-B DNA stimulation while TLR7 expressing cells showed no response (**Fig. 3.5B**). Interestingly, cells expressing TLR9 together with RAGE presented an even stronger NFκB activity compared with cells expressing TLR9 alone (Control). Intriguingly, cells expressing TLR9 together with RAGE ΔCyt showed an identical increase in NFκB activity to the one found with RAGE FL, when compared to the control cells.

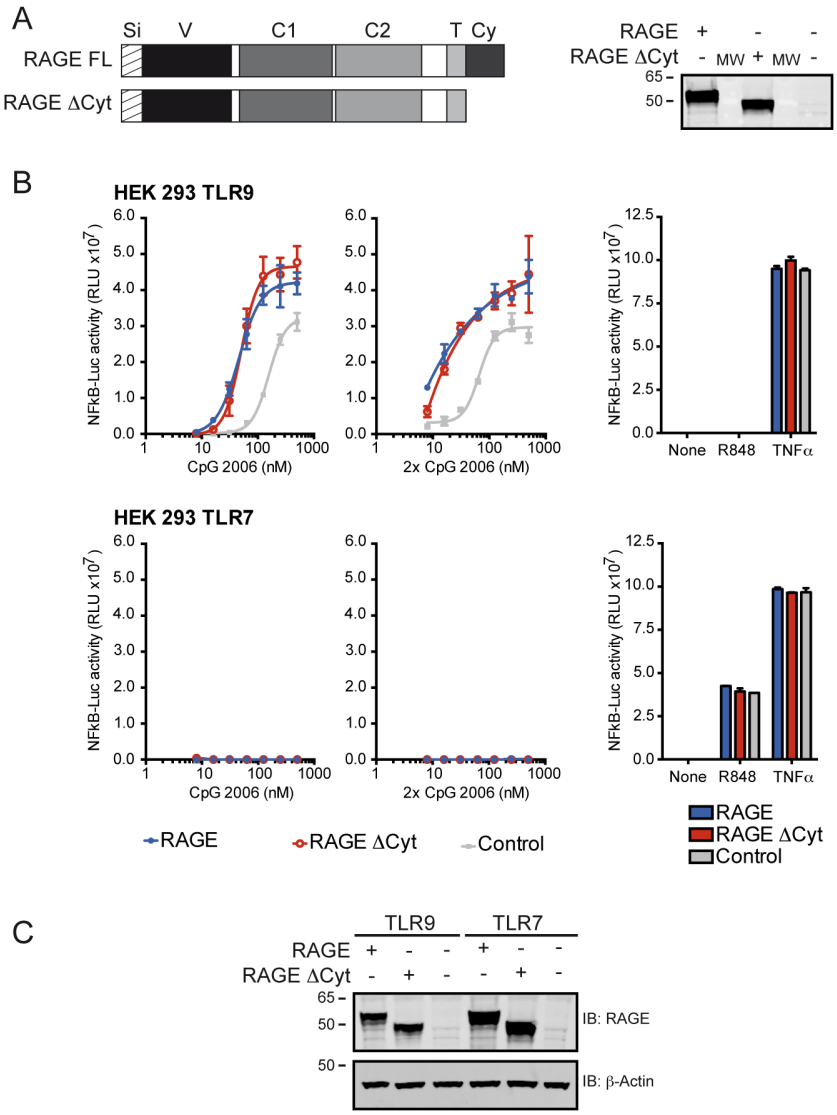

Figure 3.5 RAGE increases TLR9-dependent NFκB activation in response to DNA stimulation.

(A) Schematic representation of the RAGE full length (RAGE FL) or cytosolic domain truncated (RAGE ΔCyt) constructs used in (B). Constructs were tested for expression by transient transfection of HEK293 cells and subsequent western-blot analysis of protein content of cell lysates (right side). (B) HEK293 cells stably expressing TLR9 or TLR7 were transiently transfected with an NFκB-driven luciferase reporter and RAGE FL, RAGE ΔCyt, or mCherry (Control). Cells were stimulated for 20 h with a dose titration of ODN 2006 or a 48-mer DNA molecule corresponding to two ODN 2006 sequences (2x CpG 2006) and R848 (1 μM) or TNFα (1 ng/mL) as controls. After incubation, cell supernatants were harvested and luciferase activity measured. Data is shown as mean ± SD for duplicate samples and is representative of four similar experiments. (C) Expression level of RAGE or RAGE ΔCyt in unstimulated cells from (B) was assessed by Western blotting. Anti-β-actin antibodies were used for loading control.

Part of the experiment presented in (B-C) was included in the manuscript published in the Journal of Experimental Medicine ((228), please see joined manuscript).

This suggests that direct downstream RAGE signaling is either insignificant or nonexistent in this context. Cells expressing TLR7 together with either RAGE constructs showed no NFκB activity upon CpG-B DNA stimulation. Together with the previous finding, this showed that RAGE expression increases the activation of NFκB upon DNA stimulation in a TLR9-dependent manner. When stimulated with a longer DNA agonist (48-mer corresponding to 2x ODN 2006), TLR9 cells showed an enhanced NFκB activation when compared to cells stimulated with 24-mer ODN 2006. However, cells expressing TLR9 together with RAGE presented an even greater increase of NFκB activation than found with 24-mer DNA stimulation and this at lower doses of DNA.

Cells stimulated with TNFα showed a strong NFκB activation, which was comparable no matter whether cells expressed RAGE FL, RAGE ΔCyt or neither of them. TLR7 expressing cells stimulated with R848, a small TLR7 specific agonist, showed a good NFκB activation without any apparent effect of RAGE expression.

Together, these results showed that RAGE expression specifically increases TLR9-dependent NFκB activation upon DNA stimulation. RAGE lowered the threshold of DNA concentration for efficient activation of TLR9.

3.5 RAGE interacts with TLR9

To study potential co-localization of RAGE with TLR9, the glioma epithelial cell line U373 was used, which expressed TLR9-YFP fusion protein either alone or together with RAGE. After 1h stimulation with biotinylated ODN 2006, cells were lysed and TLR9-RAGE interaction was assessed by co-immunoprecipitation (co-IP) (**Fig. 3.6**).

Protein-A beads coated with anti-GFP antibodies were first used for co-IP with TLR9 as bait (left panel). Interestingly, RAGE was co-precipitated with TLR9 as shown by the band appearing in lane 4 and which was absent from lanes corresponding to cells expressing TLR9 alone (lane 2-3). Moreover, when cells were stimulated with ODN 2006, the amount of RAGE co-precipitating with TLR9 strongly increased (lane 5). This suggested that trafficking of RAGE to the endolysosomal compartment was increased upon DNA stimulation. It is also possible that the TLR9-RAGE interaction increases or is stabilized by DNA.

When using streptavidin-coated beads for co-IP (middle panel), unstimulated cells (lanes 1 and 3) presented bands with a size corresponding to TLR9 full-length

suggesting the co-IP to be unspecific to some extent. In the RAGE immunoblot, a band consistent with the size of RAGE also appeared for non-stimulated cells (lane 3). However, when cells were stimulated with biotinylated DNA, the amount of RAGE that co-precipitated strongly increased (lane 4). This suggested that RAGE interacted with DNA further confirming our previous results. More interestingly, in the TLR9 immunoblot, bands of approximately 115 kDa only appeared when cells had been stimulated. The size of these bands corresponded to the size of the activated TLR9, which is truncated between LRRs 14 and 15 (80, 81). The specific co-precipitation of TLR9 with biotinylated DNA indicated that the interaction between TLR9 and its DNA ligand took place in the endolysosomal compartment.

As control for TLR9 and RAGE expression, a western-blot was done using input samples. This showed a comparable expression of TLR9 across all conditions used in this experiment as well as a comparable RAGE expression in the corresponding cells.

Confirming these results, flow cytometry as well as confocal microscopy experiments were undertaken to further study the influence of RAGE on DNA internalization and trafficking (results presented on Figure 6 of the manuscript published in the Journal of Experimental Medicine, (228), please see joined manuscript).

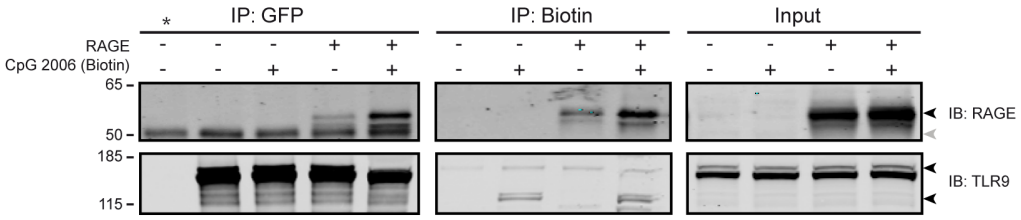

Figure 3.6 RAGE interacts with TLR9.
U373 cells expressing TLR9-YFP with or without RAGE were either left untreated or stimulated with untagged or biotin-tagged (for the biotin-IP) ODN 2006 for 1 h at 37°C before cells lysis. TLR9 or biotin were subsequently immunoprecipitated using anti-GFP-antibody- or streptavidin-coated beads respectively. TLR9 and RAGE protein content was subsequently assessed by Western blotting using specific antibodies. Cell lysates were controlled for TLR9 and RAGE total expression (Input). * To control for co-IP specificity, beads were left non-coated (lane 1). No band appeared for TLR9 and only a smaller band appeared in the RAGE immunoblot and was therefore considered to be unspecific. Black arrowheads indicate bands for TLR9 or RAGE target proteins; nonspecific band is indicated by grey arrowhead. Data is representative of three similar experiments.
Part of the data presented in this figure was included in the manuscript published in the Journal of Experimental Medicine ((228)*, please see joined manuscript).*

These experiments showed that RAGE expression induces a greater internalization of DNA to the endolysosomal compartment where RAGE and DNA colocalize together with markers of the early (Rab-5a) and late (Rab-9a) endosomal compartments.
Together, these results demonstrated that upon binding to RAGE at the cell surface, DNA is internalized and transported to the endolysosomal compartment where it is transferred to TLR9.

3.6 Conclusion to Results – Part1

The data presented in this section showed that DNA binds to RAGE through electrostatic interaction between the phosphate backbone of DNA and RAGE V-C1 ectodomain. Upon binding to RAGE at the cell surface, DNA is internalized together with RAGE and traffics towards the endo-lysosomal compartment. Through this mechanism, RAGE expression increases DNA uptake, thereby lowering the threshold of the DNA concentration necessary for TLR9-dependent immune activation and amplifying subsequent NFκB activation. Results also indicated an interaction between RAGE and TLR9, which could be part of the mechanism involved in RAGE-dependent increase of immune stimulation.

4. Results – Part 2: RAGE senses RNA at the cell surface and promotes TLR7-, TLR8- and TLR13-dependent inflammatory responses †

4.1 TLR specific RNA agonists bind to RAGE ectodomain

Results presented earlier indicated that DNA binds to RAGE via electrostatic interaction between the V and C1 domains of RAGE and the phosphate backbone of the DNA. Bases were dispensable for the interaction to take place. The backbone of RNA could therefore interact with RAGE in a manner similar to DNA.

Hence, the interaction of RAGE with immune-stimulatory RNA molecules was subsequently studied. Electrophoresis mobility shift assay (EMSA) was first used to study the mobility of Oregon green (TLR7 and TLR8 agonists) or FAM (ORN Sa19) labeled RNA molecules (Fluo-RNA) in a polyacrylamide gel after incubation with RAGE (**Fig. 4.1**). At stable concentration of labeled RNA, increasing concentration of purified RAGE V-C1-C2 ectodomain induced a dose dependent shift in the mobility of the RNA, while BSA, used as negative control, did not. All RNA molecules showed similar interaction with V-C1-C2. Interestingly, at higher concentration of V-C1-C2 protein, oligomers of lower electrophoretic mobility formed as shown by the appearance of bands in the higher part of the gel. This indicated that the V-C1-C2 domain could oligomerise around the labeled RNA. To control that RAGE interacts with the RNA and not the label, unlabeled RNA corresponding to each specific RNA sequence was used as a binding competitor. As expected, the unlabeled RNA competed efficiently with the labeled RNA, demonstrating specificity of the interaction. Together, these results showed that RNA molecules, specific agonists of the endosomal TLR7, 8 and 13, indeed interact with the extracellular domains of RAGE.

Interestingly, B-type DNA molecules (ODN 2006 and ODN 2137) could also compete with the TLR8 specific RNA for binding to RAGE (**Fig. 4.2A-B** respectively). It is

† A modified version of the results discussed in this part of the thesis is being peer reviewed for publication at the Journal of Immunology.

worth of note, that ODN 2006 also efficiently competed with TLR7 and TLR13 specific agonists for binding to RAGE (data not shown). These results suggested that the site of RNA binding to RAGE is similar to the one used by DNA for interacting with RAGE.

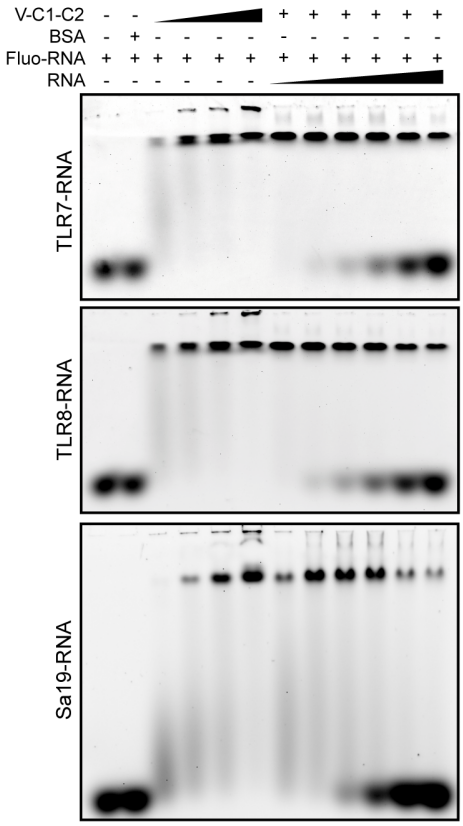

Figure 4.1 RNA binds to recombinant RAGE.
RAGE binding to RNA agonists was assessed by electrophoretic mobility shift assay (EMSA). Oregon green (TLR7- or TLR8-RNA) or FAM (Sa19-RNA) labelled RNA oligonucleotides (Fluo-RNA, 250nM) were incubated with increasing amounts of recombinant RAGE extracellular domain (V-C1-C2; 1-10 μM) or BSA (10 μM). Increasing concentration of the corresponding un-labelled RNA (RNA; 0.63-40 μM, except for Sa19-RNA; 0.63-20 μM) were added to constant concentration of Fluo-RNA (250 nM) and with RAGE (2.5 μM). Shift in labelled RNA mobility was measured by fluorescence detection. Data is representative of at least two independent experiments.

Figure 4.2 DNA can compete with RNA for binding to recombinant RAGE.
(A-B) RAGE binding to RNA agonists was assessed by electrophoretic mobility shift assay (EMSA). Oregon green labelled TLR8-RNA oligonucleotides (250nM) was incubated with increasing amounts of recombinant RAGE extracellular domain (V-C1-C2; 1-10 μM) or BSA (10 μM). Increasing concentration of un-labeled ODN 2006 (A) or ODN 2137 (B) (0.63-40 μM) were added to constant concentration of TLR8-RNA (250 nM) and with RAGE (2.5 μM). Shift in labelled RNA mobility was measured by fluorescence detection.

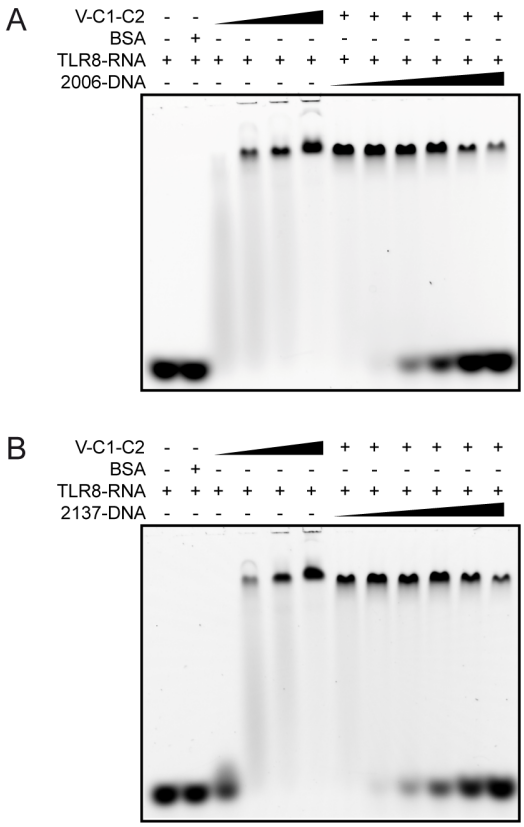

Figure 4.2 DNA can compete with RNA for binding to recombinant RAGE.
Note: For detailed legend, please see opposite page.

4.2 RNA binds to cells expressing full-length RAGE but not to cells expressing truncated RAGE lacking the V-C1 domain

The recruitment of RNA molecules at the surface of cells expressing RAGE was subsequently studied. To this end, HEK293-XL cell lines expressing TLR7-HA or TLR8-HA as well as either full-length RAGE (RAGE FL) or a mutant of RAGE lacking the V and C1 domains (RAGE ΔVC1) fused to mCitrine or TagRFP fluorescent proteins were produced (**Fig. 4.3A**).

First, flow cytometry was used to examine the cell surface binding of RNA to RAGE FL- or RAGE ΔVC1-mCitrine expressing cells (**Fig. 4.3B-C**). Measurement of mCitrine fluorescence confirmed that both cell lines expressed similar amounts of RAGE (**Fig. 4.3B**, lower panel). Cells expressing RAGE FL bound more RNA at their surface than non-transduced cells (control) or than cells expressing RAGE ΔVC1

after 15 minutes incubation at 37ºC (**Fig. 4.3B-C**). Interestingly, the amount of RNA binding to the cells expressing RAGE FL was positively correlated to the amount of RAGE-mCitrine expression (**Fig. 4.3B**, dotplots). In contrast, RNA binding to RAGE ΔVC1 expressing cells did not correlate with the amount of RAGE ΔVC1 expression. No significant binding of streptavidin-AlexaFluor647 to the cells was observed when added in absence of biotinylated nucleic acids. Together, these findings indicate that RAGE enhances RNA binding to cells. However, the recruitment of RNA to non-transduced cells or to cells expressing RAGE ΔVC1 suggested the presence of one or several RNA receptors other than RAGE at the surface of the cells used in this experiment.

To corroborate the flow-cytometry results, confocal microscopy was used to study the recruitment of labeled RNA to cells expressing either RAGE constructs (**Fig. 4.4A**). Cells expressing RAGE FL presented a strong accumulation of fluorescent RAGE at the cell-to-cell boundary, which was expected from the crystal structure mentioned earlier (**Fig. 3.2B**). Moreover, cells expressing RAGE ΔVC1 did not show such accumulation of fluorescence. When incubating labeled RNA agonist (TLR8-RNA and ORN Sa19) for 15 minutes with RAGE expressing cells, the fluorescence signal from the RNA nearly completely co-localized with that derived from RAGE FL. In contrast, cells expressing RAGE ΔVC1 showed almost no surface binding of labeled RNA. Interestingly, non-stimulatory RNA (NS-RNA) was also recruited to RAGE FL but not RAGE ΔVC1 suggesting that, as observed for DNA, RNA binds to RAGE sequence-independently. As expected, labeled single stranded CpG 2006 bound to RAGE at the cell surface in a similar manner to RNA. Streptavidin-AlexaFluor488 addition to RAGE FL and RAGE ΔVC1 expressing cells in the absence of biotinylated nucleic acids failed to bind to cells. As anticipated, Western blot analysis showed that both cell lines expressed a similar amount of RAGE (FL or dVC1, **Fig. 4.4B**).

Figure 4.3 RNA binds to cells expressing full-length RAGE but not to cells expressing truncated RAGE lacking the V-C1 domain.
(A) Schematic representation of the RAGE-fluorescent protein fusion constructs used in FACS and confocal microscopy. (B) HEK293-XL cells stably expressing TLR7-HA or TLR8-HA alone (control) or together with RAGE FL or RAGE ΔVC1 fused to mCitrine were incubated at 37ºC for 15 min with streptavidin-AlexaFluor647 labeled biotinylated RNA (5 μM). Cells were incubated with streptavidin-AlexaFluor647 alone (1 μM) to control for binding specificity. Dashed lines are representative of non-stimulated cells. Data in (B) represents FACS plots from one experiment representative of three independent experiments summarized in (C) where data represents the mean ± SEM of median fluorescence intensities from three independent experiments. p*** < 0.0001.

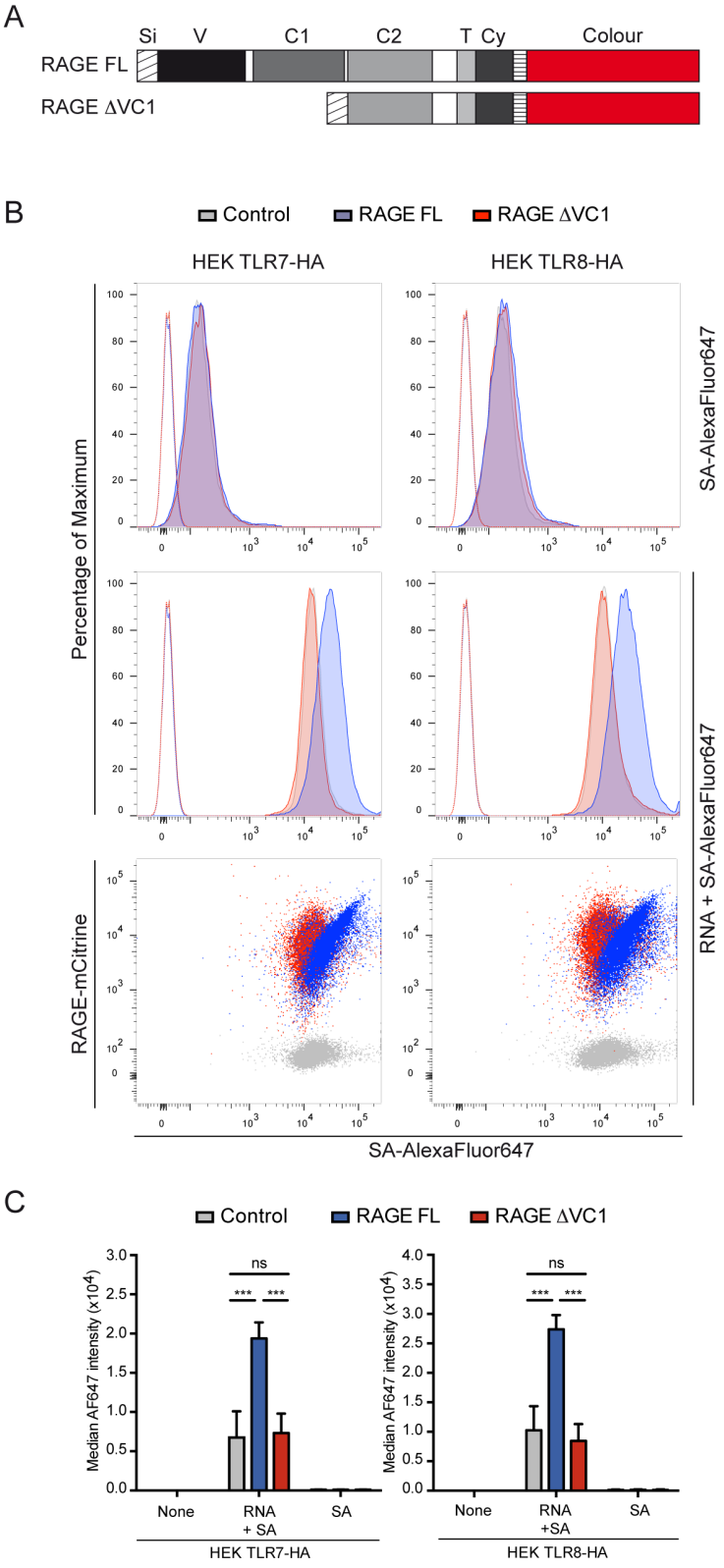

Figure 4.3 RNA binds to cells expressing full-length RAGE but not to cells expressing truncated RAGE lacking the V-C1 domain.
Note: For detailed legend, please see opposite page.

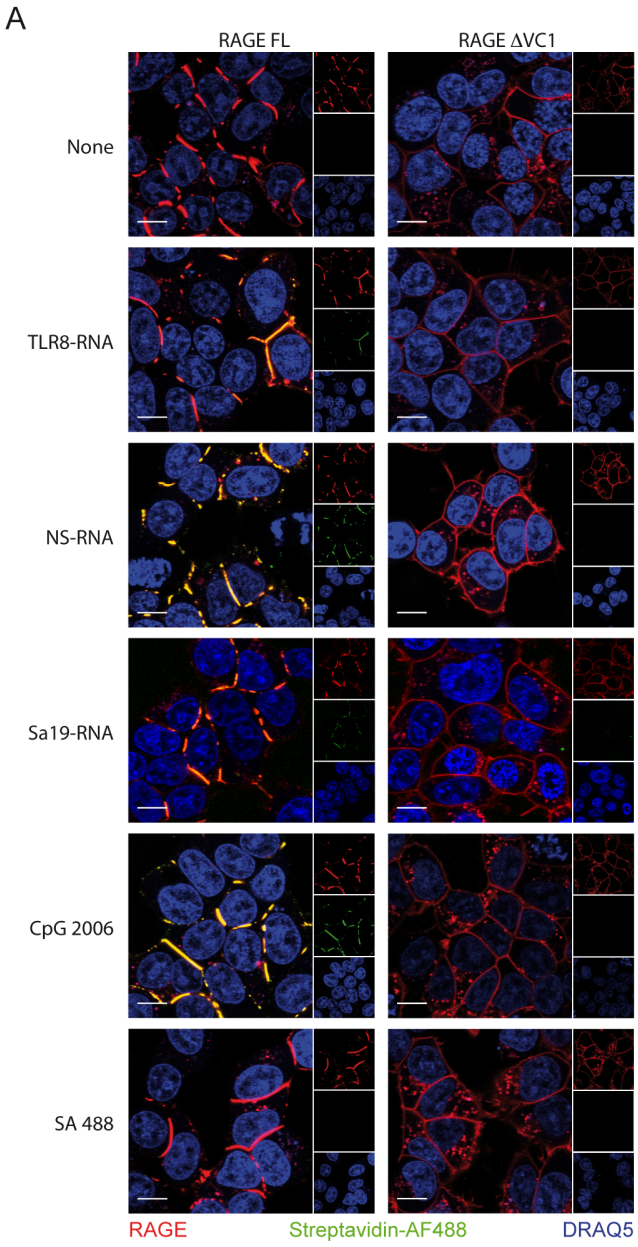

Figure 4.4 RNA binds to cells expressing full-length RAGE but not to cells expressing truncated RAGE lacking the V-C1 domain.
Note: For detailed legend, please see opposite page.

Together, these findings demonstrated that, as for DNA, RNA is recruited to RAGE at the cell surface through a sequence un-specific interaction of RNA with RAGE V-C1 domains.

4.3 RAGE increases RNA internalization

The previously published manuscript showed that RAGE expression induces increased internalization of DNA ((228), please see joined manuscript). The role of RAGE in RNA internalization was therefore further studied using confocal microscopy.

To this end, HeLa cell lines expressing RAGE FL or RAGE ΔVC1 fused to TagRFP were produced (**Fig. 4.5**). After 5 minutes incubation with labeled RNA, cells expressing RAGE FL already showed a strong recruitment of RNA to the plasma membrane that co-localized with RAGE FL forming rounded clusters (**Fig. 4.5A**). In contrast, cells expressing RAGE ΔVC1 did not show any plasma membrane recruitment of RNA. After 60 minutes incubation with labeled RNA, cells expressing RAGE FL presented a pronounced internalization of RNA in vesicles also positive for RAGE, while cells expressing RAGE ΔVC1 showed very little internalization of RNA.

To quantify RAGE-dependent internalization of RNA, analysis of the co-localization between the fluorescence signals corresponding to RNA and RAGE showed that the RNA signal strongly correlated to the RAGE signal in cells expressing RAGE FL (**Fig. 4.5B**). On the contrary, in cells expressing RAGE ΔVC1, the RNA signal showed only a very weak co-localization with RAGE.

Figure 4.4 RNA binds to cells expressing full-length RAGE but not to cells expressing truncated RAGE lacking the V-C1 domain.
(A) HEK293-XL cells stably expressing TLR8-HA together with RAGE FL or RAGE ΔVC1 fused to TagRFP were stimulated with biotinylated RNA or DNA labeled with streptavidin-AlexaFluor488 (5 µM) for 15 min at 37°C. DRAQ5 (1:2000) was used as nuclear staining. To control for binding specificity, cells were also incubated with streptavidin-AlexaFluor488 alone. The main images represent merged channels corresponding to RAGE-TagRFP (red), labeled RNA (green) and DRAQ5 (blue). Scale bars represent 10 µm. Split channels are represented on the right with the same color-coding. (B) HEK-XL TLR8-HA cells used in (A) were tested for RAGE FL- and RAGE ΔVC1-TagRFP expression by Western-blot. RAGE expression was detected using anti-TagRFP antibodies. Anti-β-actin antibodies were used as a loading control. Images are representative of at least two experiments.

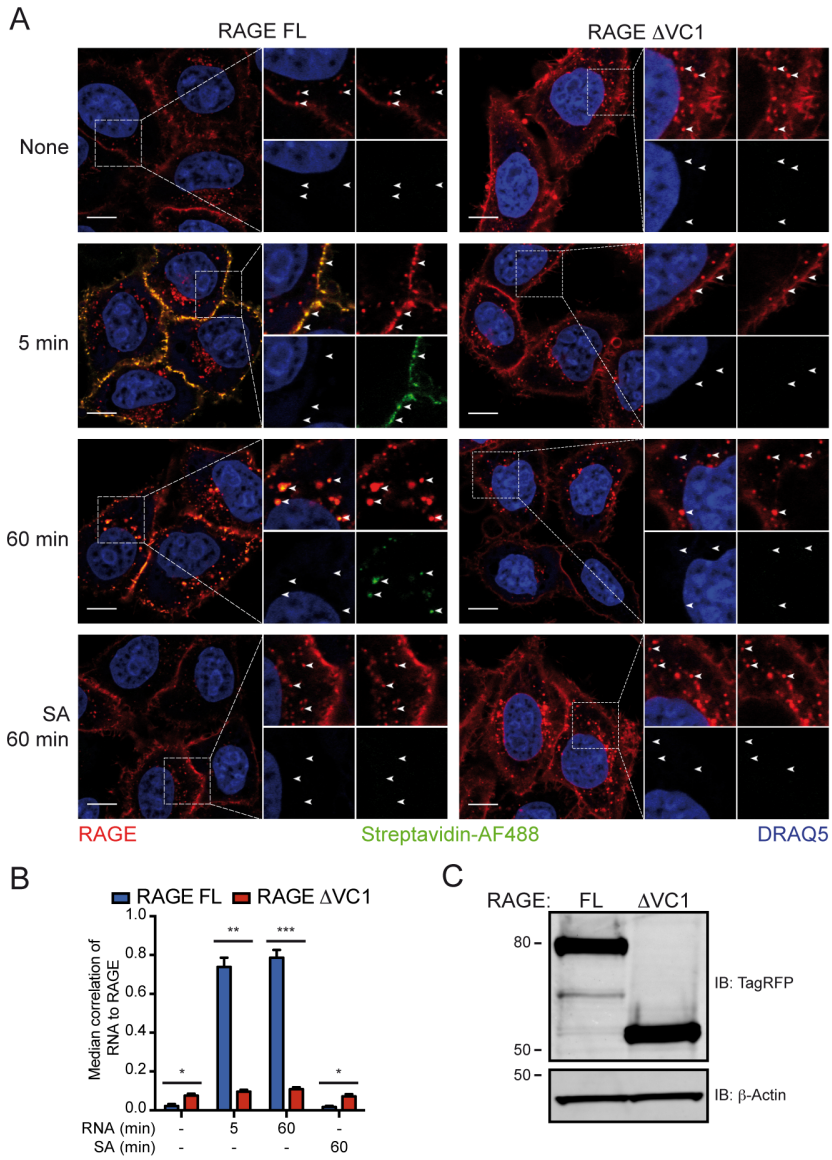

Figure 4.5 RAGE increases RNA internalization.
(A) HeLa cells stably expressing RAGE FL or RAGE ΔVC1 fused to TagRFP were stimulated with labeled RNA (5 μM) for 5 min or 60 min at 37°C prior to fixation and nuclear staining with DRAQ5. To control for binding specificity, cells were also incubated for 60 minutes with streptavidin-AlexaFluor488 alone (1 μM). Images are representative of one experiment performed three times. The main images represent merged channels corresponding to RAGE-TagRFP (red), labeled RNA (green) and DRAQ5 (blue). Scale bars are representative of 10 μm. A zoomed area of each image is represented on the right side, with merged channels (top left) and separated channels with same color coding. (B) Data represents mean ± SEM of median correlations of RNA to RAGE from three independent experiments. p* <0.05, p** <0.0005 and p*** <0.0001. (C) HeLa cells used for microscopy experiments were tested for RAGE-TagRFP expression by western-blot using anti-TagRFP antibodies. Anti-β-actin antibodies were used for loading control. Images are representative of at least two experiments.

Of note, both HeLa cell lines expressed similar amounts of RAGE (FL or ΔVC1) as shown by western-blot (**Fig. 4.5C**). Together these results suggested that, as for DNA, RAGE expression increases RNA internalization by acting as a transporter that could deliver RNA to RNA-sensing TLRs in endolysosomal compartments.

4.4 RAGE amplifies the TLR-dependent inflammatory response induced by RNA stimulation

Following the finding that expression of RAGE at the cell surface increases extracellular RNA recruitment and subsequent internalization, the impact of RAGE expression on the immune activation induced by RNA was evaluated. HEK293-XL cells expressing TLR7, TLR8 or TLR13 were transfected with a plasmid coding for full length RAGE or a control plasmid coding for mCherry.

Cells were concomitantly transfected with a reporter plasmid containing an NFκB target promoter flanked by the sequence coding for gaussia luciferase (**Fig. 4.6**). Following overnight RNA stimulation, NFκB activity of cells expressing RAGE was stronger than in cells transfected with the control plasmid (**Fig. 4.6A**). Interestingly, RAGE only increased the response of cells stimulated with TLR specific RNA agonists. Cells treated with non-stimulatory control RNA (shown previously to bind to RAGE at the cell surface, Fig. 4.3D) presented no increase of luciferase secretion regardless of RAGE expression. Furthermore, RAGE had no effect on R848 or IL-1β stimulation. This suggests that the immune response to stimulatory RNA is TLR dependent but can be increased by the presence of RAGE at the cell surface. Previous data (Fig. 3.1) showed that a minimum length of 15 nucleotides was necessary for DNA to bind to RAGE. The fact that RAGE did not affect TLR7 activation by R848 was therefore expected since R848 is a small synthetic compound. As control, RAGE expression in non-stimulated cells was detected by western-blot and showed a similar expression across all experiments (**Fig. 4.6B**). Endogenous expression of RAGE was not detectable in the HEK-XL cells used. These results demonstrate that RAGE, by recruiting RNA at the cell surface, amplifies the activation of TLRs by single stranded RNA and the ensuing pro-inflammatory NFκB pathway.

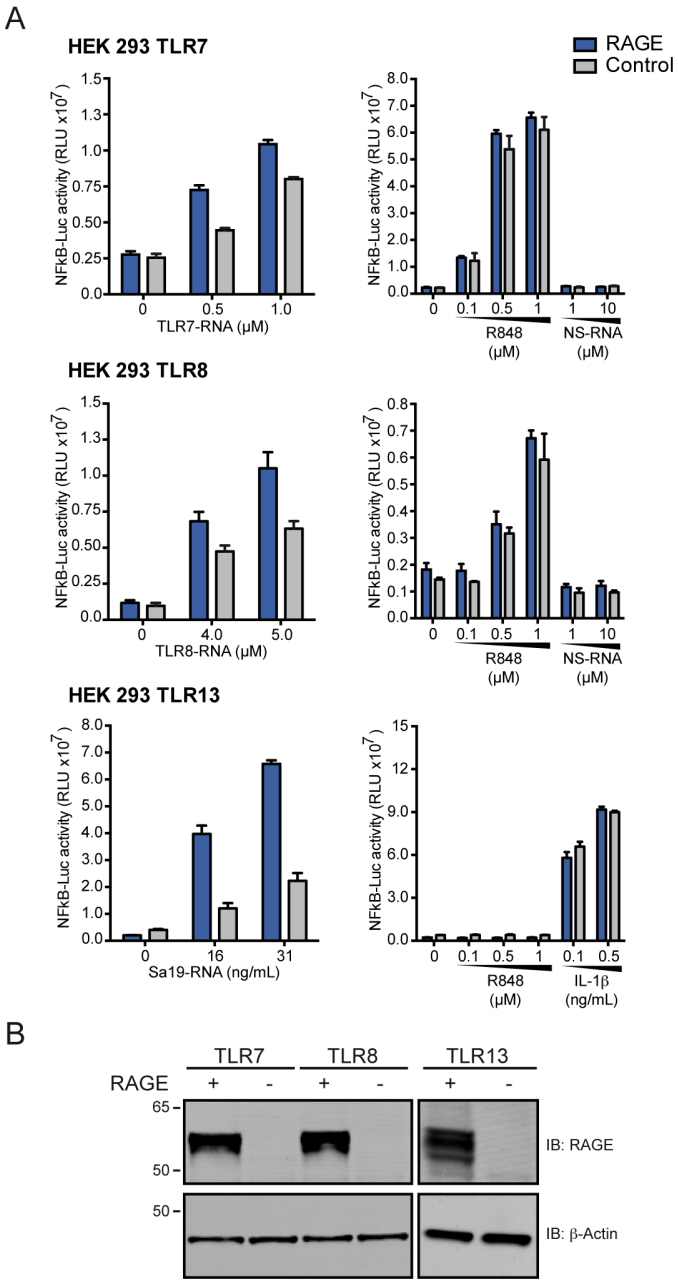

Figure 4.6 RAGE amplifies the TLR-dependent inflammatory response induced by RNA stimulation.

(A) HEK293-XL cells stably expressing human TLR7, TLR8 or mouse TLR13 were transiently transfected with an NFκB-driven luciferase reporter together with full length non-tagged human RAGE or mCherry as control. Cells were stimulated for 16h with a gradient of either specific RNA agonist (TLR7-RNA, TLR8-RNA, Sa19-RNA), R848, non-stimulatory RNA (NS-RNA) or IL-1β. After incubation, cell supernatants were harvested and luciferase activity measured. Data is shown as mean ± SD for triple experimental replicates and is representative of at least three similar experiments. (B) Unstimulated cells from (A) were lysed in LDS-loading buffer after harvest of supernatants. Samples were analyzed by Western-blotting for RAGE expression. Anti-β-actin antibodies were used for loading control. Images are representative of at least three separate experiments.

4.5 RAGE deficiency decreases the response of bone marrow cells to RNA

To test the relevance of RAGE-dependent RNA signaling, bone marrow was isolated from wild-type (WT) or RAGE deficient (KO) mice (**Fig. 4.7**).

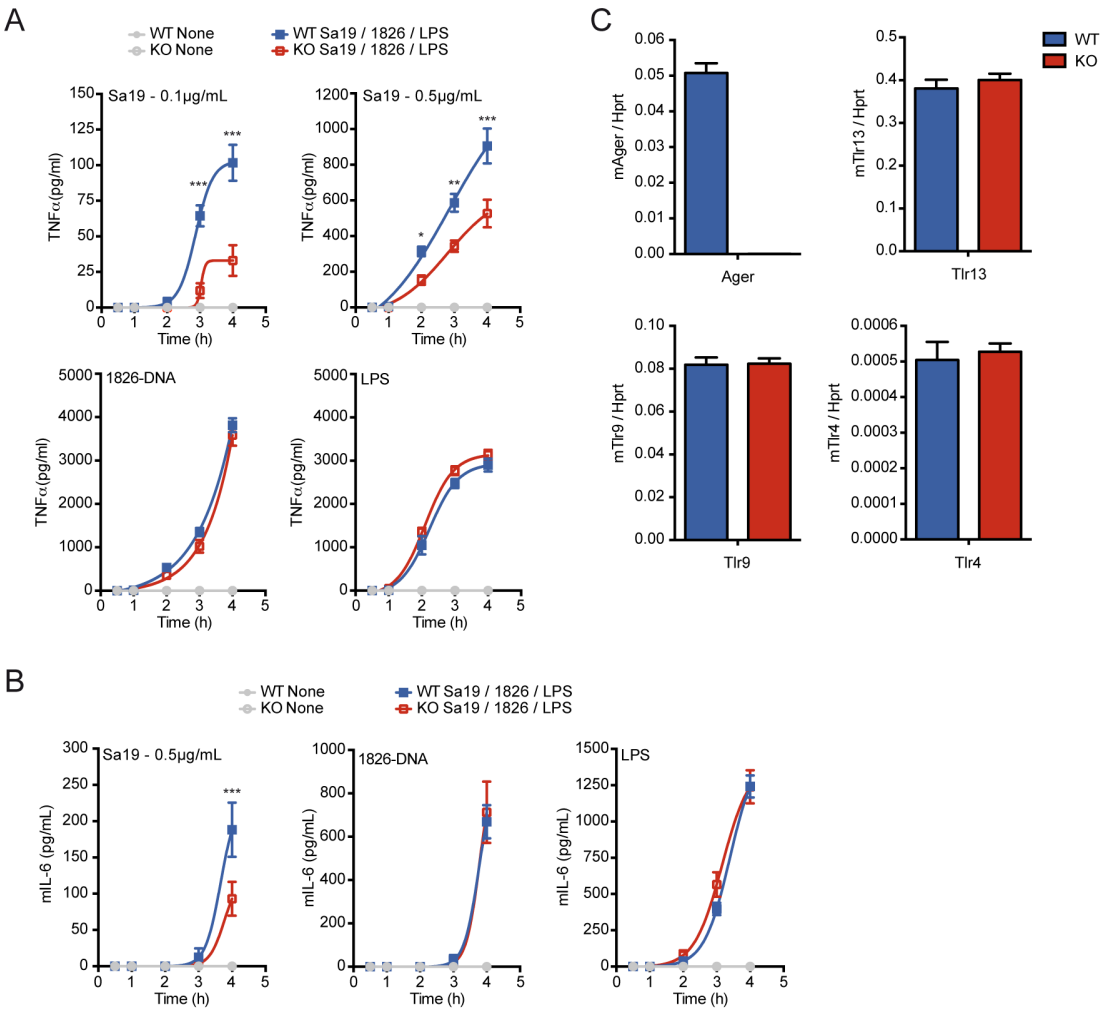

Figure 4.7 RAGE deficiency decreases the response of bone marrow cells to RNA.
(A-B) Bone marrow cells isolated from wild-type (WT) or RAGE knockout (KO) mice were stimulated with TLR13 agonist (Sa19-RNA, 0.1µg/mL and 0.5µg/mL), TLR9 agonist (ODN1826, 0.1 µM) or LPS (0.1µg/mL). TNFα (A) or IL-6 (B) secretion into supernatants was sampled over 4h at the indicated time points and quantified using HTRF. (C) Ager, Tlr4, Tlr9 and Tlr13 mRNA expression from non-stimulated cells was measured by qPCR. mRNA level of target genes was normalized to the Hprt mRNA level. Data in (A-C) represents mean ± SEM with n = 5 in both WT and KO groups. p* <0.05, p** <0.0005 and p*** <0.0001. Note: in (B) IL-6 secretion upon Sa19-RNA at 0.1µg/mL was non-detectable and therefore not represented.

Murine bone marrow has previously been used to study the effect of RAGE for DNA-HMGB1 complex sensing without need for differentiation (126). Here, bone marrow cells were directly stimulated after isolation either with TLR13 specific agonist (Sa19-RNA), type-B CpG DNA (1826-DNA) or LPS. TNFα and IL-6 content of supernatants was then sampled at indicated time-points. Interestingly, RAGE deficiency resulted in decreased and delayed TNFα secretion upon RNA stimulation (**Fig. 4.7A**, top panels), while DNA and LPS-induced cell activation were not affected (**Fig. 4.7A**, lower panels). Similar results were obtained with IL-6 cytokine levels (**Fig. 4.7B**). Indeed, RAGE deficiency resulted in decreased IL-6 secretion from cells stimulated with 0.5 µg/mL Sa19-RNA when compared to WT cells. However, cells stimulated with 0.1 µg/mL Sa19-RNA did not produce detectable IL-6 at the time points used here (data not shown). As seen with TNFα, IL-6 secretion from cells stimulated with either 1826-DNA or LPS showed no effect of RAGE deficiency. The lack of an effect of RAGE on the response of bone marrow cells to CpG-B DNA was expected since previously published data (126) indicated that complex formation of DNA with HMGB1 is necessary to detect an effect of RAGE deficiency when stimulating bone marrow cells.

To verify that the effect induced by RAGE deficiency upon RNA stimulation was not an artefact due to a possible RAGE-dependent modulation of TLR expression, RNA from unstimulated bone marrow cells was isolated and levels of Ager, Tlr4, Tlr9 and Tlr13 transcripts were measured by quantitative real-time PCR (**Fig. 4.7C**). The absence of Ager mRNA in knockout cells first confirmed the knockout of RAGE. Moreover, both WT and KO cells presented comparable levels of Tlr4, Tlr9 and Tlr13 transcripts indicating that RAGE does not regulate the gene expression of the TLRs stimulated as showed in Fig. 4.7A-B. Together, these results confirmed the importance of RAGE in cell surface sensing of extracellular RNA.

4.6 RAGE-dependent amplification of the immune response to stimulatory RNA is independent of direct RAGE signaling

Truncation of the cytoplasmic domain of RAGE had no negative effect on RAGE-induced increase of TLR9 activation by ODN 2006 (**Fig. 3.5**). The increase of NFκB induced by RAGE expression upon DNA stimulation was therefore independent of the known signaling pathways activated upon binding of other ligands to RAGE.

Consequently, involvement of the intracellular domain of RAGE in the RAGE-dependent increase of NFκB activation upon RNA stimulation was evaluated.

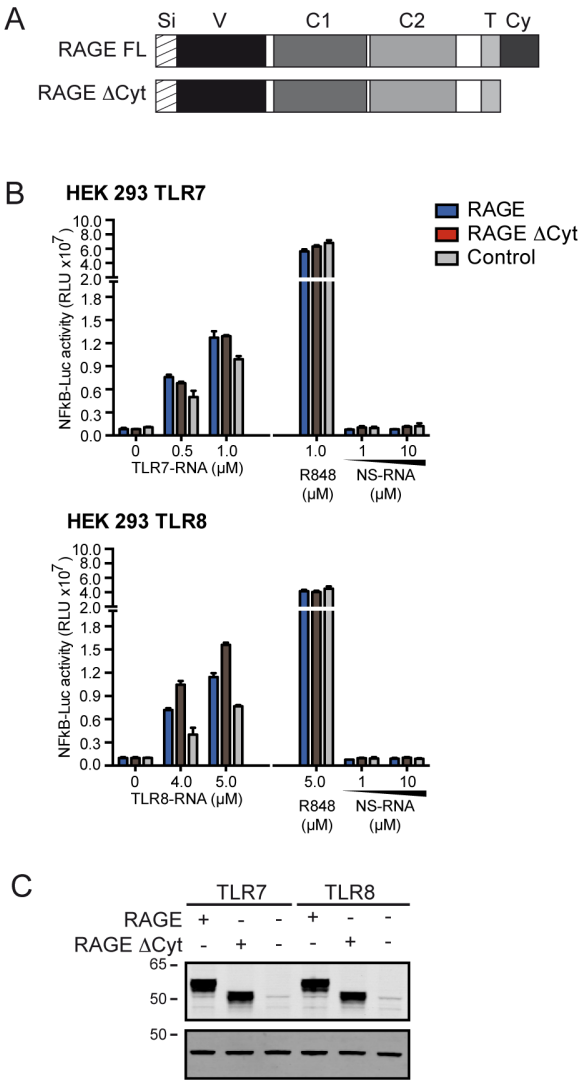

Figure 4.8 RAGE-dependent amplification of the immune response to stimulatory RNA is independent of direct RAGE signaling.
(A) Schematic representation of the RAGE full length (RAGE FL) or cytosolic domain truncated (RAGE ΔCyt) constructs used in (B). (B) HEK293-XL cells stably expressing human TLR7 or TLR8 were transiently transfected with an NFκB-driven luciferase reporter together with human RAGE FL, RAGE ΔCyt or mCherry as control. Cells were stimulated for 16h with a gradient of either specific RNA agonist (TLR7-RNA, TLR8-RNA), R848 or non-stimulatory RNA (NS-RNA). After incubation, cell supernatants were harvested and luciferase activity measured. Data is shown as mean ± SD for double experimental replicates and is representative of at least three similar experiments. (C) Expression level of RAGE and RAGE ΔCyt in unstimulated cells from (B) was assessed by Western blotting. Anti-β-actin antibodies were used for loading control. Images are representative of at least three separate experiments.

HEK293-XL cells expressing TLR7 or TLR8 were transfected with either RAGE full length (RAGE FL), cytoplasmic domain truncated RAGE (RAGE ΔCyt) or a control plasmid coding for mCherry (**Fig. 4.8A**). As for the previous experiment, cells were simultaneously transfected with a luciferase NFκB activity reporter. In TLR7 expressing cells, both RAGE FL and RAGE ΔCyt constructs induced a similar increase of NFκB activation upon RNA stimulation when compared to cells transfected with the control plasmid (**Fig. 4.8B**, top left panel). As expected, neither RAGE constructs had an effect on NFκB activation upon R848 or non-stimulatory RNA treatment. Curiously, in TLR8 expressing cells, RAGE ΔCyt further amplified the effect of RAGE FL upon RNA stimulation (**Fig. 4.8B**, lower left panel). Indeed, while RAGE FL induced an increase of NFκB activation similar to the one found before (Fig. 4.6A), RAGE ΔCyt induced an even stronger increase of gaussia luciferase release by cells stimulated with RNA. However, this amplification effect was absent in cells treated with R848 or non-stimulatory RNA. Of note, western-blot analysis of protein contents from unstimulated cells showed that both RAGE FL and RAGE ΔCyt were expressed at similar levels.

Together, these results indicated that RAGE-induced increase of NFκB activation is independent of direct RAGE downstream signaling. These results also implicated the existence of a different regulation mechanism for the effect of RAGE on RNA-induced TLR8 activation, which relies on RAGE cytoplasmic domain.

4.7 RAGE-induced RNA uptake depends on dynamin and actin polymerization

To identify the internalization mechanism involved in RAGE-dependent RNA uptake, HEK293-XL cells expressing TLR13 were transfected with either RAGE or a control plasmid coding for mCherry together with a luciferase NFκB activity reporter. Cells were subsequently treated with different inhibitors of cell internalization prior to stimulation with ORN Sa19 (**Fig. 4.9**). Cytochalasin D inhibits actin polymerization necessary to certain internalization pathways such as phagocytosis. Dynasore directly inhibits activation of dynamin, a major component of phagocytosis but also of clathrin- and caveolin-mediated endocytosis pathways. Finally, SecinH3 is a specific inhibitor of guanine nucleotide exchange factors (GEFs) necessary to recycle

adenosine diphosphate ribosylation factors (ARFs) GTPases such as ARF6, which regulate cytoskeletal organization and are involved in certain type of endocytic mechanisms. As shown previously, upon ORN Sa19 stimulation, when comparing to cells transfected with the control plasmid, RAGE expression induced an increase in luciferase expression induced by NFκB activation (**Fig. 4.9**)

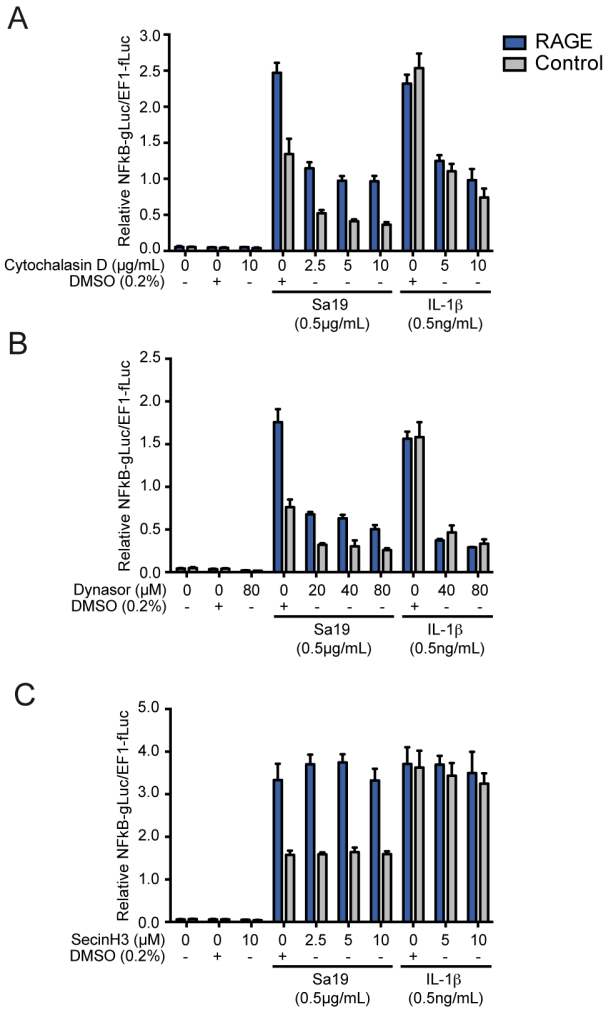

Figure 4.9 RAGE-induced RNA uptake depends on dynamin and actin polymerization.
(A-C) HEK293-XL cells stably expressing mouse TLR13 were transiently transfected with an NFκB-driven gaussia luciferase (gLuc) reporter and an EF-1-driven firefly luciferase (fLuc) reporter. Cells were concomitantly transfected with un-tagged human RAGE or mCherry as control. Cells were then incubated for 1h at 37°C in the presence of a gradient of endocytosis inhibitors (Cytochalasin D, Dynasor or SecinH3) or DMSO (0.2%, v/v). Cells were subsequently stimulated for 6h with Sa19-RNA (0.5µg/mL) or IL-1β (0.5ng/mL). After incubation, cell supernatants were harvested and cells were lysed in passive lysis buffer. Finally, gLuc and fLuc activity was measured from cell supernatants and lysates respectively. Data is shown as mean ± SD of fold gLuc/fLuc for triple experimental replicates and is representative of at least three similar experiments.

However, cells treated with Cytochalasin D or Dynasore showed a dose dependent decrease in RNA-induced luciferase expression when compared to DMSO treated cells (**Fig. 4.9A-B**). This inhibition affected both RAGE expressing cells and control cells. However, RAGE-induced increase of TLR13 activation subsisted even when inhibitors were used. Interestingly, the level of luciferase expression after treatment with Cytochalasin D and Dynasore was lower than the one found in control cells treated with DMSO, implicating that both RAGE-dependent and independent pathways were inhibited. Of note, TNFα stimulation showed no RAGE-dependent increase in NFκB activity but was also inhibited by Cytochalasin D and Dynasore (**Fig. 4.9A-B**). In stark contrast with the effect of Cytochalasin D or Dynasore, treatment with SecinH3 showed no inhibitory effect on ORN Sa19- and TNFα-induced NFκB activation and subsequent luciferase expression (**Fig. 4.9C**). Together this data showed that the RAGE-induced RNA uptake depends on dynamin activity and actin polymerization but not on ARFs. However, the RAGE-dependent RNA internalization seemed to depend on the same mechanisms involved in the RAGE-independent pathway. Further work, using a larger panel of inhibitors, will be necessary to determine whether a difference exists between RAGE-dependent and -independent RNA internalization mechanisms.

4.8 RAGE-RNA interaction, the curious case of TLR3 activation

To have a complete picture of the influence of RAGE on nucleic acid sensing by the endosomal TLRs, it was necessary to study the effect of RAGE expression on double stranded RNA (dsRNA) sensing and subsequent TLR3 activation. To this end, binding of a synthetic TLR3-specific dsRNA (TLR3-RNA, **Fig. 4.10A**, (230)) to the ectodomain of RAGE was assessed by EMSA (**Fig. 4.10B**, left panel).

First, electrophoretic mobility of synthetic TLR3-RNA labelled with Oregon green showed a more complex profile than seen before with ssRNA (Fig. 4.1). Indeed, TLR3-RNA alone yielded several bands with different mobility in the gel. Two main bands were visible (indicated by arrow heads) as well as a smeary pattern present in the lower part of the gel. This data would suggested that the TLR3-RNA molecules are able to form oligomers of heterogeneous size as suggested by the additional bands of lower electrophoretic mobility. This could be explained by the more complex

nature of this synthetic dsRNA. It is composed of “unit” sequences containing a 15-mer alignment sequence followed by a 35-mer poly (I) or poly (C) segment. One poly (I) unit is hybridized with one poly (C) unit through their complementary alignment sequences. Self-assembly of a dsRNA is permitted by hybridization of poly (I) segments with poly (C) segments (**Fig. 4.10A**).

Nevertheless, incubation of labelled TLR3-RNA with purified RAGE V-C1-C2 induced a dose-dependent shift in the mobility of TLR3-RNA in a manner similar to the one previously found with ssRNA. Moreover, with an increasing amount of V-C1-C2 protein, more bands appeared corresponding to RAGE-RNA complexes with even lower electrophoretic mobility. These indicated the capacity for RAGE ectodomains to form larger oligomers around dsRNA. However, in contrast to the previous results described for ssRNA, when labelled TLR3-RNA was placed in competition with unlabelled TLR3-RNA for binding to RAGE, only partial competition was observed. In fact, only the bands corresponding to the larger RAGE-dsRNA oligomers disappeared. This incapacity of un-labelled RNA to completely compete with the labelled RNA for binding to RAGE would suggest that the RNA oligomers can reorganise and form oligomers containing both labelled and unlabelled RNA molecules. This provided more labelled RNA oligomers that bound to RAGE, re-equilibrating the RAGE/RNA stoichiometry and decreasing the formation of higher size RAGE oligomers.

Furthermore, B-type DNA induced a dose dependent shift of the labelled TLR3-RNA to higher electrophoretic mobility comparable to those found with TLR3-RNA alone (**Fig. 4.10B**, right panel). Unlike TLR3-RNA, unlabelled DNA could not be integrated to the dsRNA oligomers and was therefore a better competitor. Although labelled TLR3-RNA formed more complicated structures of distinct electrophoretic mobility, this data demonstrated that, as for ssRNA, dsRNA could bind to RAGE ectodomain at a position close to the one used by DNA.

The effect of RAGE expression on dsRNA sensing was further characterised using HEK293 cells expressing human TLR3 (**Fig. 4.10C**). As done previously, cells were transfected with a plasmid coding for full length RAGE or a control plasmid coding for mCherry, together with a reporter plasmid containing an NFκB target promoter flanked by the sequence coding for gaussia luciferase. After 24h incubation at 37°C, cells were stimulated for 16h with either TLR3-RNA, a large synthetic mimetic of dsRNA, polyinosinic:polycytidylic acid (poly (I:C)), and IL-1β as RAGE- and TLR3-independent positive control. All stimuli induced robust gaussia luciferase expression

following NFκB activation. However, when compared to cells transfected with the control plasmid, RAGE expressing cells surprisingly showed a decreased luciferase activity upon stimulation with TLR3-RNA. This antagonistic effect of RAGE on dsRNA sensing was in opposition to the previous agonistic effect found for RAGE upon ssRNA stimulation.

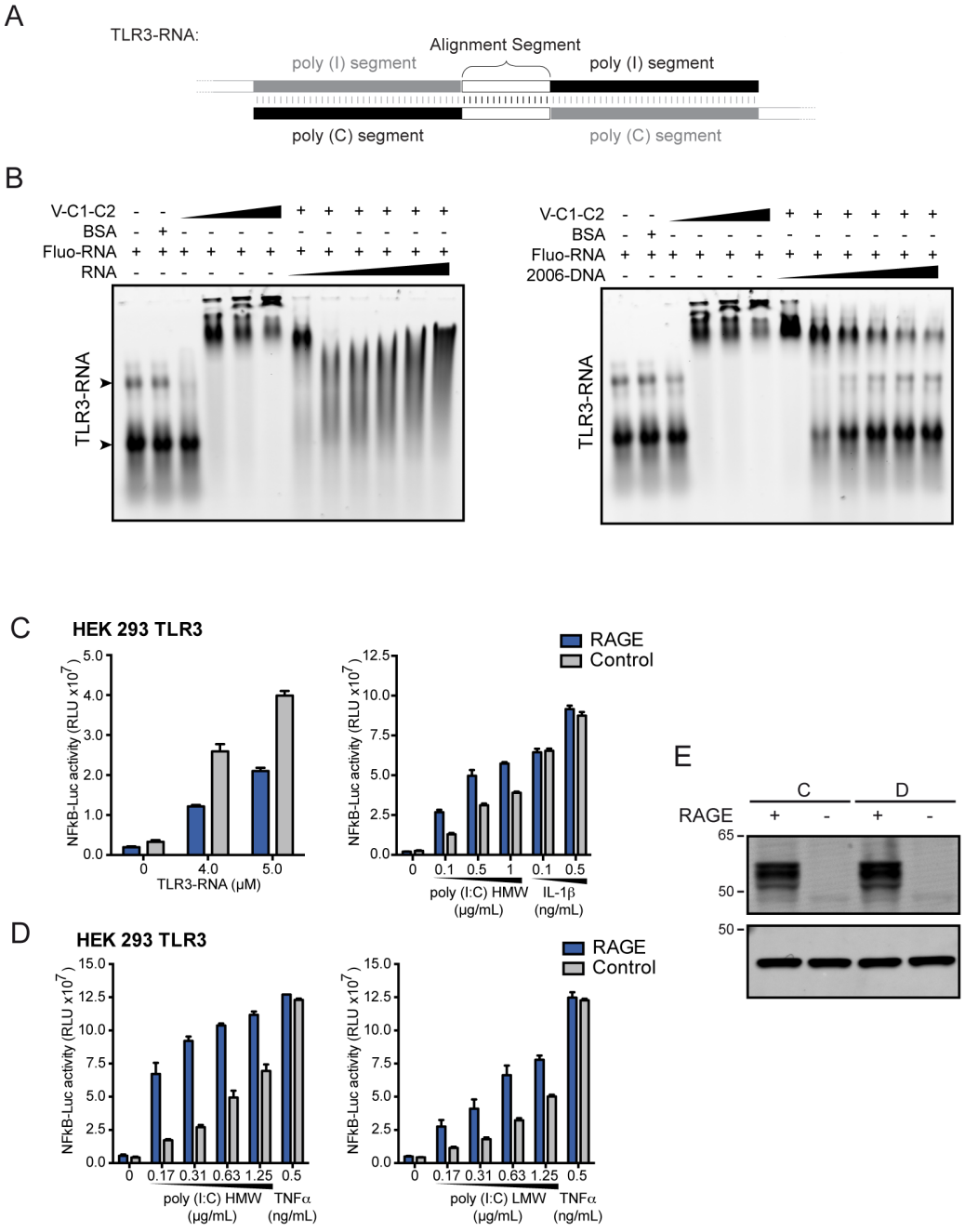

Figure 4.10 RAGE-RNA interaction, the curious case of TLR3 activation.
Note: For detailed legend, please see opposite page.

Interestingly, RAGE expression induced an increase of NFκB activation upon poly (I:C) stimulation similar to those found previously with ssRNA. Of note, RAGE expression had no effect on IL-1β induced NFκB activation.

This data suggested the existence of a singular mechanism following dsRNA binding to RAGE which negatively regulated TLR3 activation by dsRNA but not poly (I:C). One explanation for this heterogeneous effect of RAGE upon stimulation with TLR3-RNA and poly(I:C) is the difference of size. Indeed, the estimated size of the TLR3-RNA is 115 bases while the size of the high molecular weight poly (I:C) (poly (I:C) HMW) used in the previous experiment ranges between 1.5 to 8 kilobases. To test this hypothesis, TLR3 expressing HEK293 cells were transfected as described above and incubated at 37°C for 24h. Cells were subsequently stimulated with either high molecular weight (HMW) or low molecular weight (LMW, 0.2 to 1kb) poly (I:C) as well as with TNFα as RAGE-independent positive control. After 16h incubation, NFκB activation was assessed by measurement of gaussia luciferase activity (**Fig. 4.10D**). When compared to cells transfected with the control plasmid, RAGE expression induced an increased luciferase expression upon high molecular weight poly (I:C) stimulation. Unexpectedly, RAGE expression induced a similar increase in luciferase expression upon stimulation with low molecular weight poly (I:C). Of note, RAGE expression had no effect on TNFα stimulation. RAGE expression was similar in both experiments presented in figures 3.10C and D as shown by western-blot (**Fig. 4.10E**).

Figure 4.10 RAGE-RNA interaction, the curious case of TLR3 activation.
(A) Schematic representation of the structure of the TLR3-RNA agonist used in (B-C). (B) RAGE binding to TLR3-RNA agonist was assessed by electrophoretic mobility shift assay (EMSA). Oregon green labeled RNA oligonucleotides (Fluo-RNA, 250nM) were incubated with increasing amounts of recombinant RAGE extracellular domain (V-C1-C2; 1-10 μM) or BSA (10 μM). Increasing concentration of the corresponding un-labeled RNA (RNA, left panel) or ODN 2006 (2006-DNA, right panel) (0.63-40 μM) were added to constant concentration of Fluo-RNA (250 nM) and with RAGE (2.5 μM). Shift in labeled RNA mobility was measured by fluorescence detection. (C) HEK293-XL cells stably expressing human TLR3 were transiently transfected with an NFκB-driven luciferase reporter together with full length non-tagged human RAGE or mCherry (Control). Cells were stimulated for 16h with a gradient of either TLR3-RNA agonist, high molecular weight (HMW) poly (I:C), or IL-1β. After incubation, cell supernatants were harvested and luciferase activity measured. Data is shown as mean ± SD for triple experimental replicates and is representative of at least three similar experiments. (D) HEK293-XL cells stably expressing human TLR3 were transfected as in (C). Cells were then stimulated for 16h with a gradient of either high molecular weight (HMW) or low molecular weight (LMW) poly (I:C) and TNFα (0.5 ng/mL) as RAGE-independent control. After incubation, luciferase activity was measured in supernatants. (E) Unstimulated cells from (C-D) were lysed in LDS-loading buffer after harvest of supernatants. Samples were analyzed by Western-blotting for RAGE expression. Anti-β-actin antibodies were used for loading control. Images are representative of at least three separate experiments.

Together, this data showed opposite roles for RAGE towards real dsRNA and the mimetic poly (I:C) molecule. The difference of size did not explain these distinct effects since RAGE also amplified NFκB activation upon stimulation with a lower size form of poly (I:C), with a size comparable to the dsRNA.

4.9 Conclusion to Results – Part2

In this result segment, data showed that as for DNA, RNA binds to RAGE V-C1 domains in a sequence independent manner. The recruitment of ssRNA at the surface of cells expressing RAGE induced increased internalization that led to stronger immune activation. RAGE-dependent increase of the response to ssRNA was dependent on specific stimulation of endosomal TLRs. The cytoplasmic domain of RAGE was dispensable, indicating that direct RAGE signaling upon RNA-binding is negligible. RAGE internalization was essential and depended on dynamin and actin-polymerization. Finally, in stark contrast with its effect on ssRNA sensing, RAGE had an antagonistic effect on sensing of dsRNA by TLR3.

5. Discussion

Nucleic acid sensing is critical for the organism to detect infection. In the case of virus infection, it is often the only molecule detectable by the innate immune system. All nucleic acid specific PRRs are situated inside the cells, either in the cytoplasm or in the endosome. Nucleic acids mostly reach these receptors after internalization of the microorganism itself. This is the reason why much of the research done in the area of nucleic acid sensing has used liposome based transfection reagents to stimulate the diverse panel of intracellular receptors. However, it has become evident that extracellular nucleic acids exist and their concentration increases upon infection (92). Perhaps more importantly, extracellular nucleic acids of endogenous origin have been found in conditions of cell stress and tissue damage. Hence, comprehending how such extracellular molecules are internalized prior to being sensed by their putative receptor is an important step in the general understanding of the effects of infection or sterile injury on host immunity.
The work presented in this thesis supplies further clues on the mechanisms involved in extracellular nucleic acid entry and strengthens the crucial role of RAGE in the development of inflammation.

5.1 RAGE transports nucleic acids to their putative endosomal receptor

The finding that RAGE recruits nucleic acids at the surface of cells before insuring their internalization supports the idea of the existence of mechanisms that evolved to sense the abnormal presence of nucleic acids in the extracellular milieu. In fact, RAGE is not the only cell surface receptor capable of recruiting nucleic acids. Indeed, the endocytic C-type lectin receptor DEC-205 was previously shown to bind CpG-rich DNA at the surface of dendritic cells and B lymphocytes, thereby promoting a TLR9-dependent immune activation and cell maturation (9). Interestingly, as for RAGE, the CpG motif was dispensable for binding to DEC-205. This implicates a common sequence-unspecific mechanism for sensing extracellular DNA that would enable recognition of a larger array of nucleic acids from the surface, entrusting specificity to the intracellular PRR. The scavenger receptors SR-A and MARCO are

further examples of cell surface receptors for nucleic acid. Indeed, both were shown to bind CpG-rich DNA as well as RNA at the cell surface and promoted endosomal TLR stimulation (101, 102, 231).

Another common trait that these cell surface nucleic acid receptors seem to share with RAGE is the apparent absence of direct downstream signaling and the need of other putative signaling receptors for immune activation. Results presented in this thesis show that RAGE merely recruits nucleic acids at the cell surface and enhances their internalization. Use of a mutant of RAGE lacking the intracellular signaling domain showed a similar increase in NFκB activation upon stimulation with DNA or RNA than found with full-length RAGE. Furthermore, when expressed in cells lacking TLR9, RAGE alone produced no detectable immune activation. In a similar manner, cells expressing RAGE together with either TLR7 or TLR8 showed no responsiveness towards non-stimulatory RNA even though this RNA was found to bind efficiently to RAGE. Interestingly, a previous study reached a similar conclusion for S100B-dependent nitric-oxide (NO) production by microglial cells (232). Although RAGE was necessary for NO production upon stimulation with S100B, the cytosolic domain of RAGE was dispensable. It would thus appear that RAGE behaves in a 'double-standard' manner towards its ligands inducing either (1) a direct activation of pro-inflammatory pathways upon ligand binding or (2) the internalization of ligands such as nucleic acids towards a secondary receptor able to trigger downstream pro-inflammatory pathways.

Microscopy data presented in this thesis showed the concomitant cell internalization of RNA together with RAGE, further reinforcing the idea of RAGE acting as transporter of nucleic acid towards endosomal TLRs (**Fig. 5.1**). Interestingly, others had already pointed out the importance of RAGE internalization upon ligand binding (126, 224, 227). Here, experiments using endocytosis inhibitors demonstrated that RAGE-dependent RNA endocytosis requires actin polymerization and dynamin activity. Strikingly, these inhibitors repressed both RAGE-dependent and independent NFκB activation. This would suggest that nucleic acid internalization upon binding to various cell surface receptors is regulated by the same mechanisms. Even though this data provides a first clue about the mechanisms involved in RAGE-mediated nucleic acid internalization, a deeper study of these mechanisms will be necessary. The identification of the different players involved in nucleic acid endocytosis would provide a better picture of the involvement of RAGE in the

regulation of this crucial process and will help pinpoint potentially different receptor-mediated nucleic acid internalization pathways.

The surprising inhibiting effect of RAGE on TLR3 activation by dsRNA further underlined the need for a better understanding of the regulation mechanisms involved in RAGE internalization and trafficking (**Fig. 5.2**). The antagonistic effect of RAGE upon stimulation with dsRNA could be explained in several ways. One of the more plausible possibilities would be for RAGE trafficking to be directed towards a TLR7, TLR8 or TLR9 positive compartment while being unable to traffic towards TLR3 containing endosomes and therefore sequestrating dsRNA away from TLR3. In fact, some evidence exists for TLR3 distinctive trafficking that would sustain this theory. Indeed, several studies described the possible plasma membrane localization of TLR3 (233, 234). These studies suggest that TLR3 localization at the cell surface enables ligand binding and is a pre-requisite for TLR3 activation. Expression of RAGE at the cell surface and binding to dsRNA would thus compete with TLR3 for ligand binding and thereby antagonize TLR3-dependent immune activation (**Fig. 5.2**).

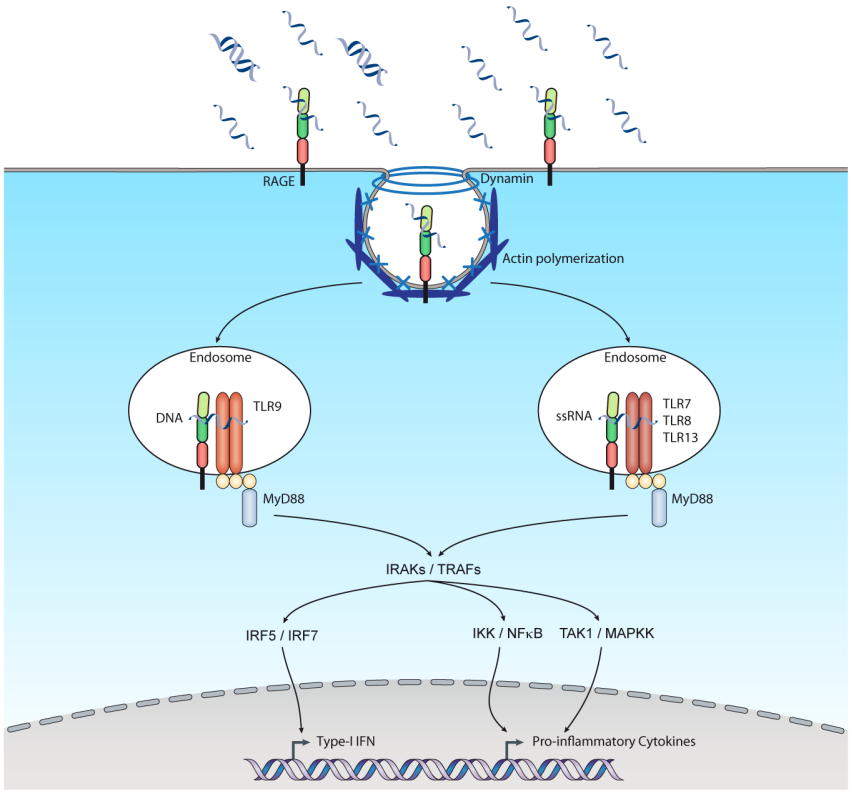

Figure 5.1 RAGE transports nucleic acids to their putative endosomal receptor. Binding of nucleic acids by RAGE at the cell surface promotes their internalization and trafficking towards TLR9 (DNA), TLR7, TLR8 and TLR13 (ssRNA). This amplified internalization of nucleic acids increases the activation of the TLRs and their downstream signaling cascades, resulting in a strengthened expression of type-I IFN and pro-inflammatory cytokines.

5.2 RAGE and cytosolic nucleic acid sensing

While investigating the role of RAGE in dsRNA sensing, a striking discrepancy appeared concerning the effect of RAGE on immune activation induced by either real dsRNA or its synthetic analog poly (I:C). In fact, while antagonizing TLR3 activation by specific dsRNA agonist, RAGE expression enhanced NFκB activation upon stimulation with poly (I:C) (**Fig. 5.2**). It is important to note that poly (I:C) has been described as an agonist of PRRs other than TLR3, namely MDA5 (235) and protein kinase R (PKR, (236, 237)). These cytosolic receptors are known inducers of downstream NFκB signaling. Hence, upon poly(I:C) treatment, RAGE might play a similar role to the one previously described for stimulation of TLR7, TLR8 and TLR13 by ssRNA. RAGE would increase dsRNA internalization and, following transfer to the cytoplasm, would promote activation of MDA5 or PKR (**Fig. 5.2**). A recent study supports this hypothesis. Indeed Liu and colleagues recently found a role for RAGE in activation of AIM2 by the HMGB1-poly(dAdT) complex (238).

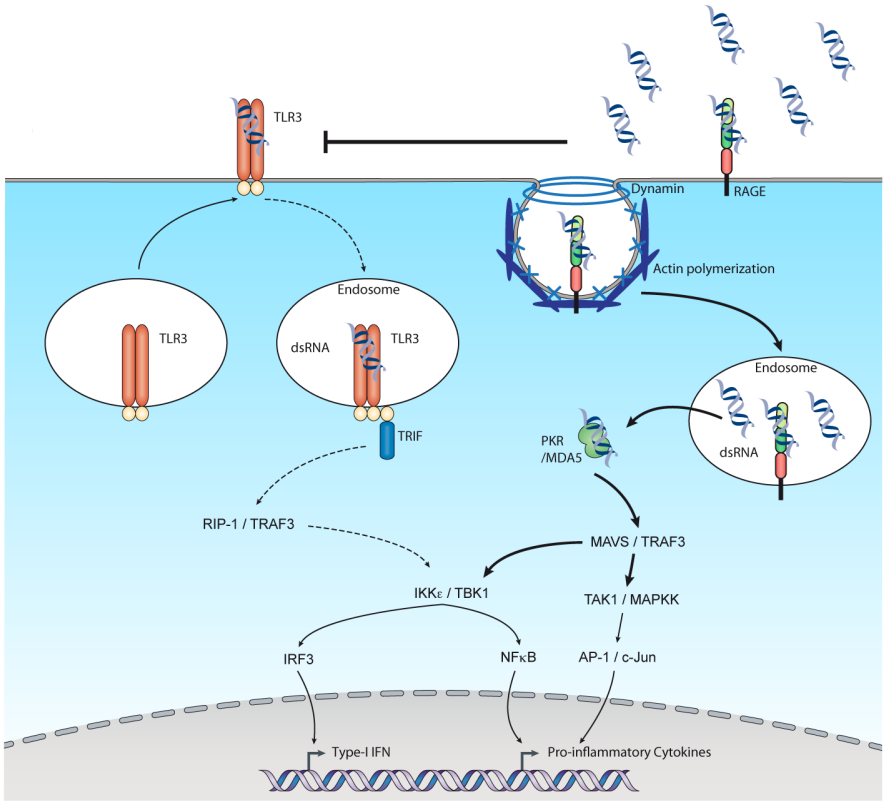

Figure 5.2 RAGE inhibits dsRNA-induced TLR3 activation and favors stimulation of cytosolic receptors.
The presence of RAGE at the cell surface competes with TLR3 for ligand binding and thereby inhibits TLR3 activation and its downstream signaling. While antagonising TLR3, the cell surface binding of dsRNA to RAGE might promote the activation of cytosolic nucleic acid receptors such as PKR and MDA5.

The authors show that RAGE expression amplifies early activation of AIM2. This would indicate that RAGE-dependent activation of cytosolic receptors by nucleic acid is possible. The activation of such cytosolic receptors by extracellular RNA through RAGE will therefore deserve further attention in the future.
Interestingly, recent publications presented DNA-RNA hybrids as agonists of TLR9 (239) and cGAS-STING (240). When placed in parallel with the results presented in this thesis, these publications call for further investigation into the role of RAGE in sensing these byproducts of viral replication and so for both TLR9- and cGAS-dependent pathways.

5.3 HMGB1, RAGE and nucleic acids

As described before, RAGE is a crucial sentinel for tissue damage and cellular stress. Indeed, RAGE senses many molecules released by damaged cells such as S100 proteins and HMGB1. HMGB1 is an important nuclear associated protein that acts as alarmin when actively or passively released by stressed cells (152, 241-243). HMGB1 has been shown to trigger inflammation in the context of infection and sepsis, but perhaps most importantly in the context of sterile tissue damage such as are found in reperfusion injury or trauma. HMGB1 triggers inflammation upon binding to several receptors such as TLR2, TLR4, IL-1R and RAGE. Interestingly, HMGB1 often interacts with these receptors while in complex with other molecules that are the primary ligand for the targeted receptor. In fact, HMGB1 was shown to interact with nucleosome or LPS thereby activating TLR2 or TLR4 respectively (244, 245). HMGB1 was also found to increase IL-1R avidity for IL-1β and thereby increase IL-1R activation (246). As mentioned earlier, similar results were found for HMGB1 in complex with DNA where RAGE-dependent inflammatory pathways were highly amplified by the presence of HMGB1 (126, 238). Importantly, HMGB1 is known to bind RNA and was previously shown to enhance the pro-inflammatory potential of RNA to activate both endosomal TLRs and cytosolic RNA receptors (247, 248). Data presented in this thesis together with the numerous studies implicating HMGB1 with DNA and RNA sensing, all point towards the function of the collaboration of RAGE and HMGB1 in amplifying sensing of DNA and RNA. While the cooperation of HMGB1 with RAGE in the exacerbation of DNA-induced TLR9 and AIM2 activation is

known, no data has yet been published that makes the link between HMGB1-RNA binding and RAGE-dependent internalization prior to a pro-inflammatory immune response. It would therefore be of great importance to test the effect of HMGB1 in the system presented herein.

5.4 RAGE, nucleic acid and disease development

Extracellular nucleic acids have been implicated in many inflammatory settings such as infection and auto-inflammatory diseases (249). One of the best described pathologies mediated by extracellular nucleic acids is systemic lupus erythematosus (SLE). This rare autoimmune disease involves the production of antibodies against the host's own nucleic acids when these are released in the extracellular milieu after cell apoptosis or necrosis. Cell death occurs in both physiological and pathological settings. The development of autoimmune diseases such as SLE therefore depends on multifactorial events that will trigger more cell death or a defective clearance of generated cell debris. Nevertheless, production of auto-antibodies allows formation of immune complexes (ICs) that contain nucleic acids and facilitates their entry into the cells leading to the activation of endosomal or cytosolic nucleic-acid sensors (249, 250). Entry of these immune complexes depends on cell surface receptors which, depending on the cell type, can be Fc-receptors, the B-cell receptor or RAGE. Indeed, as previously mentioned, RAGE is involved in the sensing of ICs that not only contain DNA but also contain HMGB1 (126). Interestingly, SLE has been shown to not only depend on the formation of DNA-ICs and TLR9 activation but also on the presence of extracellular RNA (251). In fact, TLR7 was shown to be an important mediator of inflammation during SLE and evidence pledges for the importance of RNA and RNA-containing immune complexes in the development of SLE. TLR deficiency studies found a surprising exaggeration of pDC activation and IFN-α release in TLR9$^{-/-}$ lupus mice (252). On the contrary, TLR7 deficiency or inhibition decreased the immune activation in these mice (252, 253). Furthermore, TLR7 expression in B cells was shown to exacerbate anti-RNA antibody production and disease in SLE mice (254). This data argues for the importance of extracellular RNA and RNA-ICs in the development of SLE. Together with the present results demonstrating RAGE as receptor for RNA, these studies underline the idea of a possible role for RAGE in the internalization of RNA-ICs and increase of TLR7-

dependent immune activation. However, to date, there is no published data proving this hypothesis. It would therefore be of interest to study RAGE involvement in the deleterious effect of RNA-IC in SLE.

The source of nucleic acids involved in autoimmune disease has mainly been attributed to a nuclear origin. However, on their own, endogenous nucleic acids are considered to be weak activators of the endosomal TLRs because of their modified state (255-257). This is why it is commonly believed that endogenous nucleic acids must be associated with other factors such as HMGB1 or other nuclear proteins to induce autoimmune responses. At present, how such endogenous nucleic acids acquire the potential to activate TLRs is still unclear. Providing clues on how this might happen, drug-induced SLE was found after use of hydralazine and procainamide, drugs that were shown to inhibit DNA methylation (258). On the other hand, mitochondrial RNA (mtRNA) possesses very little pseudouridine and 2'-O-methylated nucleosides, which makes them similar to bacterial RNA. Interestingly, mtRNA was shown to potentiate TLR-dependent immune responses (257). During tissue damage, it is therefore likely that mtRNA would act as a danger signal with a potential involvement of RAGE. This is supported by data showing RAGE contribution to the TLR9-depedent immune recognition of mitochondrial DNA in complex with Mitochondrial Transcription Factor A (TFAM, (259))

The role of extracellular RNA as pro-inflammatory danger signal was recently reinforced by a study showing that the micro-RNA (miRNA) let-7 is a potent TLR7 agonist (260). In fact, in Alzheimer's patients, let-7 was found to be increased in the cerebrospinal fluid. Moreover, let-7 was shown to activate TLR7 in neurons and induced neurodegeneration. Importantly, RAGE is expressed in neurons were it was shown to mediate part of Aβ deleterious effects (124, 149, 160). Together with the data presented in this thesis, the study by Lehmann and colleagues calls for further investigation of RAGE binding to let-7 and its involvement in TLR7 activation.

5.5 RAGE and cell to cell communication

Not all extracellular nucleic acids signal danger or tissue damage. Since only 1-2% of the mammalian genome is translated to proteins, great interest went into

understanding the function of such a large array of transcript deprived from translational function. Several classes of non-coding RNA (ncRNA) species ranging from 20 nucleotides to more than 200 nucleotides have been shown to regulate a large array of cellular mechanisms from gene expression to protein function (261, 262). These include the miRNA previously mentioned but also small interfering RNA (siRNA) and long non-coding RNA (lncRNA). Interestingly, certain ncRNAs were found to be secreted by cells (263). Astonishingly, plant miRNAs were also found to affect mammalian cells upon ingestion and proved that miRNAs may be involved in cross-kingdom regulation (264). However, most of the data on the existence of extracellular ncRNA is focused on miRNA and shows that such extracellular RNA are packaged into extracellular vesicles (EVs) (265, 266). Nevertheless, some evidence exists that suggests a possible regulatory effect of EV-free ncRNA present in the extracellular milieu. Initial evidence has been drawn from more primitive kingdoms. For example, the transmembrane protein SID-1 has previously been shown to mediate entry of siRNA into nematode cells enabling systemic gene silencing as a general gene expression regulation mechanism (267). SID-1 homologue proteins were later found to function in a similar way by promoting entry of siRNA and dsRNA into insect cells (268) or mammalian cells (269). Both plants and nematodes use the transfer of non-coding RNA from cell to cell as a communication mechanism enabling systemic control of gene expression (270). Furthermore, recent analysis of human plasma and blood showed the presence of EV-free miRNA (271-274). Vickers and colleagues found that plasma miRNA could be associated with high-density lipoproteins (HDL) and thereby be delivered to cells (274). Other studies found that the majority of extracellular miRNA bound to protein complexes rather than EVs. These protein complexes had a protecting effect for miRNA against RNases. For example, extracellular miRNAs were found to associate with proteins of the RNA-induced silencing complex (RISC), Argonaute 1 and 2 (Ago1/2) (271-273). These studies therefore reveal the emerging importance of ncRNA as tool for cell-to-cell communication. As mentioned earlier with the example of HMGB1, the protection of extracellular RNA by proteins could potentiate their stability and upon binding to RAGE further amplify their effect. Together with the studies described in this paragraph, ncRNA in complex with chaperone proteins such as Ago1 or Ago2 could be internalised through interaction with RAGE. Hence, the role of RAGE in such long-distance communication mechanisms would also be worth of further attention.

5.6 Conclusion and future directions

The localization of the nucleic acid sensing PRRs to the cytoplasm or the endolysosomal compartment is thought to help the organism to differentiate between self and non-self nucleic acids. This compartmentalization of signaling receptors ensures that these PRRs are only triggered under conditions where ligands achieve access to the subcellular compartment. However, under conditions of infection or tissue damage, mechanisms must be in place for the host to initiate an immune response. Thus, the presence of nucleic acid sensors or nucleic acid delivery molecules at the cell surface would sensitize cells and allow a decrease in the cellular activation threshold, enabling a faster or more pronounced response against pathogen-derived nucleic acids (**Fig. 5.3**). This model of an adjustable cellular threshold is in agreement with previous reports implicating the involvement of RAGE in sepsis or sterile injury but also in auto-inflammatory pathologies such as diabetes and atherosclerosis. Indeed, at steady state, the expression of RAGE in immune cells or vascular endothelial and smooth muscle cells is low but can be increased in pathologies where RAGE ligands accumulate.

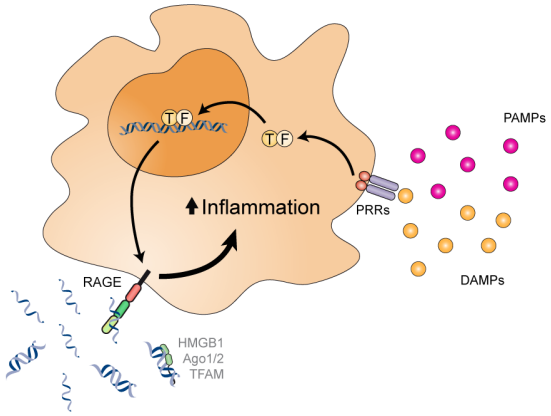

Figure 5.3 RAGE lowers the cellular threshold for immune activation by nucleic acids.
Upon cellular stress induced by infection or tissue damage, extracellular PAMPs and DAMPs stimulate RAGE expression through activation of PRRs and downstream NFκB or AP-1 transcription factors (TF). Increased expression of RAGE sensitizes the cells by lowering the threshold of immune activation induced by RAGE ligands such as extracellular nucleic acids resulting in increased inflammation.

The first hint of the involvement of RAGE in nucleic acid-derived immune stimulation came from the finding that RAGE binds DNA/HMGB1-containing immune complexes and thereby promotes their internalization and TLR9-dependent immune response.

Data presented in the first result part of this thesis, which was part of collaborative work published in 2013, further implicated RAGE in DNA sensing. These results showed that DNA can directly bind to RAGE and thereby is recruited at the surface of cells expressing RAGE. This promoted cell internalization of such DNA and a stronger immune activation upon stimulation with TLR9-specific DNA agonists (**Fig. 5.1**). RAGE was also found to interact directly with TLR9 and this interaction was amplified by DNA stimulation. The increase of RAGE expression found during the onset of inflammation could therefore act as regulatory switch enabling immune cells to lower their threshold of activation by microbial nucleic acids. This system might have evolved to reduce the risk of secondary infection.

Since RAGE sensing of DNA is controlled by sequence-unspecific interaction with the DNA phosphate backbone, RNA binding to RAGE and similar amplification of RNA-sensing appeared probable. In fact, the results presented in the second part of this thesis demonstrated this hypothesis to be true (**Fig. 5.1**). RNA was recruited to cells expressing RAGE and this strikingly promoted RNA internalization by these cells. Furthermore, in a similar manner to DNA, RAGE over-expression induced an increase of TLR7-, TLR8- or TLR13-dependent NFκB activation. This was confirmed in primary cells isolated from mouse bone marrow, where RAGE deficiency induced a marked decrease of TNFα and IL-6 secretion induced by specific stimulation of TLR13. Surprisingly, while the effect of RAGE on stimulation of all ssRNA-specific TLRs was very similar, the effect of RAGE on dsRNA proved to be different. Indeed, RAGE expression had an antagonistic effect on TLR3 specific activation. However, when using a less specific dsRNA analog, RAGE expression induced an increase of immune activation very similar to the one found with ssRNA. These results shed some light upon the importance of RAGE trafficking for regulation of endosomal TLRs activity and opened the door for a possible RAGE-dependent regulation of cytosolic RNA sensing.

In light of the role of HMGB1 in DNA sensing by RAGE, and knowing that HMGB1 is a published RNA binding protein that was shown to increase endosomal TLR activation, it would be crucial to study the effect of HMGB1 on RNA sensing through RAGE. Since HMGB1 is an important alarmin released by cells upon stress or damage, the role of the HMGB1-RAGE axis in nucleic acid sensing attests again to the function of RAGE as a central switch dropping the threshold of the immune activation in conditions of inflammation and cellular stress (**Fig. 5.3**).

Furthermore, by demonstrating the binding of extracellular RNA to RAGE, the results presented here could suggest the importance of investigating possible new roles of RAGE involving extracellular RNA sensing as a mechanism not only promoting anti-microbial immune response but also cell-to-cell communication via internalization of regulatory non-coding RNA molecules of microbial or endogenous origin.
It would also be critical to better characterise the mechanisms involved in RAGE internalization and trafficking. Is RAGE internalised upon ligand binding or is it merely following recycling pathways independently of ligand? Where is RAGE trafficking following endocytosis? Is the trafficking route dependent on the nature of RAGE ligands? What mechanisms other than actin polymerisation and dynamin activity control RAGE internalization? These questions must be answered in order to better comprehend the diverse function of RAGE in immune activation or potentially in cell communication.

As discussed earlier, RAGE was previously demonstrated to be involved in several pathologies where it was shown to promote the chronic and aberrant activation of the immune system. The data presented here further supports this fact. Targeting of RAGE by pharmacological molecules could therefore be of interest with the aim of blocking these RAGE-dependent aberrant inflammation mechanisms. Soluble forms of RAGE or RAGE-specific antibodies have been used before to block RAGE-ligand binding and proved some degree of efficiency (123, 218-220, 275). Some already optimise the production of recombinant sRAGE with a use for therapy as the end-goal (276, 277). In parallel with such a therapeutic strategy, the use of non-stimulatory nucleic acid such as the one used in experiments presented in this thesis could potentially be considered since nucleic acids are already in clinical use (278). These would target RAGE and thus inhibit ligand binding and alleviate RAGE-induced aggravation of inflammation.

In conclusion, the data presented herein established RAGE as a new cell surface sensor for nucleic acid, which promotes their recruitment and internalization into cells, thereby enhancing activation of the nucleic acid-specific TLR receptors. These findings reinforce the idea of RAGE as a central mediator of inflammation and will hopefully foster investigation into possible new roles of RAGE involving extracellular DNA/RNA sensing as a mechanism to activate either anti-microbial or danger-associated immune responses or even to promote cell-to-cell communication. Hence, the presented findings could promote RAGE as pharmacological target against devastating diseases such as Alzheimer's disease, diabetes, SLE and cancer.

6. References

1. Jandhyala, S. M., R. Talukdar, C. Subramanyam, H. Vuyyuru, M. Sasikala, and D. Nageshwar Reddy. 2015. Role of the normal gut microbiota. *World J. Gastroenterol.* 21: 8787–8803.
2. Bardoel, B. W., E. F. Kenny, G. Sollberger, and A. Zychlinsky. 2014. The balancing act of neutrophils. *Cell Host Microbe* 15: 526–536.
3. Brinkmann, V., U. Reichard, C. Goosmann, B. Fauler, Y. Uhlemann, D. S. Weiss, Y. Weinrauch, and A. Zychlinsky. 2004. Neutrophil extracellular traps kill bacteria. *Science* 303: 1532–1535.
4. Janeway, C. A. 2013. *Pillars article: approaching the asymptote? Evolution and revolution in immunology. Cold spring harb symp quant biol. 1989. 54: 1-13*. :4475–4487.
5. Poltorak, A., X. He, I. Smirnova, M. Y. Liu, C. Van Huffel, X. Du, D. Birdwell, E. Alejos, M. Silva, C. Galanos, M. Freudenberg, P. Ricciardi-Castagnoli, B. Layton, and B. Beutler. 1998. Defective LPS signaling in C3H/HeJ and C57BL/10ScCr mice: mutations in Tlr4 gene. *Science* 282: 2085–2088.
6. Qureshi, S. T., L. Larivière, G. Leveque, S. Clermont, K. J. Moore, P. Gros, and D. Malo. 1999. Endotoxin-tolerant mice have mutations in Toll-like receptor 4 (Tlr4). *The Journal of experimental medicine* 189: 615–625.
7. Hoshino, K., O. Takeuchi, T. Kawai, H. Sanjo, T. Ogawa, Y. Takeda, K. Takeda, and S. Akira. 1999. Cutting edge: Toll-like receptor 4 (TLR4)-deficient mice are hyporesponsive to lipopolysaccharide: evidence for TLR4 as the Lps gene product. *J Immunol* 162: 3749–3752.
8. Robinson, M. J., D. Sancho, E. C. Slack, S. LeibundGut-Landmann, and C. Reis e Sousa. 2006. Myeloid C-type lectins in innate immunity. *Nat Immunol* 7: 1258–1265.
9. Lahoud, M. H., F. Ahmet, J.-G. Zhang, S. Meuter, A. N. Policheni, S. Kitsoulis, C.-N. Lee, M. O'Keeffe, L. C. Sullivan, A. G. Brooks, R. Berry, J. Rossjohn, J. D. Mintern, J. Vega-Ramos, J. A. Villadangos, N. A. Nicola, M. C. Nussenzweig, K. J. Stacey, K. Shortman, W. R. Heath, and I. Caminschi. 2012. DEC-205 is a cell surface receptor for CpG oligonucleotides. *Proc Natl Acad Sci USA* 109: 16270–16275.
10. Yoneyama, M., M. Kikuchi, T. Natsukawa, N. Shinobu, T. Imaizumi, M. Miyagishi, K. Taira, S. Akira, and T. Fujita. 2004. The RNA helicase RIG-I has an essential function in double-stranded RNA-induced innate antiviral responses. *Nat Immunol* 5: 730–737.
11. Yoneyama, M., M. Kikuchi, K. Matsumoto, T. Imaizumi, M. Miyagishi, K. Taira, E. Foy, Y.-M. Loo, M. Gale, S. Akira, S. Yonehara, A. Kato, and T. Fujita. 2005. Shared and unique functions of the DExD/H-box helicases RIG-I, MDA5, and LGP2 in antiviral innate immunity. *J Immunol* 175: 2851–2858.
12. Hornung, V., A. Ablasser, M. Charrel-Dennis, F. Bauernfeind, G. Horvath, D. R. Caffrey, E. Latz, and K. A. Fitzgerald. 2009. AIM2 recognizes cytosolic dsDNA and forms a caspase-1-activating inflammasome with ASC. *Nature* 458: 514–518.
13. Unterholzner, L., S. E. Keating, M. Baran, K. A. Horan, S. B. Jensen, S. Sharma, C. M. Sirois, T. Jin, E. Latz, T. S. Xiao, K. A. Fitzgerald, S. R. Paludan, and A. G. Bowie. 2010. IFI16 is an innate immune sensor for intracellular DNA. *Nat Immunol* 11: 997–1004.
14. Ablasser, A., M. Goldeck, T. Cavlar, T. Deimling, G. Witte, I. Röhl, K.-P. Hopfner, J. Ludwig, and V. Hornung. 2013. cGAS produces a 2“-5-”linked cyclic dinucleotide second messenger that activates STING. *Nature* 498: 380–384.
15. Gao, P., M. Ascano, T. Zillinger, W. Wang, P. Dai, A. A. Serganov, B. L. Gaffney, S. Shuman, R. A. Jones, L. Deng, G. Hartmann, W. Barchet, T. Tuschl, and D. J.

Patel. 2013. Structure-function analysis of STING activation by c[G(2',5')pA(3“,5”)p] and targeting by antiviral DMXAA. *Cell* 154: 748–762.
16. O'Neill, L. A. J., D. Golenbock, and A. G. Bowie. 2013. The history of Toll-like receptors - redefining innate immunity. *Nature Publishing Group* 13: 453–460.
17. Anderson, K. V., G. Jürgens, and C. Nüsslein-Volhard. 1985. Establishment of dorsal-ventral polarity in the Drosophila embryo: genetic studies on the role of the Toll gene product. *Cell* 42: 779–789.
18. Lemaitre, B. 2004. *The road to Toll*. :521–527.
19. Lemaitre, B., E. Nicolas, L. Michaut, J. M. Reichhart, and J. A. Hoffmann. 1996. The dorsoventral regulatory gene cassette spätzle/Toll/cactus controls the potent antifungal response in Drosophila adults. *Cell* 86: 973–983.
20. Whitham, S., S. P. Dinesh-Kumar, D. Choi, R. Hehl, C. Corr, and B. Baker. 1994. The product of the tobacco mosaic virus resistance gene N: similarity to toll and the interleukin-1 receptor. *Cell* 78: 1101–1115.
21. Rock, F. L., G. Hardiman, J. C. Timans, R. A. Kastelein, and J. F. Bazan. 1998. A family of human receptors structurally related to Drosophila Toll. *Proc Natl Acad Sci USA* 95: 588–593.
22. Shimazu, R., S. Akashi, H. Ogata, Y. Nagai, K. Fukudome, K. Miyake, and M. Kimoto. 1999. MD-2, a molecule that confers lipopolysaccharide responsiveness on Toll-like receptor 4. *The Journal of experimental medicine* 189: 1777–1782.
23. Schromm, A. B., E. Lien, P. Henneke, J. C. Chow, A. Yoshimura, H. Heine, E. Latz, B. G. Monks, D. A. Schwartz, K. Miyake, and D. T. Golenbock. 2001. Molecular genetic analysis of an endotoxin nonresponder mutant cell line: a point mutation in a conserved region of MD-2 abolishes endotoxin-induced signaling. *The Journal of experimental medicine* 194: 79–88.
24. Takeuchi, O., S. Sato, T. Horiuchi, K. Hoshino, K. Takeda, Z. Dong, R. L. Modlin, and S. Akira. 2002. Cutting edge: role of Toll-like receptor 1 in mediating immune response to microbial lipoproteins. *J Immunol* 169: 10–14.
25. Takeuchi, O., T. Kawai, P. F. Mühlradt, M. Morr, J. D. Radolf, A. Zychlinsky, K. Takeda, and S. Akira. 2001. Discrimination of bacterial lipoproteins by Toll-like receptor 6. *Int. Immunol.* 13: 933–940.
26. Kawai, T., and S. Akira. 2009. The roles of TLRs, RLRs and NLRs in pathogen recognition. *Int. Immunol.* 21: 317–337.
27. Hayashi, F., K. D. Smith, A. Ozinsky, T. R. Hawn, E. C. Yi, D. R. Goodlett, J. K. Eng, S. Akira, D. M. Underhill, and A. Aderem. 2001. The innate immune response to bacterial flagellin is mediated by Toll-like receptor 5. *Nature* 410: 1099–1103.
28. Uematsu, S., K. Fujimoto, M. H. Jang, B.-G. Yang, Y.-J. Jung, M. Nishiyama, S. Sato, T. Tsujimura, M. Yamamoto, Y. Yokota, H. Kiyono, M. Miyasaka, K. J. Ishii, and S. Akira. 2008. Regulation of humoral and cellular gut immunity by lamina propria dendritic cells expressing Toll-like receptor 5. *Nat Immunol* 9: 769–776.
29. Zhang, D., G. Zhang, M. S. Hayden, M. B. Greenblatt, C. Bussey, R. A. Flavell, and S. Ghosh. 2004. A toll-like receptor that prevents infection by uropathogenic bacteria. *Science* 303: 1522–1526.
30. Andrade, W. A., M. D. C. Souza, E. Ramos-Martinez, K. Nagpal, M. S. Dutra, M. B. Melo, D. C. Bartholomeu, S. Ghosh, D. T. Golenbock, and R. T. Gazzinelli. 2013. Combined action of nucleic acid-sensing Toll-like receptors and TLR11/TLR12 heterodimers imparts resistance to Toxoplasma gondii in mice. *Cell Host Microbe* 13: 42–53.
31. Koblansky, A. A., D. Jankovic, H. Oh, S. Hieny, W. Sungnak, R. Mathur, M. S. Hayden, S. Akira, A. Sher, and S. Ghosh. 2013. Recognition of profilin by Toll-like receptor 12 is critical for host resistance to Toxoplasma gondii. *Immunity* 38: 119–130.
32. Fitzgerald, K. A., E. M. Palsson-McDermott, A. G. Bowie, C. A. Jefferies, A. S. Mansell, G. Brady, E. Brint, A. Dunne, P. Gray, M. T. Harte, D. McMurray, D. E. Smith, J. E. Sims, T. A. Bird, and L. A. O'Neill. 2001. Mal (MyD88-adapter-like) is

required for Toll-like receptor-4 signal transduction. *Nature* 413: 78–83.
33. Yamamoto, M., S. Sato, H. Hemmi, H. Sanjo, S. Uematsu, T. Kaisho, K. Hoshino, O. Takeuchi, M. Kobayashi, T. Fujita, K. Takeda, and S. Akira. 2002. Essential role for TIRAP in activation of the signalling cascade shared by TLR2 and TLR4. *Nature* 420: 324–329.
34. Lin, S.-C., Y.-C. Lo, and H. Wu. 2010. Helical assembly in the MyD88-IRAK4-IRAK2 complex in TLR/IL-1R signalling. *Nature* 465: 885–890.
35. Häcker, H., R. M. Vabulas, O. Takeuchi, K. Hoshino, S. Akira, and H. Wagner. 2000. Immune cell activation by bacterial CpG-DNA through myeloid differentiation marker 88 and tumor necrosis factor receptor-associated factor (TRAF)6. *The Journal of experimental medicine* 192: 595–600.
36. Zhang, F. X., C. J. Kirschning, R. Mancinelli, X. P. Xu, Y. Jin, E. Faure, A. Mantovani, M. Rothe, M. Muzio, and M. Arditi. 1999. Bacterial lipopolysaccharide activates nuclear factor-kappaB through interleukin-1 signaling mediators in cultured human dermal endothelial cells and mononuclear phagocytes. *J Biol Chem* 274: 7611–7614.
37. Dunne, A., and L. A. J. O'Neill. 2003. The interleukin-1 receptor/Toll-like receptor superfamily: signal transduction during inflammation and host defense. *Sci. STKE* 2003: re3.
38. Yeo, S.-J., J.-G. Yoon, and A.-K. Yi. 2003. Myeloid differentiation factor 88-dependent post-transcriptional regulation of cyclooxygenase-2 expression by CpG DNA: tumor necrosis factor-alpha receptor-associated factor 6, a diverging point in the Toll-like receptor 9-signaling. *J Biol Chem* 278: 40590–40600.
39. Yeo, S.-J., D. Gravis, J.-G. Yoon, and A.-K. Yi. 2003. Myeloid differentiation factor 88-dependent transcriptional regulation of cyclooxygenase-2 expression by CpG DNA: role of NF-kappaB and p38. *J Biol Chem* 278: 22563–22573.
40. Mellett, M., P. Atzei, R. Jackson, L. A. O'Neill, and P. N. Moynagh. 2011. Mal mediates TLR-induced activation of CREB and expression of IL-10. *J Immunol* 186: 4925–4935.
41. Kagan, J. C., T. Su, T. Horng, A. Chow, S. Akira, and R. Medzhitov. 2008. TRAM couples endocytosis of Toll-like receptor 4 to the induction of interferon-beta. *Nat Immunol* 9: 361–368.
42. Fitzgerald, K. A., D. C. Rowe, B. J. Barnes, D. R. Caffrey, A. Visintin, E. Latz, B. Monks, P. M. Pitha, and D. T. Golenbock. 2003. LPS-TLR4 signaling to IRF-3/7 and NF-kappaB involves the toll adapters TRAM and TRIF. *The Journal of experimental medicine* 198: 1043–1055.
43. Choi, Y. J., E. Im, H. K. Chung, C. Pothoulakis, and S. H. Rhee. 2010. TRIF mediates Toll-like receptor 5-induced signaling in intestinal epithelial cells. *J Biol Chem* 285: 37570–37578.
44. Oganesyan, G., S. K. Saha, B. Guo, J. Q. He, A. Shahangian, B. Zarnegar, A. Perry, and G. Cheng. 2006. Critical role of TRAF3 in the Toll-like receptor-dependent and -independent antiviral response. *Nature* 439: 208–211.
45. Yamamoto, M., S. Sato, K. Mori, K. Hoshino, O. Takeuchi, K. Takeda, and S. Akira. 2002. Cutting edge: a novel Toll/IL-1 receptor domain-containing adapter that preferentially activates the IFN-beta promoter in the Toll-like receptor signaling. *J Immunol* 169: 6668–6672.
46. Fitzgerald, K. A., S. M. McWhirter, K. L. Faia, D. C. Rowe, E. Latz, D. T. Golenbock, A. J. Coyle, S.-M. Liao, and T. Maniatis. 2003. IKKepsilon and TBK1 are essential components of the IRF3 signaling pathway. *Nat Immunol* 4: 491–496.
47. Cusson-Hermance, N., S. Khurana, T. H. Lee, K. A. Fitzgerald, and M. A. Kelliher. 2005. Rip1 mediates the Trif-dependent toll-like receptor 3- and 4-induced NF-{kappa}B activation but does not contribute to interferon regulatory factor 3 activation. *J Biol Chem* 280: 36560–36566.
48. Hemmi, H., O. Takeuchi, T. Kawai, T. Kaisho, S. Sato, H. Sanjo, M. Matsumoto, K. Hoshino, H. Wagner, K. Takeda, and S. Akira. 2000. A Toll-like receptor

recognizes bacterial DNA. *Nature* 408: 740–745.
49. Ohto, U., T. Shibata, H. Tanji, H. Ishida, E. Krayukhina, S. Uchiyama, K. Miyake, and T. Shimizu. 2015. Structural basis of CpG and inhibitory DNA recognition by Toll-like receptor 9. *Nature* 520: 702–705.
50. Krieg, A. M., A. K. Yi, S. Matson, T. J. Waldschmidt, G. A. Bishop, R. Teasdale, G. A. Koretzky, and D. M. Klinman. 1995. CpG motifs in bacterial DNA trigger direct B-cell activation. *Nature* 374: 546–549.
51. Bauer, S., C. J. Kirschning, H. Häcker, V. Redecke, S. Hausmann, S. Akira, H. Wagner, and G. B. Lipford. 2001. Human TLR9 confers responsiveness to bacterial DNA via species-specific CpG motif recognition. *Proc Natl Acad Sci USA* 98: 9237–9242.
52. Heil, F., H. Hemmi, H. Hochrein, F. Ampenberger, C. Kirschning, S. Akira, G. Lipford, H. Wagner, and S. Bauer. 2004. Species-specific recognition of single-stranded RNA via toll-like receptor 7 and 8. *Science* 303: 1526–1529.
53. Tanji, H., U. Ohto, T. Shibata, M. Taoka, Y. Yamauchi, T. Isobe, K. Miyake, and T. Shimizu. 2015. Toll-like receptor 8 senses degradation products of single-stranded RNA. *Nature Structural & Molecular Biology* 22: 109–115.
54. Kanno, A., C. Yamamoto, M. Onji, R. Fukui, S.-I. Saitoh, Y. Motoi, T. Shibata, F. Matsumoto, T. Muta, and K. Miyake. 2013. Essential role for Toll-like receptor 7 (TLR7)-unique cysteines in an intramolecular disulfide bond, proteolytic cleavage and RNA sensing. *Int. Immunol.* 25: 413–422.
55. Diebold, S. S., T. Kaisho, H. Hemmi, S. Akira, and C. Reis e Sousa. 2004. Innate antiviral responses by means of TLR7-mediated recognition of single-stranded RNA. *Science* 303: 1529–1531.
56. Alexopoulou, L., A. C. Holt, R. Medzhitov, and R. A. Flavell. 2001. Recognition of double-stranded RNA and activation of NF-kappaB by Toll-like receptor 3. *Nature* 413: 732–738.
57. Oldenburg, M., A. Krüger, R. Ferstl, A. Kaufmann, G. Nees, A. Sigmund, B. Bathke, H. Lauterbach, M. Suter, S. Dreher, U. Koedel, S. Akira, T. Kawai, J. Buer, H. Wagner, S. Bauer, H. Hochrein, and C. J. Kirschning. 2012. TLR13 recognizes bacterial 23S rRNA devoid of erythromycin resistance-forming modification. *Science* 337: 1111–1115.
58. Hidmark, A., A. von Saint Paul, and A. H. Dalpke. 2012. Cutting Edge: TLR13 Is a Receptor for Bacterial RNA. *J Immunol* 189: 2717–2721.
59. Schoenemeyer, A., B. J. Barnes, M. E. Mancl, E. Latz, N. Goutagny, P. M. Pitha, K. A. Fitzgerald, and D. T. Golenbock. 2005. The interferon regulatory factor, IRF5, is a central mediator of toll-like receptor 7 signaling. *J Biol Chem* 280: 17005–17012.
60. O'Neill, L. A. J., and A. G. Bowie. 2007. The family of five: TIR-domain-containing adaptors in Toll-like receptor signalling. *Nat Rev Immunol* 7: 353–364.
61. Häcker, H., V. Redecke, B. Blagoev, I. Kratchmarova, L.-C. Hsu, G. G. Wang, M. P. Kamps, E. Raz, H. Wagner, G. Häcker, M. Mann, and M. Karin. 2006. Specificity in Toll-like receptor signalling through distinct effector functions of TRAF3 and TRAF6. *Nature* 439: 204–207.
62. Oshiumi, H., M. Matsumoto, K. Funami, T. Akazawa, and T. Seya. 2003. TICAM-1, an adaptor molecule that participates in Toll-like receptor 3-mediated interferon-beta induction. *Nat Immunol* 4: 161–167.
63. Meylan, E., K. Burns, K. Hofmann, V. Blancheteau, F. Martinon, M. Kelliher, and J. Tschopp. 2004. RIP1 is an essential mediator of Toll-like receptor 3-induced NF-kappa B activation. *Nat Immunol* 5: 503–507.
64. Yang, Y., B. Liu, J. Dai, P. K. Srivastava, D. J. Zammit, L. Lefrançois, and Z. Li. 2007. Heat shock protein gp96 is a master chaperone for toll-like receptors and is important in the innate function of macrophages. *Immunity* 26: 215–226.
65. Latz, E., A. Schoenemeyer, A. Visintin, K. A. Fitzgerald, B. G. Monks, C. F. Knetter, E. Lien, N. J. Nilsen, T. Espevik, and D. T. Golenbock. 2004. TLR9 signals after translocating from the ER to CpG DNA in the lysosome. *Nat Immunol* 5: 190–

198.
66. Leifer, C. A., M. N. Kennedy, A. Mazzoni, C. Lee, M. J. Kruhlak, and D. M. Segal. 2004. TLR9 is localized in the endoplasmic reticulum prior to stimulation. *J Immunol* 173: 1179–1183.
67. Tabeta, K., K. Hoebe, E. M. Janssen, X. Du, P. Georgel, K. Crozat, S. Mudd, N. Mann, S. Sovath, J. Goode, L. Shamel, A. A. Herskovits, D. A. Portnoy, M. Cooke, L. M. Tarantino, T. Wiltshire, B. E. Steinberg, S. Grinstein, and B. Beutler. 2006. The Unc93b1 mutation 3d disrupts exogenous antigen presentation and signaling via Toll-like receptors 3, 7 and 9. *Nat Immunol* 7: 156–164.
68. Brinkmann, M. M., E. Spooner, K. Hoebe, B. Beutler, H. L. Ploegh, and Y.-M. Kim. 2007. The interaction between the ER membrane protein UNC93B and TLR3, 7, and 9 is crucial for TLR signaling. *J. Cell Biol.* 177: 265–275.
69. Kim, Y.-M., M. M. Brinkmann, M.-E. Paquet, and H. L. Ploegh. 2008. UNC93B1 delivers nucleotide-sensing toll-like receptors to endolysosomes. *Nature* 452: 234–238.
70. Lee, B. L., J. E. Moon, J. H. Shu, L. Yuan, Z. R. Newman, R. Schekman, and G. M. Barton. 2013. UNC93B1 mediates differential trafficking of endosomal TLRs. *Elife* 2: e00291.
71. Pelka, K., K. Phulphagar, J. Zimmermann, R. Stahl, J. L. Schmid-Burgk, T. Schmidt, J.-H. Spille, L. I. Labzin, S. Agrawal, E. R. Kandimalla, J.-L. Casanova, V. Hornung, A. Marshak-Rothstein, S. Höning, and E. Latz. 2014. Cutting edge: the UNC93B1 tyrosine-based motif regulates trafficking and TLR responses via separate mechanisms. *J Immunol* 193: 3257–3261.
72. Yi, A. K., R. Tuetken, T. Redford, M. Waldschmidt, J. Kirsch, and A. M. Krieg. 1998. CpG motifs in bacterial DNA activate leukocytes through the pH-dependent generation of reactive oxygen species. *J Immunol* 160: 4755–4761.
73. Häcker, H., H. Mischak, T. Miethke, S. Liptay, R. Schmid, T. Sparwasser, K. Heeg, G. B. Lipford, and H. Wagner. 1998. CpG-DNA-specific activation of antigen-presenting cells requires stress kinase activity and is preceded by non-specific endocytosis and endosomal maturation. *EMBO J* 17: 6230–6240.
74. Lee, J., T.-H. Chuang, V. Redecke, L. She, P. M. Pitha, D. A. Carson, E. Raz, and H. B. Cottam. 2003. Molecular basis for the immunostimulatory activity of guanine nucleoside analogs: activation of Toll-like receptor 7. *Proc Natl Acad Sci USA* 100: 6646–6651.
75. Heil, F., P. Ahmad-Nejad, H. Hemmi, H. Hochrein, F. Ampenberger, T. Gellert, H. Dietrich, G. Lipford, K. Takeda, S. Akira, H. Wagner, and S. Bauer. 2003. The Toll-like receptor 7 (TLR7)-specific stimulus loxoribine uncovers a strong relationship within the TLR7, 8 and 9 subfamily. *Eur. J. Immunol.* 33: 2987–2997.
76. de Bouteiller, O., E. Merck, U. A. Hasan, S. Hubac, B. Benguigui, G. Trinchieri, E. E. M. Bates, and C. Caux. 2005. Recognition of double-stranded RNA by human toll-like receptor 3 and downstream receptor signaling requires multimerization and an acidic pH. *J Biol Chem* 280: 38133–38145.
77. Leonard, J. N., R. Ghirlando, J. Askins, J. K. Bell, D. H. Margulies, D. R. Davies, and D. M. Segal. 2008. The TLR3 signaling complex forms by cooperative receptor dimerization. *Proc Natl Acad Sci USA* 105: 258–263.
78. Rutz, M., J. Metzger, T. Gellert, P. Luppa, G. B. Lipford, H. Wagner, and S. Bauer. 2004. Toll-like receptor 9 binds single-stranded CpG-DNA in a sequence- and pH-dependent manner. *Eur. J. Immunol.* 34: 2541–2550.
79. Ewald, S. E., B. L. Lee, L. Lau, K. E. Wickliffe, G.-P. Shi, H. A. Chapman, and G. M. Barton. 2008. The ectodomain of Toll-like receptor 9 is cleaved to generate a functional receptor. *Nature* 456: 658–662.
80. Park, B., M. M. Brinkmann, E. Spooner, C. C. Lee, Y.-M. Kim, and H. L. Ploegh. 2008. Proteolytic cleavage in an endolysosomal compartment is required for activation of Toll-like receptor 9. *Nat Immunol* 9: 1407–1414.
81. Ewald, S. E., A. Engel, J. Lee, M. Wang, M. Bogyo, and G. M. Barton. 2011.

Nucleic acid recognition by Toll-like receptors is coupled to stepwise processing by cathepsins and asparagine endopeptidase. *Journal of Experimental Medicine* 208: 643–651.
82. Hsieh, C.-S., P. deRoos, K. Honey, C. Beers, and A. Y. Rudensky. 2002. A role for cathepsin L and cathepsin S in peptide generation for MHC class II presentation. *J Immunol* 168: 2618–2625.
83. Garcia-Cattaneo, A., F.-X. Gobert, M. Müller, F. Toscano, M. Flores, A. Lescure, E. Del Nery, and P. Benaroch. 2012. Cleavage of Toll-like receptor 3 by cathepsins B and H is essential for signaling. *Proc Natl Acad Sci USA* 109: 9053–9058.
84. Murakami, Y., R. Fukui, Y. Motoi, A. Kanno, T. Shibata, N. Tanimura, S.-I. Saitoh, and K. Miyake. 2014. Roles of the cleaved N-terminal TLR3 fragment and cell surface TLR3 in double-stranded RNA sensing. *J Immunol* 193: 5208–5217.
85. Matsumoto, F., S.-I. Saitoh, R. Fukui, T. Kobayashi, N. Tanimura, K. Konno, Y. Kusumoto, S. Akashi-Takamura, and K. Miyake. 2008. Cathepsins are required for Toll-like receptor 9 responses. *Biochem Biophys Res Commun* 367: 693–699.
86. Sepulveda, F. E., S. Maschalidi, R. Colisson, L. Heslop, C. Ghirelli, E. Sakka, A.-M. Lennon-Duménil, S. Amigorena, L. Cabanie, and B. Manoury. 2009. Critical role for asparagine endopeptidase in endocytic Toll-like receptor signaling in dendritic cells. *Immunity* 31: 737–748.
87. Onji, M., A. Kanno, S.-I. Saitoh, R. Fukui, Y. Motoi, T. Shibata, F. Matsumoto, A. Lamichhane, S. Sato, H. Kiyono, K. Yamamoto, and K. Miyake. 2013. An essential role for the N-terminal fragment of Toll-like receptor 9 in DNA sensing. *Nat Comms* 4: 1949.
88. Hipp, M. M., D. Shepherd, U. Gileadi, M. C. Aichinger, B. M. Kessler, M. J. Edelmann, R. Essalmani, N. G. Seidah, C. Reis e Sousa, and V. Cerundolo. 2013. Processing of human toll-like receptor 7 by furin-like proprotein convertases is required for its accumulation and activity in endosomes. *Immunity* 39: 711–721.
89. Ishii, N., K. Funami, M. Tatematsu, T. Seya, and M. Matsumoto. 2014. Endosomal localization of TLR8 confers distinctive proteolytic processing on human myeloid cells. *J Immunol* 193: 5118–5128.
90. Hipp, M. M., D. Shepherd, S. Booth, D. Waithe, C. Reis e Sousa, and V. Cerundolo. 2015. The Processed Amino-Terminal Fragment of Human TLR7 Acts as a Chaperone To Direct Human TLR7 into Endosomes. *J Immunol* 194: 5417–5425.
91. Blasius, A. L., and B. Beutler. 2010. Intracellular toll-like receptors. *Immunity* 32: 305–315.
92. Brencicova, E., and S. S. Diebold. 2013. Nucleic acids and endosomal pattern recognition: how to tell friend from foe? *Front Cell Infect Microbiol* 3: 37.
93. Mercer, J., M. Schelhaas, and A. Helenius. 2010. Virus entry by endocytosis. *Annu. Rev. Biochem.* 79: 803–833.
94. Hall, A., and C. D. Nobes. 2000. Rho GTPases: molecular switches that control the organization and dynamics of the actin cytoskeleton. *Philos. Trans. R. Soc. Lond., B, Biol. Sci.* 355: 965–970.
95. Herre, J., A. S. J. Marshall, E. Caron, A. D. Edwards, D. L. Williams, E. Schweighoffer, V. Tybulewicz, C. Reis e Sousa, S. Gordon, and G. D. Brown. 2004. Dectin-1 uses novel mechanisms for yeast phagocytosis in macrophages. *Blood* 104: 4038–4045.
96. Brown, G. D., and S. Gordon. 2001. Immune recognition. A new receptor for beta-glucans. *Nature* 413: 36–37.
97. Rodriguez, M. E., S. M. Hellwig, D. F. Hozbor, J. Leusen, W. L. van der Pol, and J. G. van de Winkel. 2001. Fc receptor-mediated immunity against Bordetella pertussis. *J Immunol* 167: 6545–6551.
98. Pierson, T. C., and R. W. Doms. 2003. HIV-1 entry and its inhibition. *Curr. Top. Microbiol. Immunol.* 281: 1–27.
99. Marechal, V., M. C. Prevost, C. Petit, E. Perret, J. M. Heard, and O. Schwartz. 2001. Human immunodeficiency virus type 1 entry into macrophages mediated by

macropinocytosis. *Journal of virology* 75: 11166–11177.
100. Miyauchi, K., Y. Kim, O. Latinovic, V. Morozov, and G. B. Melikyan. 2009. HIV enters cells via endocytosis and dynamin-dependent fusion with endosomes. *Cell* 137: 433–444.
101. Józefowski, S., T. H. Sulahian, M. Arredouani, and L. Kobzik. 2006. Role of scavenger receptor MARCO in macrophage responses to CpG oligodeoxynucleotides. *J Leukoc Biol* 80: 870–879.
102. Limmon, G. V., M. Arredouani, K. L. McCann, R. A. Corn Minor, L. Kobzik, and F. Imani. 2008. Scavenger receptor class-A is a novel cell surface receptor for double-stranded RNA. *FASEB J* 22: 159–167.
103. Means, T. K., E. Latz, F. Hayashi, M. R. Murali, D. T. Golenbock, and A. D. Luster. 2005. Human lupus autoantibody-DNA complexes activate DCs through cooperation of CD32 and TLR9. *J Clin Invest* 115: 407–417.
104. Amigorena, S., and C. Bonnerot. 1998. Role of B-cell and Fc receptors in the selection of T-cell epitopes. *Curr Opin Immunol* 10: 88–92.
105. Gaipl, U. S., T. D. Beyer, P. Heyder, S. Kuenkele, A. Böttcher, R. E. Voll, J. R. Kalden, and M. Herrmann. 2004. Cooperation between C1q and DNase I in the clearance of necrotic cell-derived chromatin. *Arthritis Rheum* 50: 640–649.
106. Morgan, B. P., and M. J. Walport. 1991. Complement deficiency and disease. *Immunol. Today* 12: 301–306.
107. Botto, M., C. Dell'Agnola, A. E. Bygrave, E. M. Thompson, H. T. Cook, F. Petry, M. Loos, P. P. Pandolfi, and M. J. Walport. 1998. Homozygous C1q deficiency causes glomerulonephritis associated with multiple apoptotic bodies. *Nat. Genet.* 19: 56–59.
108. Bell, J. K., I. Botos, P. R. Hall, J. Askins, J. Shiloach, D. M. Segal, and D. R. Davies. 2005. The molecular structure of the Toll-like receptor 3 ligand-binding domain. *Proc Natl Acad Sci USA* 102: 10976–10980.
109. Choe, J., M. S. Kelker, and I. A. Wilson. 2005. Crystal structure of human toll-like receptor 3 (TLR3) ectodomain. *Science* 309: 581–585.
110. Liu, L., I. Botos, Y. Wang, J. N. Leonard, J. Shiloach, D. M. Segal, and D. R. Davies. 2008. Structural basis of toll-like receptor 3 signaling with double-stranded RNA. *Science* 320: 379–381.
111. Ohto, U., H. Tanji, and T. Shimizu. 2014. Structure and function of toll-like receptor 8. *Microbes Infect.* 16: 273–282.
112. Tanji, H., U. Ohto, T. Shibata, K. Miyake, and T. Shimizu. 2013. Structural reorganization of the Toll-like receptor 8 dimer induced by agonistic ligands. *Science* 339: 1426–1429.
113. Chan, M. P., M. Onji, R. Fukui, K. Kawane, T. Shibata, S.-I. Saitoh, U. Ohto, T. Shimizu, G. N. Barber, and K. Miyake. 2015. DNase II-dependent DNA digestion is required for DNA sensing by TLR9. *Nat Comms* 6: 5853.
114. Pawaria, S., K. Moody, P. Busto, K. Nündel, C.-H. Choi, T. Ghayur, and A. Marshak-Rothstein. 2015. Cutting Edge: DNase II deficiency prevents activation of autoreactive B cells by double-stranded DNA endogenous ligands. *J Immunol* 194: 1403–1407.
115. Kerkmann, M., L. T. Costa, C. Richter, S. Rothenfusser, J. Battiany, V. Hornung, J. Johnson, S. Englert, T. Ketterer, W. Heckl, S. Thalhammer, S. Endres, and G. Hartmann. 2005. Spontaneous formation of nucleic acid-based nanoparticles is responsible for high interferon-alpha induction by CpG-A in plasmacytoid dendritic cells. *J Biol Chem* 280: 8086–8093.
116. Vollmer, J., R. Weeratna, P. Payette, M. Jurk, C. Schetter, M. Laucht, T. Wader, S. Tluk, M. Liu, H. L. Davis, and A. M. Krieg. 2004. Characterization of three CpG oligodeoxynucleotide classes with distinct immunostimulatory activities. *Eur. J. Immunol.* 34: 251–262.
117. Sessa, L., E. Gatti, F. Zeni, A. Antonelli, A. Catucci, M. Koch, G. Pompilio, G. Fritz, A. Raucci, and M. E. Bianchi. 2014. The receptor for advanced glycation end-

products (RAGE) is only present in mammals, and belongs to a family of cell adhesion molecules (CAMs). *PLoS ONE* 9: e86903.
118. Hudson, B. I., A. M. Carter, E. Harja, A. Z. Kalea, M. Arriero, H. Yang, P. J. Grant, and A. M. Schmidt. 2008. Identification, classification, and expression of RAGE gene splice variants. *FASEB J* 22: 1572–1580.
119. Schmidt, A. M., S. D. Yan, S. F. Yan, and D. M. Stern. 2000. The biology of the receptor for advanced glycation end products and its ligands. *Biochim Biophys Acta* 1498: 99–111.
120. Ritthaler, U., Y. Deng, Y. Zhang, J. Greten, M. Abel, B. Sido, J. Allenberg, G. Otto, H. Roth, and A. Bierhaus. 1995. Expression of receptors for advanced glycation end products in peripheral occlusive vascular disease. *The American Journal of Pathology* 146: 688–694.
121. Abel, M., U. Ritthaler, Y. Zhang, Y. Deng, A. M. Schmidt, J. Greten, T. Sernau, P. Wahl, K. Andrassy, and E. Ritz. 1995. Expression of receptors for advanced glycosylated end-products in renal disease. *Nephrol Dial Transplant* 10: 1662–1667.
122. Greten, J., I. Kreis, K. Wiesel, E. Stier, A. M. Schmidt, D. M. Stern, E. Ritz, R. Waldherr, and P. P. Nawroth. 1996. Receptors for advance glycation end-products (AGE) - expression by endothelial cells in non-diabetic uraemic patients. *Nephrol Dial Transplant* 11: 786–790.
123. Taguchi, A., D. C. Blood, G. del Toro, A. Canet, D. C. Lee, W. Qu, N. Tanji, Y. Lu, E. Lalla, C. Fu, M. A. Hofmann, T. Kislinger, M. Ingram, A. Lu, H. Tanaka, O. Hori, S. Ogawa, D. M. Stern, and A. M. Schmidt. 2000. Blockade of RAGE-amphoterin signalling suppresses tumour growth and metastases. *Nature* 405: 354–360.
124. Yan, S. D., X. Chen, J. Fu, M. Chen, H. Zhu, A. Roher, T. Slattery, L. Zhao, M. Nagashima, J. Morser, A. Migheli, P. Nawroth, D. Stern, and A. M. Schmidt. 1996. RAGE and amyloid-beta peptide neurotoxicity in Alzheimer's disease. *Nature* 382: 685–691.
125. Tanaka, N., H. Yonekura, S. Yamagishi, H. Fujimori, Y. Yamamoto, and H. Yamamoto. 2000. The receptor for advanced glycation end products is induced by the glycation products themselves and tumor necrosis factor-alpha through nuclear factor-kappa B, and by 17beta-estradiol through Sp-1 in human vascular endothelial cells. *J Biol Chem* 275: 25781–25790.
126. Tian, J., A. M. Avalos, S.-Y. Mao, B. Chen, K. Senthil, H. Wu, P. Parroche, S. Drabic, D. Golenbock, C. Sirois, J. Hua, L. L. An, L. Audoly, G. La Rosa, A. Bierhaus, P. Naworth, A. Marshak-Rothstein, M. K. Crow, K. A. Fitzgerald, E. Latz, P. A. Kiener, and A. J. Coyle. 2007. Toll-like receptor 9-dependent activation by DNA-containing immune complexes is mediated by HMGB1 and RAGE. *Nat Immunol* 8: 487–496.
127. Moser, B., D. D. Desai, M. P. Downie, Y. Chen, S. F. Yan, K. Herold, A. M. Schmidt, and R. Clynes. 2007. Receptor for advanced glycation end products expression on T cells contributes to antigen-specific cellular expansion in vivo. *J Immunol* 179: 8051–8058.
128. Dumitriu, I. E., M. E. Bianchi, M. Bacci, A. A. Manfredi, and P. Rovere-Querini. 2007. The secretion of HMGB1 is required for the migration of maturing dendritic cells. *J Leukoc Biol* 81: 84–91.
129. Dumitriu, I. E., P. Baruah, B. Valentinis, R. E. Voll, M. Herrmann, P. P. Nawroth, B. Arnold, M. E. Bianchi, A. A. Manfredi, and P. Rovere-Querini. 2005. Release of high mobility group box 1 by dendritic cells controls T cell activation via the receptor for advanced glycation end products. *J Immunol* 174: 7506–7515.
130. Manfredi, A. A., A. Capobianco, A. Esposito, F. De Cobelli, T. Canu, A. Monno, A. Raucci, F. Sanvito, C. Doglioni, P. P. Nawroth, A. Bierhaus, M. E. Bianchi, P. Rovere-Querini, and A. Del Maschio. 2008. Maturing dendritic cells depend on RAGE for in vivo homing to lymph nodes. *J Immunol* 180: 2270–2275.
131. Li, J., and A. M. Schmidt. 1997. Characterization and functional analysis of the

promoter of RAGE, the receptor for advanced glycation end products. *J Biol Chem* 272: 16498–16506.
132. Dattilo, B. M., G. Fritz, E. Leclerc, C. W. V. Kooi, C. W. Heizmann, and W. J. Chazin. 2007. The extracellular region of the receptor for advanced glycation end products is composed of two independent structural units. *Biochemistry* 46: 6957–6970.
133. Koch, M., S. Chitayat, B. M. Dattilo, A. Schiefner, J. Diez, W. J. Chazin, and G. Fritz. 2010. Structural basis for ligand recognition and activation of RAGE. *Structure* 18: 1342–1352.
134. Fritz, G. 2011. RAGE: a single receptor fits multiple ligands. *Trends Biochem Sci*.
135. Xie, J., D. S. Burz, W. He, I. B. Bronstein, I. Lednev, and A. Shekhtman. 2007. Hexameric calgranulin C (S100A12) binds to the receptor for advanced glycated end products (RAGE) using symmetric hydrophobic target-binding patches. *J Biol Chem* 282: 4218–4231.
136. Xie, J., S. Reverdatto, A. Frolov, R. Hoffmann, D. S. Burz, and A. Shekhtman. 2008. Structural basis for pattern recognition by the receptor for advanced glycation end products (RAGE). *J Biol Chem* 283: 27255–27269.
137. Sturchler, E., A. Galichet, M. Weibel, E. Leclerc, and C. W. Heizmann. 2008. Site-specific blockade of RAGE-Vd prevents amyloid-beta oligomer neurotoxicity. *J. Neurosci.* 28: 5149–5158.
138. Ostendorp, T., E. Leclerc, A. Galichet, M. Koch, N. Demling, B. Weigle, C. W. Heizmann, P. M. H. Kroneck, and G. Fritz. 2007. Structural and functional insights into RAGE activation by multimeric S100B. *EMBO J* 26: 3868–3878.
139. Leclerc, E., G. Fritz, M. Weibel, C. W. Heizmann, and A. Galichet. 2007. S100B and S100A6 differentially modulate cell survival by interacting with distinct RAGE (receptor for advanced glycation end products) immunoglobulin domains. *J Biol Chem* 282: 31317–31331.
140. Leclerc, E., G. Fritz, S. W. Vetter, and C. W. Heizmann. 2009. Binding of S100 proteins to RAGE: an update. *Biochim Biophys Acta* 1793: 993–1007.
141. Matsumoto, S., T. Yoshida, H. Murata, S. Harada, N. Fujita, S. Nakamura, Y. Yamamoto, T. Watanabe, H. Yonekura, H. Yamamoto, T. Ohkubo, and Y. Kobayashi. 2008. Solution structure of the variable-type domain of the receptor for advanced glycation end products: new insight into AGE-RAGE interaction. *Biochemistry* 47: 12299–12311.
142. Xue, J., V. Rai, D. Singer, S. Chabierski, J. Xie, S. Reverdatto, D. S. Burz, A. M. Schmidt, R. Hoffmann, and A. Shekhtman. 2011. Advanced glycation end product recognition by the receptor for AGEs. *Structure* 19: 722–732.
143. Neeper, M., A. M. Schmidt, J. Brett, S. D. Yan, F. Wang, Y. C. Pan, K. Elliston, D. Stern, and A. Shaw. 1992. Cloning and expression of a cell surface receptor for advanced glycosylation end products of proteins. *J Biol Chem* 267: 14998–15004.
144. Hori, O., J. Brett, T. Slattery, R. Cao, J. Zhang, J. X. Chen, M. Nagashima, E. R. Lundh, S. Vijay, and D. Nitecki. 1995. The receptor for advanced glycation end products (RAGE) is a cellular binding site for amphoterin. Mediation of neurite outgrowth and co-expression of rage and amphoterin in the developing nervous system. *J Biol Chem* 270: 25752–25761.
145. Yan, S. F., R. Ramasamy, and A. M. Schmidt. 2008. Mechanisms of disease: advanced glycation end-products and their receptor in inflammation and diabetes complications. *Nat Clin Pract Endocrinol Metab* 4: 285–293.
146. Manigrasso, M. B., J. Juranek, R. Ramasamy, and A. M. Schmidt. 2014. Unlocking the biology of RAGE in diabetic microvascular complications. *Trends Endocrinol. Metab.* 25: 15–22.
147. Yan, S. F., R. Ramasamy, and A. M. Schmidt. 2009. The receptor for advanced glycation endproducts (RAGE) and cardiovascular disease. *Expert Rev. Mol. Med.* 11: e9.

148. Yamagishi, S.-I. 2011. Role of advanced glycation end products (AGEs) and receptor for AGEs (RAGE) in vascular damage in diabetes. *Exp. Gerontol.* 46: 217–224.
149. Yan, S. S., D. Chen, S. Yan, L. Guo, H. Du, and J. X. Chen. 2012. RAGE is a key cellular target for Abeta-induced perturbation in Alzheimer's disease. *Front Biosci (Schol Ed)* 4: 240–250.
150. Krieg, A. M. 2007. TLR9 and DNA “feel” RAGE. *Nat Immunol* 8: 475–477.
151. Lafyatis, R., and A. Marshak-Rothstein. 2007. Toll-like receptors and innate immune responses in systemic lupus erythematosus. *Arthritis Research & Therapy* 9: 222.
152. Sims, G. P., D. C. Rowe, S. T. Rietdijk, R. Herbst, and A. J. Coyle. 2010. HMGB1 and RAGE in inflammation and cancer. *Annu Rev Immunol* 28: 367–388.
153. Brownlee, M. 1995. Advanced protein glycosylation in diabetes and aging. *Annu. Rev. Med.* 46: 223–234.
154. Miyata, T., O. Hori, J. Zhang, S. D. Yan, L. Ferran, Y. Iida, and A. M. Schmidt. 1996. The receptor for advanced glycation end products (RAGE) is a central mediator of the interaction of AGE-beta2microglobulin with human mononuclear phagocytes via an oxidant-sensitive pathway. Implications for the pathogenesis of dialysis-related amyloidosis. *J Clin Invest* 98: 1088–1094.
155. Schmidt, A. M., S. D. Yan, and D. M. Stern. 1995. The dark side of glucose. *Nat Med* 1: 1002–1004.
156. Schmidt, A. M., O. Hori, J. X. Chen, J. F. Li, J. Crandall, J. Zhang, R. Cao, S. D. Yan, J. Brett, and D. Stern. 1995. Advanced glycation endproducts interacting with their endothelial receptor induce expression of vascular cell adhesion molecule-1 (VCAM-1) in cultured human endothelial cells and in mice. A potential mechanism for the accelerated vasculopathy of diabetes. *J Clin Invest* 96: 1395–1403.
157. Lue, L. F., D. G. Walker, L. Brachova, T. G. Beach, J. Rogers, A. M. Schmidt, D. M. Stern, and S. D. Yan. 2001. Involvement of microglial receptor for advanced glycation endproducts (RAGE) in Alzheimer's disease: identification of a cellular activation mechanism. *Experimental Neurology* 171: 29–45.
158. Yan, Du, S., H. Zhu, J. Fu, S. F. Yan, A. Roher, W. W. Tourtellotte, T. Rajavashisth, X. Chen, G. C. Godman, D. Stern, and A. M. Schmidt. 1997. Amyloid-beta peptide-receptor for advanced glycation endproduct interaction elicits neuronal expression of macrophage-colony stimulating factor: a proinflammatory pathway in Alzheimer disease. *Proc Natl Acad Sci USA* 94: 5296–5301.
159. Kim, S.-J., J.-W. Ahn, H. Kim, H.-J. Ha, S.-W. Lee, H.-K. Kim, S. Lee, H.-S. Hong, Y. H. Kim, and C. Y. Choi. 2013. Two β-strands of RAGE participate in the recognition and transport of amyloid-β peptide across the blood brain barrier. *Biochem Biophys Res Commun* 439: 252–257.
160. Origlia, N., M. Righi, S. Capsoni, A. Cattaneo, F. Fang, D. M. Stern, J. X. Chen, A. M. Schmidt, O. Arancio, S. D. Yan, and L. Domenici. 2008. Receptor for advanced glycation end product-dependent activation of p38 mitogen-activated protein kinase contributes to amyloid-beta-mediated cortical synaptic dysfunction. *J. Neurosci.* 28: 3521–3530.
161. Fang, F., L.-F. Lue, S. Yan, H. Xu, J. S. Luddy, D. Chen, D. G. Walker, D. M. Stern, S. Yan, A. M. Schmidt, J. X. Chen, and S. S. Yan. 2010. RAGE-dependent signaling in microglia contributes to neuroinflammation, Abeta accumulation, and impaired learning/memory in a mouse model of Alzheimer's disease. *FASEB J* 24: 1043–1055.
162. Takuma, K., F. Fang, W. Zhang, S. Yan, E. Fukuzaki, H. Du, A. Sosunov, G. McKhann, Y. Funatsu, N. Nakamichi, T. Nagai, H. Mizoguchi, D. Ibi, O. Hori, S. Ogawa, D. M. Stern, K. Yamada, and S. S. Yan. 2009. RAGE-mediated signaling contributes to intraneuronal transport of amyloid-beta and neuronal dysfunction. *Proc Natl Acad Sci USA* 106: 20021–20026.
163. Deane, R., S. Du Yan, R. K. Submamaryan, B. LaRue, S. Jovanovic, E. Hogg,

D. Welch, L. Manness, C. Lin, J. Yu, H. Zhu, J. Ghiso, B. Frangione, A. Stern, A. M. Schmidt, D. L. Armstrong, B. Arnold, B. Liliensiek, P. Nawroth, F. Hofman, M. Kindy, D. Stern, and B. Zlokovic. 2003. RAGE mediates amyloid-beta peptide transport across the blood-brain barrier and accumulation in brain. *Nat Med* 9: 907–913.
164. Deane, R., Z. Wu, and B. V. Zlokovic. 2004. RAGE (yin) versus LRP (yang) balance regulates alzheimer amyloid beta-peptide clearance through transport across the blood-brain barrier. *Stroke* 35: 2628–2631.
165. Marenholz, I., C. W. Heizmann, and G. Fritz. 2004. S100 proteins in mouse and man: from evolution to function and pathology (including an update of the nomenclature). *Biochem Biophys Res Commun* 322: 1111–1122.
166. Torabian, S., and M. Kashani-Sabet. 2005. Biomarkers for melanoma. *Current Opinion in Oncology* 17: 167–171.
167. Sakaguchi, M., H. Sonegawa, H. Murata, M. Kitazoe, J.-I. Futami, K. Kataoka, H. Yamada, and N.-H. Huh. 2008. S100A11, an dual mediator for growth regulation of human keratinocytes. *Mol. Biol. Cell* 19: 78–85.
168. Ghavami, S., C. Kerkhoff, W. J. Chazin, K. Kadkhoda, W. Xiao, A. Zuse, M. Hashemi, M. Eshraghi, K. Schulze-Osthoff, T. Klonisch, and M. Los. 2008. S100A8/9 induces cell death via a novel, RAGE-independent pathway that involves selective release of Smac/DIABLO and Omi/HtrA2. *Biochim Biophys Acta* 1783: 297–311.
169. Fuentes, M. K., S. S. Nigavekar, T. Arumugam, C. D. Logsdon, A. M. Schmidt, J. C. Park, and E. H. Huang. 2007. RAGE activation by S100P in colon cancer stimulates growth, migration, and cell signaling pathways. *Dis. Colon Rectum* 50: 1230–1240.
170. Kiewitz, R., C. Acklin, E. Minder, P. R. Huber, B. W. Schäfer, and C. W. Heizmann. 2000. S100A1, a new marker for acute myocardial ischemia. *Biochem Biophys Res Commun* 274: 865–871.
171. Boyd, J. H., B. Kan, H. Roberts, Y. Wang, and K. R. Walley. 2008. S100A8 and S100A9 mediate endotoxin-induced cardiomyocyte dysfunction via the receptor for advanced glycation end products. *Circ. Res.* 102: 1239–1246.
172. Kang, J. H., S. M. Hwang, and I. Y. Chung. 2015. S100A8, S100A9 and S100A12 activate airway epithelial cells to produce MUC5AC via extracellular signal-regulated kinase and nuclear factor-κB pathways. *Immunology* 144: 79–90.
173. Arumugam, T., D. M. Simeone, A. M. Schmidt, and C. D. Logsdon. 2004. S100P stimulates cell proliferation and survival via receptor for activated glycation end products (RAGE). *J Biol Chem* 279: 5059–5065.
174. Ghavami, S., I. Rashedi, B. M. Dattilo, M. Eshraghi, W. J. Chazin, M. Hashemi, S. Wesselborg, C. Kerkhoff, and M. Los. 2008. S100A8/A9 at low concentration promotes tumor cell growth via RAGE ligation and MAP kinase-dependent pathway. *J Leukoc Biol* 83: 1484–1492.
175. Wolf, R., O. M. Z. Howard, H.-F. Dong, C. Voscopoulos, K. Boeshans, J. Winston, R. Divi, M. Gunsior, P. Goldsmith, B. Ahvazi, T. Chavakis, J. J. Oppenheim, and S. H. Yuspa. 2008. Chemotactic activity of S100A7 (Psoriasin) is mediated by the receptor for advanced glycation end products and potentiates inflammation with highly homologous but functionally distinct S100A15. *J Immunol* 181: 1499–1506.
176. Rauvala, H., J. Merenmies, R. Pihlaskari, M. Korkolainen, M. L. Huhtala, and P. Panula. 1988. The adhesive and neurite-promoting molecule p30: analysis of the amino-terminal sequence and production of antipeptide antibodies that detect p30 at the surface of neuroblastoma cells and of brain neurons. *J. Cell Biol.* 107: 2293–2305.
177. Read, C. M., P. D. Cary, C. Crane-Robinson, P. C. Driscoll, and D. G. Norman. 1993. Solution structure of a DNA-binding domain from HMG1. *Nucleic Acids Res* 21: 3427–3436.
178. Bonaldi, T., G. Längst, R. Strohner, P. B. Becker, and M. E. Bianchi. 2002. The DNA chaperone HMGB1 facilitates ACF/CHRAC-dependent nucleosome sliding. *EMBO J* 21: 6865–6873.

179. Agresti, A., and M. E. Bianchi. 2003. HMGB proteins and gene expression. *Curr. Opin. Genet. Dev.* 13: 170–178.
180. Wang, H., O. Bloom, M. Zhang, J. M. Vishnubhakat, M. Ombrellino, J. Che, A. Frazier, H. Yang, S. Ivanova, L. Borovikova, K. R. Manogue, E. Faist, E. Abraham, J. Andersson, U. Andersson, P. E. Molina, N. N. Abumrad, A. Sama, and K. J. Tracey. 1999. HMG-1 as a late mediator of endotoxin lethality in mice. *Science* 285: 248–251.
181. Namiki, Y., T. Takahashi, and T. Ohno. 1998. Gene transduction for disseminated intraperitoneal tumor using cationic liposomes containing non-histone chromatin proteins: cationic liposomal gene therapy of carcinomatosa. *Gene Ther.* 5: 240–246.
182. Gardella, S., C. Andrei, D. Ferrera, L. V. Lotti, M. R. Torrisi, M. E. Bianchi, and A. Rubartelli. 2002. The nuclear protein HMGB1 is secreted by monocytes via a non-classical, vesicle-mediated secretory pathway. *EMBO Rep* 3: 995–1001.
183. Scaffidi, P., T. Misteli, and M. E. Bianchi. 2002. Release of chromatin protein HMGB1 by necrotic cells triggers inflammation. *Nature* 418: 191–195.
184. Abraham, E., J. Arcaroli, A. Carmody, H. Wang, and K. J. Tracey. 2000. HMG-1 as a mediator of acute lung inflammation. *J Immunol* 165: 2950–2954.
185. Degryse, B., T. Bonaldi, P. Scaffidi, S. Muller, M. Resnati, F. Sanvito, G. Arrigoni, and M. E. Bianchi. 2001. The high mobility group (HMG) boxes of the nuclear protein HMG1 induce chemotaxis and cytoskeleton reorganization in rat smooth muscle cells. *J. Cell Biol.* 152: 1197–1206.
186. Palumbo, R., M. Sampaolesi, F. De Marchis, R. Tonlorenzi, S. Colombetti, A. Mondino, G. Cossu, and M. E. Bianchi. 2004. Extracellular HMGB1, a signal of tissue damage, induces mesoangioblast migration and proliferation. *J. Cell Biol.* 164: 441–449.
187. Abeyama, K., D. M. Stern, Y. Ito, K.-I. Kawahara, Y. Yoshimoto, M. Tanaka, T. Uchimura, N. Ida, Y. Yamazaki, S. Yamada, Y. Yamamoto, H. Yamamoto, S. Iino, N. Taniguchi, and I. Maruyama. 2005. The N-terminal domain of thrombomodulin sequesters high-mobility group-B1 protein, a novel antiinflammatory mechanism. *J Clin Invest* 115: 1267–1274.
188. Treutiger, C. J., G. E. Mullins, A.-S. M. Johansson, A. Rouhiainen, H. M. E. Rauvala, H. Erlandsson-Harris, U. Andersson, H. Yang, K. J. Tracey, J. Andersson, and J. E. W. Palmblad. 2003. High mobility group 1 B-box mediates activation of human endothelium. *Journal of Internal Medicine* 254: 375–385.
189. Fiuza, C., M. Bustin, S. Talwar, M. Tropea, E. Gerstenberger, J. H. Shelhamer, and A. F. Suffredini. 2003. Inflammation-promoting activity of HMGB1 on human microvascular endothelial cells. *Blood* 101: 2652–2660.
190. Weber, D. J., A. S. A. Gracon, M. S. Ripsch, A. J. Fisher, B. M. Cheon, P. H. Pandya, R. Vittal, M. L. Capitano, Y. Kim, Y. M. Allette, A. A. Riley, B. P. McCarthy, P. R. Territo, G. D. Hutchins, H. E. Broxmeyer, G. E. Sandusky, F. A. White, and D. S. Wilkes. 2014. The HMGB1-RAGE axis mediates traumatic brain injury-induced pulmonary dysfunction in lung transplantation. *Sci Transl Med* 6: 252ra124.
191. Nicolls, M. R., and V. E. Laubach. 2014. Traumatic brain injury: lungs in a RAGE. *Sci Transl Med* 6: 252fs34.
192. Muhammad, S., W. Barakat, S. Stoyanov, S. Murikinati, H. Yang, K. J. Tracey, M. Bendszus, G. Rossetti, P. P. Nawroth, A. Bierhaus, and M. Schwaninger. 2008. The HMGB1 receptor RAGE mediates ischemic brain damage. *J. Neurosci.* 28: 12023–12031.
193. Bianchi, M. E. 2009. HMGB1 loves company. *J Leukoc Biol* 86: 573–576.
194. Ivanov, S., A.-M. Dragoi, X. Wang, C. Dallacosta, J. Louten, G. Musco, G. Sitia, G. S. Yap, Y. Wan, C. A. Biron, M. E. Bianchi, H. Wang, and W.-M. Chu. 2007. A novel role for HMGB1 in TLR9-mediated inflammatory responses to CpG-DNA. *Blood* 110: 1970–1981.
195. Vénéreau, E., M. Casalgrandi, M. Schiraldi, D. J. Antoine, A. Cattaneo, F. De

Marchis, J. Liu, A. Antonelli, A. Preti, L. Raeli, S. S. Shams, H. Yang, L. Varani, U. Andersson, K. J. Tracey, A. Bachi, M. Uguccioni, and M. E. Bianchi. 2012. Mutually exclusive redox forms of HMGB1 promote cell recruitment or proinflammatory cytokine release. *Journal of Experimental Medicine* 209: 1519–1528.
196. Yang, H., P. Lundbäck, L. Ottosson, H. Erlandsson-Harris, E. Vénéreau, M. E. Bianchi, Y. Al-Abed, U. Andersson, K. J. Tracey, and D. J. Antoine. 2012. Redox modification of cysteine residues regulates the cytokine activity of high mobility group box-1 (HMGB1). *Mol Med* 18: 250–259.
197. Tang, D., R. Kang, C.-W. Cheh, K. M. Livesey, X. Liang, N. E. Schapiro, R. Benschop, L. J. Sparvero, A. A. Amoscato, K. J. Tracey, H. J. Zeh, and M. T. Lotze. 2010. HMGB1 release and redox regulates autophagy and apoptosis in cancer cells. *Oncogene* 29: 5299–5310.
198. Kierdorf, K., and G. Fritz. 2013. RAGE regulation and signaling in inflammation and beyond. *J Leukoc Biol* 94: 55–68.
199. Hudson, B. I., A. Z. Kalea, M. Del Mar Arriero, E. Harja, E. Boulanger, V. D'Agati, and A. M. Schmidt. 2008. Interaction of the RAGE cytoplasmic domain with diaphanous-1 is required for ligand-stimulated cellular migration through activation of Rac1 and Cdc42. *J Biol Chem* 283: 34457–34468.
200. Rai, V., A. Y. Maldonado, D. S. Burz, S. Reverdatto, S. F. Yan, A. M. Schmidt, and A. Shekhtman. 2012. Signal transduction in receptor for advanced glycation end products (RAGE): solution structure of C-terminal rage (ctRAGE) and its binding to mDia1. *J Biol Chem* 287: 5133–5144.
201. Touré, F., G. Fritz, Q. Li, V. Rai, G. Daffu, Y. S. Zou, R. Rosario, R. Ramasamy, A. S. Alberts, S. F. Yan, and A. M. Schmidt. 2012. Formin mDia1 mediates vascular remodeling via integration of oxidative and signal transduction pathways. *Circ. Res.* 110: 1279–1293.
202. Bianchi, R., E. Kastrisianaki, I. Giambanco, and R. Donato. 2011. S100B protein stimulates microglia migration via RAGE-dependent up-regulation of chemokine expression and release. *J Biol Chem* 286: 7214–7226.
203. Fukami, K., S. Ueda, S.-I. Yamagishi, S. Kato, Y. Inagaki, M. Takeuchi, Y. Motomiya, R. Bucala, S. Iida, K. Tamaki, T. Imaizumi, M. E. Cooper, and S. Okuda. 2004. AGEs activate mesangial TGF-beta-Smad signaling via an angiotensin II type I receptor interaction. *Kidney Int* 66: 2137–2147.
204. Bu, D.-X., V. Rai, X. Shen, R. Rosario, Y. Lu, V. D'Agati, S. F. Yan, R. A. Friedman, E. Nuglozeh, and A. M. Schmidt. 2010. Activation of the ROCK1 branch of the transforming growth factor-beta pathway contributes to RAGE-dependent acceleration of atherosclerosis in diabetic ApoE-null mice. *Circ. Res.* 106: 1040–1051.
205. Lander, H. M., J. M. Tauras, J. S. Ogiste, O. Hori, R. A. Moss, and A. M. Schmidt. 1997. Activation of the receptor for advanced glycation end products triggers a p21(ras)-dependent mitogen-activated protein kinase pathway regulated by oxidant stress. *J Biol Chem* 272: 17810–17814.
206. Yeh, C. H., L. Sturgis, J. Haidacher, X. N. Zhang, S. J. Sherwood, R. J. Bjercke, O. Juhasz, M. T. Crow, R. G. Tilton, and L. Denner. 2001. Requirement for p38 and p44/p42 mitogen-activated protein kinases in RAGE-mediated nuclear factor-kappaB transcriptional activation and cytokine secretion. *Diabetes* 50: 1495–1504.
207. Yan, S. D., A. M. Schmidt, G. M. Anderson, J. Zhang, J. Brett, Y. S. Zou, D. Pinsky, and D. Stern. 1994. Enhanced cellular oxidant stress by the interaction of advanced glycation end products with their receptors/binding proteins. *J Biol Chem* 269: 9889–9897.
208. Ishihara, K., K. Tsutsumi, S. Kawane, M. Nakajima, and T. Kasaoka. 2003. The receptor for advanced glycation end-products (RAGE) directly binds to ERK by a D-domain-like docking site. *FEBS Lett.* 550: 107–113.
209. Sorci, G., F. Riuzzi, C. Arcuri, I. Giambanco, and R. Donato. 2004. Amphoterin stimulates myogenesis and counteracts the antimyogenic factors basic fibroblast

growth factor and S100B via RAGE binding. *Molecular and Cellular Biology* 24: 4880–4894.
210. Huang, J. S., J. Y. Guh, H. C. Chen, W. C. Hung, Y. H. Lai, and L. Y. Chuang. 2001. Role of receptor for advanced glycation end-product (RAGE) and the JAK/STAT-signaling pathway in AGE-induced collagen production in NRK-49F cells. *J. Cell. Biochem.* 81: 102–113.
211. Sakaguchi, T., S. F. Yan, S. D. Yan, D. Belov, L. L. Rong, M. Sousa, M. Andrassy, S. P. Marso, S. Duda, B. Arnold, B. Liliensiek, P. P. Nawroth, D. M. Stern, A. M. Schmidt, and Y. Naka. 2003. Central role of RAGE-dependent neointimal expansion in arterial restenosis. *J Clin Invest* 111: 959–972.
212. Srikrishna, G., J. Nayak, B. Weigle, A. Temme, D. Foell, L. Hazelwood, A. Olsson, N. Volkmann, D. Hanein, and H. H. Freeze. 2010. Carboxylated N-glycans on RAGE promote S100A12 binding and signaling. *J. Cell. Biochem.* 110: 645–659.
213. Park, S. J., T. Kleffmann, and P. A. Hessian. 2011. The G82S polymorphism promotes glycosylation of the receptor for advanced glycation end products (RAGE) at asparagine 81: comparison of wild-type rage with the G82S polymorphic variant. *J Biol Chem* 286: 21384–21392.
214. Raucci, A., S. Cugusi, A. Antonelli, S. M. Barabino, L. Monti, A. Bierhaus, K. Reiss, P. Saftig, and M. E. Bianchi. 2008. A soluble form of the receptor for advanced glycation endproducts (RAGE) is produced by proteolytic cleavage of the membrane-bound form by the sheddase a disintegrin and metalloprotease 10 (ADAM10). *FASEB J* 22: 3716–3727.
215. Zhang, L., M. Bukulin, E. Kojro, A. Roth, V. V. Metz, F. Fahrenholz, P. P. Nawroth, A. Bierhaus, and R. Postina. 2008. Receptor for advanced glycation end products is subjected to protein ectodomain shedding by metalloproteinases. *J Biol Chem* 283: 35507–35516.
216. Galichet, A., M. Weibel, and C. W. Heizmann. 2008. Calcium-regulated intramembrane proteolysis of the RAGE receptor. *Biochem Biophys Res Commun* 370: 1–5.
217. Metz, V. V., E. Kojro, D. Rat, and R. Postina. 2012. Induction of RAGE shedding by activation of G protein-coupled receptors. *PLoS ONE* 7: e41823.
218. Yan, S. F., R. Ramasamy, and A. M. Schmidt. 2010. Soluble RAGE: therapy and biomarker in unraveling the RAGE axis in chronic disease and aging. *Biochemical pharmacology* 79: 1379–1386.
219. Kalea, A. Z., A. M. Schmidt, and B. I. Hudson. 2011. Alternative splicing of RAGE: roles in biology and disease. *Front Biosci (Landmark Ed)* 16: 2756–2770.
220. Kalea, A. Z., F. See, E. Harja, M. Arriero, A. M. Schmidt, and B. I. Hudson. 2010. Alternatively spliced RAGEv1 inhibits tumorigenesis through suppression of JNK signaling. *Cancer Res* 70: 5628–5638.
221. Frommhold, D., A. Kamphues, I. Hepper, M. Pruenster, I. K. Lukic, I. Socher, V. Zablotskaya, K. Buschmann, B. Lange-Sperandio, J. Schymeinsky, E. Ryschich, J. Poeschl, C. Kupatt, P. P. Nawroth, M. Moser, B. Walzog, A. Bierhaus, and M. Sperandio. 2010. RAGE and ICAM-1 cooperate in mediating leukocyte recruitment during acute inflammation in vivo. *Blood* 116: 841–849.
222. Frommhold, D., A. Kamphues, S. Dannenberg, K. Buschmann, V. Zablotskaya, R. Tschada, B. Lange-Sperandio, P. P. Nawroth, J. Poeschl, A. Bierhaus, and M. Sperandio. 2011. RAGE and ICAM-1 differentially control leukocyte recruitment during acute inflammation in a stimulus-dependent manner. *BMC Immunol.* 12: 56.
223. Sorkin, A., and M. von Zastrow. 2009. Endocytosis and signalling: intertwining molecular networks. *Nat Rev Mol Cell Biol* 10: 609–622.
224. Sevillano, N., M. D. Girón, M. Salido, A. M. Vargas, J. Vilches, and R. Salto. 2009. Internalization of the receptor for advanced glycation end products (RAGE) is required to mediate intracellular responses. *J. Biochem.* 145: 21–30.
225. Wallar, B. J., and A. S. Alberts. 2003. The formins: active scaffolds that remodel the cytoskeleton. *Trends Cell Biol* 13: 435–446.

226. Reddy, M. A., S.-L. Li, S. Sahar, Y.-S. Kim, Z.-G. Xu, L. Lanting, and R. Natarajan. 2006. Key role of Src kinase in S100B-induced activation of the receptor for advanced glycation end products in vascular smooth muscle cells. *J Biol Chem* 281: 13685–13693.
227. Perrone, L., G. Peluso, and M. A. Melone. 2008. RAGE recycles at the plasma membrane in S100B secretory vesicles and promotes Schwann cells morphological changes. *J. Cell. Physiol.* 217: 60–71.
228. Sirois, C. M., T. Jin, A. L. Miller, D. Bertheloot, H. Nakamura, G. L. Horvath, A. Mian, J. Jiang, J. Schrum, L. Bossaller, K. Pelka, N. Garbi, Y. Brewah, J. Tian, C. Chang, P. S. Chowdhury, G. P. Sims, R. Kolbeck, A. J. Coyle, A. A. Humbles, T. S. Xiao, and E. Latz. 2013. RAGE is a nucleic acid receptor that promotes inflammatory responses to DNA. *Journal of Experimental Medicine*.
229. Carpenter, A. E., T. R. Jones, M. R. Lamprecht, C. Clarke, I. H. Kang, O. Friman, D. A. Guertin, J. H. Chang, R. A. Lindquist, J. Moffat, P. Golland, and D. M. Sabatini. 2006. CellProfiler: image analysis software for identifying and quantifying cell phenotypes. *Genome Biol.* 7: R100.
230. Lan, T., D. Wang, L. Bhagat, V. J. Philbin, D. Yu, J. X. Tang, M. R. Putta, T. Sullivan, N. La Monica, E. R. Kandimalla, and S. Agrawal. 2013. Design of synthetic oligoribonucleotide-based agonists of Toll-like receptor 3 and their immune response profiles in vitro and in vivo. *Org. Biomol. Chem.* 11: 1049–1058.
231. Mukhopadhyay, S., A. Varin, Y. Chen, B. Liu, K. Tryggvason, and S. Gordon. 2011. SR-A/MARCO-mediated ligand delivery enhances intracellular TLR and NLR function, but ligand scavenging from cell surface limits TLR4 response to pathogens. *Blood* 117: 1319–1328.
232. Adami, C., R. Bianchi, G. Pula, and R. Donato. 2004. S100B-stimulated NO production by BV-2 microglia is independent of RAGE transducing activity but dependent on RAGE extracellular domain. *Biochim Biophys Acta* 1742: 169–177.
233. Pohar, J., N. Pirher, M. Bencina, M. Manček-Keber, and R. Jerala. 2013. The role of UNC93B1 protein in surface localization of TLR3 receptor and in cell priming to nucleic acid agonists. *J Biol Chem* 288: 442–454.
234. Qi, R., D. Singh, and C. C. Kao. 2012. Proteolytic processing regulates Toll-like receptor 3 stability and endosomal localization. *J Biol Chem* 287: 32617–32629.
235. Gitlin, L., W. Barchet, S. Gilfillan, M. Cella, B. Beutler, R. A. Flavell, M. S. Diamond, and M. Colonna. 2006. Essential role of mda-5 in type I IFN responses to polyriboinosinic:polyribocytidylic acid and encephalomyocarditis picornavirus. *Proc Natl Acad Sci USA* 103: 8459–8464.
236. Offermann, M. K., J. Zimring, K. H. Mellits, M. K. Hagan, R. Shaw, R. M. Medford, M. B. Mathews, S. Goodbourn, and R. Jagus. 1995. Activation of the double-stranded-RNA-activated protein kinase and induction of vascular cell adhesion molecule-1 by poly (I).poly (C) in endothelial cells. *Eur J Biochem* 232: 28–36.
237. Gil, J., J. Alcamí, and M. Esteban. 2000. Activation of NF-kappa B by the dsRNA-dependent protein kinase, PKR involves the I kappa B kinase complex. *Oncogene* 19: 1369–1378.
238. Liu, L., M. Yang, R. Kang, Y. Dai, Y. Yu, F. Gao, H. Wang, X. Sun, X. Li, J. Li, H. Wang, L. Cao, and D. Tang. 2014. HMGB1-DNA complex-induced autophagy limits AIM2 inflammasome activation through RAGE. *Biochem Biophys Res Commun* 450: 851–856.
239. Rigby, R. E., L. M. Webb, K. J. Mackenzie, Y. Li, A. Leitch, M. A. M. Reijns, R. J. Lundie, A. Revuelta, D. J. Davidson, S. Diebold, Y. Modis, A. S. MacDonald, and A. P. Jackson. 2014. RNA:DNA hybrids are a novel molecular pattern sensed by TLR9. *EMBO J* 33: 542–558.
240. Mankan, A. K., T. Schmidt, D. Chauhan, M. Goldeck, K. Höning, M. Gaidt, A. V. Kubarenko, L. Andreeva, K.-P. Hopfner, and V. Hornung. 2014. Cytosolic RNA:DNA hybrids activate the cGAS-STING axis. *EMBO J* 33: 2937–2946.

241. Hirsiger, S., H.-P. Simmen, C. M. L. Werner, G. A. Wanner, and D. Rittirsch. 2012. Danger signals activating the immune response after trauma. *Mediators Inflamm* 2012: 315941.
242. Yanai, H., T. Ban, and T. Taniguchi. 2012. High-mobility group box family of proteins: ligand and sensor for innate immunity. *Trends Immunol.* 33: 633–640.
243. Li, G., X. Liang, and M. T. Lotze. 2013. HMGB1: The Central Cytokine for All Lymphoid Cells. *Front Immunol* 4: 68.
244. Urbonaviciute, V., B. G. Fürnrohr, S. Meister, L. Munoz, P. Heyder, F. De Marchis, M. E. Bianchi, C. Kirschning, H. Wagner, A. A. Manfredi, J. R. Kalden, G. Schett, P. Rovere-Querini, M. Herrmann, and R. E. Voll. 2008. Induction of inflammatory and immune responses by HMGB1-nucleosome complexes: implications for the pathogenesis of SLE. *Journal of Experimental Medicine* 205: 3007–3018.
245. Youn, J. H., Y. J. Oh, E. S. Kim, J. E. Choi, and J.-S. Shin. 2008. High mobility group box 1 protein binding to lipopolysaccharide facilitates transfer of lipopolysaccharide to CD14 and enhances lipopolysaccharide-mediated TNF-alpha production in human monocytes. *J Immunol* 180: 5067–5074.
246. Sha, Y., J. Zmijewski, Z. Xu, and E. Abraham. 2008. HMGB1 develops enhanced proinflammatory activity by binding to cytokines. *J Immunol* 180: 2531–2537.
247. Yanai, H., T. Ban, Z. Wang, M. K. Choi, T. Kawamura, H. Negishi, M. Nakasato, Y. Lu, S. Hangai, R. Koshiba, D. Savitsky, L. Ronfani, S. Akira, M. E. Bianchi, K. Honda, T. Tamura, T. Kodama, and T. Taniguchi. 2009. HMGB proteins function as universal sentinels for nucleic-acid-mediated innate immune responses. *Nature* 462: 99–103.
248. Bell, A. J., S. Chauhan, S. A. Woodson, and N. R. Kallenbach. 2008. Interactions of recombinant HMGB proteins with branched RNA substrates. *Biochem Biophys Res Commun* 377: 262–267.
249. Smith, S., and C. Jefferies. 2014. Role of DNA/RNA sensors and contribution to autoimmunity. *Cytokine Growth Factor Rev.* 25: 745–757.
250. Shrivastav, M., and T. B. Niewold. 2013. Nucleic Acid sensors and type I interferon production in systemic lupus erythematosus. *Front Immunol* 4: 319.
251. Vollmer, J., S. Tluk, C. Schmitz, S. Hamm, M. Jurk, A. Forsbach, S. Akira, K. M. Kelly, W. H. Reeves, S. Bauer, and A. M. Krieg. 2005. Immune stimulation mediated by autoantigen binding sites within small nuclear RNAs involves Toll-like receptors 7 and 8. *The Journal of experimental medicine* 202: 1575–1585.
252. Christensen, S. R., J. Shupe, K. Nickerson, M. Kashgarian, R. A. Flavell, and M. J. Shlomchik. 2006. Toll-like receptor 7 and TLR9 dictate autoantibody specificity and have opposing inflammatory and regulatory roles in a murine model of lupus. *Immunity* 25: 417–428.
253. Pawar, R. D., A. Ramanjaneyulu, O. P. Kulkarni, M. Lech, S. Segerer, and H.-J. Anders. 2007. Inhibition of Toll-like receptor-7 (TLR-7) or TLR-7 plus TLR-9 attenuates glomerulonephritis and lung injury in experimental lupus. *J. Am. Soc. Nephrol.* 18: 1721–1731.
254. Hwang, S.-H., H. Lee, M. Yamamoto, L. A. Jones, J. Dayalan, R. Hopkins, X. J. Zhou, F. Yarovinsky, J. E. Connolly, M. A. Curotto de Lafaille, E. K. Wakeland, and A.-M. Fairhurst. 2012. B cell TLR7 expression drives anti-RNA autoantibody production and exacerbates disease in systemic lupus erythematosus-prone mice. *J Immunol* 189: 5786–5796.
255. Jöckel, S., G. Nees, R. Sommer, Y. Zhao, D. Cherkasov, H. Hori, G. Ehm, M. Schnare, M. Nain, A. Kaufmann, and S. Bauer. 2012. The 2'-O-methylation status of a single guanosine controls transfer RNA-mediated Toll-like receptor 7 activation or inhibition. *Journal of Experimental Medicine* 209: 235–241.
256. Bauer, S., S. Pigisch, D. Hangel, A. Kaufmann, and S. Hamm. 2008. Recognition of nucleic acid and nucleic acid analogs by Toll-like receptors 7, 8 and 9.

Immunobiology 213: 315–328.
257. Karikó, K., M. Buckstein, H. Ni, and D. Weissman. 2005. Suppression of RNA recognition by Toll-like receptors: the impact of nucleoside modification and the evolutionary origin of RNA. *Immunity* 23: 165–175.
258. Cornacchia, E., J. Golbus, J. Maybaum, J. Strahler, S. Hanash, and B. Richardson. 1988. Hydralazine and procainamide inhibit T cell DNA methylation and induce autoreactivity. *J Immunol* 140: 2197–2200.
259. Julian, M. W., G. Shao, Z. C. VanGundy, T. L. Papenfuss, and E. D. Crouser. 2013. Mitochondrial Transcription Factor A, an Endogenous Danger Signal, Promotes TNFα Release via RAGE- and TLR9-Responsive Plasmacytoid Dendritic Cells. *PLoS ONE* 8: e72354.
260. Lehmann, S. M., C. Krüger, B. Park, K. Derkow, K. Rosenberger, J. Baumgart, T. Trimbuch, G. Eom, M. Hinz, D. Kaul, P. Habbel, R. Kälin, E. Franzoni, A. Rybak, D. Nguyen, R. Veh, O. Ninnemann, O. Peters, R. Nitsch, F. L. Heppner, D. Golenbock, E. Schott, H. L. Ploegh, F. G. Wulczyn, and S. Lehnardt. 2012. An unconventional role for miRNA: let-7 activates Toll-like receptor 7 and causes neurodegeneration. *Nat. Neurosci.* 15: 827–835.
261. Fu, X.-D. 2014. Non-coding RNA: a new frontier in regulatory biology. *Natl Sci Rev* 1: 190–204.
262. Cech, T. R., and J. A. Steitz. 2014. The noncoding RNA revolution-trashing old rules to forge new ones. *Cell* 157: 77–94.
263. Dinger, M. E., T. R. Mercer, and J. S. Mattick. 2008. RNAs as extracellular signaling molecules. *J. Mol. Endocrinol.* 40: 151–159.
264. Zhang, L., D. Hou, X. Chen, D. Li, L. Zhu, Y. Zhang, J. Li, Z. Bian, X. Liang, X. Cai, Y. Yin, C. Wang, T. Zhang, D. Zhu, D. Zhang, J. Xu, Q. Chen, Y. Ba, J. Liu, Q. Wang, J. Chen, J. Wang, M. Wang, Q. Zhang, J. Zhang, K. Zen, and C.-Y. Zhang. 2012. Exogenous plant MIR168a specifically targets mammalian LDLRAP1: evidence of cross-kingdom regulation by microRNA. *Cell Res.* 22: 107–126.
265. Chen, X., Y. Ba, L. Ma, X. Cai, Y. Yin, K. Wang, J. Guo, Y. Zhang, J. Chen, X. Guo, Q. Li, X. Li, W. Wang, Y. Zhang, J. Wang, X. Jiang, Y. Xiang, C. Xu, P. Zheng, J. Zhang, R. Li, H. Zhang, X. Shang, T. Gong, G. Ning, J. Wang, K. Zen, J. Zhang, and C.-Y. Zhang. 2008. Characterization of microRNAs in serum: a novel class of biomarkers for diagnosis of cancer and other diseases. *Cell Res.* 18: 997–1006.
266. Zhang, Y., D. Liu, X. Chen, J. Li, L. Li, Z. Bian, F. Sun, J. Lu, Y. Yin, X. Cai, Q. Sun, K. Wang, Y. Ba, Q. Wang, D. Wang, J. Yang, P. Liu, T. Xu, Q. Yan, J. Zhang, K. Zen, and C.-Y. Zhang. 2010. Secreted monocytic miR-150 enhances targeted endothelial cell migration. *Molecular Cell* 39: 133–144.
267. Winston, W. M., C. Molodowitch, and C. P. Hunter. 2002. Systemic RNAi in C. elegans requires the putative transmembrane protein SID-1. *Science* 295: 2456–2459.
268. Feinberg, E. H., and C. P. Hunter. 2003. Transport of dsRNA into cells by the transmembrane protein SID-1. *Science* 301: 1545–1547.
269. Duxbury, M. S., S. W. Ashley, and E. E. Whang. 2005. RNA interference: a mammalian SID-1 homologue enhances siRNA uptake and gene silencing efficacy in human cells. *Biochem Biophys Res Commun* 331: 459–463.
270. Jose, A. M., and C. P. Hunter. 2007. Transport of sequence-specific RNA interference information between cells. *Annu. Rev. Genet.* 41: 305–330.
271. Turchinovich, A., L. Weiz, A. Langheinz, and B. Burwinkel. 2011. Characterization of extracellular circulating microRNA. *Nucleic Acids Res* 39: 7223–7233.
272. Arroyo, J. D., J. R. Chevillet, E. M. Kroh, I. K. Ruf, C. C. Pritchard, D. F. Gibson, P. S. Mitchell, C. F. Bennett, E. L. Pogosova-Agadjanyan, D. L. Stirewalt, J. F. Tait, and M. Tewari. 2011. Argonaute2 complexes carry a population of circulating microRNAs independent of vesicles in human plasma. *Proc Natl Acad Sci USA* 108: 5003–5008.

273. Turchinovich, A., and B. Burwinkel. 2012. Distinct AGO1 and AGO2 associated miRNA profiles in human cells and blood plasma. *RNA Biol* 9: 1066–1075.
274. Vickers, K. C., B. T. Palmisano, B. M. Shoucri, R. D. Shamburek, and A. T. Remaley. 2011. MicroRNAs are transported in plasma and delivered to recipient cells by high-density lipoproteins. *Nat Cell Biol* 13: 423–433.
275. Miller, A. L., G. P. Sims, Y. A. Brewah, M. C. Rebelatto, J. Kearley, E. Benjamin, A. E. Keller, P. Brohawn, R. Herbst, A. J. Coyle, A. A. Humbles, and R. Kolbeck. 2012. Opposing roles of membrane and soluble forms of the receptor for advanced glycation end products in primary respiratory syncytial virus infection. *J. Infect. Dis.* 205: 1311–1320.
276. Bowman, M. A. H., and A. M. Schmidt. 2013. The next generation of RAGE modulators: implications for soluble RAGE therapies in vascular inflammation. *J. Mol. Med.* 91: 1329–1331.
277. Tae, H.-J., J. M. Kim, S. Park, N. Tomiya, G. Li, W. Wei, N. Petrashevskaya, I. Ahmet, J. Pang, S. Cruschwitz, R. A. Riebe, Y. Zhang, C. H. Morrell, D. Browe, Y. C. Lee, R.-P. Xiao, M. I. Talan, E. G. Lakatta, and L. Lin. 2013. The N-glycoform of sRAGE is the key determinant for its therapeutic efficacy to attenuate injury-elicited arterial inflammation and neointimal growth. *J. Mol. Med.* 91: 1369–1381.
278. Krieg, A. M. 2012. CpG still rocks! Update on an accidental drug. *nucleic acid therapeutics* 22: 77–89.

7. Annexes

7.1 Plasmid and gene sequences

Note: bold underlined sequences correspond to the restriction sites described in the Material and Method section.

pRP plasmid sequence

GACGGATCGGGAGATCTCCCGATCCCCTATGGTGCACTCTCAGTACAATCTGCTCTGATGCCGCATAGTTAAGCCAGTATCTGCTC
CCTGCTTGTGTGTTGGAGGTCGCTGAGTAGTGCGCGAGCAAAATTTAAGCTACAACAAGGCAAGGCTTGACCGACAATTGCATGAA
GAATCTGCTTAGGGTTAGGCGTTTTGCGCTGCTTCGCGAGTTGACATTGATTATTGACTAGTTATTAATAGTAATCAATTACGGGG
TCATTAGTTCATAGCCCATATATGGAGTTCCGCGTTACATAACTTACGGTAAATGGCCCGCCTGGCTGACCGCCCAACGACCCCCG
CCCATTGACGTCAATAATGACGTATGTTCCCATAGTAACGCCAATAGGGACTTTCCATTGACGTCAATGGGTGGAGTATTTACGGT
AAACTGCCCACTTGGCAGTACATCAAGTGTATCATATGCCAAGTACGCCCCCTATTGACGTCAATGACGGTAAATGGCCCGCCTGG
CATTATGCCCAGTACATGACCTTATGGGACTTTCCTACTTGGCAGTACATCTACGTATTAGTCATCGCTATTACCATGGTGATGCG
GTTTTGGCAGTACATCAATGGGCGTGGATAGCGGTTTGACTCACGGGGATTTCCAAGTCTCCACCCCATTGACGTCAATGGGAGTT
TGTTTTGGCACCAAAATCAACGGGACTTTCCAAAATGTCGTAACAACTCCGCCCCATTGACGCAAATGGGCGGTAGGCGTGTACGG
TGGGAGGTCTATATAAGCAGAGCTCAATAAAAGAGCCCACAACCCCTCACTCCGCGCGCCAGTCTTCCGATAGACTGCGTCGCCCG
GGTACCCGTATTCCCAATAAAGCCTCTTGCTGTTTGCATCCGAATCGTGGTCTCGCTGTTCCTTGGGAGGGTCTCCTCTGAGTGAT
TGACTACCCACGACGGGGGTCTTTCATTTGGGGGCTCGTCCGGGATTTGGAGACCCCTGCCCAGGGACCACCGACCCACCACCGGG
AGGTAAGCTGGCCAGCAACTTATCTGTGTCTGTCCGATTGTCTAGTGTCTATGTTTGATGTTATGCGCCTGCGTCTGTACTAGTTA
GCTAACTAGCTCTGTATCTGGCGGACCCGTGGTGGAACTGACGAGTTCTGAACACCCGGCCGCAACCCTGGGAGACGTCCCAGGGA
CTTTGGGGGCCGTTTTTGTGGCCCGACCTGAGGAAGGGAGTCGATGTGGAATCCGACCCCGTCAGGATATGTGGTTCTGGTAGGAG
ACGAGAACCTAAAACAGTTCCCGCCTCCGTCTGAATTTTTGCTTTCGGTTTGGAACCGAAGCCGCGCGTCTTGTCTGCTGCAGCGC
TGCAGCATCGTTCTGTGTTGTCTCTGTCTGACTGTGTTTCTGTATTTGTCTGAAAATTAGGGCCAGACTGTTACCACTCCCTTAAG
TTTGACCTTAGGTCACTGGAAAGATGTCGAGCGGATCGCTCACAACCAGTCGGTAGATGTCAAGAAGAGACGTTGGGTTACCTTCT
GCTCTGCAGAATGGCCAACCTTTAACGTCGGATGGCCGCGAGACGGCACCTTTAACCGAGACCTCATCACCCAGGTTAAGATCAAG
GTCTTTTCACCTGGCCCGCATGGACACCCAGACCAGGTCCCCTACATCGTGACCTGGGAAGCCTTGGCTTTTGACCCCCCTCCCTG
GGTCAAGCCCTTTGTACACCCTAAGCCTCCGCCTCCTCTTCCTCCATCCGCCCCGTCTCTCCCCCTTGAACCTCCTCGTTCGACCC
CGCCTCGATCCTCCCTTTATCCAGCCCTCACTCCTTCTCTAGGCGCCTCCGGTATGACCGAGTACAAGCCCACGGTGCGCCTCGCC
ACCCGCGACGACGTCCCCAGGGCCGTACGCACCCTCGCCGCCGCGTTCGCCGACTACCCCGCCACGCGCCACACCGTCGATCCGGA
CCGCCACATCGAGCGGGTCACCGAGCTGCAAGAACTCTTCCTCACGCGCGTCGGGCTCGACATCGGCAAGGTGTGGGTCGCGGACG
ACGGCGCCGCGGTGGCGGTCTGGACCACGCCGGAGAGCGTCGAAGCGGGGGCGGTGTTCGCCGAGATCGGCCCGCGCATGGCCGAG
TTGAGCGGTTCCCGGCTGGCCGCGCAGCAACAGATGGAAGGCCTCCTGGCGCCGCACCGGCCCAAGGAGCCCGCGTGGTTCCTGGC
CACCGTCGGCGTCTCGCCCGACCACCAGGGCAAGGGTCTGGGCAGCGCCGTCGTGCTCCCCGGAGTGGAGGCGGCCGAGCGCGCCG
GGGTGCCCGCCTTCCTGGAGACCTCCGCGCCCCGCAACCTCCCCTTCTACGAGCGGCTCGGCTTCACCGTCACCGCCGACGTCGAG
GTGCCCGAAGGACCGCGCACCTGGTGCATGACCCGCAAGCCCGGTGCCTGAGGATCGATCCGGCCATTAGCCATATTATTCATTGG
TTATATAGCATAAATCAATATTGGCTATTGGCCATTGCATACGTTGTATCCATATCATAATATGTACATTTATATTGGCTCATGTC
CAACATTACCGCCATGTTGACATTGATTATTGACTAGTTATTAATAGTAATCAATTACGGGGTCATTAGTTCATAGCCCATATATG
GAGTTCCGCGTTACATAACTTACGGTAAATGGCCCGCCTGGCTGACCGCCCAACGACCCCCGCCCATTGACGTCAATAATGACGTA
TGTTCCCATAGTAACGCCAATAGGGACTTTCCATTGACGTCAATGGGTGGAGTATTTACGGTAAACTGCCCACTTGGCAGTACATC
AAGTGTATCATATGCCAAGTACGCCCCCTATTGACGTCAATGACGGTAAATGGCCCGCCTGGCATTATGCCCAGTACATGACCTTA
TGGGACTTTCCTACTTGGCAGTACATCTACGTATTAGTCATCGCTATTACCATGGTGATGCGGTTTTGGCAGTACATCAATGGGCG
TGGATAGCGGTTTGACTCACGGGGATTTCCAAGTCTCCACCCCATTGACGTCAATGGGAGTTTGTTTTGGCACCAAAATCAACGGG
ACTTTCCAAAATGTCGTAACAACTCCGCCCCATTGACGCAAATGGGCGGTAGGCGTGTACGGTGGGAGGTCTATATAAGCAGAGCT
CGTTTAGTGAACCGTCAGATCGCCTGGAGACGCCATCCACGCTGTTTTGACCTCCATAGAAGACACCGGGACCGATCCAGCCTCCG
CGGCCCCAAGCTTTGCTAGCCAATTGTCGCGCGCGTCTTCTAGAGGATCTGGTACCTCTTCTGGATCCTCTTCT**GGCGCGCC**TTCT
TCT**GCGGCCGC**TAAACCTAGGAGACTCGAGTCTTCTCCATCTGGCTGGTCTTCTGGGCCCTAATTAGTTGAACGCCGGCGGTCGAG
GCCGCATCGATAAAATAAAAGATTTTATTTAGTCTCCAGAAAAAGGGGGGAATGAAAGACCCCACCTGTAGGTTTGGCAAGCTAGC
TTAAGTAACGCCATTTTGCAAGGCATGGAAAAATACATAACTGAGAATAGAGAAGTTCAGATCAAGGTCAGGAACAGATGGAACAG
CTGAATATGGGCCAAACAGGATATCTGTGGTAAGCAGTTCCTGCCCCGGCTCAGGGCCAAGAACAGATGGTCCCCAGATGCGGTCCAGCCCTCAGCA
GTTTCTAGAGAACCATCAGATGTTTCCAGGGTGCCCCAAGGACCTGAAATGACCCTGTGCCTTATTTGAACTAACCAATCAGTTCG
CTTCTCGCTTCTGTTCGCGCGCTTCTGCTCCCCGAGCTCAATAAAAGAGCCCACAACCCCTCACTCGGGGCGCCAGTCCTCCGATT
GACTGAGTCGCCCGGGTACCCGTGTATCCAATAAACCCTCTTGCAGTTGCATCCGACTTGTGGTCTCGCTGTTCCTTGGGAGGGTC
TCCTCTGAGTGATTGACTACCCGTCAGCGGGGGTCTTTCATTTGGGGGCTCGTCCGGGATCGGGAGACCCCTGCCCAGGGACCACC
GACCCACCACCGGGAGGTAAGCTGGGAACTAATTCTGTGGAATGTGTGTCAGTTAGGGTGTGGAAAGTCCCCAGGCTCCCCAGCAG
GCAGAAGTATGCAAAGCATGCATCTCAATTAGTCAGCAACCAGGTGTGGAAAGTCCCCAGGCTCCCCAGCAGGCAGAAGTATGCAA
AGCATGCATCTCAATTAGTCAGCAACCATAGTCCCGCCCCTAACTCCGCCCATCCCGCCCCTAACTCCGCCCAGTTCCGCCCATTC
TCCGCCCCATGGCTGACTAATTTTTTTTATTTATGCAGAGGCCGAGGCCGCCTCTGCCTCTGAGCTATTCCAGAAGTAGTGAGGAG
GCTTTTTTGGAGGCCTAGTACCGTCGACCTCTAGCTAGAGCTTGGCGTAATCATGGTCATAGCTGTTTCCTGTGTGAAATTGTTAT
CCGCTCACAATTCCACACAACATACGAGCCGGAAGCATAAAGTGTAAAGCCTGGGGTGCCTAATGAGTGAGCTAACTCACATTAAT
TGCGTTGCGCTCACTGCCCGCTTTCCAGTCGGGAAACCTGTCGTGCCAGCTGCATTAATGAATCGGCCAACGCGCGGGGAGAGGCG
GTTTGCGTATTGGGCGCTCTTCCGCTTCCTCGCTCACTGACTCGCTGCGCTCGGTCGTTCGGCTGCGGCGAGCGGTATCAGCTCAC
TCAAAGGCGGTAATACGGTTATCCACAGAATCAGGGGATAACGCAGGAAAGAACATGTGAGCAAAAGGCCAGCAAAAGGCCAGGAA
CCGTAAAAAGGCCGCGTTGCTGGCGTTTTTCCATAGGCTCCGCCCCCCTGACGAGCATCACAAAAATCGACGCTCAAGTCAGAGGT
GGCGAAACCCGACAGGACTATAAAGATACCAGGCGTTTCCCCCTGGAAGCTCCCTCGTGCGCTCTCCTGTTCCGACCCTGCCGCTT

ACCGGATACCTGTCCGCCTTTCTCCCTTCGGGAAGCGTGGCGCTTTCTCAATGCTCACGCTGTAGGTATCTCAGTTCGGTGTAGGT
CGTTCGCTCCAAGCTGGGCTGTGTGCACGAACCCCCCGTTCAGCCCGACCGCTGCGCCTTATCCGGTAACTATCGTCTTGAGTCCA
ACCCGGTAAGACACGACTTATCGCCACTGGCAGCAGCCACTGGTAACAGGATTAGCAGAGCGAGGTATGTAGGCGGTGCTACAGAG
TTCTTGAAGTGGTGGCCTAACTACGGCTACACTAGAAGGACAGTATTTGGTATCTGCGCTCTGCTGAAGCCAGTTACCTTCGGAAA
AAGAGTTGGTAGCTCTTGATCCGGCAAACAAACCACCGCTGGTAGCGGTGGTTTTTTTGTTTGCAAGCAGCAGATTACGCGCAGAA
AAAAAGGATCTCAAGAAGATCCTTTGATCTTTTCTACGGGGTCTGACGCTCAGTGGAACGAAAACTCACGTTAAGGGATTTTGGTC
ATGAGATTATCAAAAAGGATCTTCACCTAGATCCTTTTAAATTAAAAATGAAGTTTTAAATCAATCTAAAGTATATATGAGTAAAC
TTGGTCTGACAGTTACCAATGCTTAATCAGTGAGGCACCTATCTCAGCGATCTGTCTATTTCGTTCATCCATAGTTGCCTGACTCC
CCGTCGTGTAGATAACTACGATACGGGAGGGCTTACCATCTGGCCCCAGTGCTGCAATGATACCGCGAGACCCACGCTCACCGGCT
CCAGATTTATCAGCAATAAACCAGCCAGCCGGAAGGGCCGAGCGCAGAAGTGGTCCTGCAACTTTATCCGCCTCCATCCAGTCTAT
TAATTGTTGCCGGGAAGCTAGAGTAAGTAGTTCGCCAGTTAATAGTTTGCGCAACGTTGTTGCCATTGCTACAGGCATCGTGGTGT
CACGCTCGTCGTTTGGTATGGCTTCATTCAGCTCCGGTTCCCAACGATCAAGGCGAGTTACATGATCCCCCATGTTGTGCAAAAAA
GCGGTTAGCTCCTTCGGTCCTCCGATCGTTGTCAGAAGTAAGTTGGCCGCAGTGTTATCACTCATGGTTATGGCAGCACTGCATAA
TTCTCTTACTGTCATGCCATCCGTAAGATGCTTTTCTGTGACTGGTGAGTACTCAACCAAGTCATTCTGAGAATAGTGTATGCGGC
GACCGAGTTGCTCTTGCCCGGCGTCAATACGGGATAATACCGCGCCACATAGCAGAACTTTAAAAGTGCTCATCATTGGAAAACGT
TCTTCGGGGCGAAAACTCTCAAGGATCTTACCGCTGTTGAGATCCAGTTCGATGTAACCCACTCGTGCACCCAACTGATCTTCAGC
ATCTTTTACTTTCACCAGCGTTTCTGGGTGAGCAAAAACAGGAAGGCAAAATGCCGCAAAAAAGGGAATAAGGGCGACACGGAAAT
GTTGAATACTCATACTCTTCCTTTTTCAATATTATTGAAGCATTTATCAGGGTTATTGTCTCATGAGCGGATACATATTTGAATGT
ATTTAGAAAAATAAACAAATAGGGGTTCCGCGCACATTTCCCCGAAAAGTGCCACCTGACGTC

RAGE FL coding sequence

GGCGCGCCTGCCACCATGGCAGCCGGAACAGCAGTTGGAGCCTGGGTGCTGGTCCTCAGTCTGTGGGGGGCAGTAGTAGGTGCTCA
AAACATCACAGCCCGGATTGGCGAGCCACTGGTGCTGAAGTGTAAGGGGGCCCCCAAGAAACCACCCCAGCGGCTGGAATGGAAAC
TGAACACAGGCCGGACAGAAGCTTGGAAGGTCCTGTCTCCCCAGGGAGGAGGCCCCTGGGACAGTGTGGCTCGTGTCCTTCCCAAC
GGCTCCCTCTTCCTTCCGGCTGTCGGGATCCAGGATGAGGGGATTTTCCGGTGCCAGGCAATGAACAGGAATGGAAAGGAGACCAA
GTCCAACTACCGAGTCCGTGTCTACCAGATTCCTGGGAAGCCAGAAATTGTAGATTCTGCCTCTGAACTCACGGCTGGTGTTCCCA
ATAAGGTGGGGACATGTGTGTCAGAGGGAAGCTACCCTGCAGGGACTCTTAGCTGGCACTTGGATGGGAAGCCCCTGGTGCCTAAT
GAGAAGGGAGTATCTGTGAAGGAACAGACCAGGAGACACCCTGAGACAGGGCTCTTCACACTGCAGTCGGAGCTAATGGTGACCCC
AGCCCGGGGAGGAGATCCCCGTCCCACCTTCTCCTGTAGCTTCAGCCCAGGCCTTCCCCGACACCGGGCCTTGCGCACAGCCCCCA
TCCAGCCCCGTGTCTGGGAGCCTGTGCCTCTGGAGGAGGTCCAATTGGTGGTGGAGCCAGAAGGTGGAGCAGTAGCTCCTGGTGGA
ACCGTAACCCTGACCTGTGAAGTCCCTGCCCAGCCCTCTCCTCAAATCCACTGGATGAAGGATGGTGTGCCCTTGCCCCTTCCCCC
CAGCCCTGTGCTGATCCTCCCTGAGATAGGGCCTCAGGACCAGGGAACCTACAGCTGTGTGGCCACCCATTCCAGCCACGGGCCCC
AGGAAAGCCGTGCTGTCAGCATCAGCATCATCGAACCAGGCGAGGAGGGGCCAACTGCAGGCTCTGTGGGAGGATCAGGGCTGGGA
ACTCTAGCCCTGGCCCTGGGGATCCTGGGAGGCCTGGGGACAGCCGCCCTGCTCATTGGGGTCATCTTGTGGCAAAGGCGGCAACG
CCGAGGAGAGGAGAGGAAGGCCCCAGAAAACCAGGAGGAAGAGGAGGAGCGTGCAGAACTGAATCAGTCGGAGGAACCTGAGGCAG
GCGAGAGTAGTACTGGAGGGCCT(TGA)**GCGGCCGC**

RAGE ΔCyt coding sequence

GGCGCGCCTGCCACCATGGCAGCCGGAACAGCAGTTGGAGCCTGGGTGCTGGTCCTCAGTCTGTGGGGGGCAGTAGTAGGTGCTCA
AAACATCACAGCCCGGATTGGCGAGCCACTGGTGCTGAAGTGTAAGGGGGCCCCCAAGAAACCACCCCAGCGGCTGGAATGGAAAC
TGAACACAGGCCGGACAGAAGCTTGGAAGGTCCTGTCTCCCCAGGGAGGAGGCCCCTGGGACAGTGTGGCTCGTGTCCTTCCCAAC
GGCTCCCTCTTCCTTCCGGCTGTCGGGATCCAGGATGAGGGGATTTTCCGGTGCCAGGCAATGAACAGGAATGGAAAGGAGACCAA
GTCCAACTACCGAGTCCGTGTCTACCAGATTCCTGGGAAGCCAGAAATTGTAGATTCTGCCTCTGAACTCACGGCTGGTGTTCCCA
ATAAGGTGGGGACATGTGTGTCAGAGGGAAGCTACCCTGCAGGGACTCTTAGCTGGCACTTGGATGGGAAGCCCCTGGTGCCTAAT
GAGAAGGGAGTATCTGTGAAGGAACAGACCAGGAGACACCCTGAGACAGGGCTCTTCACACTGCAGTCGGAGCTAATGGTGACCCC
AGCCCGGGGAGGAGATCCCCGTCCCACCTTCTCCTGTAGCTTCAGCCCAGGCCTTCCCCGACACCGGGCCTTGCGCACAGCCCCCA
TCCAGCCCCGTGTCTGGGAGCCTGTGCCTCTGGAGGAGGTCCAATTGGTGGTGGAGCCAGAAGGTGGAGCAGTAGCTCCTGGTGGA
ACCGTAACCCTGACCTGTGAAGTCCCTGCCCAGCCCTCTCCTCAAATCCACTGGATGAAGGATGGTGTGCCCTTGCCCCTTCCCCC
CAGCCCTGTGCTGATCCTCCCTGAGATAGGGCCTCAGGACCAGGGAACCTACAGCTGTGTGGCCACCCATTCCAGCCACGGGCCCC
AGGAAAGCCGTGCTGTCAGCATCAGCATCATCGAACCAGGCGAGGAGGGGCCAACTGCAGGCTCTGTGGGAGGATCAGGGCTGGGA
ACTCTAGCCCTGGCCCTGGGGATCCTGGGAGGCCTGGGGACAGCCGCCCTGCTCATTGGGGTCATCTTGTGGCAAAGGCGGTGA**GC
GGCCGC**

RAGE ΔVC1 coding sequence

GGCGCGCCTGCCACCATGGCAGCCGGAACAGCAGTTGGAGCCTGGGTGCTGGTCCTCAGTCTGTGGGGGGCAGTAGTAGGTCCCCG
TGTCTGGGAGCCTGTGCCTCTGGAGGAGGTCCAATTGGTGGTGGAGCCAGAAGGTGGAGCAGTAGCTCCTGGTGGAACCGTAACCC
TGACCTGTGAAGTCCCTGCCCAGCCCTCTCCTCAAATCCACTGGATGAAGGATGGTGTGCCCTTGCCCCTTCCCCCCAGCCCTGTG
CTGATCCTCCCTGAGATAGGGCCTCAGGACCAGGGAACCTACAGCTGTGTGGCCACCCATTCCAGCCACGGGCCCCAGGAAAGCCG
TGCTGTCAGCATCAGCATCATCGAACCAGGCGAGGAGGGGCCAACTGCAGGCTCTGTGGGAGGATCAGGGCTGGGAACTCTAGCCC
TGGCCCTGGGGATCCTGGGAGGCCTGGGGACAGCCGCCCTGCTCATTGGGGTCATCTTGTGGCAAAGGCGGCAACGCCGAGGAGAG
GAGAGGAAGGCCCCAGAAAACCAGGAGGAAGAGGAGGAGCGTGCAGAACTGAATCAGTCGGAGGAACCTGAGGCAGGCGAGAGTAG
TACTGGAGGGCCT**GCGGCCGC**

Linker-mCitrine coding sequence

GCGGCCGCTTTTTTCCCGCTCGAGGGAGGCGGTGGGAGTGGAGGCGGTGGCAGATCCGTGAGCAAGGGCGAGGAGCTGTTCACCGG
GGTGGTGCCCATCCTGGTCGAGCTGGACGGCGACGTAAACGGCCACAAGTTCAGCGTGTCCGGCGAGGGCGAGGGCGATGCCACCT
ACGGCAAGCTGACCCTGAAGTTCATCTGCACCACCGGCAAGCTGCCCGTGCCCTGGCCCACCCTCGTGACCACCTTCGGCTACGGC
CTGATGTGCTTCGCCCGCTACCCCGACCACATGAAGCAGCACGACTTCTTCAAGTCCGCCATGCCCGAAGGCTACGTCCAGGAGCG
CACCATCTTCTTCAAGGACGACGGCAACTACAAGACCCGCGCCGAGGTGAAGTTCGAGGGCGACACCCTGGTGAACCGCATCGAGC
TGAAGGGCATCGACTTCAAGGAGGACGGCAACATCCTGGGGCACAAGCTGGAGTACAACTACAACAGCCACAACGTCTATATCATG
GCCGACAAGCAGAAGAACGGCATCAAGGTGAACTTCAAGATCCGCCACAACATCGAGGACGGCAGCGTGCAGCTCGCCGACCACTA
CCAGCAGAACACCCCCATCGGCGACGGCCCCGTGCTGCTGCCCGACAACCACTACCTGAGCTACCAGTCCAAGCTGAGCAAAGACC
CCAACGAGAAGCGCGATCACATGGTCCTGCTGGAGTTCGTGACCGCCGCCGGGATCACTCTCGGCATGGACGAGCTGTACAAGACT
AGG**CCATCTGGCTGG**

Linker-TagRFP coding sequence

GCGGCCGCTGAGGGAGGCGGTGGGAGTGGAGGCGGTGGCCCTGCAGGGGTGTCTAAGGGCGAAGAGCTGATTAAGGAGAACATGCA
CATGAAGCTGTACATGGAGGGCACCGTGAACAACCACCACTTCAAGTGCACATCCGAGGGCGAAGGCAAGCCCTACGAGGGCACCC
AGACCATGAGAATCAAGGTGGTCGAGGGCGGCCCTCTCCCCTTCGCCTTCGACATCCTGGCTACCAGCTTCATGTACGGCAGCAGA
ACCTTCATCAACCACACCCAGGGCATCCCCGACTTCTTTAAGCAGTCCTTCCCTGAGGGCTTCACATGGGAGAGAGTCACCACATA
CGAAGACGGGGGCGTGCTGACCGCTACCCAGGACACCAGCCTCCAGGACGGCTGCCTCATCTACAACGTCAAGATCAGAGGGGTGA
ACTTCCCATCCAACGGCCCTGTGATGCAGAAGAAAACACTCGGCTGGGAGGCCAACACCGAGATGCTGTACCCCGCTGACGGCGGC
CTGGAAGGCAGAAGCGACATGGCCCTGAAGCTCGTGGGCGGGGGCCACCTGATCTGCAACTTCAAGACCACATACAGATCCAAGAA
ACCCGCTAAGAACCTCAAGATGCCCGGCGTCTACTATGTGGACCACAGACTGGAAAGAATCAAGGAGGCCGACAAAGAGACCTACG
TCGAGCAGCACGAGGTGGCTGTGGCCAGATACTGCGACCTCCCTAGCAAACTGGGGCACAAACTTAATTGAGGGCCCTAATTAGTT
GAA**CGCCGGCG**

NFκB-gLuc plasmid sequence

GGTACCGCCAAGNTAGGGGACTTTCCGCTTGGGGACTTTCCGCTGGGGACTTTCCGCTGGGGACTTTCCGCTGGGGACTTTCCGCG
GAGACTCTAGAGGGTATATAATGGAAGCTCGAATTGATCTGCGATCTAAGTAAGCTTGGCATTCCGGTACTGTTGGTAAAGCCACC
ATGGGAGTCAAAGTTCTGTTTGCCCTGATCTGCATCGCTGTGGCCGAGGCCAAGCCCACCGAGAACAACGAAGACTTCAACATCGT
GGCCGTGGCCAGCAACTTCGCGACCACGGATCTCGATGCTGACCGCGGGAAGTTGCCCGGCAAGAAGCTGCCGCTGGAGGTGCTCA
AAGAGATGGAAGCCAATGCCCGGAAAGCTGGCTGCACCAGGGGCTGTCTGATCTGCCTGTCCCACATCAAGTGCACGCCCAAGATG
AAGAAGTTCATCCCAGGACGCTGCCACACCTACGAAGGCGACAAAGAGTCCGCACAGGGCGGCATAGGCGAGGCGATCGTCGACAT
TCCTGAGATTCCTGGGTTCAAGGACTTGGAGCCSATGGAGCAGTTCATCGCACAGGTCGATCTGTGTGTGGACTGCACAACTGGCT
GCCTCAAAGGGCTTGCCAACGTGCAGTGTTCTGACCTGCTCAAGAAGTGGCTGCCGCAACGCTGTGCGACCTTTGCCAGCAAGATC
CAGGGCCAGGTGGACAAGATCAAGGGGGCCGGTGGTGACTAATCTAGAGTCGGGGCGGCCGGCCGCTTCGAGCAGACATGATAAGA
TACATTGATGAGTTTGGACAAACCACAACTAGAATGCAGTGAAAAAAATGCTTTATTTGTGAAATTTGTGATGCTATTGCTTTATT
TGTAACCATTATAAGCTGCAATAAACAAGTTAACAACAACAATTGCATTCATTTTATGTTTCAGGTTCAGGGGGAGGTGTGGGAGG
TTTTTTAAAGCAAGTAAAACCTCTACAAATGTGGTAAAATCGATAAGGATCCGTCGACCGATGCCCTTGAGAGCCTTCAACCCAGT
CAGCTCCTTCCGGTGGGCGCGGGGCATGACTATCGTCGCCGCACTTATGACTGTCTTCTTTATCATGCAACTCGTAGGACAGGTGC
CGGCAGCGCTCTTCCGCTTCCTCGCTCACTGACTCGCTGCGCTCGGTCGTTCGGCTGCGGCGAGCGGTATCAGCTCACTCAAAGGC
GGTAATACGGTTATCCACAGAATCAGGGGATAACGCAGGAAAGAACATGTGAGCAAAAGGCCAGCAAAAGGCCAGGAACCGTAAAA
AGGCCGCGTTGCTGGCGTTTTTCCATAGGCTCCGCCCCCCTGACGAGCATCACAAAAATCGACGCTCAAGTCAGAGGTGGCGAAAC
CCGACAGGACTATAAAGATACCAGGCGTTTCCCCCTGGAAGCTCCCTCGTGCGCTCTCCTGTTCCGACCCTGCCGCTTACCGGATA
CCTGTCCGCCTTTCTCCCTTCGGGAAGCGTGGCGCTTTCTCATAGCTCACGCTGTAGGTATCTCAGTTCGGTGTAGGTCGTTCGCT
CCAAGCTGGGCTGTGTGCACGAACCCCCCGTTCAGCCCGACCGCTGCGCCTTATCCGGTAACTATCGTCTTGAGTCCAACCCGGTA
AGACACGACTTATCGCCACTGGCAGCAGCCACTGGTAACAGGATTAGCAGAGCGAGGTATGTAGGCGGTGCTACAGAGTTCTTGAA
GTGGTGGCCTAACTACGGCTACACTAGAAGAACAGTATTTGGTATCTGCGCTCTGCTGAAGCCAGTTACCTTCGGAAAAAGAGTTG
GTAGCTCTTGATCCGGCAAACAAACCACCGCTGGTAGCGGTGGTTTTTTTGTTTGCAAGCAGCAGATTACGCGCAGAAAAAAAGGA
TCTCAAGAAGATCCTTTGATCTTTTCTACGGGGTCTGACGCTCAGTGGAACGAAAACTCACGTTAAGGGATTTTGGTCATGAGATT
ATCAAAAAGGATCTTCACCTAGATCCTTTTAAATTAAAAATGAAGTTTTAAATCAATCTAAAGTATATATGAGTAAACTTGGTCTG
ACAGTTACCAATGCTTAATCAGTGAGGCACCTATCTCAGCGATCTGTCTATTTCGTTCATCCATAGTTGCCTGACTCCCCGTCGTG
TAGATAACTACGATACGGGAGGGCTTACCATCTGGCCCCAGTGCTGCAATGATACCGCGAGACCCACGCTCACCGGCTCCAGATTT
ATCAGCAATAAACCAGCCAGCCGGAAGGGCCGAGCGCAGAAGTGGTCCTGCAACTTTATCCGCCTCCATCCAGTCTATTAATTGTT
GCCGGGAAGCTAGAGTAAGTAGTTCGCCAGTTAATAGTTTGCGCAACGTTGTTGCCATTGCTACAGGCATCGTGGTGTCACGCTCG
TCGTTTGGTATGGCTTCATTCAGCTCCGGTTCCCAACGATCAAGGCGAGTTACATGATCCCCCATGTTGTGCAAAAAAGCGGTTAG
CTCCTTCGGTCCTCCGATCGTTGTCAGAAGTAAGTTGGCCGCAGTGTTATCACTCATGGTTATGGCAGCACTGCATAATTCTCTTA
CTGTCATGCCATCCGTAAGATGCTTTTCTGTGACTGGTGAGTACTCAACCAAGTCATTCTGAGAATAGTGTATGCGGCGACCGAGT
TGCTCTTGCCCGGCGTCAATACGGGATAATACCGCGCCACATAGCAGAACTTTAAAAGTGCTCATCATTGGAAAACGTTCTTCGGG
GCGAAAACTCTCAAGGATCTTACCGCTGTTGAGATCCAGTTCGATGTAACCCACTCGTGCACCCAACTGATCTTCAGCATCTTTTA
CTTTCACCAGCGTTTCTGGGTGAGCAAAAACAGGAAGGCAAAATGCCGCAAAAAAGGGAATAAGGGCGACACGGAAATGTTGAATA
CTCATACTCTTCCTTTTTCAATATTATTGAAGCATTTATCAGGGTTATTGTCTCATGAGCGGATACATATTTGAATGTATTTAGAA
AAATAAACAAATAGGGGTTCCGCGCACATTTCCCCGAAAAGTGCCACCTGACGCGCCCTGTAGCGGCGCATTAAGCGCGGCGGGTG
TGGTGGTTACGCGCAGCGTGACCGCTACACTTGCCAGCGCCCTAGCGCCCGCTCCTTTCGCTTTCTTCCCTTCCTTTCTCGCCACG
TTCGCCGGCTTTCCCCGTCAAGCTCTAAATCGGGGGCTCCCTTTAGGGTTCCGATTTAGTGCTTTACGGCACCTCGACCCCAAAAA
ACTTGATTAGGGTGATGGTTCACGTAGTGGGCCATCGCCCTGATAGACGGTTTTTCGCCCTTTGACGTTGGAGTCCACGTTCTTTA
ATAGTGGACTCTTGTTCCAAACTGGAACAACACTCAACCCTATCTCGGTCTATTCTTTTGATTTATAAGGGATTTTGCCGATTTCG
GCCTATTGGTTAAAAAATGAGCTGATTTAACAAAAATTTAACGCGAATTTTAACAAAATATTAACGCTTACAATTTGCCATTCGCC
ATTCAGGCTGCGCAACTGTTGGGAAGGGCGATCGGTGCGGGCCTCTTCGCTATTACGCCAGCCCAAGCTACCATGATAAGTAAGTA

ATATTAAGGTACGGGAGGTACTTGGAGCGGCCGCAATAAAATATCTTTATTTTCATTACATCTGTGTGTTGGTTTTTTGTGTGAAT
CGATAGTACTAACATACGCTCTCCATCAAAACAAAACGAAACAAAACAAACTAGCAAAATAGGCTGTCCCCAGTGCAAGTGCAGGT
GCCAGAACATTTCTCTATCGATA

EF-1α-fLuc plasmid sequence

AATGTAGTCTTATGCAATACTCTTGTAGTCTTGCAACATGGTAACGATGAGTTAGCAACATGCCTTACAAGGAGAGAAAAAGCACC
GTGCATGCCGATTGGTGGAAGTAAGGTGGTACGATCGTGCCTTATTAGGAAGGCAACAGACGGGTCTGACATGGATTGGACGAACC
ACTGAATTGCCGCATTGCAGAGATATTGTATTTAAGTGCCTAGCTCGATACATAAACGGGTCTCTCTGGTTAGACCAGATCTGAGC
CTGGGAGCTCTCTGGCTAACTAGGGAACCCACTGCTTAAGCCTCAATAAAGCTTGCCTTGAGTGCTTCAAGTAGTGTGTGCCCGTC
TGTTGTGTGACTCTGGTAACTAGAGATCCCTCAGACCCTTTTAGTCAGTGTGGAAAATCTCTAGCAGTGGCGCCCGAACAGGGACT
TGAAAGCGAAAGGGAAACCAGAGGAGCTCTCTCGACGCAGGACTCGGCTTGCTGAAGCGCGCACGGCAAGAGGCGAGGGGCGGCGA
CTGGTGAGTACGCCAAAAATTTTGACTAGCGGAGGCTAGAAGGAGAGAGATGGGTGCGAGAGCGTCAGTATTAAGCGGGGGAGAAT
TAGATCGCGATGGGAAAAAATTCGGTTAAGGCCAGGGGGAAAGAAAAAATATAAATTAAAACATATAGTATGGGCAAGCAGGGAGC
TAGAACGATTCGCAGTTAATCCTGGCCTGTTAGAAACATCAGAAGGCTGTAGACAAATACTGGGACAGCTACAACCATCCCTTCAG
ACAGGATCAGAAGAACTTAGATCATTATATAATACAGTAGCAACCCTCTATTGTGTGCATCAAAGGATAGAGATAAAAGACACCAA
GGAAGCTTTAGACAAGATAGAGGAAGAGCAAAACAAAAGTAAGACCACCGCACAGCAAGGCCATTACGGCCTGATCTTCAGACCTG
GAGGAGGAGATATGAGGGACAATTGGAGAAGTGAATTATATAAATATAAAGTAGTAAAAATTGAACCATTAGGAGTAGCACCCACC
AAGGCAAAGAGAAGAGTGGTGCAGAGAGAAAAAAGAGCAGTGGGAATAGGAGCTTTGTTCCTTGGGTTCTTGGGAGCAGCAGGAAG
CACTATGGGCGCAGCGTCAATGACGCTGACGGTACAGGCCAGACAATTATTGTCTGGTATAGTGCAGCAGCAGAACAATTTGCTGA
GGGCTATTGAGGCGCAACAGCATCTGTTGCAACTCACAGTCTGGGGCATCAAGCAGCTCCAGGCAAGAATCCTGGCTGTGGAAAGA
TACCTAAAGGATCAACAGCTCCTGGGGATTTGGGGTTGCTCTGGAAAACTCATTTGCACCACTGCTGTGCCTTGGAATGCTAGTTG
GAGTAATAAATCTCTGGAACAGATTTGGAATCACACGACCTGGATGGAGTGGGACAGAGAAATTAACAATTACACAAGCTTAATAC
ACTCCTTAATTGAAGAATCGCAAAACCAGCAAGAAAAGAATGAACAAGAATTATTGGAATTAGATAAATGGGCAAGTTTGTGGAAT
TGGTTTAACATAACAAATTGGCTGTGGTATATAAAATTATTCATAATGATAGTAGGAGGCTTGGTAGGTTTAAGAATAGTTTTTGC
TGTACTTTCTATAGTGAATAGAGTTAGGCAGGGATATTCACCATTATCGTTTCAGACCCACCTCCCAACCCCGAGGGGACCCGACA
GGCCCGAAGGAATAGAAGAAGAAGGTGGAGAGAGAGACAGAGACAGATCCATTCGATTAGTGAACGGATCTCGACGGTATCGATGC
GGATACTGCAGACAAATGGCAGTATTCATCCACAATTTTAAAAGAAAAGGGGGGATTGGGGGGTACAGTGCAGGGGAAAGAATAGT
AGACATAATAGCAACAGACATACAAACTAAAGAATTACAAAAACAAATTACAAAAATTCAAAATTTTCGGGTTTATTACAGGGACA
GCAGAGATCCAGTGGCGCGCCCGACGATAAGCTTTGCAAAGATGGATAAAGTTTTAAACAGAGAGGAATCTTTGCAGCTAATGGAC
CTTCTAGGTCTTGAAAGGAGTGGGAATTGGCTCCGGTGCCCGTCAGTGGGCAGAGCGCACATCGCCCACAGTCCCCGAGAAGTTGG
GGGGAGGGGTCGGCAATTGAACCGGTGCCTAGAGAAGGTGGCGCGGGGTAAACTGGGAAAGTGATGTCGTGTACTGGCTCCGCCTT
TTTCCCGAGGGTGGGGGAGAACCGTATATAAGTGCAGTAGTCGCCGTGAACGTTCTTTTTCGCAACGGGTTTGCCGCCAGAACACA
GGTAAGTGCCGTGTGTGGTTCCCGCGGGCCTGGCCTCTTTACGGGTTATGGCCCTTGCGTGCCTTGAATTACTTCCACTGGCTGCA
GTACGTGATTCTTGATCCCGAGCTTCGGGTTGGAAGTGGGTGGGAGAGTTCGAGGCCTTGCGCTTAAGGAGCCCCTTCGCCTCGTG
CTTGAGTTGAGGCCTGGCCTGGGCGCTGGGGCCGCCGCGTGCGAATCTGGTGGCACCTTCGCGCCTGTCTCGCTGCTTTCGATAAG
TCTCTAGCCATTTAAAATTTTTGATGACCTGCTGCGACGCTTTTTTTCTGGCAAGATAGTCTTGTAAATGCGGGCCAAGATCTGCA
CACTGGTATTTCGGTTTTTGGGGCCGCGGGCGGCGACGGGGCCCGTGCGTCCCAGCGCACATGTTCGGCGAGGCGGGGCCTGCGAG
CGCGGCCACCGAGAATCGGACGGGGGTAGTCTCAAGCTGGCCGGCCTGCTCTGGTGCCTGGCCTCGCGCCGCCGTGTATCGCCCCG
CCCTGGGCGGCAAGGCTGGCCCGGTCGGCACCAGTTGCGTGAGCGGAAAGATGGCCGCTTCCCGGCCCTGCTGCAGGGAGCTCAAA
ATGGAGGACGCGGCGCTCGGGAGAGCGGGCGGGTGAGTCACCCACACAAAGGAAAAGGGCCTTTCCGTCCTCAGCCGTCGCTTCAT
GTGACTCCACGGAGTACCGGGCGCCGTCCAGGCACCTCGATTAGTTCTCGAGCTTTTGGAGTACGTCGTCTTTAGGTTGGGGGGAG
GGGTTTTATGCGATGGAGTTTCCCCACACTGAGTGGGTGGAGACTGAAGTTAGGCCAGCTTGGCACTTGATGTAATTCTCCTTGGA
ATTTGCCCTTTTTGAGTTTGGATCTTGGTTCATTCTCAAGCCTCAGACAGTGGTTCAAAGTTTTTTTCTTCCATTTCAGGTGTCGT
GAGGAATTTCGACCCTGCAGGTGATCTACTAGTGCGGATATCTAGTGAACCGTCAGATCCGCTAGCGCTACCGGACTCAGATCTCG
AGCTCAAGCTTCGAATTCTGCAGTCGAGGTCGACGCCACCATGGAAGATGCCAAAAACATTAAGAAGGGCCCAGCGCCATTCTACC
CACTCGAAGACGGGACCGCCGGCGAGCAGCTGCACAAAGCCATGAAGCGCTACGCCCTGGTGCCCGGCACCATCGCCTTTACCGAC
GCACATATCGAGGTGGACATTACCTACGCCGAGTACTTCGAGATGAGCGTTCGGCTGGCAGAAGCTATGAAGCGCTATGGGCTGAA
TACAAACCATCGGATCGTGGTGTGCAGCGAGAATAGCTTGCAGTTCTTCATGCCCGTGTTGGGTGCCCTGTTCATCGGTGTGGCTG
TGGCCCCAGCTAACGACATCTACAACGAGCGCGAGCTGCTGAACAGCATGGGCATCAGCCAGCCCACCGTCGTATTCGTGAGCAAG
AAAGGGCTGCAAAAGATCCTCAACGTGCAAAAGAAGCTACCGATCATACAAAAGATCATCATCATGGATAGCAAGACCGACTACCA
GGGCTTCCAAAGCATGTACACCTTCGTGACTTCCCATTTGCCACCCGGCTTCAACGAGTACGACTTCGTGCCCGAGAGCTTCGACC
GGGACAAAACCATCGCCCTGATCATGAACAGTAGTGGCAGTACCGGATTGCCCAAGGGCGTAGCCCTACCGCACCGCACCGCTTGT
GTCCGATTCAGTCATGCCCGCGACCCCATCTTCGGCAACCAGATCATCCCCGACACCGCTATCCTCAGCGTGGTGCCATTTCACCA
CGGCTTCGGCATGTTCACCACGCTGGGCTACTTGATCTGCGGCTTTCGGGTCGTGCTCATGTACCGCTTCGAGGAGGAGCTATTCT
TGCGCAGCTTGCAAGACTATAAGATTCAATCTGCCCTGCTGGTGCCCACACTATTTAGCTTCTTCGCTAAGAGCACTCTCATCGAC
AAGTACGACCTAAGCAACTTGCACGAGATCGCCAGCGGCGGGGCGCCGCTCAGCAAGGAGGTAGGTGAGGCCGTGGCCAAACGCTT
CCACCTACCAGGCATCCGCCAGGGCTACGGCCTGACAGAAACAACCAGCGCCATTCTGATCACCCCCGAAGGGGACGACAAGCCTG
GCGCAGTAGGCAAGGTGGTGCCCTTCTTCGAGGCTAAGGTGGTGGACTTGGACACCGGTAAGACACTGGGTGTGAACCAGCGCGGC
GAGCTGTGCGTCCGTGGCCCCATGATCATGAGCGGCTACGTTAACAACCCCGAGGCTACAAACGCTCTCATCGACAAGGACGGCTG
GCTGCACAGCGGCGACATCGCCTACTGGGACGAGGACGAGCACTTCTTCATCGTGGACCGGCTGAAGAGCCTGATCAAATACAAGG
GCTACCAGGTAGCCCCAGCCGAACTGGAGAGCATCCTGCTGCAACACCCCAACATCTTCGACGCCGGGGTCGCCGGCCTGCCCGAC
GACGATGCCGGCGAGCTGCCCGCCGCAGTCGTCGTGCTGGAACACGGTAAAACCATGACCGAGAAGGAGATCGTGGACTATGTGGC
CAGCCAGGTTACAACCGCCAAGAAGCTGCGCGGTGGTGTTGTGTTCGTGGACGAGGTGCCTAAAGGACTGACCGGCAAGTTGGACG
CCCGCAAGATCCGCGAGATTCTCATTAAGGCCAAGAAGGGCGGCAAGATCGCCGTGTGAGCGGCCGCGACTCTAGATCATAATCAG
CCATACCACATTTGACGCGTGTCATATGATAATCAACCTCTGGATTACAAAATTTGTGAAAGATTGACTGGTATTCTTAACTATGT
TGCTCCTTTTACGCTATGTGGATACGCTGCTTTAATGCCTTTGTATCATGCTATTGCTTCCCGTATGGCTTTCATTTTCTCCTCCT
TGTATAAATCCTGGTTGCTGTCTCTTTATGAGGAGTTGTGGCCCGTTGTCAGGCAACGTGGCGTGGTGTGCACTGTGTTTGCTGAC
GCAACCCCCACTGGTTGGGGCATTGCCACCACCTGTCAGCTCCTTTCCGGGACTTTCGCTTTCCCCCTCCCTATTGCCACGGCGGA
ACTCATCGCCGCCTGCCTTGCCCGCTGCTGGACAGGGGCTCGGCTGTTGGGCACTGACAATTCCGTGGTGTTGTCGGGGAAGCTGA
CGTCCTTTCCATGGCTGCTCGCCTGTGTTGCCACCTGGATTCTGCGCGGGACGTCCTTCTGCTACGTCCCTTCGGCCCTCAATCCA
GCGGACCTTCCTTCCCGCGGCCTGCTGCCGGCTCTGCGGCCTCTTCCGCGTCTTCGCCTTCGCCCTCAGACGAGTCGGATCTCCCT
TTGGGCCGCCTCCCCGCATCGGTACGTACGCGTACCGGTTAGTAATGAGTTTGGAATTAATTCTGTGGAATGTGTGTCAGTTAGGG
TGTGGAAAGTCCCCAGGCTCCCCAGCAGGCAGAAGTATGCAAAGCATGCATCTCAATTAGTCAGCAACCAGGTGTGGAAAGTCCCC
AGGCTCCCCAGCAGGCAGAAGTATGCAAAGCATGCATCTCAATTAGTCAGCAACCATAGTCCCGCCCCTAACTCCGCCCATCCCGC
CCCTAACTCCGCCCAGTTCCGCCCATTCTCCGCCCCATGGCTGACTAATTTTTTTTATTTATGCAGAGGCCGAGGCCGCCTCTGCC

TCTGAGCTATTCCAGAAGTAGTGAGGAGGCTTTTTTGGAGGCCTAGGCTTTTGCAAAAAGCTCCCGGGAGCTTGTATATCCATTTT
CGGATCTGATCAGCACGTGTTGACAATTAATCATCGGCATAGTATATCGGCATAGTATAATACGACAAGGTGAGGAACTAAACCAT
GGCCAAGCCTTTGTCTCAAGAAGAATCCACCCTCATTGAAAGAGCAACGGCTACAATCAACAGCATCCCCATCTCTGAAGACTACA
GCGTCGCCAGCGCAGCTCTCTCTAGCGACGGCCGCATCTTCACTGGTGTCAATGTATATCATTTTACTGGGGGACCTTGTGCAGAA
CTCGTGGTGCTGGGCACTGCTGCTGCTGCGGCAGCTGGCAACCTGACTTGTATCGTCGCGATCGGAAATGAGAACAGGGGCATCTT
GAGCCCCTGCGGACGGTGCCGACAGGTGCTTCTCGATCTGCATCCTGGGATCAAAGCCATAGTGAAGGACAGTGATGGACAGCCGA
CGGCAGTTGGGATTCGTGAATTGCTGCCCTCTGGTTATGTGTGGGAGGGCTAAGCACAATTCGAGCTCGGTACCTTTAAGACCAAT
GACTTACAAGGCAGCTGTAGATCTTAGCCACTTTTTAAAAGAAAAGGGGGGACTGGAAGGGCTAATTCACTCCCAACGAAGACAAG
ATCTGCTTTTTGCTTGTACTGGGTCTCTCTGGTTAGACCAGATCTGAGCCTGGGAGCTCTCTGGCTAACTAGGGAACCCACTGCTT
AAGCCTCAATAAAGCTTGCCTTGAGTGCTTCAAGTAGTGTGTGCCCGTCTGTTGTGTGACTCTGGTAACTAGAGATCCCTCAGACC
CTTTTAGTCAGTGTGGAAAATCTCTAGCAGTAGTAGTTCATGTCATCTTATTATTCAGTATTTATAACTTGCAAAGAAATGAATAT
CAGAGAGTGAGAGGAACTTGTTTATTGCAGCTTATAATGGTTACAAATAAAGCAATAGCATCACAAATTTCACAAATAAAGCATTT
TTTTCACTGCATTCTAGTTGTGGTTTGTCCAAACTCATCAATGTATCTTATCATGTCTGGCTCTAGCTATCCCGCCCCTAACTCCG
CCCATCCCGCCCCTAACTCCGCCCAGTTCCGCCCATTCTCCGCCCCATGGCTGACTAATTTTTTTTATTTATGCAGAGGCCGAGGC
CGCCTCGGCCTCTGAGCTATTCCAGAAGTAGTGAGGAGGCTTTTTTGGAGGCCTAGGGACGTACCCAATTCGCCCTATAGTGAGTC
GTATTACGCGCGCTCACTGGCCGTCGTTTTACAACGTCGTGACTGGGAAAACCCTGGCGTTACCCAACTTAATCGCCTTGCAGCAC
ATCCCCCTTTCGCCAGCTGGCGTAATAGCGAAGAGGCCCGCACCGATCGCCCTTCCCAACAGTTGCGCAGCCTGAATGGCGAATGG
GACGCGCCCTGTAGCGGCGCATTAAGCGCGGCGGGTGTGGTGGTTACGCGCAGCGTGACCGCTACACTTGCCAGCGCCCTAGCGCC
CGCTCCTTTCGCTTTCTTCCCTTCCTTTCTCGCCACGTTCGCCGGCTTTCCCCGTCAAGCTCTAAATCGGGGGCTCCCTTTAGGGT
TCCGATTTAGTGCTTTACGGCACCTCGACCCCAAAAAACTTGATTAGGGTGATGGTTCACGTAGTGGGCCATCGCCCTGATAGACG
GTTTTTCGCCCTTTGACGTTGGAGTCCACGTTCTTTAATAGTGGACTCTTGTTCCAAACTGGAACAACACTCAACCCTATCTCGGT
CTATTCTTTTGATTTATAAGGGATTTTGCCGATTTCGGCCTATTGGTTAAAAAATGAGCTGATTTAACAAAAATTTAACGCGAATT
TTAACAAAATATTAACGCTTACAATTTAGGTGGCACTTTTCGGGGAAATGTGCGCGGAACCCCTATTTGTTTATTTTTCTAAATAC
ATTCAAATATGTATCCGCTCATGAGACAATAACCCTGATAAATGCTTCAATAATATTGAAAAAGGAAGAGTATGAGTATTCAACAT
TTCCGTGTCGCCCTTATTCCCTTTTTTGCGGCATTTTGCCTTCCTGTTTTTGCTCACCCAGAAACGCTGGTGAAAGTAAAAGATGC
TGAAGATCAGTTGGGTGCACGAGTGGGTTACATCGAACTGGATCTCAACAGCGGTAAGATCCTTGAGAGTTTTCGCCCCGAAGAAC
GTTTTCCAATGATGAGCACTTTTAAAGTTCTGCTATGTGGCGCGGTATTATCCCGTATTGACGCCGGGCAAGAGCAACTCGGTCGC
CGCATACACTATTCTCAGAATGACTTGGTTGAGTACTCACCAGTCACAGAAAAGCATCTTACGGATGGCATGACAGTAAGAGAATT
ATGCAGTGCTGCCATAACCATGAGTGATAACACTGCGGCCAACTTACTTCTGACAACGATCGGAGGACCGAAGGAGCTAACCGCTT
TTTTGCACAACATGGGGGATCATGTAACTCGCCTTGATCGTTGGGAACCGGAGCTGAATGAAGCCATACCAAACGACGAGCGTGAC
ACCACGATGCCTGTAGCAATGGCAACAACGTTGCGCAAACTATTAACTGGCGAACTACTTACTCTAGCTTCCCGGCAACAATTAAT
AGACTGGATGGAGGCGGATAAAGTTGCAGGACCACTTCTGCGCTCGGCCCTTCCGGCTGGCTGGTTTATTGCTGATAAATCTGGAG
CCGGTGAGCGTGGGTCTCGCGGTATCATTGCAGCACTGGGGCCAGATGGTAAGCCCTCCCGTATCGTAGTTATCTACACGACGGGG
AGTCAGGCAACTATGGATGAACGAAATAGACAGATCGCTGAGATAGGTGCCTCACTGATTAAGCATTGGTAACTGTCAGACCAAGT
TTACTCATATATACTTTAGATTGATTTAAAACTTCATTTTTAATTTAAAAGGATCTAGGTGAAGATCCTTTTTGATAATCTCATGA
CCAAAATCCCTTAACGTGAGTTTTCGTTCCACTGAGCGTCAGACCCCGTAGAAAAGATCAAAGGATCTTCTTGAGATCCTTTTTTT
CTGCGCGTAATCTGCTGCTTGCAAACAAAAAAACCACCGCTACCAGCGGTGGTTTGTTTGCCGGATCAAGAGCTACCAACTCTTTT
TCCGAAGGTAACTGGCTTCAGCAGAGCGCAGATACCAAATACTGTTCTTCTAGTGTAGCCGTAGTTAGGCCACCACTTCAAGAACT
CTGTAGCACCGCCTACATACCTCGCTCTGCTAATCCTGTTACCAGTGGCTGCTGCCAGTGGCGATAAGTCGTGTCTTACCGGGTTG
GACTCAAGACGATAGTTACCGGATAAGGCGCAGCGGTCGGGCTGAACGGGGGGTTCGTGCACACAGCCCAGCTTGGAGCGAACGAC
CTACACCGAACTGAGATACCTACAGCGTGAGCTATGAGAAAGCGCCACGCTTCCCGAAGGGAGAAAGGCGGACAGGTATCCGGTAA
GCGGCAGGGTCGGAACAGGAGAGCGCACGAGGGAGCTTCCAGGGGGAAACGCCTGGTATCTTTATAGTCCTGTCGGGTTTCGCCAC
CTCTGACTTGAGCGTCGATTTTTGTGATGCTCGTCAGGGGGGCGGAGCCTATGGAAAAACGCCAGCAACGCGGCCTTTTTACGGTT
CCTGGCCTTTTGCTGGCCTTTTGCTCACATGTTCTTTCCTGCGTTATCCCCTGATTCTGTGGATAACCGTATTACCGCCTTTGAGT
GAGCTGATACCGCTCGCCGCAGCCGAACGACCGAGCGCAGCGAGTCAGTGAGCGAGGAAGCGGAAGAGCGCCCAATACGCAAACCG
CCTCTCCCCGCGCGTTGGCCGATTCATTAATGCAGCTGGCACGACAGGTTTCCCGACTGGAAAGCGGGCAGTGAGCGCAACGCAAT
TAATGTGAGTTAGCTCACTCATTAGGCACCCCAGGCTTTACACTTTATGCTTCCGGCTCGTATGTTGTGTGGAATTGTGAGCGGAT
AACAATTTCACACAGGAAACAGCTATGACCATGATTACGCCAAGCGCGCAATTAACCCTCACTAAAGGGAACAAAAGCTGGAGCTG
CAAGCTT

VSV-G plasmid sequence

GAGCTTGGCCCATTGCATACGTTGTATCCATATCATAATATGTACATTTATATTGGCTCATGTCCAACATTACCGCCATGTTGACA
TTGATTATTGACTAGTTATTAATAGTAATCAATTACGGGGTCATTAGTTCATAGCCCATATATGGAGTTCCGCGTTACATAACTTA
CGGTAAATGGCCCGCCTGGCTGACCGCCCAACGACCCCCGCCCATTGACGTCAATAATGACGTATGTTCCCATAGTAACGCCAATA
GGGACTTTCCATTGACGTCAATGGGTGGAGTATTTACGGTAAACTGCCCACTTGGCAGTACATCAAGTGTATCATATGCCAAGTAC
GCCCCCTATTGACGTCAATGACGGTAAATGGCCCGCCTGGCATTATGCCCAGTACATGACCTTATGGGACTTTCCTACTTGGCAGT
ACATCTACGTATTAGTCATCGCTATTACCATGGTGATGCGGTTTTGGCAGTACATCAATGGGCGTGGATAGCGGTTTGACTCACGG
GGATTTCCAAGTCTCCACCCCATTGACGTCAATGGGAGTTTGTTTTGGCACCAAAATCAACGGGACTTTCCAAAATGTCGTAACAA
CTCCGCCCCATTGACGCAAATGGGCGGTAGGCGTGTACGGTGGGAGGTCTATATAAGCAGAGCTCGTTTAGTGAACCGTCAGATCG
CCTGGAGACGCCATCCACGCTGTTTTGACCTCCATAGAAGACACCGGGACCGATCCAGCCTCCGGTCGACCGATCCTGAGAACTTC
AGGGTGAGTTTGGGGACCCTTGATTGTTCTTTCTTTTTCGCTATTGTAAAATTCATGTTATATGGAGGGGGCAAAGTTTTCAGGGT
GTTGTTTAGAATGGGAAGATGTCCCTTGTATCACCATGGACCCTCATGATAATTTTGTTTCTTTCACTTTCTACTCTGTTGACAAC
CATTGTCTCCTCTTATTTTCTTTTCATTTTCTGTAACTTTTTCGTTAAACTTTAGCTTGCATTTGTAACGAATTTTTAAATTCACT
TTTGTTTATTTGTCAGATTGTAAGTACTTTCTCTAATCACTTTTTTTTCAAGGCAATCAGGGTATATTATATTGTACTTCAGCACA
GTTTTAGAGAACAATTGTTATAATTAAATGATAAGGTAGAATATTTCTGCATATAAATTCTGGCTGGCGTGGAAATATTCTTATTG
GTAGAAACAACTACACCCTGGTCATCATCCTGCCTTTCTCTTTATGGTTACAATGATATACACTGTTTGAGATGAGGATAAAATAC
TCTGAGTCCAAACCGGGCCCCTCTGCTAACCATGTTCATGCCTTCTTCTCTTTCCTACAGCTCCTGGGCAACGTGCTGGTTGTTGT
GCTGTCTCATCATTTTGGCAAAGAATTCCTCGACGGATCCCTCGAGGAATTCTGACACTATGAAGTGCCTTTTGTACTTAGCCTTT
TTATTCATTGGGGTGAATTGCAAGTTCACCATAGTTTTTCCACACAACCAAAAAGGAAACTGGAAAAATGTTCCTTCTAATTACCA
TTATTGCCCGTCAAGCTCAGATTTAAATTGGCATAATGACTTAATAGGCACAGCCTTACAAGTCAAAATGCCCAAGAGTCACAAGG
CTATTCAAGCAGACGGTTGGATGTGTCATGCTTCCAAATGGGTCACTACTTGTGATTTCCGCTGGTATGGACCGAAGTATATAACA
CATTCCATCCGATCCTTCACTCCATCTGTAGAACAATGCAAGGAAAGCATTGAACAAACGAAACAAGGAACTTGGCTGAATCCAGG
CTTCCCTCCTCAAAGTTGTGGATATGCAACTGTGACGGATGCCGAAGCAGTGATTGTCCAGGTGACTCCTCACCATGTGCTGGTTG
ATGAATACACAGGAGAATGGGTTGATTCACAGTTCATCAACGGAAAATGCAGCAATTACATATGCCCCACTGTCCATAACTCTACA

ACCTGGCATTCTGACTATAAGGTCAAAGGGCTATGTGATTCTAACCTCATTTCCATGGACATCACCTTCTTCTCAGAGGACGGAGA
GCTATCATCCCTGGGAAAGGAGGGCACAGGGTTCAGAAGTAACTACTTTGCTTATGAAACTGGAGGCAAGGCCTGCAAAATGCAAT
ACTGCAAGCATTGGGGAGTCAGACTCCCATCAGGTGTCTGGTTCGAGATGGCTGATAAGGATCTCTTTGCTGCAGCCAGATTCCCT
GAATGCCCAGAAGGGTCAAGTATCTCTGCTCCATCTCAGACCTCAGTGGATGTAAGTCTAATTCAGGACGTTGAGAGGATCTTGGA
TTATTCCCTCTGCCAAGAAACCTGGAGCAAAATCAGAGCGGGTCTTCCAATCTCTCCAGTGGATCTCAGCTATCTTGCTCCTAAAA
ACCCAGGAACCGGTCCTGCTTTCACCATAATCAATGGTACCCTAAAATACTTTGAGACCAGATACATCAGAGTCGATATTGCTGCT
CCAATCCTCTCAAGAATGGTCGGAATGATCAGTGGAACTACCACAGAAAGGGAACTGTGGGATGACTGGGCACCATATGAAGACGT
GGAAATTGGACCCAATGGAGTTCTGAGGACCAGTTCAGGATATAAGTTTCCTTTATACATGATTGGACATGGTATGTTGGACTCCG
ATCTTCATCTTAGCTCAAAGGCTCAGGTGTTCGAACATCCTCACATTCAAGACGCTGCTTCGCAACTTCCTGATGATGAGAGTTTA
TTTTTTGGTGATACTGGGCTATCCAAAAATCCAATCGAGCTTGTAGAAGGTTGGTTCAGTAGTTGGAAAAGCTCTATTGCCTCTTT
TTTCTTTATCATAGGGTTAATCATTGGACTATTCTTGGTTCTCCGAGTTGGTATCCATCTTTGCATTAAATTAAAGCACACCAAGA
AAAGACAGATTTATACAGACATAGAGATGAACCGACTTGGAAAGTAACTCAAATCCTGCACAACAGATTCTTCATGTTTGGACCAA
ATCAACTTGTGATACCATGCTCAAAGAGGCCTCAATTATATTTGAGTTTTTAATTTTTATGAAAAAAAAAAAAAAAAACGGAATTC
CTCGAGGGATCCGTCGAGGAATTCACTCCTCAGGTGCAGGCTGCCTATCAGAAGGTGGTGGCTGGTGTGGCCAATGCCCTGGCTCA
CAAATACCACTGAGATCTTTTTCCCTCTGCCAAAAATTATGGGGACATCATGAAGCCCCTTGAGCATCTGACTTCTGGCTAATAAA
GGAAATTTATTTTCATTGCAATAGTGTGTTGGAATTTTTTGTGTCTCTCACTCGGAAGGACATATGGGAGGGCAAATCATTTAAAA
CATCAGAATGAGTATTTGGTTTAGAGTTTGGCAACATATGCCCATATGCTGGCTGCCATGAACAAAGGTTGGCTATAAAGAGGTCA
TCAGTATATGAAACAGCCCCCTGCTGTCCATTCCTTATTCCATAGAAAAGCCTTGACTTGAGGTTAGATTTTTTTTATATTTTGTT
TTGTGTTATTTTTTTCTTTAACATCCCTAAAATTTTCCTTACATGTTTTACTAGCCAGATTTTTCCTCCTCTCCTGACTACTCCCA
GTCATAGCTGTCCCTCTTCTCTTATGGAGATCCCTCGACGGATCGGCCGCAATTCGTAATCATGTCATAGCTGTTTCCTGTGTGAA
ATTGTTATCCGCTCACAATTCCACACAACATACGAGCCGGAAGCATAAAGTGTAAAGCCTGGGGTGCCTAATGAGTGAGCTAACTC
ACATTAATTGCGTTGCGCTCACTGCCCGCTTTCCAGTCGGGAAACCTGTCGTGCCAGCTGCATTAATGAATCGGCCAACGCGCGGG
GAGAGGCGGTTTGCGTATTGGGCGCTCTTCCGCTTCCTCGCTCACTGACTCGCTGCGCTCGGTCGTTCGGCTGCGGCGAGCGGTAT
CAGCTCACTCAAAGGCGGTAATACGGTTATCCACAGAATCAGGGGATAACGCAGGAAAGAACATGTGAGCAAAAGGCCAGCAAAAG
GCCAGGAACCGTAAAAAGGCCGCGTTGCTGGCGTTTTTCCATAGGCTCCGCCCCCCTGACGAGCATCACAAAAATCGACGCTCAAG
TCAGAGGTGGCGAAACCCGACAGGACTATAAAGATACCAGGCGTTTCCCCCTGGAAGCTCCCTCGTGCGCTCTCCTGTTCCGACCC
TGCCGCTTACCGGATACCTGTCCGCCTTTCTCCCTTCGGGAAGCGTGGCGCTTTCTCATAGCTCACGCTGTAGGTATCTCAGTTCG
GTGTAGGTCGTTCGCTCCAAGCTGGGCTGTGTGCACGAACCCCCCGTTCAGCCCGACCGCTGCGCCTTATCCGGTAACTATCGTCT
TGAGTCCAACCCGGTAAGACACGACTTATCGCCACTGGCAGCAGCCACTGGTAACAGGATTAGCAGAGCGAGGTATGTAGGCGGTG
CTACAGAGTTCTTGAAGTGGTGGCCTAACTACGGCTACACTAGAAGAACAGTATTTGGTATCTGCGCTCTGCTGAAGCCAGTTACC
TTCGGAAAAAGAGTTGGTAGCTCTTGATCCGGCAAACAAACCACCGCTGGTAGCGGTGGTTTTTTTGTTTGCAAGCAGCAGATTAC
GCGCAGAAAAAAAGGATCTCAAGAAGATCCTTTGATCTTTTCTACGGGGTCTGACGCTCAGTGGAACGAAAACTCACGTTAAGGGA
TTTTGGTCATGAGATTATCAAAAAGGATCTTCACCTAGATCCTTTTAAATTAAAAATGAAGTTTTAAATCAATCTAAAGTATATAT
GAGTAAACTTGGTCTGACAGTTACCAATGCTTAATCAGTGAGGCACCTATCTCAGCGATCTGTCTATTTCGTTCATCCATAGTTGC
CTGACTCCCCGTCGTGTAGATAACTACGATACGGGAGGGCTTACCATCTGGCCCCAGTGCTGCAATGATACCGCGAGACCCACGCT
CACCGGCTCCAGATTTATCAGCAATAAACCAGCCAGCCGGAAGGGCCGAGCGCAGAAGTGGTCCTGCAACTTTATCCGCCTCCATC
CAGTCTATTAATTGTTGCCGGGAAGCTAGAGTAAGTAGTTCGCCAGTTAATAGTTTGCGCAACGTTGTTGCCATTGCTACAGGCAT
CGTGGTGTCACGCTCGTCGTTTGGTATGGCTTCATTCAGCTCCGGTTCCCAACGATCAAGGCGAGTTACATGATCCCCCATGTTGT
GCAAAAAAGCGGTTAGCTCCTTCGGTCCTCCGATCGTTGTCAGAAGTAAGTTGGCCGCAGTGTTATCACTCATGGTTATGGCAGCA
CTGCATAATTCTCTTACTGTCATGCCATCCGTAAGATGCTTTTCTGTGACTGGTGAGTACTCAACCAAGTCATTCTGAGAATAGTG
TATGCGGCGACCGAGTTGCTCTTGCCCGGCGTCAATACGGGATAATACCGCGCCACATAGCAGAACTTTAAAAGTGCTCATCATTG
GAAAACGTTCTTCGGGGCGAAAACTCTCAAGGATCTTACCGCTGTTGAGATCCAGTTCGATGTAACCCACTCGTGCACCCAACTGA
TCTTCAGCATCTTTTACTTTCACCAGCGTTTCTGGGTGAGCAAAAACAGGAAGGCAAAATGCCGCAAAAAAGGGAATAAGGGCGAC
ACGGAAATGTTGAATACTCATACTCTTCCTTTTTCAATATTATTGAAGCATTTATCAGGGTTATTGTCTCATGAGCGGATACATAT
TTGAATGTATTTAGAAAAATAAACAAATAGGGGTTCCGCGCACATTTCCCCGAAAAGTGCCACCTAAATTGTAAGCGTTAATATTT
TGTTAAAATTCGCGTTAAATTTTTGTTAAATCAGCTCATTTTTTAACCAATAGGCCGAAATCGGCAAAATCCCTTATAAATCAAAA
GAATAGACCGAGATAGGGTTGAGTGTTGTTCCAGTTTGGAACAAGAGTCCACTATTAAAGAACGTGGACTCCAACGTCAAAGGGCG
AAAAACCGTCTATCAGGGCGATGGCCCACTACGTGAACCATCACCCTAATCAAGTTTTTTGGGGTCGAGGTGCCGTAAAGCACTAA
ATCGGAACCCTAAAGGGAGCCCCCGATTTAGAGCTTGACGGGGAAAGCCGGCGAACGTGGCGAGAAAGGAAGGGAAGAAAGCGAAA
GGAGCGGGCGCTAGGGCGCTGGCAAGTGTAGCGGTCACGCTGCGCGTAACCACCACACCCGCCGCGCTTAATGCGCCGCTACAGGG
CGCGTCCCATTCGCCATTCAGGCTGCGCAACTGTTGGGAAGGGCGATCGGTGCGGGCCTCTTCGCTATTACGCCAGCTGGCGAAAG
GGGGATGTGCTGCAAGGCGATTAAGTTGGGTAACGCCAGGGTTTTCCCAGTCACGACGTTGTAAAACGACGGCCAGTGAGCGCGCG
TAATACGACTCACTATAGGGCGAATTGGAGCTCCACCGCGGTGGCGGCCGCTCTAGA

Gag-pol plasmid sequence

GAGCTTGGCCCATTGCATACGTTGTATCCATATCATAATATGTACATTTATATTGGCTCATGTCCAACATTACCGCCATGTTGACA
TTGATTATTGACTAGTTATTAATAGTAATCAATTACGGGGTCATTAGTTCATAGCCCATATATGGAGTTCCGCGTTACATAACTTA
CGGTAAATGGCCCGCCTGGCTGACCGCCCAACGACCCCCGCCCATTGACGTCAATAATGACGTATGTTCCCATAGTAACGCCAATA
GGGACTTTCCATTGACGTCAATGGGTGGAGTATTTACGGTAAACTGCCCACTTGGCAGTACATCAAGTGTATCATATGCCAAGTAC
GCCCCCTATTGACGTCAATGACGGTAAATGGCCCGCCTGGCATTATGCCCAGTACATGACCTTATGGGACTTTCCTACTTGGCAGT
ACATCTACGTATTAGTCATCGCTATTACCATGGTGATGCGGTTTTGGCAGTACATCAATGGGCGTGGATAGCGGTTTGACTCACGG
GGATTTCCAAGTCTCCACCCCATTGACGTCAATGGGAGTTTGTTTTGGCACCAAAATCAACGGGACTTTCCAAAATGTCGTAACAA
CTCCGCCCCATTGACGCAAATGGGCGGTAGGCGTGTACGGTGGGAGGTCTATATAAGCAGAGCTCGTTTAGTGAACCGTCAGATCG
CCTGGAGACGCCATCCACGCTGTTTTGACCTCCATAGAAGACACCGGGACCGATCCAGCCTCCCCTCGAAGCTTACATGTGGTACC
GAGCTCGGATCCTGAGAACTTCAGGGTGAGTCTATGGGACCCTTGATGTTTTCTTTCCCCTTCTTTTCTATGGTTAAGTTCATGTC
ATAGGAAGGGGAGAAGTAACAGGGTACACATATTGACCAAATCAGGGTAATTTTGCATTTGTAATTTTAAAAAATGCTTTCTTCTT
TTAATATACTTTTTTGTTTATCTTATTTCTAATACTTTCCCTAATCTCTTTCTTTCAGGGCAATAATGATACAATGTATCATGCCT
CTTTGCACCATTCTAAAGAATAACAGTGATAATTTCTGGGTTAAGGCAATAGCAATATTTCTGCATATAAATATTTCTGCATATAA
ATTGTAACTGATGTAAGAGGTTTCATATTGCTAATAGCAGCTACAATCCAGCTACCATTCTGCTTTTATTTTATGGTTGGGATAAG
GCTGGATTATTCTGAGTCCAAGCTAGGCCCTTTTGCTAATCATGTTCATACCTCTTATCTTCCTCCCACAGCTCCTGGGCAACGTG
CTGGTCTGTGTGCTGGCCCATCACTTTGGCAAAGAATTCATGGGCCAGACTGTTACCACTCCCTTAAGTTTGACCTTAGGTCACTG
GAAAGATGTCGAGCGGATCGCTCACAACCAGTCGGTAGATGTCAAGAAGAGACGTTGGGTTACCTTCTGCTCTGCAGAATGGCCAA
CCTTTAACGTCGGATGGCCGCGAGACGGCACCTTTAACCGAGACCTCATCACCCAGGTTAAGATCAAGGTCTTTTCACCTGGCCCG
CATGGACACCCAGACCAGGTCCCCTACATCGTGACCTGGGAAGCCTTGGCTTTTGACCCCCCTCCCTGGGTCAAGCCCTTTGTACA

CCCTAAGCCTCCGCCTCCTCTTCCTCCATCCGCCCCCGTCTCTCCCCCTTGAACCTCCTCGTTCGACCCCGCCTCGATCCTCCCTTT
ATCCAGCCCTCACTCCTTCTCTAGGCGCCAAACCTAAACCTCAAGTTCTTTCTGACAGTGGGGGGCCGCTCATCGACCTACTTACA
GAAGACCCCCCGCCTTATAGGGACCCAAGACCACCCCCTTCCGACAGGGACGGAAATGGTGGAGAAGCGACCCCTGCGGGAGAGGC
ACCGGACCCCTCCCCAATGGCATCTCGCCTACGTGGGAGACGGGAGCCCCCTGTGGCCGACTCCACTACCTCGCAGGCATTCCCCC
TCCGCGCAGGAGGAAACGGACAGCTTCAATACTGGCCGTTCTCCTCTTCTGACCTTTACAACTGGAAAAATAATAACCCTTCTTTT
TCTGAAGATCCAGGTAAACTGACAGCTCTGATCGAGTCTGTCCTCATCACCCATCAGCCCACCTGGGACGACTGTCAGCAGCTGTT
GGGGACTCTGCTGACCGGAGAAGAAAAACAACGGGTGCTCTTAGAGGCTAGAAAGGCGGTGCGGGGCGATGATGGGCGCCCCACTC
AACTGCCCAATGAAGTCGATGCCGCTTTTCCCCTCGAGCGCCCAGACTGGGATTACACCACCCAGGCAGGTAGGAACCACCTAGTC
CACTATCGCCAGTTGCTCCTAGCGGGTCTCCAAAACGCGGGCAGAAGCCCCACCAATTTGGCCAAGGTAAAAGGAATAACACAAGG
GCCCAATGAGTCTCCCTCGGCCTTCCTAGAGAGACTTAAGGAAGCCTATCGCAGGTACACTCCTTATGACCCTGAGGACCCAGGGC
AAGAAACTAATGTGTCTATGTCTTTCATTTGGCAGTCTGCCCCAGACATTGGGAGAAAGTTAGAGAGGTTAGAAGATTTAAAAAAC
AAGACGCTTGGAGATTTGGTTAGAGAGGCAGAAAAGATCTTTAATAAACGAGAAACCCCGGAAGAAAGAGAGGAACGTATCAGGAG
AGAAACAGAGGAAAAAGAAGAACGCCGTAGGACAGAGGATGAGCAGAAAGAGAAAGAAAGAGATCGTAGGAGACATAGAGAGATGA
GCAAGCTATTGGCCACTGTCGTTAGTGGACAGAAACAGGATAGACAGGGAGGAGAACGAAGGAGGTCCCAACTCGATCGCGACCAG
TGTGCCTACTGCAAAGAAAAGGGGCACTGGGCTAAAGATTGTCCCAAGAAACCACGAGGACCTCGGGGACCAAGACCCCAGACCTC
CCTCCTGACCCTAGATGACTAGGGAGGTCAGGGTCAGGAGCCCCCCCCTGAACCCAGGATAACCCTCAAAGTCGGGGGGCAACCCG
TCACCTTCCTGGTAGATACTGGGGCCCAACACTCCGTGCTGACCCAAAATCCTGGACCCCTAAGTGATAAGTCTGCCTGGGTCCAA
GGGGCTACTGGAGGAAAGCGGTATCGCTGGACCACGGATCGCAAAGTACATCTAGCTACCGGTAAGGTCACCCACTCTTTCCTCCA
TGTACCAGACTGTCCCTATCCTCTGTTAGGAAGAGATTTGCTGACTAAACTAAAAGCCCAAATCCACTTTGAGGGATCAGGAGCTC
AGGTTATGGGACCAATGGGGCAGCCCCTGCAAGTGTTGACCCTAAATATAGAAGATGAGTATCGGCTACATGAGACCTCAAAAGAG
CCAGATGTTTCTCTAGGGTCCACATGGCTGTCTGATTTTCCTCAGGCCTGGGCGGAAACCGGGGGCATGGGACTGGCAGTTCGCCA
AGCTCCTCTGATCATACCTCTGAAAGCAACCTCTACCCCCGTGTCCATAAAACAATACCCCATGTCACAAGAAGCCAGACTGGGGA
TCAAGCCCCACATACAGAGACTGTTGGACCAGGGAATACTGGTACCCTGCCAGTCCCCCTGGAACACGCCCCTGCTACCCGTTAAG
AAACCAGGGACTAATGATTATAGGCCTGTCCAGGATCTGAGAGAAGTCAACAAGCGGGTGGAAGACATCCACCCCACCGTGCCCAA
CCCTTACAACCTCTTGAGCGGGCTCCCACCGTCCCACCAGTGGTACACTGTGCTTGATTTAAAGGATGCCTTTTTCTGCCTGAGAC
TCCACCCCACCAGTCAGCCTCTCTTCGCCTTTGAGTGGAGAGATCCAGAGATGGGAATCTCAGGACAATTGACCTGGACCAGACTC
CCACAGGGTTTCAAAAACAGTCCCACCCTGTTTGATGAGGCACTGCACAGAGACCTAGCAGACTTCCGGATCCAGCACCCAGACTT
GATCCTGCTACAGTACGTGGATGACTTACTGCTGGCCGCCACTTCTGAGCTAGACTGCCAACAAGGTACTCGGGCCCTGTTACAAA
CCCTAGGGAACCTCGGGTATCGGGCCTCGGCCAAGAAAGCCCAAATTTGCCAGAAACAGGTCAAGTATCTGGGGTATCTTCTAAAA
GAGGGTCAGAGATGGCTGACTGAGGCCAGAAAAGAGACTGTGATGGGGCAGCCTACTCCGAAGACCCCTCGACAACTAAGGGAGTT
CCTAGGGACGGCAGGCTTCTGTCGCCTCTGGATCCCTGGGTTTGCAGAAATGGCAGCCCCCTTGTACCCTCTCACCAAAACGGGGA
CTCTGTTTAATTGGGGCCCAGACCAACAAAAGGCCTATCAAGAAATCAAGCAAGCTCTTCTAACTGCCCCAGCCCTGGGGTTGCCA
GATTTGACTAAGCCCTTTGAACTCTTTGTCGACGAGAAGCAGGGCTACGCCAAAGGTGTCCTAACGCAAAAACTGGGACCTTGGCG
TCGGCCGGTGGCCTACCTGTCCAAAAAGCTAGACCCAGTAGCAGCTGGGTGGCCCCCTTGCCTACGGATGGTAGCAGCCATTGCCG
TACTGACAAAGGATGCAGGCAAGCTAACCATGGGACAGCCACTAGTCATTCTGGCCCCCCATGCAGTAGAGGCACTAGTCAAACAA
CCCCCCGACCGCTGGCTTTCCAACGCCCGGATGACTCACTATCAGGCCTTGCTTTTGGACACGGACCGGGTCCAGTTCGGACCGGT
GGTAGCCCTGAACCCGGCTACGCTGCTCCCACTGCCTGAGGAAGGGCTGCAACACAACTGCCTTGATATCCTGGCCGAAGCCCACG
GAACCCGACCCGACCTAACGGACCAGCCGCTCCCAGACGCCGACCACACCTGGTACACGGATGGAAGCAGTCTCTTACAAGAGGGA
CAGCGTAAGGCGGGAGCTGCGGTGACCACCGAGACCGAGGTAATCTGGGCTAAAGCCCTGCCAGCCGGGACATCCGCTCAGCGGC
TGAACTGATAGCACTCACCCAGGCCCTAAAGATGGCAGAAGGTAAGAAGCTAAATGTTTATACTGATAGCCGTTATGCTTTTGCTA
CTGCCCATATCCATGGAGAAATATACAGAAGGCGTGGGTTGCTCACATCAGAAGGCAAAGAGATCAAAAATAAAGACGAGATCTTG
GCCCTACTAAAAGCCCTCTTTCTGCCCAAAAGACTTAGCATAATCCATTGTCCAGGACATCAAAAGGGACACAGCGCCGAGGCTAG
AGGCAACCGGATGGCTGACCAAGCGGCCCGAAAGGCAGCCATCACAGAGACTCCAGACACCTCTACCCTCCTCATAGAAAATTCAT
CACCCTACACCTCAGAACATTTTCATTACACAGTGACTGATATAAAGGACCTAACCAAGTTGGGGGCCATTTATGATAAAACAAAG
AAGTATTGGGTCTACCAAGGAAAACCTGTGATGCCTGACCAGTTTACTTTTGAATTATTAGACTTTCTTCATCAGCTGACTCACCT
CAGCTTCTCAAAAATGAAGGCTCTCCTAGAGAGAAGCCACAGTCCCTACTACATGCTGAACCGGGATCGAACACTCAAAAATATCA
CTGAGACCTGCAAAGCTTGTGCACAAGTCAACGCCAGCAAGTCTGCCGTTAAACAGGGAACTAGGGTCCGCGGGCATCGGCCCGGC
ACTCATTGGGAGATCGATTTCACCGAGATAAAGCCCGGATTGTATGGCTATAAATATCTTCTAGTTTTTATAGATACCTTTTCTGG
CTGGATAGAAGCCTTCCCAACCAAGAAAGAAACCGCCAAGGTCGTAACCAAGAAGCTACTAGAGGAGATCTTCCCCAGGTTCGGCA
TGCCTCAGGTATTGGGAACTGACAATGGGCCTGCCTTCGTCTCCAAGGTGAGTCAGACAGTGGCCGATCTGTTGGGGATTGATTGG
AAATTACATTGTGCATACAGACCCCAAAGCTCAGGCCAGGTAGAAAGAATGAATAGAACCATCAAGGAGACTTTAACTAAATTAAC
GCTTGCAACTGGCTCTAGAGACTGGGTGCTCCTACTCCCCTTAGCCCTGTACCGAGCCCGCAACACGCCGGGCCCCCATGGCCTCA
CCCCATATGAGATCTTATATGGGGCACCCCCGCCCCTTGTAAACTTCCCTGACCCTGACATGACAAGAGTTACTAACAGCCCCTCT
CTCCAAGCTCACTTACAGGCTCTCTACTTAGTCCAGCACGAAGTCTGGAGACCTCTGGCGGCAGCCTACCAAGAACAACTGGACCG
ACCGGTGGTACCTCACCCTTACCGAGTCGGCGACACAGTGTGGGTCCGCCGACACCAGACTAAGAACCTAGAACCTCGCTGGAAAG
GACCTTACCCAGTCCTGCTGACCACCCCCACCGCCCTCAAAGTAGACGGCATCGCAGCTTGGATACACGCCGCCCACGTGAAGGCT
GCCGACCCCGGGGGTGGACCATCCTCTAGACTGACATGGCGCGTTCAACGCTCTCAAAACCCCTTAAAAATAAGGTTAACCCGCGA
GGCCCCCGTGGCTCAAATCCTGCACAACAGATTCTTCATGTTTGGACCAAATCAACTTGTGATACCATGCTCAAAGAGGCCTCAAT
TATATTTGAGTTTTTAATTTTTATGAAAAAAAAAAAAAAAAAACGGAATTCCTCGAGGGATCCGTCGAGGAATTCACTCCTCAGGTG
CAGGCTGCCTATCAGAAGGTGGTGGCTGGTGTGGCCAATGCCCTGGCTCACAAATACCACTGAGATCTTTTTCCCTCTGCCAAAAA
TTATGGGGACATCATGAAGCCCCTTGAGCATCTGACTTCTGGCTAATAAAGGAAATTTATTTTCATTGCAATAGTGTGTTGGAATT
TTTTGTGTCTCTCACTCGGAAGGACATATGGGAGGGCAAATCATTTAAAACATCAGAATGAGTATTTGGTTTAGAGTTTGGCAACA
TATGCCCATATGCTGGCTGCCATGAACAAAGGTTGGCTATAAAGAGGTCATCAGTATATGAAACAGCCCCCTGCTGTCCATTCCTT
ATTCCATAGAAAAGCCTTGACTTGAGGTTAGATTTTTTTTATATTTTGTTTTGTGTTATTTTTTTCTTTAACATCCCTAAAATTTT
CCTTACATGTTTTACTAGCCAGATTTTTCCTCCTCTCCTGACTACTCCCAGTCATAGCTGTCCCTCTTCTCTTATGGAGATCCCTC
GACGGATCGGCCGCAATTCGTAATCATGTCATAGCTGTTTCCTGTGTGAAATTGTTATCCGCTCACAATTCCACACAACATACGAG
CCGGAAGCATAAAGTGTAAAGCCTGGGGTGCCTAATGAGTGAGCTAACTCACATTAATTGCGTTGCGCTCACTGCCCGCTTTCCAG
TCGGGAAACCTGTCGTGCCAGCTGCATTAATGAATCGGCCAACGCGCGGGGAGAGGCGGTTTGCGTATTGGGCGCTCTTCCGCTTC
CTCGCTCACTGACTCGCTGCGCTCGGTCGTTCGGCTGCGGCGAGCGGTATCAGCTCACTCAAAGGCGGTAATACGGTTATCCACAG
AATCAGGGGATAACGCAGGAAAGAACATGTGAGCAAAAGGCCAGCAAAAGGCCAGGAACCGTAAAAAGGCCGCGTTGCTGGCGTTT
TTCCATAGGCTCCGCCCCCCTGACGAGCATCACAAAAATCGACGCTCAAGTCAGAGGTGGCGAAACCCGACAGGACTATAAAGATA
CCAGGCGTTTCCCCCTGGAAGCTCCCTCGTGCGCTCTCCTGTTCCGACCCTGCCGCTTACCGGATACCTGTCCGCCTTTCTCCCTT
CGGGAAGCGTGGCGCTTTCTCATAGCTCACGCTGTAGGTATCTCAGTTCGGTGTAGGTCGTTCGCTCCAAGCTGGGCTGTGTGCAC
GAACCCCCCGTTCAGCCCGACCGCTGCGCCTTATCCGGTAACTATCGTCTTGAGTCCAACCCGGTAAGACACGACTTATCGCCACT
GGCAGCAGCCACTGGTAACAGGATTAGCAGAGCGAGGTATGTAGGCGGTGCTACAGAGTTCTTGAAGTGGTGGCCTAACTACGGCT
ACACTAGAAGAACAGTATTTGGTATCTGCGCTCTGCTGAAGCCAGTTACCTTCGGAAAAAGAGTTGGTAGCTCTTGATCCGGCAAA
CAAACCACCGCTGGTAGCGGTGGTTTTTTTGTTTGCAAGCAGCAGATTACGCGCAGAAAAAAAGGATCTCAAGAAGATCCTTTGAT
CTTTTCTACGGGGTCTGACGCTCAGTGGAACGAAAACTCACGTTAAGGGATTTTGGTCATGAGATTATCAAAAAGGATCTTCACCT
AGATCCTTTTAAATTAAAAATGAAGTTTTAAATCAATCTAAAGTATATATGAGTAAACTTGGTCTGACAGTTACCAATGCTTAATC

AGTGAGGCACCTATCTCAGCGATCTGTCTATTTCGTTCATCCATAGTTGCCTGACTCCCCGTCGTGTAGATAACTACGATACGGGA
GGGCTTACCATCTGGCCCCAGTGCTGCAATGATACCGCGAGACCCACGCTCACCGGCTCCAGATTTATCAGCAATAAACCAGCCAG
CCGGAAGGGCCGAGCGCAGAAGTGGTCCTGCAACTTTATCCGCCTCCATCCAGTCTATTAATTGTTGCCGGGAAGCTAGAGTAAGT
AGTTCGCCAGTTAATAGTTTGCGCAACGTTGTTGCCATTGCTACAGGCATCGTGGTGTCACGCTCGTCGTTTGGTATGGCTTCATT
CAGCTCCGGTTCCCAACGATCAAGGCGAGTTACATGATCCCCCATGTTGTGCAAAAAAGCGGTTAGCTCCTTCGGTCCTCCGATCG
TTGTCAGAAGTAAGTTGGCCGCAGTGTTATCACTCATGGTTATGGCAGCACTGCATAATTCTCTTACTGTCATGCCATCCGTAAGA
TGCTTTTCTGTGACTGGTGAGTACTCAACCAAGTCATTCTGAGAATAGTGTATGCGGCGACCGAGTTGCTCTTGCCCGGCGTCAAT
ACGGGATAATACCGCGCCACATAGCAGAACTTTAAAAGTGCTCATCATTGGAAAACGTTCTTCGGGGCGAAAACTCTCAAGGATCT
TACCGCTGTTGAGATCCAGTTCGATGTAACCCACTCGTGCACCCAACTGATCTTCAGCATCTTTTACTTTCACCAGCGTTTCTGGG
TGAGCAAAAACAGGAAGGCAAAATGCCGCAAAAAAGGGAATAAGGGCGACACGGAAATGTTGAATACTCATACTCTTCCTTTTTCA
ATATTATTGAAGCATTTATCAGGGTTATTGTCTCATGAGCGGATACATATTTGAATGTATTTAGAAAAATAAACAAATAGGGGTTC
CGCGCACATTTCCCCGAAAAGTGCCACCTAAATTGTAAGCGTTAATATTTTGTTAAAATTCGCGTTAAATTTTTGTTAAATCAGCT
CATTTTTTAACCAATAGGCCGAAATCGGCAAAATCCCTTATAAATCAAAAGAATAGACCGAGATAGGGTTGAGTGTTGTTCCAGTT
TGGAACAAGAGTCCACTATTAAAGAACGTGGACTCCAACGTCAAAGGGCGAAAAACCGTCTATCAGGGCGATGGCCCACTACGTGA
ACCATCACCCTAATCAAGTTTTTTGGGGTCGAGGTGCCGTAAAGCACTAAATCGGAACCCTAAAGGGAGCCCCCGATTTAGAGCTT
GACGGGGAAAGCCGGCGAACGTGGCGAGAAAGGAAGGGAAGAAAGCGAAAGGAGCGGGCGCTAGGGCGCTGGCAAGTGTAGCGGTC
ACGCTGCGCGTAACCACCACACCCGCCGCGCTTAATGCGCCGCTACAGGGCGCGTCCCATTCGCCATTCAGGCTGCGCAACTGTTG
GGAAGGGCGATCGGTGCGGGCCTCTTCGCTATTACGCCAGCTGGCGAAAGGGGGATGTGCTGCAAGGCGATTAAGTTGGGTAACGC
CAGGGTTTTCCCAGTCACGACGTTGTAAAACGACGGCCAGTGAGCGCGCGTAATACGACTCACTATAGGGCGAATTGGAGCTCCAC
CGCGGTGGCGGCCGCTCTAGA

8. List of Publications

1) **Bertheloot D.**, Naumovski A.L., Langhoff P., Horvath G.L., Jin T., Xiao T.S., Garbi N., Agrawal S., Kolbeck R. and Latz E., *RAGE enhances TLR responses through binding and internalization of RNA*.
(Under peer review at the Journal of Immunology)

2) **Bertheloot D.**, Latz E., *HMGB1, IL-1α, IL-33 and S100 proteins: dual-function alarmins*.
(Under peer review at the Journal of Cellular and Molecular Immunology)

3) S.K. Fassl, J. Austermann, O. Papantonopoulou, M. Riemenschneider, J. Xue, **D. Bertheloot**, Freise N., Spiekermann C., Witten A., Viemann D., Kirschnek S., Stoll M., Latz E., Schultze J.L., Roth J., T. Vogl., 2014. *Transcriptome assessment reveals a dominant role for TLR4 in the activation of human monocytes by the alarmin MRP8*. Journal of Immunology.
doi: 10.4049/jimmunol.1401085

4) Sirois, C.M., Jin, T., Miller, A.L., **Bertheloot, D.**, Nakamura H., Horvath G.L., Mian A., Jiang J., Schrum J., Bossaller L., Pelka K., Garbi N., Brewah Y., Tian J., Chang C., Chowdhury P.S., Sims G.P., Kolbeck R., Coyle A.J., Humbles A.A., Xiao T.S., Latz E., 2013. *RAGE is a nucleic acid receptor that promotes inflammatory responses to DNA*. Journal of Experimental Medicine.
doi: 10.1084/jem.20120201

5) Stutz, A., **Bertheloot, D.** & Latz, E., 2011. *Innate immune receptors for nucleic acids*. Methods in molecular biology.
doi: 10.1007/978-1-61779-139-0_5